University of Sheffield

ADAMTS5 and integrin crosstalk in controlling ovarian cancer migration and invasion

Rachele Bacchetti

This thesis is submitted in partial fulfilment of the requirements for the degree of Doctor of Philosophy

The University of Sheffield, School of Biosciences

Faculty of Science

March 2025

ABSTRACT

Ovarian cancer is the most common cause of female gynaecological cancer death and ~80% of patients will have developed metastasis at diagnosis. For this reason, it is fundamental to discover novel mechanisms controlling ovarian cancer metastasis. Ovarian cancer metastasis relies on cancer cell migration and interaction with the extracellular matrix (ECM), mediated by surface receptors like integrins. Extracellular proteases, like ADAMTSs, are fundamental to degrade the ECM and facilitate cell migration, leading to the formation of a tumour-promoting environment. The small GTPase Rab25 has been shown to control cancer cell migration in 3D environments, increasing integrin recycling. We have recently demonstrated that ADAMTS5 was upregulated by Rab25. Moreover, ADAMTS5 inhibition reduced the migration and invasion of ovarian cancer cells over-expressing Rab25.

In this thesis we showed that the ECM component fibronectin promoted ADAMTS5 expression. Mechanistically, we found that the fibronectin co-receptor syndecan-4 was required for Rab25-driven ADAMTS5 expression. We also found that ADAMTS5 was necessary and sufficient to stimulate ovarian cancer cell migration through matrix, while ADAMTS5 inhibition and knockdown prevented ovarian cancer spheroid invasion and migration through mesothelial cell layers. Furthermore, we developed an *in vivo* Zebrafish model to elucidate the contribution of Rab25 to ovarian cancer metastasis and found that Rab25 overexpression promoted ovarian cancer metastasis formation. Altogether, these data identify ADAMTS5 as a novel regulator of ovarian cancer cell migration and invasion, suggesting it might represent a novel therapeutic target to prevent ovarian cancer metastasis.

ACKNOWLEDGEMENTS

I would like to thank my supervisor **Dr Elena Rainero** for providing me with the opportunity to work in her laboratory, but even more for the support, kindness, patience, and mentorship given throughout the PhD journey. I am truly grateful for the time spent in her lab, the meeting discussing everything and anything, and the confidence placed in my work, it was great to have her as a mentor.

I would also like to thank my advisors, **Dr Mark Bass** and **Dr Emily Noël** for their support during my PhD. A special thanks to Dr Mark Bass for the help during the fibronectin fragments purification and to Dr Emily Noël for our great chats over coffee. I would also like to thank my co-supervisor, **Dr Freek van Eeden**, who helped me set up the zebrafish model, I would not have managed without your advice and knowledge. I would also like to thank **Dr Nick van Hateren** and **Dr Darren Robinson** for the training and help troubleshooting in the LMF. I would also like to thank **Claire E Allen** and all the aquarium staff for their support setting everything up and the training given. In addition, I would like to express my deepest thanks to past and present members of **Kathryn Ayscough**, **Freek van Eeden**, **Helen Matthews**, and **Elena Rainero labs**. Many thanks to **Shahd Alhadid** and **Shengnan Yuan** for always being there, the best friends someone could have ever needed, hopefully we will see each other soon. Thanks to **Dr Mona Nazemi** and **Bian Yanes** for all the help given in and out the lab you will always be like big sisters. Thanks to **Dr Monserrat Llanses Marínez** for all the help, the late nights in the lab and multiple dinners (sorry Nick if she was late for the videocall, it was my fault!), I truly have missed sharing lab bench with you. Thanks to **Dr Victoria H Hart** and **Rachel H Lawson**, it's great to share lab space with you. Thanks **Isabella J Davis** for the morning chats and early morning math questions, it has been great to be a Rep with you, best of luck. Thanks to **Zhe Bao**, **Ifeoluwa F Oyelade**, **Dr Haya Alomaim** and **Dr Eric Vancauwenberghe** for being great lab mates. Thanks to **Eleanor R Markham** and **Cathrine**

Hyde, for their help with the zebrafish, sharing techniques, protocols, and materials. Thanks to **Anthony J Hobber** for his help in the lab and his support completing the Puzzler collection magazines in between experiments, I would have not managed without you. A special thanks to **Charly A Pain**, your support and motivation during writing made it possible, and to all the coffees taken at table 29 or 13 while writing.

A special thanks to **Nada Ghorab,** for your help, support, and encouragement. It has been great to share this journey with you from the really first day of university, it's a pleasure to be able to call you a friend, can't wait to see what the future holds for us.

I would also like to specially thank my partner, **Mattia Coppola**, for always being by my side, his support and constant encouragement. I am extremely grateful for his positivity and cheering in my worst days. I would have not managed to finish writing this thesis without your support.

I want to extend my thanks to my **all my family** for their support over the years, specially to my parents, **Roberta Margutti** and **Stefano Bacchetti**, for their constant support, love and believing I can achieve anything I set my mind on. Thanks for their efforts and sacrifices which allowed me to go to university, study abroad and follow my dreams. An enormous thanks to **my grandparents**, for always listening to my stories, believing in me, and encouraging me to study. Finally, I would like to dedicate my thesis in loving memory of my grandad, **Guerrino Margutti**, whose support, love and strength will never be forgotten. I know you always wondered when I will be done, I am glad to report that I have officially finished!

DECLARATION

I, Rachele Bacchetti, declare that this thesis is the result of my sole work, except where explicitly stated otherwise, for the degree of Doctor of Philosophy at the University of Sheffield, and it has not been previously submitted to this or any other institution. I am aware of the University's guidance on the Use of Unfair Means (www.sheffield.ac.uk/ssid/unfair-means). I confirm that where I have quoted from the work of others, the source is always given. This Thesis has been written using the inclusive first-person plural.

Part of the work presented in figure 3.4 (Chapter 3) and work presented in figure 4.1 (Chapter 4) has been accepted for publication, in press, and is currently available in the form of a BioRxiv article titled 'The protease ADAMTS5 controls ovarian cancer cell invasion, downstream of Rab25' by Shengnan Yuan, *Rachele Bacchetti*, Jamie Adams and Elena Rainero*. Work in figure 4.10, figure 4.11 and figure 4.12 has been analysed by Elena Rainero*.

*Supervisor

Rachele Bacchetti, 15 Mar. 2025

Table of content

List of figures

Chapter 1: Introduction

Chapter 2: Methods

Chapter 3: Rab25 overexpression drives ADAMTS5 expression in a FN dependent manner via syndecan-4 in ovarian cancer cells

Chapter 4: ADAMTS5 is needed for ovarian cancer cell migration

Chapter 5: ADAMTS5 is required for ovarian cancer cell clearance of mesothelial monolayers

Chapter 6: Establishment of an in vivo model for ovarian cancer cell invasion, zebrafish as a cancer metastasis animal model

Chapter 7: Discussion

List of Tables

Chapter 1: Introduction

Chapter 2: Methods

ABBREVIATIONS

A disintegrin and metalloproteinase (ADAM)

A disintegrin and metalloproteinase with thrombospondin motifs (ADAMTS)

Antigen presenting CAF (apCAF)

Basement membrane (BM)

Bone morphogenic protein (BMP)

Bovine serum albumin (BSA)

Cancer associated mesothelial cells (CAMCS)

Cancer-associated fibroblasts (CAFS)

Carbohydrate antigen 125 (CA125)

Cell derived matrix (CDM)

chloride intracellular channel 3 (CLIC3)

cluster of differentiation 44 (CD44)

CUB and Sushi multiple domain 3 (CSMD3)

Cyclin E1 (CCNE1)

Cyclin-dependent kinase 12 (CDK12)

Days post-fertilization (dpf)

Dulbeecco's Modified Eagle Medium (DMEM)

Endoplasmic reticulum (ER)

Epidermal growth factor (EGF)

Epithelial ovarian cancer (EOC)

Epithelial-Mesenchymal Transition (EMT)

Ets proto-oncogene 1 (ETS1)

Extracellular matrix (ECM)

Extracellular signal-regulated kinase (ERK)

FAT Atypical cadherin 3 FAT3

Fatty acid binding protein 4 (FABP4)

Fibronectin (FN)

Focal adhesion kinase (FAK)

Foetal bovine serum (FBS)

Gamma-aminobutyric acid receptor subunit alpha-6 (GABRA6)

GDP dissociation inhibitor (GDI)

Glycosaminoglycan (GAG)

GTPase activating proteins (GAPs)

Guanine nucleotide exchange factors (gefs)

Gynecology Oncology Group (GOG)

Hepatocellular carcinoma (HCC)

Hepatocyte growth factor (HGF)

High grade serous ovarian carcinoma (HGSC)

Hormone-sensitive lipase (HSL)

Hours post-fertilization (hpf)

Human epididymis protein 4 (HE4)

Immunofluorescence wash (IFw)

Inflammatory CAF (iCAF)

Insulin growth factor binding protein 3 (IGFBP-3)

Interleukin (IL)

International federation of Gynaecology and Obstetrics (FIGO)

Interstitial matrix (IM)

Lysyl-oxidase (LOX)

Matrix metalloproteinases (MMP)

Methylcellulose (MTC)

Mitogen-activated protein kinase (MAPK)

Mouse embryonic fibroblasts (MEFs)

Myelocytomatosis oncogene (MYC)

Myofibroblastic (mycaf)

Neurofibromin (NF1)

Nuclear factor kappa-B (NFκB)

Phosphatase and tensin homolog (PTEN)

Phosphoinositide 3-kinase (PI3K)

Placental growth factor 2 (plgf-2)

Platelet-derived endothelial cell growth factor (PD-ECGF)

Polyvinylpyrrolidone (PVP)

Protein kinase B (AKT)

Retinoblastoma (RB1)

Risk of Ovarian Cancer Algorithm (ROCA)

Room temperature (RT)

Syndecan-1 (SDC1)

Syndecan-2 (SDC2)

Syndecan-3 (SDC3)

Syndecan-4 (SDC4)

The Cancer Genome Atlas (TCGA)

Thrombospondin motif type I (TSR1)

Tissue inhibitors of metalloproteinases (TIMPs)

Transforming growth factor beta (TGF-β)

Tumour microenvironment (TME)

v-raf murine sarcoma viral oncogene homolog B1 (BRAF)

Breast Cancer gene (BRCA)

Vascular endothelial growth factor (VEGF)

World health organization (WHO)

α-smooth muscle actin (αSMA)

CHAPTER 1: Introduction

In this chapter, I will cover the basics of ovarian cancer development, progression, and metastasis; explore the role of the extracellular matrix (ECM) in cancer progression and introduce regulators of cancer cell migration.

1.1 Ovarian cancer:

Cancer is a group of diseases characterised by the abnormal growth and transformation of cells. It is one of the leading causes of death worldwide that led to 10 million deaths in 2020 (WHO, 2021), being one of the major societal, public health and economic problems of the 21st century. Studies working on prediction of cancer cases estimate that there will be a 77% increase in cancer cases by 2050 compared to 2022, if the projected changes in population growth and cancer rates remain the same (Bray et al., 2024), highlighting the need to invest in prevention and treatments. In this thesis, I will focus on ovarian cancer, the most common cause of female cancer death when looking at gynaecological malignancies.

1.1.1 Epidemiology

Breast (23.8%), cervical (6.8%), uterine (4.3%) and ovarian (3.4%), are among the most frequently diagnosed cancers in women, together they account for almost 40% of all cancers affecting women (Bray et al., 2024). In 2018 there were approximately 7,500 new cases of ovarian cancer and 4,200 deaths in the UK (Cancer Research UK, 2021). Early-stage ovarian cancer is normally symptom free, and when symptoms start to appear, they tend to be non-specific leading women to be diagnosed at an advanced stage. This reduces 5-year survival rate to 29% compared to early-stage detection survival rate and increases reoccurrence, as 80% of the patients will already have developed metastasis by the time of diagnosis (Dhaliwal and Shepherd, 2021). Furthermore, despite advances in precision medicine and cytotoxic therapies; treatment safety and efficacy (due to chemoresistance) are not consistent when looking at solid

tumour treatments. Anti-invasive and antimetastatic drugs have been overlooked in the past years as the drug end point is not tumour shrinkage but metastatic reduction. Recent regulatory changes have been implemented allowing for metastatic endpoints for solid tumour therapies, which will lead to new opportunities to develop migrastatics; drugs that block cell movement or invasion, broadening cancer treatment options (Rosel et al., 2019). This is a great advancement as metastasis is considered the most life-threatening event for patients with cancer, accounting for 90% of tumour-related deaths (Riggio et al., 2021). However, this often repeated claim can be considered overly simplistic as it lacks robust evidence, due to the multifactorial nature of cancer including primary tumour burden, organ dysfunction, systemic effects, treatment related toxicity and other pathologies (Boire et al., 2024). Nevertheless, a better understanding of the metastatic events is necessary, as a high frequency of ovarian cancer patients have micro-metastasis that are not detectable with current technologies.

1.1.2 Pathological classification, development, and progression

Ovarian cancer can be classified into epithelial or non-epithelial cancers (figure 1.1). Epithelial ovarian cancer (EOC) accounts for more than 90% of ovarian cancer cases while non-epithelial include germ-cell, accounting for approximately 5%, sex-cord stromal and small cell carcinoma, accounting for the rest. EOC can be further classified in six different subtypes: serous, clear cell, endometrioid, mucinous, squamous carcinoma and transitional cell (Worzfeld, et al., 2017). Historically all subtypes were classified by clinicians and researchers as of ovarian epithelial origin, as the dominant mass was located on the ovary, but lesions to other areas (fallopian tubes or peritoneum) were reported (Piek et al., 2001; Woolas et al., 1994). Recently, high-grade serous ovarian cancer, accounting for 75% of all EOC, has been shown to arise predominantly from tissue within the fallopian tube (Köbel and Kang, 2022). The world health organization (WHO) has now reclassified female genital tumours using combined terminology for the site of origin to tubo-ovarian high-grade serous carcinoma

(WHO, 2020). Other ovarian cancer types, such as endometroid and clear cell carcinoma, do also not develop from the ovarian tissue but arise from ectopic endometrium. Mucinous ovarian cancer tissue of origin has been controversial, most of these tumours were misdiagnosed metastasis from other organs like uterus, pancreas, colon and stomach (Ledermann et al., 2014), but a small rate of them do actually originate from the epithelium of the ovaries. Ovarian cancer origin heterogeneity presents extra challenges for the study and treatment of this disease (Blagden, 2015). To aid advancing therapies better nomenclature and classification are needed to optimise treatment. To achieve this, further research to determine early events leading to ovarian cancer development is required.

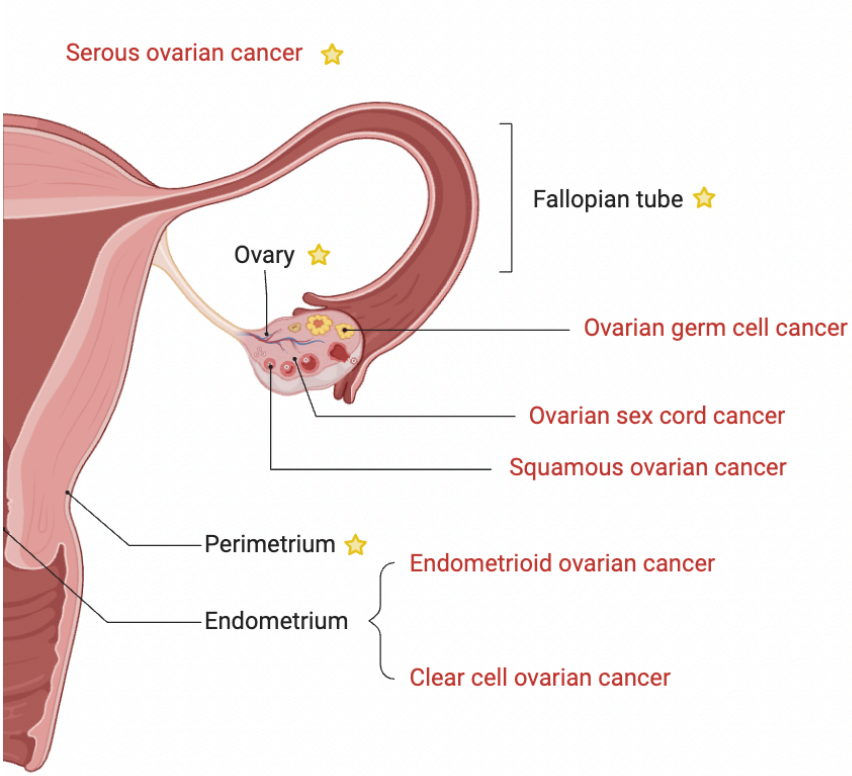

Figure 1.1. ***Location of origin of the different ovarian cancer subtypes.*** Diagram showing different parts of the female reproductive system. Ovarian cancer types have been labelled in red next to the current known tissues from which they develop. Due to the multiple tissues of origin of serous ovarian cancer a star was used to mark the different location of origin of this subtype. Image created using BioRender.

Moreover, ovarian cancer can be further classified by stage and grade that will define tumour progression. The International federation of Gynaecology and Obstetrics (FIGO) have defined the staging system for ovarian, fallopian and peritoneum cancers. There are four stages, I-IV,

that describe how advanced the tumour has grown, I being the earliest and IV the most advanced (Berek et al., 2021). The criteria for each stage are summarised in figure 1.2. In addition, EOC can be categorised by grade. Multiple grading systems are currently used, the most common ones are the FIGO, WHO or Gynecology Oncology Group, USA, (GOG). Based on the FIGO system, there are a total of three grades based on architectural features depending on the ratio between granular and papillary structures against solid tumour structures. In low grade cancers (grade I) there is less than 5% solid tumour, moderate grade cancers (grade II) have between 5% and 50% solid tumour growth and finally high-grade cancers (grade III) are more than 50% solid tumour, growing more quickly and being more likely to spread. As these grading systems were not useful in classifying all ovarian cancer subtypes, were not universally applied and were not always prognostically meaningful when comparing early and late stages, Silverberg and colleagues proposed a grading system that considers the architectural pattern, nuclear pleomorphism and mitotic activity (Silverberg, 2000). Each of these parameters scores 1 to 3 points, following guidelines. If the final score is between 3-5, it is a well-differentiated grade I tumour; between 6-7 a moderately differentiated grade II tumour; while between 8-9 a poorly differentiated grade III tumour.

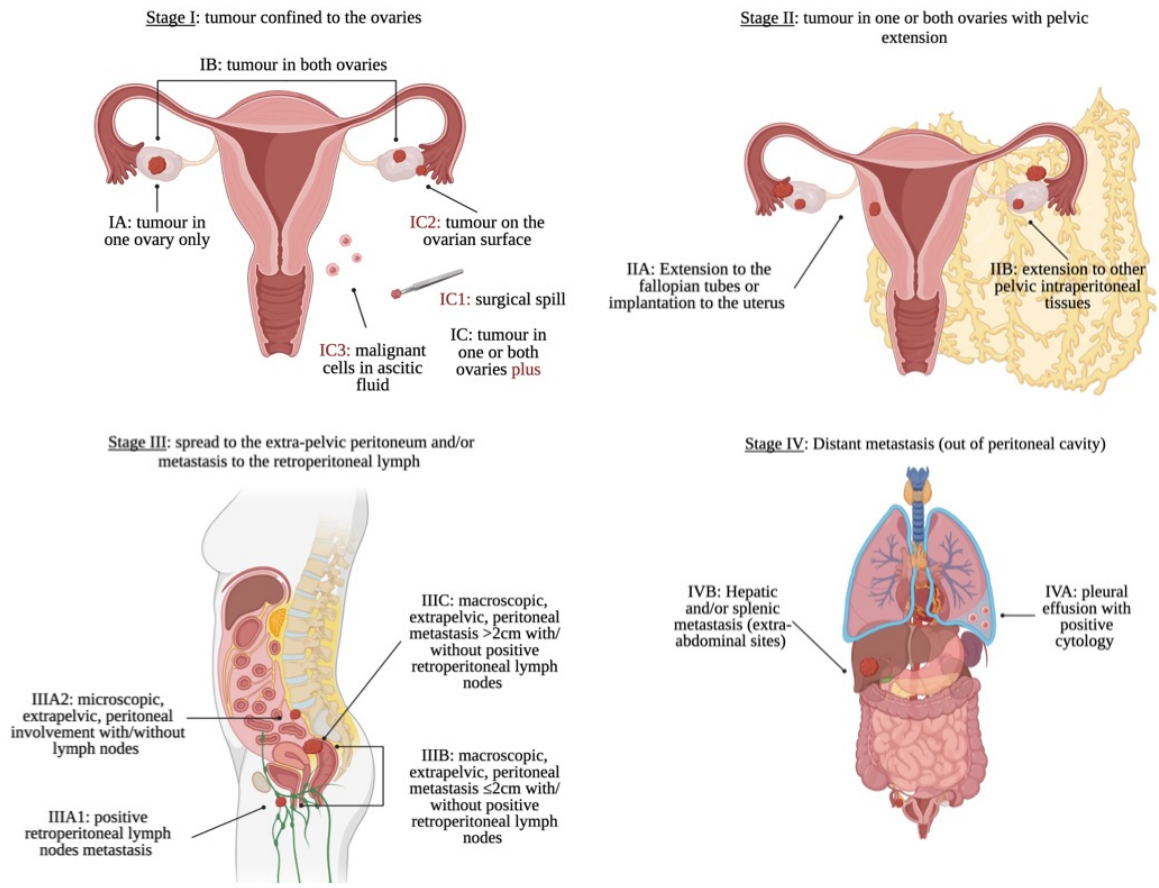

Figure 1.2. ***Stages of ovarian cancer.*** The illustration shows where cancer cells are located during the different ovarian cancer stages, including the description of the four main stages (I to IV) and substages of the disease as classified in the FIGO staging system. Illustration made using BioRender.

1.1.3 Molecular abnormalities underlying ovarian cancer

The most common EOC subtype is high grade serous ovarian carcinoma (HGSC), also classified as the most lethal. HGSC are associated with mutations in the TP53 gene. The majority of TP53 mutations are missense variants, but frameshift, nonsense or splice junction variants leading to complete loss of protein have also been observed (Salani et al., 2008). TP53 is a tumour suppressor gene involved in G2 checkpoint, controlling cell cycle arrest, senescence or apoptosis in response to cellular stress (Bieging et al., 2014). In contrast to what could be expected, a study analysing The Cancer Genome Atlas (TCGA) data found that TP53 wildtype tumours could lead to worse prognosis than mutated (missense, frameshift, splice-site and nonsense) TP53 tumours (Wong et al., 2013), potentially due to upregulation in EDAR2, which

regulates NFκB leading to survival and invasion. Moreover, approximately 50% of HGSC show defective homologous recombination of somatic and germline breast cancer gene (BRCA) mutations, epigenetic activations of BRCA or abnormalities in DNA repair genes (Testa et al., 2018). BRCA1/2 are components of the homologous recombination repair machinery for double strand DNA breaks; mutations in others members, such as, RAD51C, RAD51D and BRIP1, have also been associated with increased risk of developing ovarian cancer (Ramus et al., 2015). Furthermore, omics studies have confirmed the high chromosomal instability of this types of cancer. RB1 (encoding for retinoblastoma, a negative regulator of cell cycle progression), NF1 (neurofibromin, a negative regulator of cell growth), FAT3 (FAT Atypical cadherin 3, coordinating cell-cell adhesion), CSMD3 (CUB and Sushi multiple domain 3, an activator of mitogen-activated protein kinase (MAPK) signalling pathway), GABRA6 (gamma-aminobutyric acid receptor subunit alpha-6) and CDK12 (cyclin-dependent kinase 12, regulating gene transcription, RNA splicing and DNA replication) were further found mutated in HGSC and 113 focal somatic copy number alterations were detected, like amplification of CCNE1 (Cyclin E1, cell cycle regulator), MYC (myelocytomatosis oncogene, playing a role in cell cycle progression and apoptosis) and MECOM and deletions in PTEN (phosphatase and tensin homolog, negative regulator of cell division and growth), RB1 and NF1 (Bell et al., 2011). Other alterations are commonly located in the Notch, phosphoinositide 3-kinase (PI3K) and RAS-MEK signalling pathways (Matulonis, et al., 2016).

When looking at other ovarian cancer subtypes, v-raf murine sarcoma viral oncogene homolog B1 (BRAF) mutations are normally only found in serous borderline tumours or low-grade serous carcinomas. Even if low grade serous carcinomas show more mutational stability and have been proven to be less aggressive than HGSC, these tumours tend to be less responsive to chemotherapy, leading to poor long-term prognosis (Tone et al., 2014). Loss of PTEN and activation of PIK3CA are common in endometroid and clear cell subtypes, but not in serous or

mucinous (Kuo et al., 2009). Moreover, clear cell carcinoma frequently has inactivating mutations of ARID1A, a subunit of the SWI/SNF chromatin remodelling complex which facilitates gene activation, as it is associated to endometriosis, while HER2 amplification has been reported in this and mucinous subtypes. Mucinous subtype has also been reported to exhibit KRAS mutations (Cuatrecasas et al., 1997; Lheureux et al., 2019; Wiegand et al., 2010). Small cell carcinoma of the ovary, currently with unknown tissue of origin, is associated with somatic and germline inactivating mutations in SMARCA4, part of the SWI/SNF chromatin remodelling complex together with ARID1A, associated with loss of protein expression (Jelinic et al., 2014).

Not only is ovarian cancer a highly heterogenic disease, with multiple tissues of origin, but it also displays a varied genetic and molecular background. It is known that genome instability and mutations to tumour suppressor genes and oncogenes drive the transformation of normal cells into neoplastic states forming malignant tumours. Hanahan (2022) has recently proposed the concept of "enabling characteristics", molecular or cellular mechanisms that aid cancer cells to adopt functional trails; among these, non-mutational epigenetic reprograming can be found. Multiple epigenetic events have been reported in ovarian cancer, many of them linked to tumour progression and chemotherapy resistance. To mention a few examples, hypermethylation of MLH1, involved in DNA repair, is found in more than 50% of ovarian cancer with platinum resistance while epigenetic silencing of the tumour suppressor gene DLEC1 is linked to ovarian cancer recurrence (Lin et al., 2018; Zeller et al., 2012).

1.1.4 Current detection and treatments

There is no screening test for ovarian cancer to increase early detection. As it occurs with many other cancer types, the risk of developing ovarian carcer increases with age. This is mostly due to accumulation of genetic alterations and exposure to environmental factors, being 5 times more common in women over 60 years of age than under (National Cancer Institute, 2024).

Most patients are asymptomatic during early stages of ovarian cancer, and when showing symptoms, they can be misdiagnosed due to similarities with other pathologies like gastrointestinal conditions, as there are no clear or unique symptoms specific to ovarian cancer. Another common issue for early detection is that early lesions do not occur in the ovaries, which makes it harder to know where to look. Common diagnosis tests are transvaginal ultrasound or high blood levels of carbohydrate antigen 125 (CA125). CA125 is an epitope located on mucin 16, a glycoprotein expressed on epithelial cells from the ovaries, fallopian tube and peritoneum, among other tissues, which is not normally found in the bloodstream, but under pathological conditions, such as ovarian cancer, levels can rise. However, CA125 can also be elevated in endometriosis and benign tumours or be non-detectable in early-stage ovarian cancer (Whitwell, et al., 2020), increasing the risk of misdiagnosis. Increased levels of CA125 are most frequent in HGSC compared to other subtypes; it is found elevated in 50% of stage I patients, with better detection in later stages (Jacobs et al., 1999; Tian et al., 2009). The Prostate, Lung, Colorectal and Ovarian (PLCO) Cancer Screening trial tested the efficacy of CA125 as a screening tool by enrolling more than 78,000 women, between the ages of 55-78, and assigning them randomly to two groups: one where normal care screening was provided (examination with ovarian palpation) and the other where annual screening with CA125 blood test and transvaginal ultrasound was provided. Ovarian cancer was diagnosed in both groups at a similar rate (4.7 and 5.7 per 10.000 persons/year respectively). Independently of the screening technique, approximately 80% of cases were late stage (III or IV), which led to no reduction in overall mortality (Buys et al., 2011). A further trial carried out in the UK (United Kingdom Collaborative Trial of Ovarian Cancer Screening - UKCTOCS) that enrolled 200,000 post-menopausal women aimed to investigate the effect of early detection using the Risk of Ovarian Cancer Algorithm (ROCA) in ovarian cancer mortality. ROCA uses baseline levels of CA125, serially collected levels, age, menopausal status, and other genetic risk factors. A small

increase in survival, due to annual screening using ROCA, was reported in the study but the results were not statistically significant (Jacobs et al., 2016).

Human epididymis protein 4 (HE4), a surface glycoprotein like CA125, has been reported to be elevated in serous and endometroid tumours, with changes in levels occurring earlier than CA125 (Abbink et al., 2018; Drapkin et al., 2005).

There are currently two FDA approved multivariate index assays, OVA1 and ROMA. OVA1 assay measures multiple serum biomarkers including CA125 and calculates the risk index of ovarian malignancy. As it uses more than one biomarker, it is able to identify higher levels of early stage ovarian cancer and subtypes frequently misdiagnosed due to low levels of CA125 (Dunton et al., 2021; Ueland et al., 2011). ROMA incorporates levels of CA125 and HE4 with menopausal status and carries out a regression model. This was shown to be more sensitive than CA125 serum levels alone at detecting early-stage disease, with higher sensitivity in premenopausal women than postmenopausal, potentially due to postmenopausal women needed to be further subdivided in early and late postmenopausal stages so that better cut-offs for the levels of CA125 and HE4 could be applied (Chan et al., 2013; Moore et al., 2009). These screening and detection issues lead to most patients being diagnosed at late or advanced stage presenting metastasis. Activation of invasion and metastasis, covered in detail in section 1.2, is one of the hallmarks of cancer, associated with higher pathological grades, poor prognosis, and higher mortality (Hanahan and Weinberg, 2011). Therefore, finding therapy targets that can prevent metastasis is fundamental.

First line of treatment for ovarian cancer involves surgery, that depending on woman age and cancer stage, type, and grade, may lead to bilateral or unilateral oophorectomy. If patients are classified with well-differentiated stage I ovarian cancer, after debulking of the macroscopic tumours they will not receive chemotherapy. For all other cases, platinum-based chemotherapy, like cisplatin or carboplatin, is administered post-surgery. In some cases, the use of taxane

agents, like paclitaxel, is also administered as a combination therapy. Improvement in survival has been observed when paclitaxel is incorporated weekly (dose-dense) instead of every 3 weeks together with carboplatin every 3 weeks (Armstrong et al., 2006; Katsumata et al., 2009). Platinum derived chemotherapies lead to cytotoxicity by crosslinking with DNA, forming platinum-DNA adducts recognised by proteins involved in nucleotide excision repair, mismatch repair and high mobility group proteins, leading to apoptosis via a still unclear process hypothesised to be mediated via activation of c-ABL and JNK/SAPK pathway (Kartalou and Essigmann, 2001; Nehmé et al., 1997). Even if platinum-based chemotherapy is effective, 75% of patients will recur, developing resistance to chemotherapy and succumbing to the disease (Agarwal and Kaye, 2003). Over the last decades, PARP inhibitors have been approved by the FDA for use in ovarian cancer management together with bevacizumab, a monoclonal antibody that binds VEGF, as second-line chemotherapy for patients with resistance or BRCA mutations. Emerging therapies are being developed to bridge the gap of demand for novel treatment approaches. For instance, clinical trials for immunotherapy pembrolizumab, durvalumab or rintatolimod have just finished (estimated completion dates 2024 up to late 2025), while small molecule kinase inhibitors and gene therapies are also being considered (Tavares et al., 2024).

Overall, ovarian cancer is the most lethal reproductive cancer for females, refinement of screening techniques and development of more targeted treatments to enhance patient outcome are needed. Therefore, research focusing on understanding the development and progression of the disease may help identify new targets and biomarkers for earlier diagnosis and improved survival.

1.2 Ovarian cancer cell migration and dissemination

Most solid tumour cancers like breast, lung, colon, and liver metastasise via the lymphatic system or blood system following a series of processes, termed the invasion/metastasis cascade.

This involves local invasion, intravasation, survival in the circulation, extravasation, and colonization of distant tissues. On the contrary, ovarian cancer metastasis occurs mostly passively (figure 1.3). The ovary has no anatomical barrier, allowing cancer cells to move freely in the peritoneal cavity once detached from the primary tumour (Motohara, et al., 2019). Ascites formation, a condition which refers to the build-up of fluid in the abdominal cavity, is one of the complications of ovarian cancer. Movement of the ascitic fluid can lead to cells shedding from the primary tumour, either as spheroids including stromal components or single cells. Detached spheroids/cells then float in the ascitic fluid and reach the omentum and peritoneum, the most common metastatic sites, and rarely the liver or lungs (Yeung, et al., 2015). After shedding from the primary tumour, ovarian cancer cells must avoid anoikis, the process by which adherent cells undergo apoptosis when they lose cell-matrix interactions (Hanahan and Weinberg, 2011). It was shown that while floating in ascitic fluid ovarian cancer cells gained anoikis resistance via $\alpha v\beta 3$ integrin activation, which led to decreased caspase-3 activation and increased expression of Bcl-2, resulting in cell survival (Dolinschek et al., 2021). Additionally, it has been shown that amplification of chromosome 1q22, which leads to overexpression of Rab25 in breast and ovarian cancer, is linked to preventing apoptosis and anoikis and increasing proliferation in both anchored and non-anchored cancer cells (Tan et al., 2006). As multiple spheroids can shed from the primary tumour, metastasis to the intraperitoneal cavity occurs rapidly and dissemination occurs in multiple areas (Lengyel, 2010). Previous research and clinical observations have revealed that ovarian cancer cells have a preference for adipose-rich surfaces in the peritoneal cavity, such as the omentum, with approximately 80% of women showing omental metastasis (Schild et al., 2018). Boyden chamber experiments, where ovarian cancer cells were seeded in the top compartment and either adipocytes or conditioned media from adipocytes were placed in the bottom compartment, showed increased ovarian cancer cell migration when adipocytes were present

and an even bigger effect with the conditioned media, suggesting the involvement of a soluble factor. Five cytokines were further identified as abundantly secreted by adipocytes: IL-6, IL-8, MCP-1, TIMP-1, and adiponectin. Addition of inhibitory antibodies against IL-6, IL-8, MCP-1 and TIMP-1 resulted in at least 50% decreased migration of cancer cells towards matrigel plugs containing adipocytes when compared to the absence of antibodies (Nieman et al., 2011). Moreover, it was further investigated if adipocytes provided energy to cancer cells in the form of lipids to sustain metastatic growth. An increase of lipid droplets was observed when ovarian cancer cells were cocultured with adipocytes. Thanks to the use of adipocytes loaded with fluorescently labelled lipids, it was possible to observe that lipids were transferred from adipocytes to cancer cells. It was discovered that ovarian cancer metastatic cells upregulate fatty acid binding protein 4 (FABP4) in comparison to primary tumours. FABP4 is a small fatty acid binding protein that assists in the trafficking of lipids in the cells, functioning as a chaperone during lipolysis, the breakdown of triglycerides to fatty acids and glycerol. When ovarian cancer cells were cocultured with adipocytes, increased in fatty acids release and increased phosphorylation of hormone-sensitive lipase (HSL) were observed, which led to lipolysis. Moreover, when cancer cells were cocultured with adipocytes, they showed increased MAPK phosphorylation, activation of protein kinase A and β-oxidation, all signs of lipid metabolism adaptation for energy production (Nieman et al., 2011; Scheja et al., 1999).

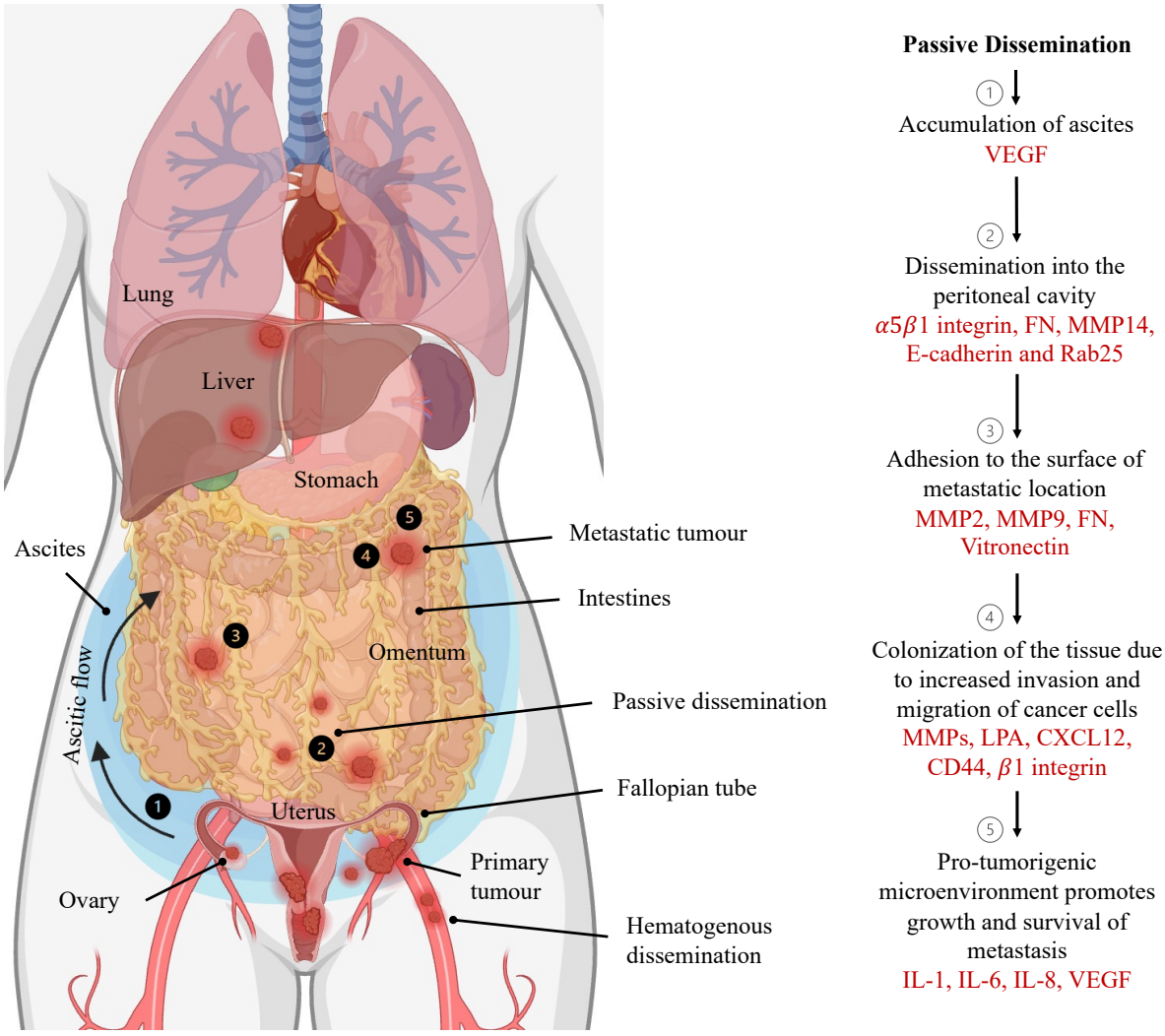

Figure 1.3. ***Ovarian cancer dissemination.*** The illustration shows the process through which ovarian cancer cells migrate and metastasise. Firstly, ascitic fluid builds up. VEGF has been linked to accumulation of ascitic fluid in the abdomen and its inhibition was found to reduce ascites formation in mouse models (1), then cells shed from the primary tumour into the peritoneal cavity. Increase FN and $\alpha5\beta1$ integrin promotes cell detachment from the primary tumour, while MMP14 cleavage of $\alpha3$ integrin decreases adhesion of cancer cells. Loss of E-cadherin leading to activation of epithelial to mesenchymal transition (EMT) and overexpression of Rab25, which supports anchorage-independent proliferation, are also linked to cancer cell shedding from the primary tumour (2), after which cells adhere to the tissue where metastasis will occur. Adhesion to the mesothelial layer of cells that cover the abdominal organs have been shown to be promoted by MMP2 and MMP9, which can cleave collagen and fibronectin located on top of mesothelial cells. Furthermore, FN and vimentin have been shown to promote anchorage via $\alpha5\beta1$ and $\alpha v\beta3$ integrin interactions (3). Once cells have attached, colonization of the tissue occurs. Multiple MMPs have been shown to promote invasion of ovarian cancer cells. Stimulation of cluster of differentiation 44 (CD44) expression in cancer cells by ascites increases binding to hyaluronic acid which in turn promotes adhesion and migration of cancer cells. CXCL12 found on ascitic fluid engages with its receptor CXCR4 located in ovarian cancer cells promoting $\beta1$ integrin expression, which increases migratory potential. Additionally, lysophosphatidic acid (LPA), also upregulated in the ascitic fluid, promotes cancer cell motility by inducing MMP secretion (4). Finally, a pro-tumorigenic microenvironment is achieved to support cancer cell growth and survival in the new tissue. After implantation, inflammation of the tissue results in stromal cell secretion of IL-1, IL-6 and IL-8, which stimulate angiogenesis by increasing ovarian cancer cell secretion of VEGF, leading to new vasculature formation and survival of the metastasis (5). In red some of the factors known to promote the different stages of ovarian cancer progression are listed. Illustration made using BioRender, adapted from (Yeung et al., 2015).

Once the spheroids reach the secondary site, they interact with the mesothelium, a single epithelial cell layer that covers the organs in the peritoneal cavity, before colonization occurs (Yeung, et al., 2015). Early adhesion of the ovarian cancer spheroids to the mesothelium has been found to be mediated by matrix metalloproteinases (MMP), that are upregulated during ovarian cancer progression (Egeblad and Werb, 2002). MT1-MMP (also known as MMP14) was found to cleave mucin 16 from the surface of ovarian cancer cells, which led to enhanced adhesion of cancer cells to the mesothelium in an integrin-dependent manner. It was suggested that mucin 16 initially facilitates weak binding to the mesothelial monolayer via interaction with mesothelin located on peritoneal mesothelial cells, while shedding of the ectodomain via MT1-MMP-mediated cleavage leads to potential exposure of integrin $\beta 1$ which further stabilises the adhesion (Bruney et al., 2014). On the other hand, MMP2 was found to enhance adhesion by cleaving FN and vitronectin into smaller fragments to which cells adhere more strongly (Kenny et al., 2008). Once cancer cells are attached to the mesothelium, they start to proliferate and invade the surrounding tissues. These processes have been found to be promoted by ascitic components, including lysophosphatidic acid, which promotes motility and invasiveness of cancer cells (Fang et al., 2002); CXCL12 binding to CXCR4, which increases $\beta 1$ integrin expression and cancer cell migratory potential (Balkwill, 2004); and increased CD44 expression in cancer cells that binds to hyaluronic acid, increasing migration (Casey and Skubitz, 2000). Finally, the formation of macrometastasis is achieved when ovarian cancer cells implant in secondary tissues. This stimulates the release of cytokines due to inflammation in the tissue, such as interleukin 1, 6 and 8, that in turn lead to increased vascular endothelial growth factor (VEGF) secretion, creating an optimal microenvironment for metastatic growth (Freedman et al., 2004; Stadlmann et al., 2005).

Passive dissemination is not the only way ovarian cancer can metastasise. Pradeep and colleagues have shown that ovarian cancer metastasis can also occur hematogenously by using

a parabiosis model (Pradeep et al., 2014). They excised the skin of female mice and connected their circulation via anastomosis. Successful connection of the circulation was confirmed by injecting dye into one mouse and the appearance of dye in the other. Host mice were injected with ovarian cancer cells in the ovaries to investigate metastatic spread in host and guest mice. Mice were separated 2 weeks after injection and omental metastasis was found after 25 days with no micrometastases present in other organs of the guest mice, confirming that ovarian cancer cells can spread hematogenously having a predilection for the omental tissue (Pradeep et al., 2014).

Altogether, ovarian cancer metastasis occurs mainly via passive dissemination to the peritoneal cavity. Cancer cells shed from the primary tumour, often as spheroids, and if they survive into the ascitic fluid they reach the omentum or peritoneum, where they adhere. Adhesion is facilitated by upregulation of ECM protein, cell surface receptors and MMPs which create a supportive microenvironment for metastasis to occur.

1.3 Importance of the ECM in tumour progression

It has become apparent that cancer is not only the accumulation of genetic mutations. These are necessary, but not sufficient for cancer progression. Instead, cancer is a complex ecosystem, that includes cancer cells, stromal cells, and ECM, figure 1.4. Interactions between these players are fundamental for tumour development, survival and progression (de Visser and Joyce, 2023). The foundation of this theory comes from the "seed and soil hypothesis" described by Paget, where it was suggested that to understand cancer it was not only important to look at the cancer cells, or "seed", but also at their surrounding cells, matrix, nutrients and signals, or "soil"; this is now defined as the tumour microenvironment (TME) (Paget, 1889).

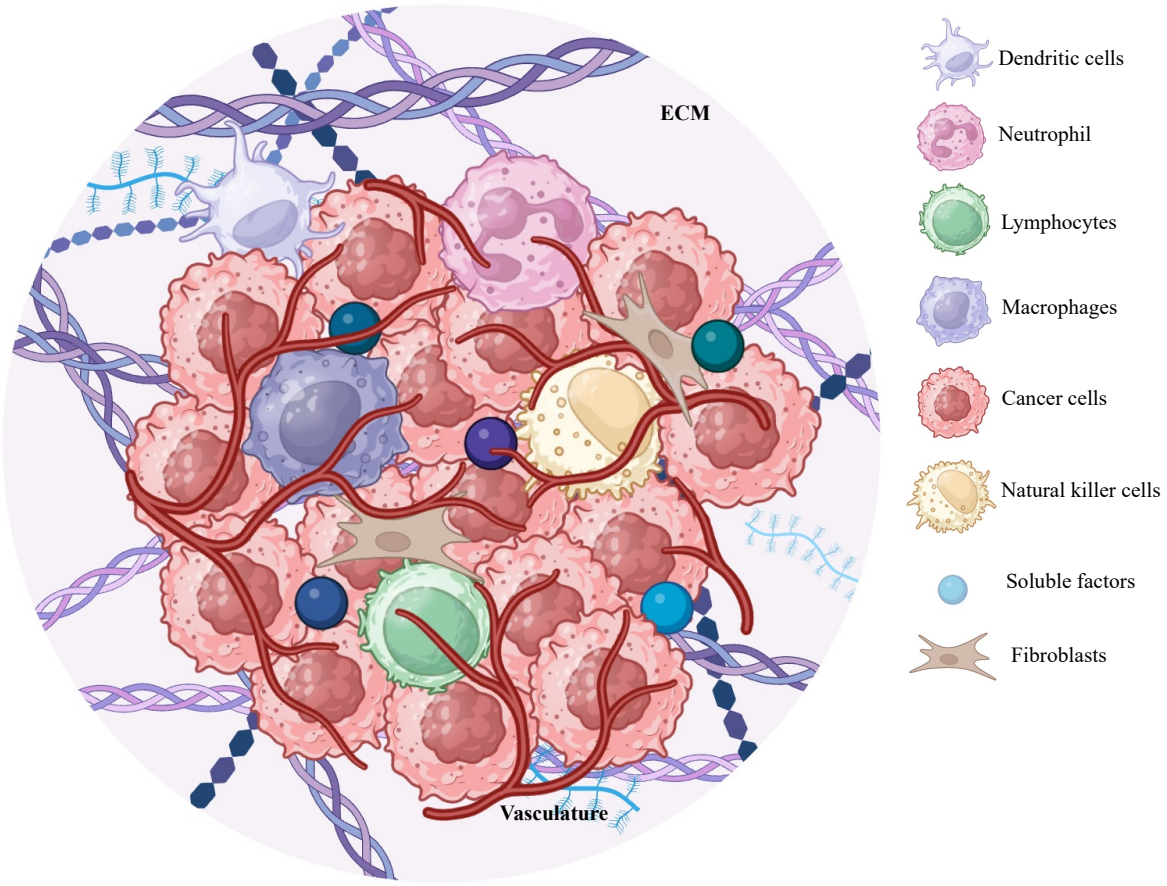

Figure 1.4. ***Tumour microenvironment.*** The illustration shows the main components of the tumour microenvironment, including cancer cells, different types of stromal cells, the ECM and vasculature. Image made using Biorender.

The TME composition varies between tumour types and subtypes, showing heterogeneity from patient to patient. However, some core factors are always present, like tumour cells, vasculature, cancer-associated stomal cells, immune cells, ECM, and secreted factors (Bharadwaj and Mandal, 2024). The interactions between the different cell types and the ECM lead to a complex and dynamic signalling network, which has been found to promote several hallmarks of cancer, such as angiogenesis (Watnick, 2012), metastasis (Neophytou et al., 2021) and drug resistance (Salemme et al., 2023).

The ECM is a non-cellular component essential for the maintenance of tissue homeostasis, as it promotes cell-cell communication, adhesion and proliferation (Frantz et al., 2010). During cancer development and progression, the ECM is dysregulated and undergoes continuous remodelling, giving rise to biochemical and biophysical cues that influence cell adhesion and

migration (Walker et al., 2018). Mass spectrometry approaches were used to clarify matrix composition in tumours. 1056 genes were found to be linked to the matrisome, by combining in silico prediction with proteomic analysis; of these 278 were defined as core matrisome genes, encoding for 200 glycoproteins (including FN, laminins and tenascins), 35 proteoglycans and 43 collagens, while 778 genes were considered matrisome-associated genes, which included secreted factors (such as growth factors and cytokines), ECM regulators (including MMPs, ADAM, LOX) and ECM-affiliated (like semaphorins and mucin) (Naba et al., 2012).

1.3.1 ECM proteins in ovarian cancer TME

In ovarian cancer several ECM proteins have been found dysregulated, contributing to primary tumour growth, survival in ascitic fluid and metastasis (Brown et al., 2023). There are two main types of ECM: basement membrane (BM) and interstitial matrix (IM). The BM is secreted mostly by epithelial or endothelial cells, it is located beneath them separating them from the IM, and it is mainly formed by non-fibrillar collagen IV, laminin, nidogens and perlecan. On the other hand, the IM, located in the lamina propria, is mainly secreted by mesenchymal cells, and is composed of fibrillar collagens I and III, fibronectin, elastin, decorin and hyaluronic acid (Pompili et al., 2021). During ovarian cancer peritoneal metastasis, ovarian cancer cells interact with both the BM and IM proteins of the pelvis and abdomen. In this section, I will discuss the major components of ovarian cancer ECM.

a. Collagens

Collagens are the most abundant ECM protein, comprising 28 different types that can be categorised into three major groups: fibrillar, non-fibrillar and fibril-associated (Ricard-Blum, 2011), with fibrillar collagens being the predominant group.

Collagens are formed by three polypeptide, α, chains of different sizes (from 662 to 3152 amino acids) that form homo- or heterodimers (Ricard-Blum et al., 2005). The three α chains arrange

by forming a right-handed triple helix that is stabilised by the presence of glycine, located at every third residue, resulting in the formation of a triple helix comprised of Gly-X-Y repeats (Persikov et al., 2005). The X and Y locations are mainly prolines and 4-hydoxyprolines but their composition is variable (Weis et al., 2010).

Collagen is synthetised as procollagen (figure1.5). Firstly, pro-α chains undergo multiple post-transitional modifications in the ER, resulting in the formation of the triple helix facilitated by heat shock protein 47 (Sauk et al., 2005). Further modifications, like hydroxylation, are added to the pro-collagen before it is transported to the Golgi apparatus, where final modifications occur before being assembled into secretory vesicles (Wu et al., 2025). Once in the extracellular space, the N-terminus is cleaved by a disintegrin and metalloproteinase with thrombospondin motifs 2 (ADAMTS2), except for the N-terminus of the pro- $\alpha 1$ V chain that is cleaved by bone morphogenic protein 1 (BMP-1). BMP-1 also cleaves the C-terminus of the pro-peptides, resulting in a functional collagen molecule (Hopkins et al., 2007).

Collagens can be divided in subfamilies depending on the supramolecular assembly into fibrils, beaded filaments or anchoring fibrils (fibril-associated collagens with interrupted triple-helices - FACIT) and networks (Ricard-Blum, 2011). Lysyl-oxidase (LOX) mediates the assembly of collagen into fibrils, by crosslinking the telopeptides that are left exposed after the removal of the pro-peptides. The obtained fibrils are heterotypic in nature formed by 3 components; a major fibrillar collagen (collagen I or II), a minor fibrillar collagen (collagen V or XI), and a FACIT (collagen IX, XII or XIV) (Revell et al., 2021).

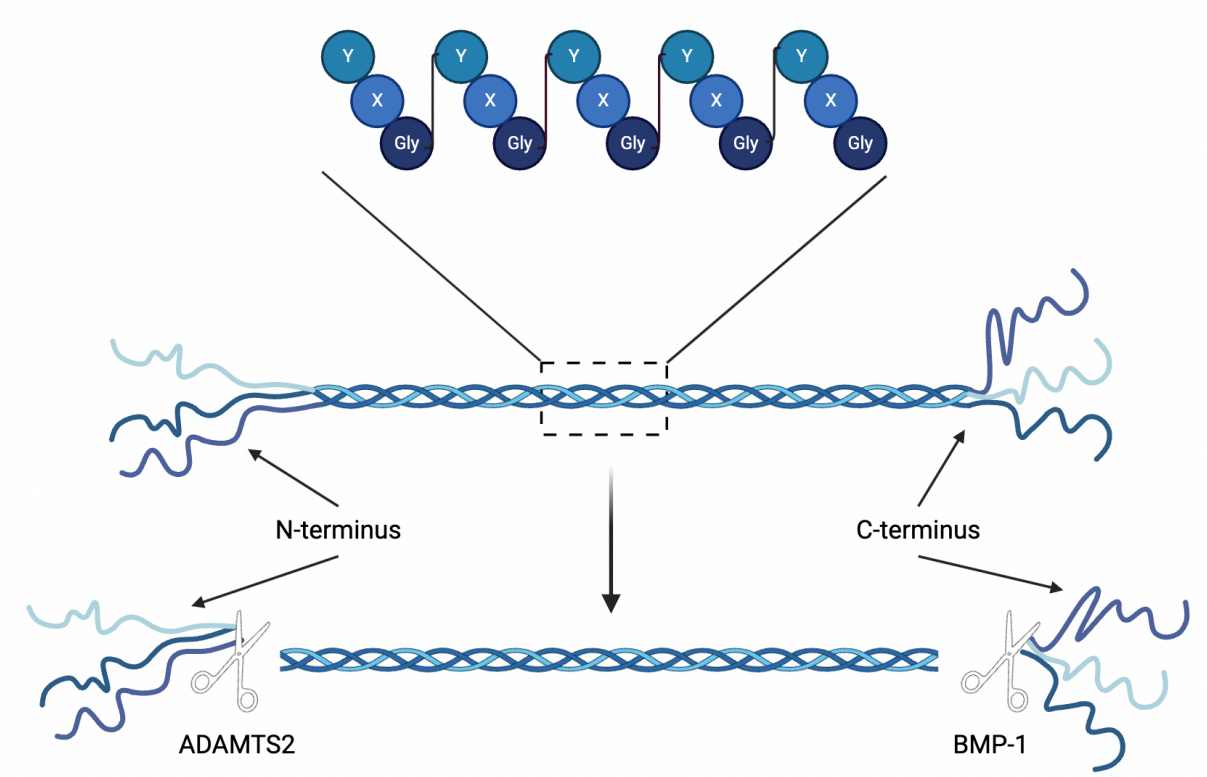

Figure 1.5. ***Collagen structure.*** Collagen chains are formed by Gly-X-Y repeats, where X and Y mostly represent proline and 4-nhydroxyproline, respectively. Three alpha chains form the procollagen triple helix structure. The N- and C-terminus domains are cleaved by ADAMTS2 and BMP-1 respectively, giving rise to mature collagen. Image made using Biorender.

In the normal ovarian tissue, collagen fibrils are thin, long, and wavy, running parallel to the epithelial boundary, while during cancer development the fibrils become short and thick running in a perpendicular direction to the boundary. The formation of these collagen tracks is known as tumour-associated collagen signature, linked to loss of elasticity and increase in stiffness (Adur et al., 2014). Increased collagen deposition by CAFs and tumour-associated macrophages is observed in multiple cancers (Xu et al., 2019); for instance, in breast cancer it has been linked to increased invasiveness and tumour progression (Provenzano et al., 2006). In ovarian cancer, collagen I has been linked to increased adhesion and migration of different ovarian cancer cell lines (Shen et al., 2012) and spheroids (Burleson et al., 2004) and to paclitaxel resistance (Gurler et al., 2015). Collagen VI has been shown to increase chemoresistance to cisplatin (Sherman-Baust et al., 2003), while collagen XI has been correlated to high stages of disease and poor survival, it has been identified as a recurrence

predictor, it was found elevated in metastasis and it can be considered a biomarker for platinum-resistance (Cheon et al., 2014; Teng et al., 2014; Wu et al., 2014).

b. Laminins

Laminins are the second major component of the BM after collagen IV. There are twelve different mammalian laminin heterodimers formed by the assembly of three disulphide-linked polypeptides, α, β and γ chains, into the shape of an asymmetrical cross (Colognato and Yurchenco, 2000). The N-terminus of laminins normally interact with other BM molecules, helping in the assembly and stability of the BM, while the C-terminus interacts with cell surface receptors mediating signalling between the cells and the ECM, this allows cells to mediate adhesion, migration and survival by regulating apoptosis among other functions, figure 1.6 (Aumailley, 2013). In ovarian cancer laminin delimits the area between epithelial cells and the stroma. This is found disrupted in proximity to areas with invading cells, during early stages of invasion (Campo et al., 1992). This work did not specify which specific laminin heterodimer was studied. During later stages of ovarian cancer, high levels of laminin are found in ascitic fluid which could be linked with metastasis promotion. Due to the type of antibodies used, authors could not determine if the change was observed in whole laminin or fragments (Byers et al., 1995). Moreover, it was suggested that ovarian cancer cells may produce laminin at later stage of metastasis to promote migration and invasion by binding to cell surface receptors that are also dysregulated during cancer progression, such as integrins and CD44. Injection of ovarian cancer cells in mouse ovaries together with laminin-111 was found to be linked to bigger tumours and more ascites production when compared to cancer cells co-injected with gelatine. Moreover, laminin-111 and its peptides led to increased cell adhesion and increase in survival gene expression in vivo (Yoshida et al., 2001). Moreover, laminin-511 secreted in exosomes by ovarian cancer cells was found to be taken up by omental macrophages, leading to a pro-tumoral phenotype (H. Li et al., 2022). On the contrary, laminin subunit α3 gene

(LAMA3) expression was found to be lower in carcinoma tissue when compared to normal, potentially due to DNA methylation. Low LAMA3 expression was linked to lower recurrence-free survival and overall survival when compared to high LAMA3 expression (Tang et al., 2019), potentially functioning as a tumour suppressor.

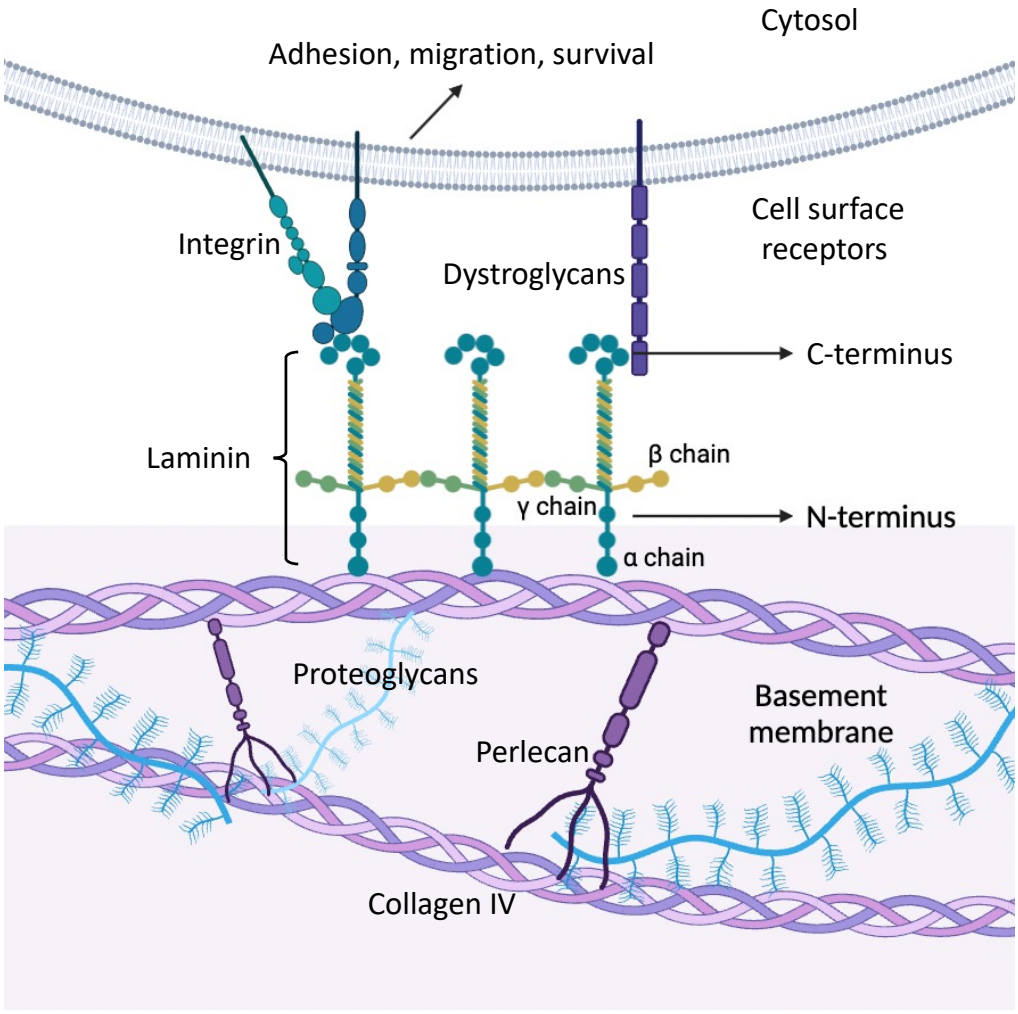

Figure 1.6. ***Laminin structure and function.*** Laminins are composed of three polypeptide chains, α, β and χ. Laminin binds to cell surface receptors, such as integrins and dystroglycans, via the C-terminus and to the BM via the N-terminus; this triggers downstream signalling pathways mediating adhesion, migration, survival and preventing apoptosis. Image made using Biorender.

c. Fibronectin

Fibronectin (FN) is a glycoprotein that mediates cell-ECM interaction during development (George et al., 1993). FN interacts with other ECM proteins, cell surface receptors, glycosaminoglycans and other FN molecules (Hynes and Yamada, 1982). FN exists as a dimer linked via a pair of antiparallel disulphide bonds at the C terminus. Each monomer is composed

of repeating units, including twelve type I, two type II and fifteen to seventeen type III motifs, forming a modular protein (Zollinger and Smith, 2017). FN adopts a compact conformation where the type III^{2-4} of one subunit covalently interacts with the type III^{12-14} from the other, folding on itself (Lemmon et al., 2011). This conformation is a soluble form that is then assembled by cells into a insoluble fibrillar network, that is incorporated in the ECM (Hynes, 1990). This assembly occurs as a multistep process. Adherent cells interact with the soluble FN dimer via integrins located in focal adhesions. FN/integrin binding unfolds the FN molecule into a linear structure that, by stretching the domains, allows further FN binding, leading to the formation of a network in an irreversible manner (Morla and Ruoslahti, 1992), figure 1.7. FN has been shown to promote cell growth, migration and differentiation during wound healing, embryonic development and tumorigenesis (To and Midwood, 2011).

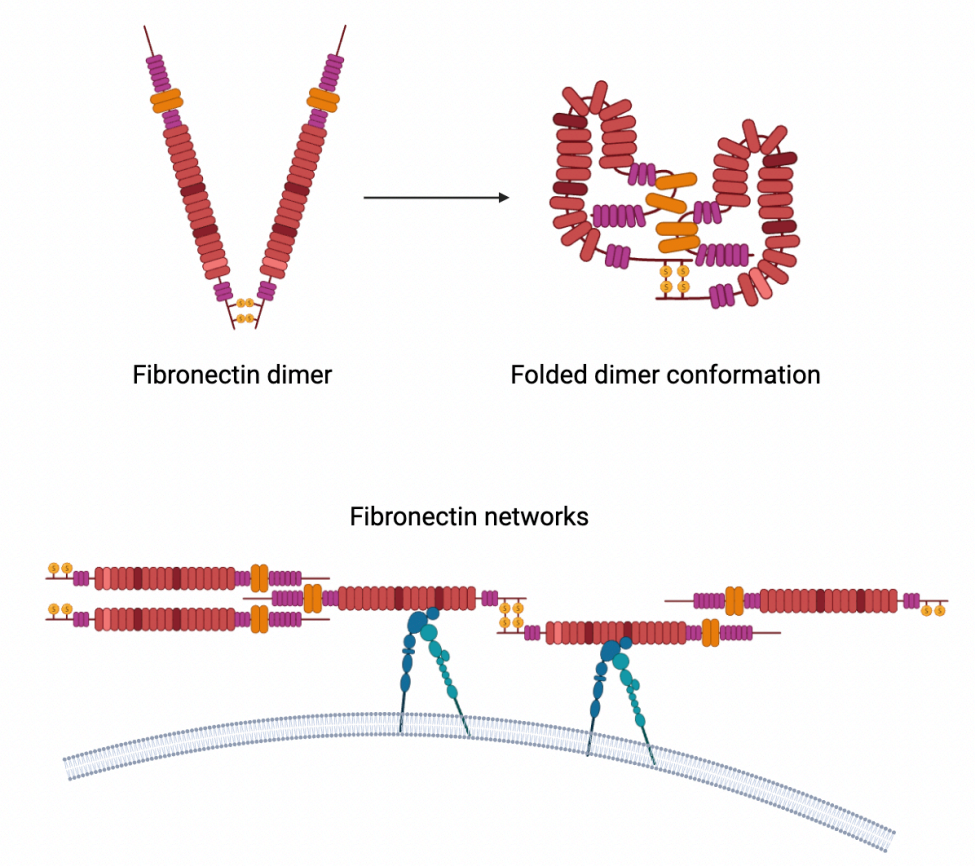

Figure 1.7. ***Fibronectin assembly.*** Fibronectin dimers interact via disulfuric bonds and are further folded via ionic interactions. Once FN bind to cell surface receptors of the integrin family, the dimer undergoes a conformational change becoming linear where other FN molecules can anchor. Image made using Biorender.

In ovarian cancer FN is an indicator of poor prognosis, that has been shown to promote cancer cell migration and invasion. Its expression was found elevated in omental metastasis and ascites (Franke et al., 2003; Kenny et al., 2008; Lou et al., 2013; Wilhelm et al., n.d.). Higher FN expression is found in patients with higher FIGO stages (stage III and IV) when compared to lower FIGO stages (stage I and II) (Bao et al., 2021). Moreover, it was also shown to promote migration of ovarian cancer cells in an $\alpha 5\beta 1$ integrin dependent manner (Caswell et al., 2007). FN also promotes adhesion and migration of ovarian cancer spheroids to the peritoneum during early metastatic events. FN expression and secretion is induced in mesothelial cells by ovarian cancer cell interacting in a transforming growth factor beta (TGF- β)/RAC1 signalling-dependent manner (Kenny et al., 2014; Rieppi et al., 1999). Indeed, knock down of FN in mesothelial cells reduced cancer cell proliferation and migration. In vivo models confirmed the need for FN during omental metastasis, as mice with FN deficiency developed less metastasis post ovarian cancer cell injection (Kenny et al., 2014).

d. Proteoglycans

All ECM contains proteoglycans at different concentrations, for example they are the major component of the cartilage matrix. They were firstly identified in the ECM, where they can vary in form and function, from the small leucine-rich decorin to the big aggrecan (Aspberg, 2012; Reed and Iozzo, 2002). Proteoglycans can also be located on the cell surface, mostly as transmembrane proteins, such as syndecans and CD44; while others, like glypicans, are anchored to the outer face of the plasma membrane via glycosylphosphatidylinositol (Dick et al., 2012). Serglycin is the only proteoglycan known to be located intracellularly in mast cell granules and endothelial cells, where it is thought to regulate the secretion of the chemokine CXCL1 (Meen et al., 2011), figure 1.8. Finally, a few proteoglycans, including syndecan and glypicans, have been reported in the nucleus, but this remains controversial, as is not clear how proteoglycans are transported into the nuclei, due to their size. It has been suggested that

syndecans could be cleaved by MMPs, and syndecan fragments could be transported to the nucleus (Couchman and Pataki, 2012; Richardson et al., 2001). Proteoglycans are a complex macromolecule with a protein core, containing functional domains that can affect cell-matrix dynamics, and one or more glycosaminoglycan (GAG) chains that contains alternating units of hexosamine acid, hexuronic acid or galactose, contributing to the heterogeneity of the proteoglycan family (Karamanos et al., 2018). The type of GAG chain attached to the protein core is determined by the core protein structure, the linker tetrasaccharide that extends from the anchor site modifications, and the Golgi apparatus biochemical environment (Prydz, 2015).

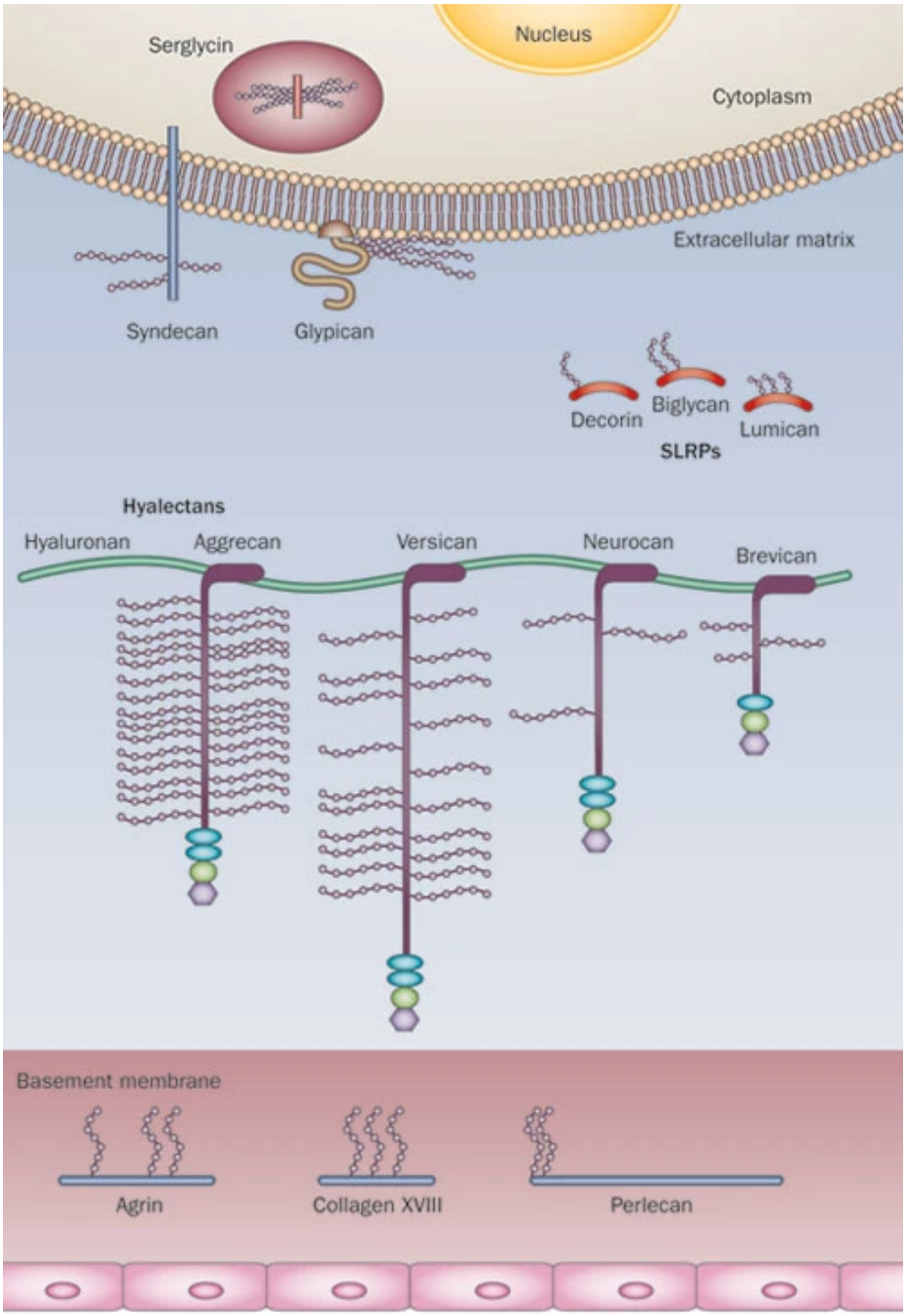

Figure 1.8. ***Proteoglycans family members.*** Extracellular matrix proteoglycans, such as versican, aggrecan and neurocan, are shown linked to hyaluronic acid; cell surface proteoglycans, like syndecan and glypican are located at the plasma membrane by their transmembrane domain or via glycosylphosphatidylinositol. Serglycin is located intracellularly in vesicles. Image from (Edwards, 2012).

In normal tissues, proteoglycans provide hydration and compressive resistance (Hynes and Naba, 2012), while during ovarian cancer they have been found associated with multiple processes. Decorin loss of expression in ovarian cancer ECM is linked to cancer progression (Nash et al., 2002). Another small leucine-rich repeat proteoglycan, lumican, was also found

to be reduced in the ovarian cancer stroma, but no link with cancer progression was established (Amankwah et al., 2011). Loss of perlecan expression in the BM correlated to higher invasion, as staining was absent at the invasive front of tumours in patient samples, but it was retained close to new vasculature (Davies et al., 2004). Hyaluronic acid high levels correlates with higher tumour grades and metastasis, as it is known to promote cancer cells adhesion to the peritoneum (Casey and Skubitz, 2000; Catterall et al., 1999; Hiltunen et al., 2002). Moreover, it has been linked to reduction of carboplatin chemotherapy efficiency. Carboplatin has been shown to increase production of hyaluronic acid, which leads to increased ABC transporter expression, which transport different substances out of the cells including drugs, that in turn induce chemotherapy resistance (Ricciardelli et al., 2013). Versican is also found elevated in many malignant tumours. In ovarian cancer, increase levels of versican in the stroma correlated with increase in hyaluronic acid. Moreover versican is known to interact with hyaluronan acid and CD44, cell surface receptor for hyaluronan acid, which is potentially linked to promoting cancer progression (Ghosh et al., 2010; Voutilainen et al., 2003; Ween et al., 2011). Versican overexpression was linked to increased microvessel density, invasion potential and poorer overall and progression-free survival in ovarian cancer patients (Ghosh et al., 2010). Furthermore, it facilitates adhesion of ovarian cancer cells and spheroids to the mesothelial monolayer as it promotes disaggregation and cell migration. This suggests that versican might drive metastasis, as reduction in its expression impaired the ability of cancer cells to generate peritoneal metastasis *in vivo* (Desjardins et al., 2014).

1.3.2 ECM degradation and remodelling

The ECM is constantly being deposited, degraded, and remodelled to maintain tissue homeostasis (Walker et al., 2018). During tumour progression, normal tissue homeostasis is lost. A highly aligned, anisotropic, and organised ECM is a sign of desmoplasia, as normal ECM has a random isotropic arrangement of fibres. This ECM alignment serves as trails for

cancer cells to migrate (Provenzano et al., 2006). Importantly, biochemical and biophysical cues are also released while the ECM is actively remodelled, as it serves as a reservoir of growth factors and bioactive molecules, further influencing adhesion and migration of cells (Geiger and Yamada, 2011). As changes occur during tumour progression, an increased secretion of fibronectin, collagen I, III and IV, and cancer type-specific ECM proteins, such as increased expression of hyaluronan acid in pancreatic cancer or chondroitin sulphate proteoglycan in glioblastomas, occurs thanks to cross-communication between the ECM and tumour cells (Malik et al., 2015). The changes in ECM composition between cancer types can be used as prognostic biomarkers (Cirri and Chiarugi, 2011), such as laminin $\beta 3$ chain expression, which was identified as a poor prognostic factor in colorectal cancer and hyaluronan acid accumulation in the tumour is linked to poor prognosis in pancreatic cancer (M.-S. Kim et al., 2021; Sato et al., 2016).

For cancer cells to invade and migrate, they need to breach though the BM, which normally functions as a physical barrier to cell migration. This is why cancer cells that need to become motile adopt different migratory behaviours to move through the ECM barrier (Kelley et al., 2014). One way in which cancer cells can breach through the BM is mediated by the build-up of mechanical force. As cancer cells proliferate, they are spatially constricted by the BM. This results in an increase in the mechanical stress that may lead to BM rupture (Chang and Chaudhuri, 2019). Another method is mediated by protrusive invadopodia, actin rich protrusions of the plasma membrane on the basal surface of cells, into the BM, creating a breach in the membrane that allows the cell to squeeze in the gap as it widens (Walker et al., 2018). Evidence has found high levels of matrix degrading enzymes at the breaching sites. Interestingly, optical highlighting and landmark photobleaching experiments has shown that gap formation is not correlated with degradation of the matrix. All together it suggests that degradation of the matrix is only partial and laminin and collagen IV are also pushed to the

side by invadopodia, suggesting the involvement of multiple factors during cancer cell invasion (Kelley et al., 2014; Morrissey et al., 2013).

1.3.2.1 Stromal cells in ECM remodelling: cancer associated fibroblasts and cancer associated mesothelial cells

Fibroblasts secrete most of the components of the ECM, moreover they also secrete MMPs, which degrade ECM, and their counterparts tissue inhibitors of metalloproteinases (TIMPs), helping to maintain normal ECM turnover (Kalluri and Zeisberg, 2006). During cancer progression, fibroblasts and other stromal cells become activated, similarly to activation during wound healing processes, and together with cancer cells they can regulate matrix alignment (Cukierman and Bassi, 2010). Cancer-associated fibroblasts (CAFs) can be activated by various mechanisms, including inflammatory cues, changes in ECM stiffness or composition, and metabolite secretion by cancer cells (Kalluri and Zeisberg, 2006). A well-known regulator of CAF activation is TGFβ, that has been established to promote the activation of SMAD transcription factors. This drives the expression of α-smooth muscle actin (αSMA), increasing contractility of the cytoskeleton and promoting ECM remodelling. In addition, stimulation with IL-1, IL-6 and TNFα can also lead to CAF activation while loss of Notch signalling can promote CAF phenotype in some cancer types (Sahai et al., 2020). CAFs can be classified into three main groups based on their genetic and epigenetic profile, although more subtypes have been identified in the tumour stoma in a cancer type-dependent manner (de Visser and Joyce, 2023): inflammatory (iCAF), myofibroblastic (myCAF) and antigen presenting CAF (apCAF). iCAF are linked to metastasis, angiogenesis and immunosuppression and have been shown to be induced by TNFα and IL-1α; myCAFs have been shown to promote matrix deposition, migration, invasion and metastasis, they are characterised by high αSMA expression; finally, apCAF are linked to immunosuppression (Louault et al., 2020). CAF heterogeneity could be due to the diverse cell precursors. CAFs mainly derive from fibroblasts or pericytes located

close to the tumour, but they can also derive from; 1) mesenchymal stem cells located in the bone marrow, 2) epithelial or mesenchymal cells that have undergone EMT or 3) endothelial cells (Cirri and Chiarugi, 2011).

CAFs have been shown to promote cancer cell proliferation in multiple cancer types, by releasing hepatocyte growth factor (HGF), epidermal growth factor and cytokines. For example HGF secreted by CAFs has been shown to increase proliferation of lung cancer cells via activation of c-Met receptor which led to activation of PI3K/Akt (protein kinase B) in cancer cells (Yao et al., 2024). Similarly, CAF-derived HGF increased proliferation and drug resistance of ovarian cancer cells by the activation of c-Met signalling pathway (Deying et al., 2017). Moreover, CAFs secrete several proteases which mediate the degradation of the ECM and cleavage of growth factors, leading to tumour expansion, invasion and angiogenesis (Roy et al., 2009). Beside this, CAFs have also been shown to promote angiogenesis, via the expression of connective tissue growth factor, resulting in the formation of micro-vessels. Additionally the secretion of MMP9 and MMP13 by CAFs indirectly activate VEGF by releasing it from the ECM (Joshi et al., 2021). In addition to primary tumour growth, CAFs have been linked to invasion and distant metastasis by accelerating the process of EMT. CAFs were found to regulate EMT via regulation of β-catenin mediated by cytokine secretion and extracellular vesicles (Liu et al., 2024). For example, CXCL12 secreted by CAFs activates β-catenin signalling in tumour cells, which in turn leads to the expression of genes promoting EMT. Moreover, microRNA from CAFs have been shown to downregulate PTEN expression and activate β-catenin and PI3K/Akt signalling in bladder cancer, further promoting EMT (Shan et al., 2021). EMT can also be activated by CAFs in an β-catenin independent manner, as it was shown that loss of caveolin-1 in CAFs led to increase in the migration and invasion ability of breast cancer cells, via the secretion of TGFβ and activation of TGFβRII receptors in breast cancer cells (Huang et al., 2022). Finally, CAFs were also found to facilitate cancer

progression by inducing inflammation in tumours, recruiting macrophages, neutrophils and lymphocytes to the tumour stroma, resulting in the formation of a pro-tumorigenic TME and facilitating tumour progression (Chiarugi, 2013).

In ovarian cancer, CAFs have been shown to promote tumour growth, proliferation, and metastasis via the activation of EGFR/Extracellular signal-regulated kinase (ERK)/Akt pathways in cancer cells (Zhang et al., 2022). Moreover, it was found that co-culturing fibroblasts with ovarian cancer cells led to increased motility of the cancer cells in a TGFβ dependent manner. Furthermore, in fibroblasts co-cultures with ovarian cancer cells, higher levels of versican were observed compared to fibroblast only cultures. This process was found to be dependent on TGFβ secreted by cancer cells, as it was prevented in the presence of a TGFβ neutralising antibody. The CAF-mediated versican upregulation then promoted ovarian cancer cell motility by activating NFκB signalling pathway and expression of CD44 and MMP9 in cancer cells (Yeung et al., 2013).

One of the major causes of death in ovarian cancer is recurrence, due to metastasis and resistance to chemotherapy. In these processes, cancer associated mesothelial cells (CAMCs) in the ovarian cancer TME play an important role.

Mesothelial cells from a monolayer that lines the organs of the abdominal cavity, including the omentum and small intestines, and are the primary barrier to ovarian cancer dissemination. Similar to fibroblasts, when mesothelial cells become activated, they undergo morphological changes, with increase in αSMA and vimentin expression, fibronectin secretion, and reduction of E-cadherin, which in turn leads to EMT (Lv et al., 2011). CAMCs have been found to promote adhesion and invasion of ovarian cancer cells to the peritoneum by increasing secretion of IL-8 and CCL2 (Zheng et al., 2022). Moreover, CAMCs have been shown to secrete hyaluronic acid, which binds to the CD44 receptor highly expressed on the ovarian cancer cell surface, which was shown to promote adhesion the mesothelium (Casey et al., 2003;

Gardner et al., 1996; Jones et al., 1995). CAMCs can further facilitate metastasis by secreting VEGF, in response to TGFβ secreted from ovarian cancer cells, which acts on epithelial cells boosting their migratory potential and vasculature formation abilities of human umbilical venous endothelial cells (Fujikake et al., 2018). TGFβ, secreted form ovarian cancer cells, further activates RAC1/SMAD3 pathway via binding to the TGFβRI in CAMCs, which induces the upregulation of fibronectin expression. This has been shown to support adhesion and migration of ovarian cancer cells expressing $\alpha 5\beta 1$ integrin to fibronectin deposited on CAMCs (Kenny et al., 2014).

1.3.2.2 Matrix degrading enzymes

For tumour invasion to succeed, infiltration, dissemination, and substitution of normal tissue by tumorigenic tissue is needed. To support these processes, degradation of the ECM and formation of new tumour supporting ECM that aids the growing tumour mass need to be achieved (Madsen and Bugge, 2015). This is mediated by the secretion of matrix degrading enzymes. In this section I will discuss MMPs, ADAMs and ADAMTSs, together denominated the metzincin protease superfamily, as they have a methionine residue next to the zinc-dependent metalloproteinase active site (Kelwick et al., 2015).

a. Matrix metalloproteases (MMPs)

MMPs are a family of 24 zinc-dependent endopeptidases that play crucial roles in various physiological processes, such as embryonic development, tissue remodelling, and wound healing, as well as in pathological conditions like cancer, arthritis, and cardiovascular diseases (Birkedal-Hansen et al., 1993; Sekhon, 2010). They are capable of degrading a diverse array of ECM proteins, including collagens, elastin, and gelatine (Zitka et al., 2010). Depending on their structure, function, and cellular localization, they can be grouped in eight subcategories. From the N-terminus to the C-terminus, MMPs typically consist of a pro-peptide, a catalytic

domain, a linker peptide or hinge region and a hemopexin domain (Cui et al., 2017). MMPs are synthesised as inactive proenzymes, which once in the ECM, or on the cell surface in some cases, need to be activated. Most MMPs are activated by furin cleavage of the RXKR or RRKR sequence located between the pro-domain and the catalytic domain (Ra and Parks, 2007). Activation of MMPs can also occur via furin-independent mechanisms, including cleavage by other MMPs, such as pro-MMP2 that is cleaved by MMP14 (Ra and Parks, 2007). To ensure that ECM turnover is tightly regulated, MMPs are inhibited by α_2-macroglobulin or TIMPs. α_2-macroglobulin sequesters the enzyme while TIMPs chelate the catalytic zinc atom with their N-terminal domain (Löffek et al., 2011).

In cancer, MMPs have been found commonly overexpressed both by cancer cells and stromal cells, promoting ECM degradation and growth factor release (Deryugina and Quigley, 2006) and being implicated in different stages of tumour progression and metastasis (figure 1.9). Invasion and intravasation (figure 1.9-1) were found to be promoted by MMP-1, -2, -3, -7, and -14. MMP-1 secreted from CAFs was found to cleave PAR-1 which drove cancer cell migration and invasion in an *in vivo* mouse xenograft model of breast cancer (Boire et al., 2005). PAR-1 is a G-protein-coupled receptor that when cleaved can activate proinflammatory and proliferative signalling, including IL-8. MMP-2 and MMP-14 were known to release TGF-β from the ECM, that can then stimulate cancer cell invasion, migration, immune responses and proliferation (Kessenbrock et al., 2010). MMP-3 overexpression leads to cleavage of E-cadherin, which in turn promotes EMT, leading to migration of premalignant mammary epithelial cells (Lochter et al., 1997). Multiple MMPs are associated with cancer spread, MMP-2 and 3 with lymph node metastasis and vascular invasion in oesophageal squamous cell carcinoma (Shima et al., 1992), MMP-11 is linked to increased local invasiveness in head and neck cancer (Muller et al., 1993) while MMP13 correlates with increased metastatic capacity in head and neck, and vulvar squamous cell carcinoma (Johansson et al., 1999, 1997). MMPs

also promote tumour growth by stimulating angiogenesis (figure 1.9-2); for example, MMP-1 promotes the expression of VEGF receptor 2 by stimulation of MAPK and activation of nuclear factor kappa-B (NFκB) which leads to the promotion of endothelial cells proliferation (Quintero-Fabián et al., 2019). MMP-9 is known to control angiogenesis by regulating availability of VEGF. In pancreatic cancer, it was found that infiltrating cells expressed MMP-9 which cleaved ECM-bound VEGF improving availability for its receptor in pancreatic islet cells (Bergers et al., 2000). On the contrary, MMPs can also inhibit angiogenesis. MMP-2, -9 and -12 have been shown to produce angiostatin by degrading plasminogen, which has been found to inhibit human microvascular endothelial cells proliferation and differentiation *in vitro* (Cornelius et al., 1998). Tumstatin is a fragment produced from the cleavage of plasminogen by MMP-9, which has been identified as a suppressor of vasculature formation. Indeed, MMP-9 deficient mice showed increased tumour growth as they had reduced levels of tumstatin in blood (Hamano et al., 2003). Moreover, inflammation of the tumour microenvironment can be regulated by MMPs (figure 1.9-3). TNF-α, a known proinflammatory cytokine, is expressed as a membrane-bound precursor. The removal of its prodomain is mediated by ADAM-17 and MMPs, such as MMP-1, -2, -3, 9 and -12. Secretion of TNF-α by macrophages, natural killer cells and T-cells, leading to TNF-α receptors, TNFR1 and TNFR2, activation on cancer cells induces tumour cell death and tumour-associated endothelial cell death, which increases vasculature permeability due to disruption of the vasculature, increasing immune cell infiltration into the tumour (Alim et al., 2024). MMP-7 was found to indirectly regulate neutrophil infiltration by cleaving syndecan-1 (SDC1) from cell surfaces. SDC1 is known to form complexes with CXCL1, which once released by MMP-7 cleavage leads to the formation of a gradient attracting neutrophils (Li et al., 2002). Similarly, MMP-9 cleavage of CXCL8/interleukin-8 complex leads to increased chemotaxis gradients, which attract neutrophils (Van den Steen et al., 2000). Finally, MMPs can support the formation of metastatic

niches (figure 1.9-4). MMP-9 ability to release VEGF and Kit ligand from the ECM promoting angiogenesis has been linked to the formation of the metastatic niche which recruits stem cells and progenitors cells from the bone marrow to metastatic sites that are tumour-type specific, as injection of Lewis lung carcinoma cells lead to metastasis in lung and liver and melanoma cells disseminated more widely in mice models (Kaplan et al., 2005). In addition, MMP-1 correlates with poor prognosis in colorectal and oesophageal carcinomas (Reunanen and Kähäri, 2013), MMP-1, -2 and -9 serum levels correlate with poor prognosis in breast cancer (Kwon, 2023), while MMP-7 serum levels correlates with bladder cancer poor prognosis (Szarvas et al., 2014). In ovarian cancer, increased expression of MMP-9 was found to corelate with poor prognosis (Sillanpää et al., 2006).

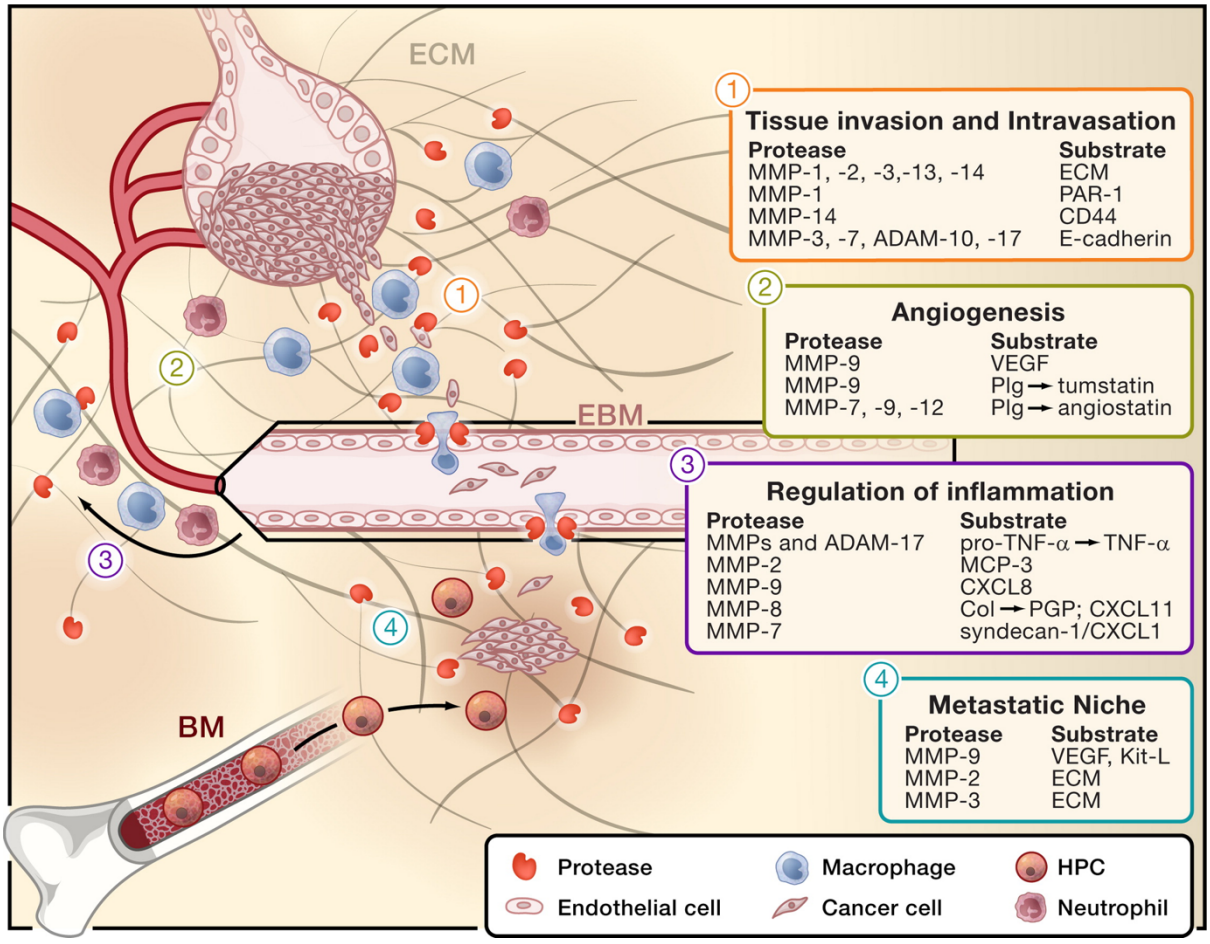

Figure 1.9. ***MMP functions in the TME.*** The illustration shows the different roles of MMP in tumour progression and their substrates. Image from (Kessenbrock et al., 2010).

In ovarian cancer, MMP-2 and MMP-9 are associated with tumour aggressiveness (Brun et al., 2008), invasion (Moser et al., 1994) and promotion of metastasis (Schmalfeldt et al., 2001). Furthermore, MMP-7 overexpression was linked to promotion of invasion and migration (Wang et al., 2005; Zhao et al., 2012). Additionally, MMP-7 has been shown to be elevated in 80% of malignant ovarian cancers compared to 40% borderline and normal samples (Al-Alem and Curry, 2015), but controversially, high expression was also found to correlate with better 10-year disease free survival (Sillanpää et al., 2006), leaving the role of this enzyme uncertain. MMP-8 expression levels were identified to correlate with tumour grade, tumour stage and poor prognosis. Furthermore, its production was upregulated in response to interlukin-1 beta potentially promoting an invasive phenotype. MMP-8 was found to correlate with tumour progression in a study that examined 302 patients with different types of ovarian cancer (Stadlmann et al., 2003). Stratification of patients into short survival and long survival population showed that MMP-13 expression in ascitic fluid correlated with decreased overall survival (Hantke et al., 2003)

b. A disintegrin and metalloproteases (ADAMs)

ADAMs are a family of 21 metalloendopeptidase proteins, which cleave membrane protein extracellular domains. Unlike MMPs they are all membrane bound, but variant proteins have been found secreted, as multiple ADAM genes have alternative spliced transcripts (Edwards et al., 2008). For example ADAM12 encodes for full length ADAM12 protein and short length ADAM12 protein which does not have the transmembrane and cytoplasmic domains (Wewer et al., 2006). ADAMs are composed of a pro-domain, a disintegrin domain, a metalloproteinase domain, a cysteine-rich domain and an EGF like domain, followed by the transmembrane domain and the cytoplasmic domain (H. Zhu et al., 2021), figure 1.10. After ADAMs are synthetised in the endoplasmic reticulum, they are transported to the Golgi for further maturation. Once at the plasma membrane, ADAMs are inactive until the pro-domain is

removed, mostly by furin-mediated cleavage (Seals and Courtneidge, 2003). ADAMs take their name due to similarities to the disintegrin domain of snake venom metalloproteinases, that contain RGD sequences which allows them to interact with integrins. On the contrary, ADAMs disintegrin domain lack RGD binding sites (Evans, 2001); however, there is now evidence that a motif present in their disintegrin loop allows interaction with integrins (White et al., 2005), influencing cell adhesion and cell-cell interactions. The ADAM cysteine-domain was found to mediate cell adhesion, in addition to shedding of membrane bound proteins. ADAM12 cysteine-domain was found to bind to syndecans located on the cell surface of mesothelial cells promoting initial integrin-independent adhesion (Iba et al., 2000). The secreted form of ADAM-9 (ADAM-9S), lacking transmembrane and cytoplasmic domains, was shown to regulate colon cancer cell invasion *in vitro* through binding to $\alpha 2\beta 1$ and $\alpha 6\beta 4$ integrins via its disintegrin domain. Indeed, when integrin blocking antibodies were present ADAM-9S-driven invasion was strongly reduced (Mazzocca et al., 2005). Moreover, ADAM-9S was shown to be catalytically active against laminin-1, resulting in increased invasion in laminin-1 containing matrices.

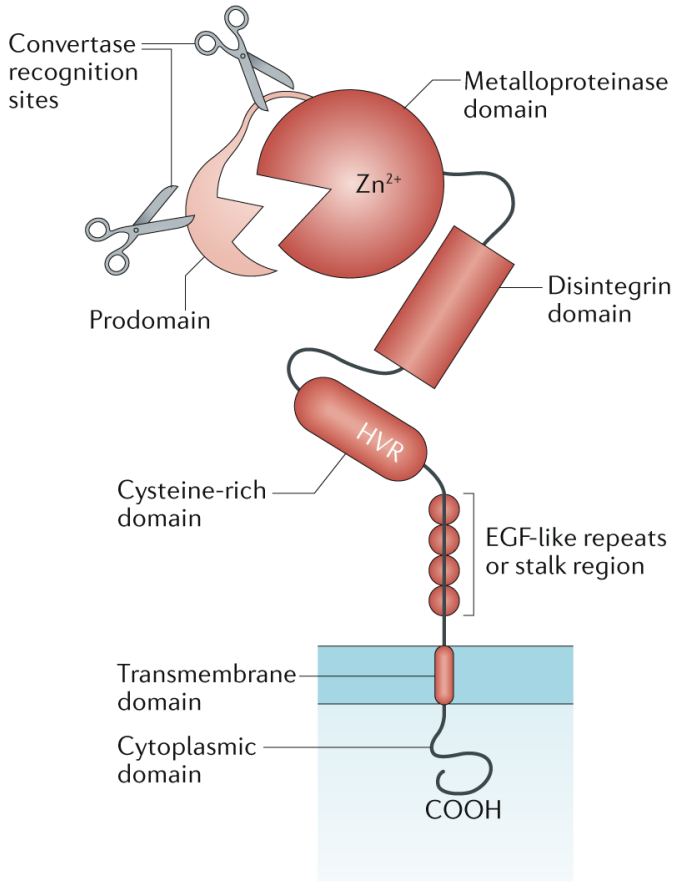

Figure 1.10. ***ADAM structure.*** The illustration shows the general structure of the ADAM family members and their activation by cleavage of the pro-domain by convertases like furin proteases. Image from (Lambrecht et al., 2018).

ADAM-10 and 17 have been shown to release EGFR ligands from the membrane of cells, including EGF, TGF-α and amphiregulin, which are known to be implicated in cancer development and progression (Sahin et al., 2004). ADAM-9 was found highly expressed in epithelial cells from well differentiated prostate tumours, while its expression was reduced as cancer progressed to advanced stages. ADAM-9 knockout in mice led to the development of smaller prostate tumours when compared to controls carrying either one or two alleles of ADAM-9. Furthermore, overexpression of ADAM-9 in mouse prostate epithelial cells led to abnormal epithelium and neoplasia (Peduto et al., 2005). ADAM-12 overexpression in mouse models of breast cancer has been linked to increase tumour progression (Kveiborg et al., 2005). Moreover, ADAM-15 knocked out mice showed less neovasculature and smaller tumours after

being injections with melanoma cells (Horiuchi et al., 2003), while others have found that its downregulation in prostate cancer cells led to reduced migration and adhesion to fibronectin, vimentin and lamin (Najy et al., 2008).

In ovarian cancer, low expression levels of ADAM-23 in epithelial cells is associated with poor survival, higher FIGO stages and lymph node metastasis (Ma et al., 2018). ADAM-10 and 17 have been shown to mediate the shedding of the adhesion protein nectin-4, suggesting that it may promote cancer cell migration, as shed nectin-4 has been found to promote tumour cell survival via translocation of the endo-domain to the nucleus, and migration and EMT activation via activation of PI3K/Akt signalling pathway via the ecto-domain (Buchanan et al., 2017; Wang et al., 2025). Moreover, ADAM-17 has also been found to decrease cisplatin efficacy by increased shedding of its substrates which in turn activate downstream cell survival signalling. Therefore, combination of inhibition of ADAM-17, using the small molecule inhibitor GW280264X, with cisplatin led to increased sensitivity to chemotherapy (Hedemann et al., 2021).

c. A disintegrin and metalloprotease with thrombospondin motifs (ADAMTSs)

ADAMTSs are secreted enzymes, associated to zinc metalloproteases as they contain a methionine residue close to the zinc-dependent active site, found to have multiple roles in tissue morphogenesis and pathologies, inflammation and vasculature formation (Gomis-Rüth, 2009). There are 19 genes that encode for ADAMTSs. ADAMTSs family members are named 1 to 20, excluding ADAMTS11 which was assigned to the same protein as ADAMTS5 (Apte, 2009). Their structure includes a signal peptide, a pro-region, a metalloproteinase domain, a disintegrin like domain, a central thrombospondin type I repeat, a cysteine rich domain, followed by a spacer region (figure 1.11). All family members have the same structure for the protease domain that spans up to the thrombospondin type I repeat, while the ancillary domain is where the variability is introduced (Apte, 2009). Depending on their domain organization,

ADAMTSs can be subdivided into eight categories, with different substrate preferences summarised in table 1.1. ADAMTSs can be activated in multiple ways. The pro-domain maintains the protein folded correctly and inactive; all ADAMTSs contain a furin-like pro-protein convertase cleavage site, pro-ADAMTS1 and 4 can also be activated in the Golgi and secreted in an active state, while others are activated by furin extracellularly (ADAMTS5) or in the cell surface (ADAMTS9) (Koo et al., 2007). Furthermore, some members do not need the removal of the pro-domain to be catalytically active, like ADAMTS13, that contains an extremely short pro-domain which appears to not be involved in activation of the protease but potentially in binding of other proteins (Majerus et al., 2003). ADAMTSs substrate-binding preferences, catalytic activity regulation and association with the ECM depends on the ancillary domain (Kelwick et al., 2015). Similarly to the other metalloproteinases, their activity is inhibited by TIMPs (Murphy, 2011) or by internalization and degradation via low-density lipoprotein-related protein 1 (LRP-1) (Yamamoto et al., 2014).

Figure 1.11. ***ADAMTS generic structure.*** The illustration shows the general structure of the ADAMTS family members. Starting from the N-terminus, a signal peptide (S), a pro-region (Pro), a metalloproteinase domain (Met), a disintegrin like domain (Dis), a central thrombospondin type I repeat (T1), a cysteine rich domain (Cys), a spacer region (Spa) with a variable C-terminus which can contain more thrombospondin type I repeat.

Table 1.1. ***ADAMTS family members classification.*** In the table is possible to see the classification of the different members and the substrates they are known to cleave

Classification	ADAMTS member	Main Substrate
Aggrecanases and proteoglycanases	ADAMTS1 ADAMTS4 ADAMTS5 ADAMTS8 ADAMTS9 ADAMTS15 ADAMTS20	Aggrecan, versican, brevican, neurocan, fibromodulin, decorin, syndecan, biglycan
COMP proteinases	ADAMTS7 ADAMTS12	COMP
Procollagen N-peptidases	ADAMTS2 ADAMTS3 ADAMTS14	Pro-collagen
Von-Willebrand factor proteinases	ADAMTS13	Von-Willebrand coagulation factor
Unclassified	ADAMTS6 ADAMTS10 ADAMTS16 ADAMTS17 ADAMTS18 ADAMTS19	Unknown

Multiple ADAMTSs have been found dysregulated in cancer, functioning both as tumour suppressors and tumour promoters. This dual role could be due to the different ECM substrates, the cleavage of which could have different impacts in the TME. We have recently reviewed ADAMTS role in modulating ECM dynamics, cancer cell-ECM interactions and oncogenic signalling pathways during cancer metastasis (Bacchetti et al., 2024).

A pan-cancer analysis demonstrated that most ADAMTS were upregulated in pancreatic cancer while ADAMTS1, 8, 9, 10 and 15 were found downregulated in multiple cancer types (Bacchetti et al., 2024). Moreover, their expression was found to vary depending on cancer stage, for example ADAMTS1 was found downregulated in early stages of breast and head and neck cancers, but it latter appears to be overexpress, promoting metastasis at later stages (Demircan et al., 2009; Porter et al., 2004; Tan et al., 2013). Their ability to regulate cancer not

only resides in the remodelling of the ECM, but also via direct interaction or cleavage of growth factors that modulate downstream signalling pathways, including activation of TGF-β by ADAMTS1, 6, 10 and 16 leading to cell migration (Bacchetti et al., 2024).

To summarize ECM composition and remodelling are fundamental for tumour development, growth, and metastasis. The different ECM proteins, secreted either by the cancer cells or cancer supporting stromal cells, play a fundamental role in cancer cell adhesion, migration, and survival. Moreover, degradation of the ECM by matrix degrading enzymes, like MMPs, ADAMs and ADAMTSs is also needed to allow cancer cells to escape the primary tumour, breach through the BM and establish a supportive TME for growth and metastasis.

1.4 ADAMTS5 role in cancer initiation and progression

ADAMTS5 has numerous proteoglycan substrates, and it has been well characterised in osteoarthritis, where it cleaves aggrecan, one of the major components of the cartilage matrix. Similarly to ADAMTS1 and ADAMTS4 (Kumar et al., 2012a), it has been identified as a tumour promoter and a tumour suppressor, in a context-dependent manner.

On the one hand, its role as a tumour suppressor has been observed in prostate cancer and head and neck carcinomas (Stokes et al., 2010). In prostate cancer, ADAMTS5 mRNA expression levels were low in cancer cell lines, while stromal cell cultures expressed higher levels of ADAMTS5, while addition of TGFβ1 to the latter led to decreased expression of ADAMTS5. In these tumours, an increase in versican deposition was linked to increased cell migration, potentially due to the decreased expression of ADAMTS5 or due to the increase in versican translation (Cross et al., 2005). Furthermore, in breast cancer expression levels of ADMATS5 were found to be decreased compared to normal breast tissue (Porter et al., 2004). Hypermethylation of the ADAMTS5 gene was observed in colorectal cancer when compared to normal mucosa, using bead-chip arrays, suggesting that it might be a potential diagnostic

marker (Kim et al., 2011). Moreover, the thrombospondin motif type I (TSR1) of ADAMTS5 has been found linked to angiogenesis *in vivo*, as it was shown to inhibit formation of new vasculature. The authors suggested this could be due to inhibition of the attachment of endothelial cells to the matrix, blocking their migration and induction of apoptosis by blocking the VEGF-induced stress fibres via suppression of RhoA activation (Sharghi-Namini et al., 2008). Moreover, this could also be mediated by sequestration of VEGF, as it has been previously shown that the C-terminus domain of the TSR motif in ADAMTS1 can bind and sequester VEGF (Luque et al., 2003). Further work is needed to confirm the ability of ADAMTS5 TSR motif to sequester VEGF. Similar results were also shown in melanoma, where the TSR1 domain of ADAMTS5 was shown to inhibit cell growth *in vivo* independently of the catalytic activity. This effect was linked to reduced formation of new vasculature, reduced tumour cell proliferation and increased apoptosis (Kumar et al., 2012b). In this study the overexpression of ADAMTS5 in tumours led to down-regulation of pro-angiogenic factors such as VEGF, insulin growth factor binding protein 3 (IGFBP-3), placental growth factor 2 (PlGF-2) and platelet-derived endothelial cell growth factor (PD-ECGF), identifying ADAMTS5 as an anti-angiogenic and anti-tumorigenic protein. Interestingly, in gastric cancer the anti-angiogenic properties of ADAMTS5 were not mediated via VEGF. It was found that ADAMTS5 expression was downregulated in gastric tumour samples when compared to normal tissues, and a negative correlation between ADAMTS5 expression and micro-vessel density was detected by immunohistochemical staining. The transcription factor Ets proto-oncogene 1 (ETS1) is known to regulate cell differentiation, tumour progression and angiogenesis. ETS1 expression was shown to be downregulated upon ADAMTS5 over-expression, while ADAMTS5 knockdown increased ETS1 levels, suggesting that ADAMTS5 might regulate angiogenesis in part by downregulation of ETS1 (Huang et al., 2019). A more detailed examination of the role of ADAMTS5 in controlling ETS1 expression and the

molecular mechanism behind this is required. Additionally, *in vitro* experiments showed an increase adhesion of cancer cells to FN leading to decreased cancer cell migration and invasion when ADAMTS5 was upregulated in gastric cancer (Huang et al., 2019). Similarly, to gastric cancer, in hepatocellular carcinoma (HCC) ADAMTS5 was found to be downregulated. When stably expressed in an HCC cell line, ADAMTS5 led to VEGF downregulation in the media. As a result of this, application of ADAMTS5 containing media, from ADAMTS5 expressing hepatocellular carcinoma cells, on human umbilical vein endothelial cells impaired their migration and invasion, reducing vasculature formation via downregulation of VEGF (C. Li et al., 2015). ADAMTS5 ability to reduce angiogenesis reflected on patient survival, as HCC patients with higher levels of ADAMTS5 had higher overall survival compared to patients with low expression. However, other studies have reported that higher levels of ADAMTS5 resulted in poorer overall survival and correlated with pathological stages in HCC (Z. Zhu et al., 2021). The difference between these studies could be in the nature of the experiments. Li et al, identified low expression rate of ADAMTS5 in patient tumour tissue samples compared to normal tissue, 50% of the samples did stain for ADAMTS5, which was mainly in the cytoplasm and then transfected HCC cells to stably express ADAMTS5 for future experiments. On the other hand, Zhu et al, carried out bioinformatic analysis using different GEO datasets and TCGA profiles, using potentially a bigger pool of data. It is therefore possible that mRNA levels do not correlate with protein levels. Thus, the role of ADAMTS5 in HCC is still unclear. On the other hand, ADAMTS5 has also been observed as a tumour promoter. ADAMTS5 is overexpressed in glioblastomas via activation of IL-1. In this context, it was found to colocalise with brevican, one of its substrates, which it was proven to cleave into two major fragments, which in turn increase glioblastoma invasive potential (Held-Feindt et al., 2006; Nakada et al., 2005). Moreover, ADAMTS5 expression was found to correlate with lymph node invasion, higher pathological stages, and poorer overall survival in colorectal cancer (Haraguchi et al.,

2017). Similarly, high expression correlates with poorer prognosis and promotion of invasion in non-small lung cancer (Gu et al., 2016). A549 lung cancer cells transfected with ADAMTS5 shRNA showed decreased migration compared to control, also showing decrease E-cadherin and increase vimentin protein levels. In breast cancer, cleavage of fibulin-2 by ADAMTS4 and 5 also leads to higher invasion and migration of cancer cells (Fontanil et al., 2017).

In ovarian cancer, ADAMTS5 was identified as overexpressed in malignant tumours when compared to benign or borderline ovarian tumours. Its expression was mainly located in epithelial cells, with higher expression of brevican, versican and aggrecan in malignant subtypes compared to benign tumours (Lima et al., 2016), suggesting a potential role in advanced stages of ovarian cancer. Moreover, we looked at ovarian cancer patient survival, using Gyorffy and colleagues platform, Kaplan-Meier Plotter (Gyorffy et al., 2012; Győrffy, 2023), where it was possible to observe that higher expression of ADAMTS5 in ovarian cancer patients leads to worse overall survival when compared to low ADAMTS5 expression patients (Yuan et al., 2024).

In conclusion ADAMTS5 can have a dual role in cancer. It has been identified as a tumour suppressor in cancer types like colorectal, gastric, and prostate, but it was also identified as a tumour promoter in cancers such as ovarian, lung and glioblastomas. Depending on the tumour type where its expression is dysregulated, it can affect angiogenesis, and migration and invasion of cancer cells.

1.5 Molecular mechanisms underpinning cell migration

Cell migration is fundamental to establish and maintain a tissue. In cancer, cells need to acquire the expression of genes that enable them to alter their shape and attachment to other cells and the ECM (Hanahan and Weinberg, 2011). Cancer cell migration can be classified as individual or collective migration, which depends on the cell morphology, molecular profile, actin cytoskeleton dynamics, matrix adhesion and protease activity (Wu et al., 2021). Cells that move

individually can adopt two behaviours: amoeboid or mesenchymal migration. On one hand, amoeboid migration is characterised by rapid movement, round and deformable cell shape, and poor cell-ECM interactions, with no degradation of the surrounding ECM, as their deformability allows cells to squeeze through narrow gaps (Holle et al., 2019). On the other hand, mesenchymal migration is characterised by epithelial cancer cell morphological and genetical changes which leads cells to downregulate epithelial markers and upregulate mesenchymal ones in a process called epithelial to mesenchymal transition (EMT) (Kalluri and Weinberg, 2009). During EMT cancer cells lose expression of E-cadherin, and other epithelial markers, and increase expression of mesenchymal markers, including N-cadherin, vimentin, α-smooth muscle actin and fibronectin. Moreover an increase in the expression levels of EMT-related transcription factors can be observed such as ZEB1, SNAI1 and TWIST (Grigore et al., 2016). Mesenchymal cancer cells have an elongated spindle-like shape that can form plasma membrane protrusions, like pseudopodia and filopodia. As mesenchymal cells cannot squeeze through the ECM pores, this type of migration is characterised by proteolytic degradation of the ECM, mediated by the recruitment of proteases at the leading edge of the cell to break down ECM barriers (Chang and Chaudhuri, 2019). Movement of the cancer cells is achieved by integrin-mediated ECM adhesion, focal adhesion kinase (FAK) and Src dependent cytoskeletal rearrangement and contractility via focal adhesion formation, which create tension and a pulling force towards the ECM at the leading edge of the cell. By integrin turnover and recycling, adhesion at the rear of the cell is reduced and increased at the front resulting in slow forward movement of the cell (Sadok and Marshall, 2014).

Finally, cancer cells can migrate collectively, for this to occur cancer cells retain some cell-cell connections, moving as a group. Their movement is dependent on the actin dynamics, proteolysis of the ECM and integrin-mediated ECM adhesion. During collective migration cells are polarised, forming a leading edge and a following edge (Wu et al., 2017).

Regulation of integrin-dependent cell-ECM adhesion is critical in controlling mesenchymal cell migration. A key mechanisms modulating integrin function is vesicular trafficking, which is tightly controlled by small GTPases of the Rab family. This process will be discussed in more detail below.

1.5.1 Rab GTPases

Rab GTPases form the largest family of small GTPases, comprising more than 70 members. They belong to the Ras superfamily and function as molecular switches (Wennerberg et al., 2005). Rab GTPases cycle between a GTP-bound active and a GDP-bound inactive form. The hydrolysis of GTP into GDP is promoted by GTPase activating proteins (GAPs), which stimulate the GTPase activity of the Rab GTPases. In addition, recognition by a GDP dissociation inhibitor (GDI) retain the Rab GTPase in the cytosol, preventing their activation. To activate the GTPases, guanine nucleotide exchange factors (GEFs) mediate the removal of GDP and addition of GTP (Goody et al., 2005), figure 1.12.

Once activated, Rab GTPases promote membrane trafficking and intracellular signalling in a temporal and spatial manner (Zerial and McBride, 2001). Rabs are located at the plasma membrane and organelle membranes, controlling the endocytic and exocytic trafficking, shuttling cargo to and from the cell surface and within the cell. This allows them to contribute to plasma membrane delivery, organelle biosynthesis and degradation (autophagy) and regulate functions such as secretion, synaptic transmission, cell polarity and phagocytosis (Schwartz et al., 2007). Rab GTPase activation is controlled by cell signalling, with GAPs and GEFs being phosphorylated in response to cellular stress or growth factors stimulation (Xu et al., 2021). To increase specificity Rab GTPases are located into specific cellular compartments and linked to specific cargos. For example Rab2 is located in the endoplasmic reticulum (ER) mediating trafficking between the ER and Golgi; Rab5 is located in clathrin coated vesicles and early endosomes while Rab11 localises in recycling endosomes (Schwartz et al., 2007).

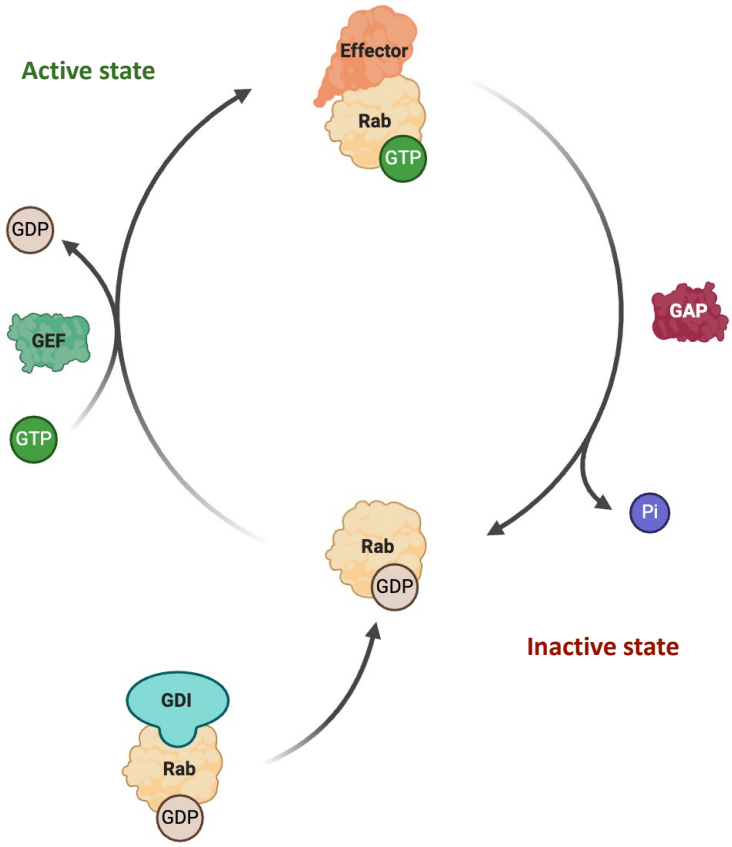

Figure 1.12. ***Rab GTPases activation.*** Rab GTPases switch between an GTP-active state to a GDP-inactive state. This swich is mediated by GTPase activating proteins (GAPs) and guanine nucleotide exchange factors (GEFs). Furthermore, GDP dissociation inhibitor (GDI) retains inactive Rab GTPases in the cytosol. Image made using BioRender.

Rab GTPases have been found to be altered in different cancer types, as dysregulation of receptor signalling and trafficking is linked to cancer development, table 1.2. Many Rab family members are expressed at higher levels in cancer types like breast, liver, and lung, promoting tumour progression and metastasis as they increase vesicle trafficking of cell adhesion molecules, stimulating invasion and migration. Gene mutations and post-transitional modifications have also been observed in many cancers leading to regulation of tumorigenic potential, cell invasion and metastasis. Some Rab GTPases have been found to have dual roles, and depending on the cancer type, they can be tumour promoting or tumour suppressing. For instance, Rab1 is tumour promoting in liver cancer and tumour suppressing in breast cancer, while Rab27 is tumour promoting in breast cancer and tumour suppressing in lung cancer (Xu et al., 2024). Dysregulation of the Rab11 subfamily is particularly linked to metastasis

progression, due to the alteration in integrin recycling to the plasma membrane, as described below (Caswell et al., 2007; Wang et al., 2000).

Table 1.2. ***Summary of Rab GTPases in different cancer types.*** *Table adapted from* (Xu et al., 2024).

Cancer type	Rab's implicated
Liver	Rab1, Rab10, Rab13, Rab22 and Rab32
Breast	Rab1, Rab2A, Rab5, Rab8, Rab11, Rab21, Rab22, Rab25, Rab27, Rab35 and Rab40B
Colorectal	Rab1, Rab13 and Rab31
Melanoma	Rab1 and Rab4A
Pancreatic	Rab5 and Rab27
Cervical	Rab5, Rab10, Rab11, Rab13, Rab21, Rab31 and Rab35
Gastric	Rab11, Rab14 and Rab18
Ovarian	Rab14 and Rab25
Lung	Rab25

1.5.1.1 Rab25

Rab25, also called Rab11c, is a member of the Rab11 subfamily that regulates endosomal recycling in epithelial cells (Jagoe et al., 2006). Rab25 has been found to function as an oncogene in ovarian, breast, renal, gastric, liver, bladder, lung, prostate cancer and glioblastoma, but also as a tumour suppressor in colon, head and neck, oesophageal, oral, and oropharyngeal cancers; therefore, its function changes depending on the cancer type (Wang et al., 2017).

Rab25 is a small GTPase, of 23kDa, its function is regulated by the guanine nucleotide binding motif and the carboxyl-terminal region. The former allows binding of the GTP/GDP and the latter contains a CCXXX motif that allows binding to specific membranes via prenylation of the cystine residues, namely vesicles that will be recycled to the apical membrane in polarised epithelial cells (Bhuin and Roy, 2014).

Rab25 has been found mutated in ovarian, prostate, bladder and invasive breast cancer, producing a constitutively activated GTP-bound protein that promotes migration (Kessler et al., 2012). Multiple evidence has associated Rab25 to an oncogenic function. Rab25 was identified as a driver of 1q22 region amplification, which increased DNA, RNA and protein expression levels associating it with poor patient prognosis in ovarian, breast and Wilms tumours (Cheng et al., 2004; Mitra et al., 2012). Increased expression of Rab25 allows survival of cells without growth factors, improves growth without anchorage, suppresses apoptosis and increases tumour development, by promoting recycling of integrins to the plasma membrane and activating intracellular signalling pathways. For example, direct interaction of Rab25 with $\alpha 5\beta 1$ integrin was linked to increased tumour aggressiveness, cancer cell migration and cell invasion (Caswell et al., 2007). $\alpha 5\beta 1$ integrin was found to coprecipitate with HA-Rab25 stably expressed in ovarian cancer cells, but not with Rab11A or Rab11B. Furthermore, chimeras of Rab25, with partial or total replacement of the c-terminus with the corresponding region of Rab11, were used to confirm Rab25 variable region is the one able to associate with $\beta 1$ integrin. The opposite experiment was also carried out, where Rab11 with total replacement of the variable region with the corresponding Rab25 one was able to bind to β1 integrin. Invasion assays were then carried out showing increased invasion in Rab25 expressing ovarian cancer cells in a $\alpha 5\beta 1$ and FN dependent manner, as addition of FN to the matrix further boosted migration. Chimeras were also used confirming the need of Rab25 interaction with $\beta 1$ integrin to promote invasion, as full length Rab11 and Rab25 with Rab11 c-terminal region did not promote migration while full length Rab25 and Rab11 with Rab25 c-terminal region did (Caswell et al., 2007). Rab25 has been shown to also activate Akt and Wnt signalling pathways and suppress apoptosis. Overexpression of Rab25 led to increased anchorage dependent and independent cell proliferation. This was associated with elevated Akt phosphorylation levels, which in turn stimulated ovarian cancer cell proliferation by blocking apoptotic signalling via

decreased BCL2 expression and PI3K activation (Cheng et al., 2004). Similarly, Rab25 expression was found elevated in glioblastoma cells (Ding et al., 2017), hepatocellular cells (Geng et al., 2016) and in bladder cancer cells (Zhang et al., 2013), where it was found to regulate Akt phosphorylation leading to migration and invasion. On the other hand, Rab25 overexpression was detected in HCC patient tissues and correlated with advance tumour stages and nodal metastasis. Rab25 downregulation was found to inhibit the expression of Wnt signalling target genes like c-Myc, cyclin D1 and MMP7, negatively regulating cancer cells ability to invade (Geng et al., 2016). Moreover, Src signalling pathway and ERK were also found affected by Rab25 expression. Rab25 was also reported to stabilise HIF-1α, in an oxygen-independent manner, promoting aggressiveness of ovarian cancer and a cisplatin resistance phenotype (Gomez-Roman et al., 2016). Tumour cell proliferation, migration and invasiveness were as also enhanced by Rab25 expression in renal cancer cells. Consistently, Rab25 expression correlated with high invasion classification, lymph node metastasis and pathological stage in renal cancer patients (Y. Li et al., 2015).

On the other hand, several studies have shown that loss of Rab25 expression can lead to tumour progression, suggesting a tumour suppressive role in colorectal and head and neck cancer (Goldenring and Nam, 2011; Seven et al., 2015; Tong et al., 2012). Rab25 was found to be downregulated in colorectal cancer when compared to normal colon tissue, correlating with lower survival rates. Moreover deficiency of Rab25 in mice led to the formation of multiple polyps in the small bowel and colon (Nam et al., 2010). Another group also showed that ectopic expression of Rab25 in colorectal cancer cell lines reduced invasiveness and wound closure rates in 2D and colony formation in 3D matrices by upregulating claudin-7 expression, a tight junction protein known to suppress proliferation and invasion in multiple cancer types. Mechanistically, the inhibition of cell invasion was mediated by Rab25 increased recycling of claudin-7 which reduced the phosphorylation of EGFR, decreasing downstream signalling

pathway activation, demonstrated by the reduction of its effector Ras (Cho et al., 2024). Moreover, $\alpha 5\beta 1$ localisation in polarised Caco2-BBE cells, a clone of the Caco2 cell line able to form an apical bush border, was altered in Rab25 knockdown. A reduction in $\alpha 5\beta 1$ integrin at the plasma membrane was found, altering the apical brush border formation, leading to clustering of microvilli. Depletion of Rab25 also reduced claudin expression, disrupting tight junctions. All together alteration to integrin expression and localization, and disruption of tight junctions increased colorectal cancer cell migration and colony formation in Rab25 knock down cells (Krishnan et al., 2013).

Rab25 expression in cancer is still under investigation as correlation between its expression and cancer progression is still unclear due to the diverse behaviours depending on cancer type. Rab25 function is likely to be determined by the cancer type. Literature suggests that regulators of Rab, like Rab coupling protein, or effectors, like chloride intracellular channel 3 (CLIC3) may determine if Rab25 has an oncogenic or a tumour suppressor function (Chen, 2021).

1.5.2 Integrins

Integrins are a superfamily of cell adhesion transmembrane receptors that bind mostly to the ECM (Hynes, 2002). They are heterodimers formed by an α and a β subunit. Currently, 18 α subunits and 8 β have been identified in humans that bind through a noncovalent association (Hynes, 2002). The extracellular portion of the dimer contains 700 to a 1000 amino acids forming an elongated stalk and a globular ligand binding head region (Xiong et al., 2001). In the head region there are seven repeats and an insertion called the I-domain, which contains a metal ion-dependent adhesion site; when the ligand binds, it switches from a closed to an open conformation, strengthening the adhesion (Liddington and Ginsberg, 2002). The cytoplasmic tails are smaller, containing approximately 75 amino acids, tails of the different β subunits share high similarity, while α subunit tails are diverse. Many cytoskeletal and signalling proteins binds to the β tails, and a few have been found to also interact with the α (Calderwood

et al., 2003; Hughes et al., 1996). Integrins have different ligand specificity, allowing them to bind to different ECM proteins, figure 1.13 (Takada et al., 2007).

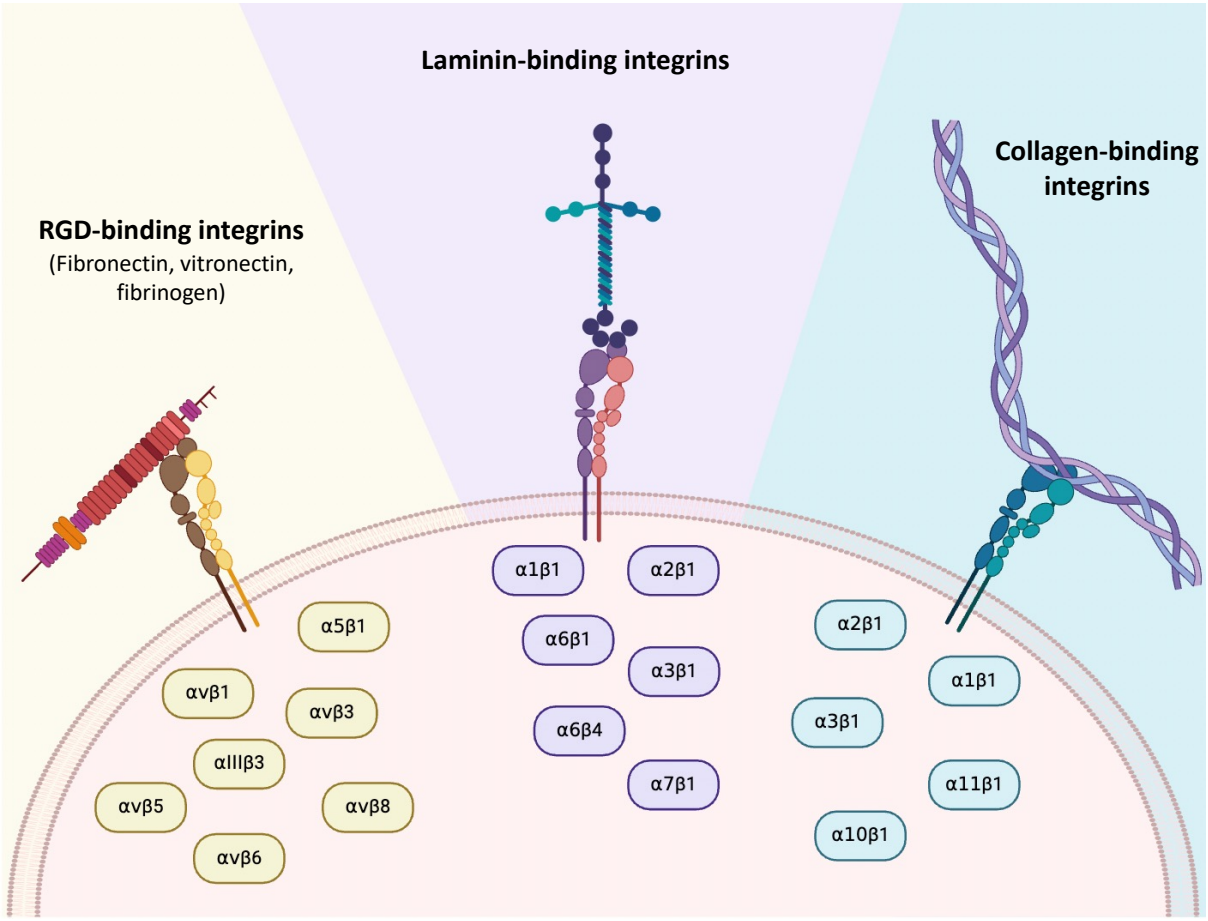

Figure 1.13. ***Integrin ligand-specificity.*** Integrins can be classified in three broad categories based on the ECM specificity: RGD-binding, laminin-binding and collagen-binding integrins. Image made using BioRender.

Once integrins bind to their corresponding ligand, they stimulate intracellular signals, modulating cell behaviours like adhesion, proliferation, survival, shape, polarity, motility, gene expression and differentiation, mostly by regulating cytoskeletal changes (Clark and Brugge, 1995). Integrins can be activated either via the extracellular portion (outside-in signalling) or from the intracellular region (inside-out signalling). Integrins exists in three conformations, bent (low-affinity), medium-affinity and extended (high-affinity); the switch between them depends on the affinity with the ligand (ECM proteins) and downstream effectors. The bent conformation is normally maintained by shank-associated RH domain-interacting proteins which bind to the α integrin tails. Contrarily, the extended conformation is maintained by the

interaction of the β integrin tail with α-actin, talin, vinculin and paxillin, among others. This binding triggers conformational changes that extend the extracellular domains of the subunits and rearrange the α and β interface in the ligand-binding domain, leading to increased affinity - this process is termed inside-out signalling (Pang et al., 2023). Integrins can also be activated by the binding of the ligand to the extracellular domain of the integrin - outside-in signalling. Integrins clustered at the cell surface interact with the ECM ligands, which stimulate conformational changes, leading to the activation of FAK. FAK is then auto-phosphorylated which contributes to Src binding next to the intracellular β integrin tail. In turn the complex activates adhesion associated adaptor proteins like paxillin (Li et al., 2023).

Due to their multiple functions in normal cellular states, integrins have been found linked to almost every step of cancer progression, from cancer initiation to metastatic colonization, including local invasion, survival and intra- and extravasation (Hamidi and Ivaska, 2018). In ovarian cancer, $\alpha 2\beta 1$ was found highly expressed, being identified as a marker for poor prognosis (Dötzer et al., 2021). $\alpha 2\beta 1$ was also found to promote ovarian cancer peritoneal dissemination by influencing spheroid disaggregation during mesothelial cell invasion, by increasing the levels of MMP2 and 9 (Burleson et al., 2005; Shield et al., 2007). However, it was also found that $\alpha 2\beta 1$ promotes spheroids formation in epithelial cancer ovarian cells, as a reduction in spheroid diameter was observed when cancer cells with α2 knockout were allowed to form spheroids compared to α2 expressing cells, ability to bind collagen was also reduced in the α2 knockout cells (Huang et al., 2020). This difference in $\alpha 2\beta 1$ function in ovarian cancer spheroid formation could depend on the dual role of α2β1 integrin being needed to both aggregate cells together and maintain cell-cell connections in the early stages of dissemination, and spheroid adhesion to the mesothelium. α2β1-dependent collagen binding at the metastatic site could then increase the levels of MMP2 and 9, favouring disaggregation of the spheroids

and promoting migration and invasion. Furthermore, $\alpha 2\beta 1$ was also observed to promote chemoresistance via activation of PI3K/Akt signalling pathway (Zheng et al., 2020).

$\alpha 5\beta 1$ has also been linked to ovarian cancer progression. Loss of E-cadherin in ovarian cancer was shown to promote the upregulation of $\alpha 5$ integrin, which in turn enhanced adhesion to FN-containing matrices and migration in matrigel (Sawada et al., 2008). The omentum, one of the main metastatic sites of ovarian cancer cells, was shown to contain high levels of FN. In addition, mesothelial cells, lining the omentum, are known to secrete FN and deposit it on their cell surface. It was demonstrated that 3D cultures of ovarian cancer cells bind to the mesothelial cells in a FN- and $\alpha 5\beta 1$ integrin-dependent manner. Indeed, $\alpha 5\beta 1$ blocking antibodies prevented ovarian cancer cells adhesion to the mesothelium *in vivo*, indicating that α5β1 is required for the early step in metastasis (Sawada et al., 2008). Other groups also demonstrated that either $\beta 1$ expression or addition of exogenous FN induced spheroid formation, which could be blocked by $\alpha 5\beta 1$ blocking antibodies (Casey et al., 2001). Additionally, blocking the RGD binding site in FN with specific antibodies abolished ovarian cancer cell binding to mesothelial cells, confirming the need of integrin-mediated adhesion for metastasis initiation (Strobel and Cannistra, 1999).

Integrins surface levels are tightly regulated by endocytosis and recycling. This is fundamental to regulate cell migration, as integrins establish several weak interactions with the ECM. As they are internalised, sorted and re-delivered in other areas of the cells, integrin density increases establishing stronger adhesions that allow the cells to move; this is called Velcro principle (Alberts et al., 2002). Integrin endocytosis has been found to be mediated by a variety of pathways, including clathrin-dependent, caveolin-dependent endocytosis or via macropinocytosis (Moreno-Layseca et al., 2019). After internalisation, integrins can be recycled back to the plasma membrane by two different pathways, the Rab4 dependent short-loop and the Rab11-dependent long-loop (De Franceschi et al., 2015). In ovarian cancer cells,

it was found that Rab25 directly interacts with $\alpha 5\beta 1$ integrin (Caswell et al., 2007). Furthermore, Rab25 expressing cells were found to promote the expression of CLIC3 in a matrix dependent manner, as when A2780-Rab25 cells were seeded on a 3D fibrillar cell-derived matrix CLIC3 gene expression was increased, compared to plastic or control cells lacking Rab25 expression. CLIC3 was founds enriched in late endosome/lysosomes, where it colocalised with Rab25. Moreover, FN-bound α5β1 was delivered to CLIC3-positive lysosomes, but rather than being degraded, it was recycled back to the plasma membrane, in a Rab25 and CLIC3-dependent manner. Interestingly, in the absence of CLIC3, Rab25 promoted integrin degradation. These observations might shed light on the dual role of Rab25 that has been observed in cancer, as the presence of CLIC3 might dictate whether Rab25 promotes (by driving integrin recycling) or prevent cell migration (by stimulating integrin degradation) (Dozynkiewicz et al., 2012).

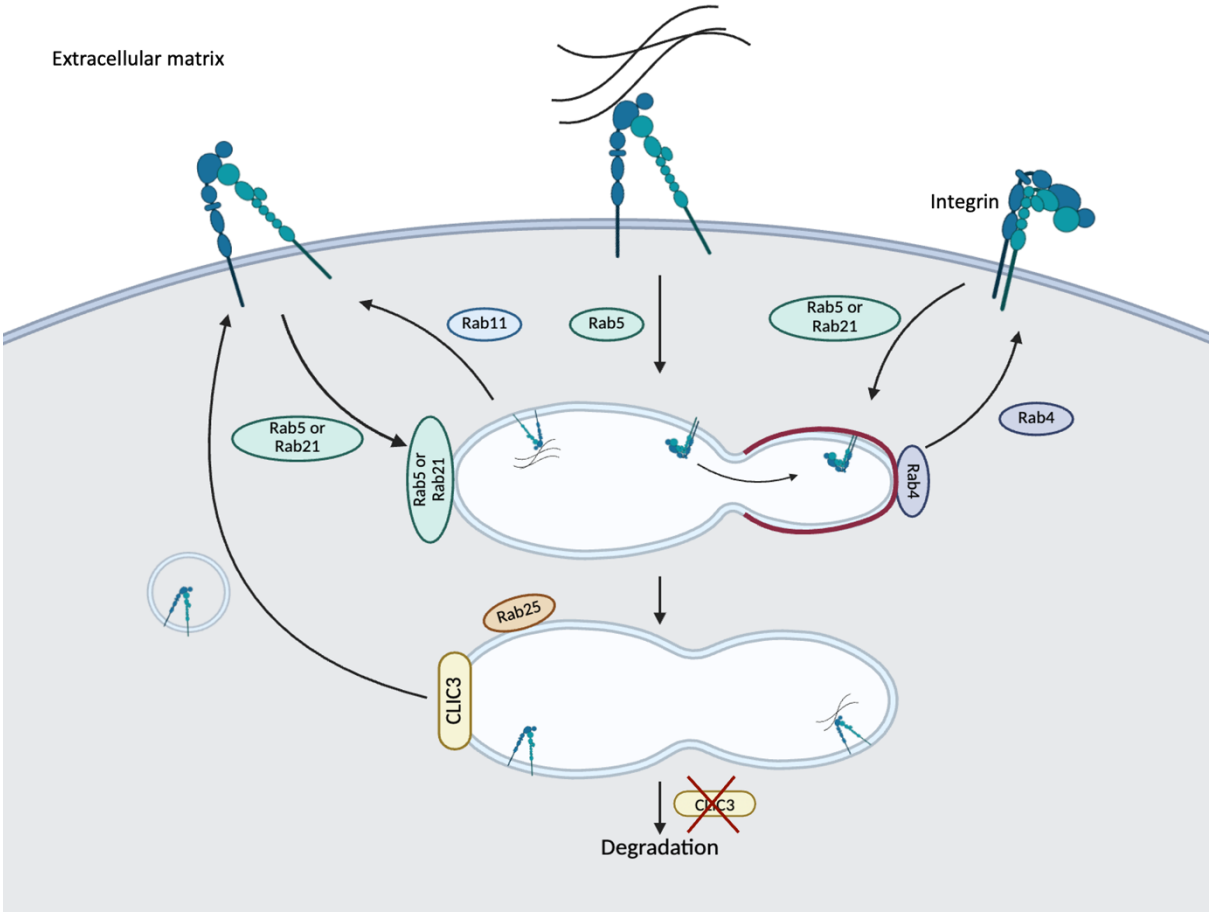

Figure 1.14. ***Integrin recycling.*** The illustration shows the trafficking routs of integrins. At the plasma membrane integrins are internalised in a Rab5- or Rab21-dependent manner. Inactive integrins are mostly recycled from

early endosomes in a Rab4 dependent manner, via the short loop pathway. They can be further recycled in a Rab11 dependent manner from early endosomes, via the long loop pathway. Moreover, active integrins can be recycled from CLIC3-positive late endosomes positive in a Rab25-dependent manner, preventing degradation. In the absence of CLIC3 integrins are degraded. Image made using BioRender.

1.5.2. Other ECM receptors

Other ECM receptors have been identified as important regulators of cancer cell migration, these include CD44 and syndecans.

a. CD44

CD44 is a transmembrane glycoprotein that is expressed at different degrees in multiple cell types and used as a cell surface marker to recognise cancer stem cells. The main ECM ligand of CD44 is hyaluronic acid, that as previously mentioned is found in ovarian cancer TME. Upon ligand binding, CD44 undergoes a conformational change that activates multiple signalling pathways to induce cell proliferation, adhesion, migration, and invasion (Ponta et al., 2003). Versican, a proteoglycan, is known to bind to hyaluronic acid forming the pericellular matrix of the cell. This serves as scaffold for other proteins, such as newly secreted collagen and fibronectin, that can be retained in the pericellular matrix before assembly, forming tracks that promote cell proliferation and migration (Evanko et al., 2007; Wight, 2017). In ovarian cancer, TGF-β upregulates versican in CAFs, which promotes motility and invasion by binding to CD44 at the ovarian cancer cell membrane. This results in the activation of NFκB and JNK signalling, which in turn upregulates CD44, hyaluronan-mediated motility receptor and MMP9, and potentially further activates CD44-mediated signalling pathways (Yeung et al., 2013). Expression of CD44 has been found to correlate with higher stages of disease and poor prognosis in ovarian cancer patients (Lin and Ding, 2017; Sacks and Barbolina, 2015). Moreover, it was linked to EMT via regulation of Snail, metastasis and relapse (Gao et al., 2015; Zhou et al., 2019). Research has also shown that CD44 together with β1 integrin mediate

ovarian carcinoma cell adhesion to mesothelial cells during early steps of metastasis (Lessan et al., 1999).

b. Syndecans

Syndecan family is composed of four members (syndecan 1-4), all transmembrane heparan sulphate glycoproteins. Syndecans have mainly three domains, a highly conserved C-terminus cytoplasmic domain, a transmembrane domain, and a variable N-terminus extracellular domain that contains multiple GAG chains (Czarnowski, 2021), figure 1.15. The GAG chains allow syndecans to interact with multiple growth factors, like VEGF and FGF2, chemokines, ECM molecules like fibronectin, proteinases, and lipases. The extracellular domain also allows syndecan to interact directly or indirectly with integrins. Moreover, this domain can be shed from the membrane, which has been linked to tumour progression. The cytoplasmic domain can be further subdivided into three regions: a C1 region, a variable region and a C2 region. The C1 region is linked with cytoskeleton interactions while the C2 region can mediate trafficking and exosome production (Chung et al., 2016).

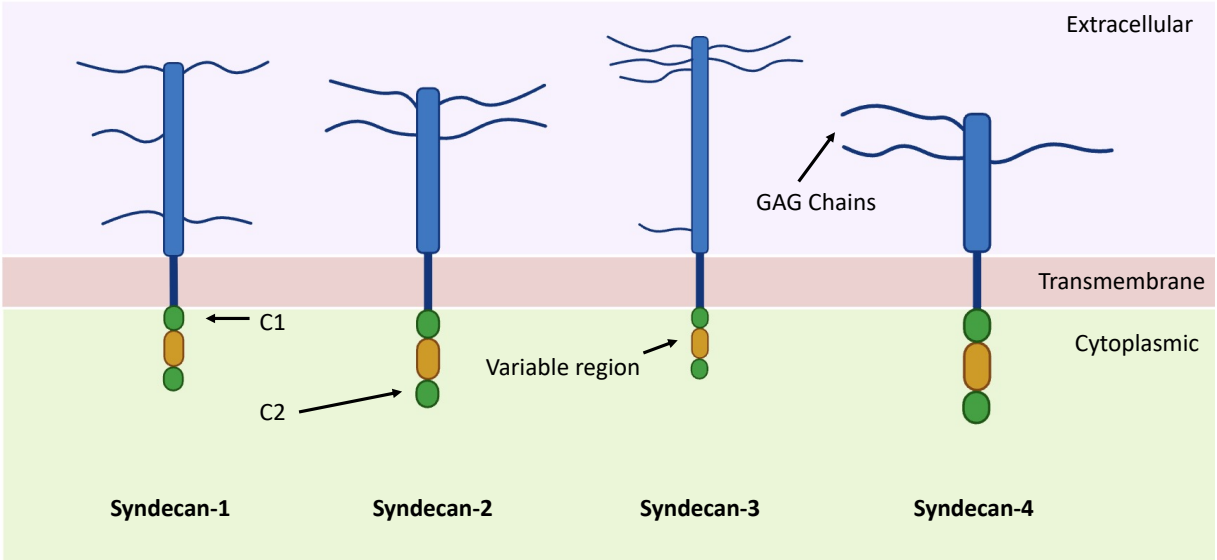

Figure 1.15. ***Syndecan structure.*** The illustration shows the main structure of the four syndecans. Syndecans are composed of three major domains, the extracellular, transmembrane, and cytoplasmic. The cytoplasmic domain can be further divided into three regions, C1, variable region and C2. Image made using Biorender.

Location of syndecans may vary between cell types as they are not expressed ubiquitously. SDC1 is located in epithelial cells and leukocytes, and its expression is found dysregulated in many cancer types. In bladder cancer, low levels of SDC1 correlated with lower stage and grade and could predict recurrence free survival (Kim and Park, 2014). Other studies have confirmed the decreased levels of SDC1 in tumour samples but interestingly found high levels in the serum, providing evidence of SDC1shedding. This process was linked to high stage and grade bladder cancer, indicating that shedding may contribute to aggressiveness (Szarvas et al., 2014). On the contrary, elevated SDC1 levels correlated with poor prognosis in breast cancer, resulting in increased tumour bulk, high grade and oestrogen and progesterone receptor negative phenotype (Barbareschi et al., 2003). Furthermore, high SDC1 expression was associated with higher patient death when patients were treated with cyclophosphamide-methotrexate-fluorouracil chemotherapy, while no other therapy showed correlation with SDC1 expression. Additionally, SDC1was linked to aggressive triple-negative inflammatory breast cancer and was found to be co-expressed with the cancer stem cell marker CD44, suggesting a role in cancer stem cell-like behaviour via the modulation of IL-6/STAT3, Notch and EGFR signalling pathways (Ibrahim et al., 2017). Moreover, in ovarian cancer, SDC1 has been found expressed in borderline and malignant tumours, but not in benign tissues. Its expression in the stoma was found associated with shorter patient survival and disease progression (Davies et al., 2004). This was supported by another study that found high levels in the stoma and low levels in the epithelium, suggesting that SDC1 may have a tumour promoting role in the stroma and a tumour suppressor role in the epithelial cells (Kusumoto et al., 2010). Syndecans have been involved in cell-cell and cell-ECM interactions. Loss of SDC1 in epithelial cells could lead to decreased intracellular cohesion, allowing for migration to occur, increasing metastatic potential; while increased expression in the stroma could be

needed to promote tumour angiogenesis, supporting tumour survival and growth, due to SDC1 ability to bind to growth factors.

Syndecan-2 (SDC2) localises to synapses and it is expressed by mesenchymal cells, known to have a role in matrix formation (Klass et al., 2000). SDC2 increased expression was found mainly in lung, colorectal and pancreatic cancer. In pancreatic cancer, SDC2 was expressed in the stroma and epithelial cells of tumour tissues but not in normal tissue in stromal cells, and contrarily to SDC1, high expression in epithelial cells was associated with longer survival and no association with its expression in the stroma and survival was found (Hrabar et al., 2010). On the contrary, in lung cancer SDC2 expression was increased in malignant cells and promoted cell invasiveness (Tsoyi et al., 2019). Moreover, in colorectal cancer upregulation of SDC2 was associated with vascular invasion, cancer stage, lymph node and distant metastasis, playing a role in activating EMT (Hua et al., 2020). Syndecan-3 (SDC3) expression was found increased in pancreatic cancer and it was associated with perineural invasion and correlated with increased tumour size (Yao et al., 2017, 2014). However, further elucidation of the role of SDC2 and 3 in cancer is needed.

Finally, syndecan-4 (SDC4), the most ubiquitously expressed member of the family, has been found dysregulated in numerous cancer types. It has been found overexpressed in breast, liver, melanoma, glioma, testicular, osteosarcoma, thyroid, kidney and bladder cancer, while it was shown to be downregulated in neuroblastoma (Onyeisi et al., 2021). SDC4 and $\alpha 5$ integrin gene expression and protein cell surface localisation were found increased in colorectal cancer cells under hypoxia. Similar increase in SDC4 and $\alpha 5$ gene expression was also found in colorectal cancer patient tissues. Moreover, an increased adhesion of the colorectal cancer cells was observed on FN under hypoxic conditions (Koike et al., 2004), consistent with an increase in FN receptor expression. In glioma tissues and cell lines, all four syndecans were detected at an mRNA level. It was found that SDC1 expression was promoted by NFκB (Watanabe et al.,

2006). SDC4 is a marker for poor prognosis, used as predictive biomarker for long term survival after administration of the Wilms' tumour 1 targeting cancer vaccine WT1 peptide, as low syndecan-4 mRNA expression was linked to 64% of the patients responding well to the therapy (Takashima et al., 2016). SDC4 was shown to correlate with oestrogen and progesterone receptors presence in breast cancer. In addition, a negative correlation between SDC1 and SDC4 was observed in breast cancer. In high-grade breast tumours low SDC4 and high SDC1 expression was found, while in tumours with oestrogen and progesterone receptors the opposite trend, high SDC4 and low SDC1, was observed (Lendorf et al., 2011). In osteosarcoma, an increase of SDC4 and its ligand FN was observed in high grade tissues when compared to others. High SDC4 expression was associated with larger tumour size, distant metastasis and shorter overall survival (Na et al., 2012).

In ovarian cancer, multiple syndecans are dysregulated. SDC1 is upregulated in ovarian carcinoma when compared to normal tumour, and in secondary metastasis compared to normal omentum tissue (Casey et al., 2003; Salani et al., 2007). SDC3 was identified as a potential biomarker, as it was significantly overexpressed in tumour stroma compared to normal stroma, to improve diagnosis of EOC (Kulbe et al., 2019), while SDC4 correlates with poor prognosis and its expression increases as tumour stage increases (S. Kim et al., 2021).

Recapitulating, cell migration is a key process for cancer progression. Cancer cells can adopt different strategies to migrate, having to change cell shape, degrade and adhere to the surrounding ECM. Rab GTPases are fundamental regulators of integrin recycling. Integrins are receptors that mediate cell-ECM interactions influencing adhesion, survival, and motility, which facilitate metastatic spread. Understanding the molecular mechanisms governing these processes is essential for developing targeted therapies aimed at disrupting cancer spread.

1.6 Hypothesis, aims and objectives

As metastasis is the leading cause of death of ovarian cancer patients, understanding how ovarian cancer cell migration is regulated at the molecular level is essential. In this thesis, we aimed to investigate the role of ADAMTS5 in regulating ovarian cancer cell migration and invasion downstream of Rab25 and to elucidate the molecular mechanism behind Rab25-mediated upregulation of ADAMTS5.

Rab25 overexpression in A2780 ovarian cancer cells was found to promote FN-dependent invasion. This was mediated by Rab25 driven recycling of α5β1 integrin to the invasive front of migrating cells which promoted adhesion to FN surfaces, enhancing tumour cell invasion into the ECM (Caswell et al., 2007). Furthermore, recently published data from our lab, (Yuan et al., 2025), demonstrated that Rab25 overexpression promoted ADAMTS5 expression compared to the empty vector control, and this upregulation was further promoted by the presence of cell derived matrix. Moreover, we showed that ADAMTS5 is required for Rab25-dependent ovarian cancer cell migration in 3D environments (Yuan et al., 2024). Indeed, a reduction of pseudopod elongation and directional cell migration was observed in Rab25-overexpressing cells in the presence of 2 different ADAMTS5 inhibitor, as well as upon ADAMTS5 knockdown. Furthermore, when spheroids generated from Rab25 expressing cells were embedded in a 3D matrix, the presence of ADAMTS5 inhibitor and ADAMTS5 knockdown significantly reduced in the invasion area. Taken together. we found that Rab25 upregulates ADAMTS5 in 3D environments and that its catalytic activity is needed for ovarian cancer cell migration and invasion in the presence of ECM. In addition, FN is highly enriched in cell derived matrices and was found to be expressed in ovarian cancer ECM and ascites (Kenny et al., 2014). We, therefore, hypothesised that FN is the ECM component driving the upregulation of ADAMTS5 downstream of Rab25 overexpression, in ovarian cancer cells. Rab25 could be coordinating cell adhesion to FN via the promotion of α5β1 integrin recycling to the plasma membrane which, together with SDC4, regulates focal adhesion formation, which

in turn might promote ADAMTS5 expression. High levels of this protease then drive migration, mesothelial cell invasion and ultimately metastasis, in a catalytic activity-dependent manner. The objectives of this project are to elucidate:

a. The molecular mechanism through which Rab25 controls ADAMTS5 expression and the role of FN in promoting this upregulation.

b. The requirement of Rab25 and ADAMTS5 for ovarian cancer cell migration and invasion, using a physiologically relevant 3D *in vitro* system.

c. The role of Rab25 and ADAMTS5 in promoting ovarian cancer cell invasion *in vivo* using a zebrafish cancer model.

CHAPTER 2: Materials and Methods

2.1 Materials

Table 2.1. ***Materials***

Material	*Supplier*
0.22µm syringe filter	Gilson
10 cm petri dishes, 200mm deep	Greiner bio-one
12 well plates Cell Star	Greiner bio-one
24 well plates CytoOne	StarLab
25 Culture-Inserts 2 Well for self-insertion	Ibidi
4% PFA	ThermoFisher
5X siRNA buffer	Horizon Discovery by Perkin Elmer
6 well plates Cell Star	Greiner bio-one
ADAMTS5 Inhibitor	MedChemExpress
ADAMTS5 Inhibitor	SantaCruz
alpha5 integrin, mouse	BD Transduction Laboratories
Ambion^{TM} Nuclease-Free Water	Invitrogen
Amicon Ultra® - 4 Centrifugal filters 10k	Milipore
Ammonium chloride	Sigma
Ampicillin	Sigma
anti ADAMTS5, rabbit	abcam
anti-Fibronectin, mouse	BD Transduction Laboratories
anti-Integrin alpha 2 antibody	abcam
anti-Mouse Alexa 488, donkey	Invitrogen
anti-Mouse Alexa 647, goat	Invitrogen
anti-Rabbit Alexa 594, donkey	Invitrogen
anti-Rabbit Alexa 647, goat	Invitrogen

ATN161	TOCRIS
Beta1 integrin - Alexa647, mouse (clone TS2/16)	BioLegend
Bisindolylmaleimide I (BIM)	Cayman
Calcium chloride	Fisher
Collagen I HC rat tail	Corning
Color Prestained Protein Standard Broad Range	BioLabs
DarmaFect 1 Reagent	Dharmacone
Dimethyl sulfoxide (DMSO)	Sigma
Disodium phosphate	Fisher
Dithiothreitol (DTT)	Bio-Rad
Dulbecco's Modified Eagle Medium (DMEM), high glucose, pyruvate	Gibco
EGF	Sigma
Fibronectin bocine plasma	Sigma
Foetal bovine serum (FBS)	Gilson
Glass-bottomed 3.5cm dishes	StarLab
Glucose	Fisher
Glycerol	Fisher
Glycine	Sigma
High-Capacity cDNA Reverse Transcription Kit	Appliedbiosystems
Hs_ADAMTS5_1_SG QuantiTect Primer Assay	Qiagen
Hs_CXCL8_1_SG QuantiTect Primer Assay	Qiagen
Hs_GAPDH_1_SG QuantiTect Primer Assay	Qiagen
Hs_SDC4_1_SG QuantiTect Primer Assay	Qiagen
Insulin	SLS
InvitrogenTM LipofectamineTM 2000 Transfection Reagent	ThermoFisher
Lactose	Sigma
Luna® Universal One-Step RT-qPCR Kit	New England Biolabs

Magnesium sulphate	AnalaR
Matrigel BM matrix, GF reduced	Corning
GeneJet Plasmid Maxiprep kit	Fisher
Medium 199	Sigma
Methanol	Fisher
Methylcellulose	Sigma
Microplate PCR 384 well	Alphalaboratories
Mm_Adamts5_1_SG QuantiTect Primer Assay	Qiagen
Mm_Gapdh_3_SG QuantiTect Primer Assay	Qiagen
NuPAGE, LDS Sample Buffer (4X)	Fisher
On target plus control siRNA non-targeting siRNA #4	Horizon
ON-TARGETplus Human RAB25 siRNA	Horizon
ON-TARGETplus Human SDC4 siRNA	Horizon
Phalloidin Alexa Fluor 555	ThermoFisher
Phalloidin Alexa Fluor 647	ThermoFisher
Potassium dihydrogen phosphate	Fisher
Purified mouse andt-CD29	BD Transduction Laboratories
PVDF membrane	IMMOBILON-FL
Polyvinylpyrrolidone **(**PVP)	Sigma
QiaShredder	QIAGEN
qPCRBIO SyGreen Blue Mix Lo-ROX	PCRBIOSYSTEMS
QuantiNova® SYBR® Green PCR Kit	QIAGEN
Rnase-free water	Cleaver scientific and Horizon Discovery
RNeasy Mini Kit (50)	QIAGEN
RPMI-1640, L-Glutamine	Gibco
Sodium chloride	Sigma-Aldrich
Sodium deoxycholate	Sigma-Aldrich

Sodium sulphate	
Soluble collagen I	Bio Engineering
Tris(hydroxymethyl)aminomethane (Tris)	Sigma-Aldrich
Triton X-100	Sigma
Trypsin-EDTA	Sigma
Tryptone	Gibco
Tween-20	Sigma
Ultra-LEAF™ Purified Rat IgG1, κ Isotype Ctrl Antibody, Rat (IgG1k)	BioLegend
VECTASHIELD Antifade Mounting Medium with DAPI	VECTOR laboratories
Yeast	ForMedium

2.2 Cell culture

A2780 ovarian cancer cells, gifted by Prof Jim Norman's lab (Cancer Research UK Scotland Institute) and generated as described in Cheng et al., 2004, established from an ovarian endometroid adenocarcinoma with Rab25 overexpression (A2780-Rab25), or with control vector pcDNA3 (A2780-DNA3); Ovcar3 cells, obtained from Prof Patrick Caswell (The University of Manchester), established from the ascites of a patient with progressive ovarian adenocarcinoma; and Ovcar4 cells, established from a high-grade serous ovarian adenocarcinoma from a patient refractory to cisplatin, were cultured in RPMI media supplemented with 10% foetal bovine serum (FBS). MDA-MB-231, a metastatic breast cancer cell line, and SKOV3, established from the ascitic fluid of a 64-year-old caucasian female with an ovarian cancer, were cultured in DMEM supplemented with 10% FBS. Epithelial cell line from the mesothelium isolated from pleural fluid of non-cancerous individuals and immortalised by transfection of pRSV-T plasmid, MET-5a-GFP, was obtained from Francis Jacobs lab (Department of Biomedicine, University Hospital Basel). It was cultured in Medium 199 supplemented with 10% FBS, 3.3 nM epidermal growth factor (EGF), 400 nM

hydrocortisone, 870 nM bovine insulin and 20 mM HEPES. All cell lines were maintained at 37 degrees C with 5% $C0_2$ and split as needed (max every 4 days). Mouse embryonic fibroblasts (MEFs) from a SDC4 knock-out mouse and wild type MEF were cultured in DMEM with 10%FBS and 10nM interferon gamma (from Dr Bass lab, University of Sheffield). They were maintained at 33 degrees C with 5% CO_2, to maintain the KO stable as it is expressed under a temperature-sensitive promoter with interferon gamma.

For cell splitting, media was removed from the cells, and they were washed with phosphate buffer saline (PBS), after which cells were incubated with 0.25% trypsin-EDTA or TrypLE for 5 to a maximum of 10 minutes. Trypsin was then neutralised by resuspending the cells in complete medium. The cells are then seeded in 10 cm tissue culture dishes. Ovcar3 and Met-5a-GFP were split at a ratio of 1:3 while A2780's at a ratio of 1/20 every 3 to 4 days.

For long term storage, cells were cryopreserved. Once cells reached more than 70% confluency, they were trypsinised and neutralised in complete medium after which they were centrifuged at 1000 rpm for 3 minutes at room temperature (RT). Two solutions were prepared for preservation: A) 50% complete medium and 50% FBS for a total of 500µl and B) 80% FBS and 20% DMSO for a total of 500 µl, per 10cm dish that needed freezing. The pellet was then suspended in solution A and added into cryovials. Solution B was added on top by gently pipetting the solution into the wall of the vial. Each vial was then gently inverted and placed into Corning ™ CoolCell cell freezing container into a -80 degrees C freezer for a few days before being moved to liquid nitrogen. Cells were recovered from cryo by fully thawing the vial in a water bath before adding the whole millilitre of solution to a 10 cm dish containing 10 ml of media. Cells are split the next day and passaged again before using for experiments to ensure normal behaviour.

2.3 Ovcar3/MET-5a-GFP Coculture assay

35 mm glass bottom dishes were coated with 25 µg/ml FN for 1 hour at 37 degrees C to allow polymerization. 1/20 Ovcar3 cells and 1/20 MET-5a-GFP cells, from a confluent 10cm dish, were added to the dish together with a 50/50 mix of RPMI and Medium 199 media for a total of 2 ml. Cells were incubated at 37 degrees C for 6 days with no media change or 12 days with one media change at day 6. Cells were then assessed by immunofluorescence.

2.4 2D and 3D Immunofluorescence staining

For any type of staining cells were fixed with 4% paraformaldehyde (PFA) for 15 minutes in sterile conditions. After which cells were washed with PBS and permeabilised with 0.25% Triton X-100 in PBS for 5 minutes.

For 2D antibody staining, cells were blocked using 1% bovine serum albumin (BSA) for 1 hour at RT. Respective primary antibodies or conjugated antibodies were diluted in PBS and added to the dishes for 1 hour at RT (table 2.2). Cells were washed 3 times with PBS. If the antibody was not conjugated, a secondary antibody, anti-mouse IgG Alexa Fluor 555 or anti-mouse IgG Alexa Fluor 488, was added and incubated for 45 minutes at RT. Cells were washed again with PBS and incubated with Phalloidin Alexa Fluor 555 or Phalloidin Alexa Fluor 647 when needed, for 10 minutes at RT. Cells were finally washed twice with PBS, once with dH_2O and Vectashield antifade mounting medium with DAPI was added for preservation. Dishes were then kept at 4 degrees C until imaged.

For 3D antibody staining, cells were blocked using Immunofluorescence wash (IFw) (1xPBS with 0.3gNaN_3, 0.5g BSA, 1 ml Triton X-100 and 0.2ml Tween for a total of 500ml, pH 7.4) for 2 hours at RT on a rocker. Respective primary antibodies or conjugated antibodies in IFw were added to the dishes and incubated overnight at 4 degrees C. Cells were washed 3 times with PBS-1%Tween for 5 minutes. If the antibody was not conjugated, a secondary antibody was added in IFw to the sample and incubated for 4 hours at RT. Cells were washed again with

PBS-Tween and incubated with Phalloidin Alexa Fluor 555 or Phalloidin Alexa Fluor 647, when needed, for 1 hour at RT. Cells were finally washed 3 times with PBS-1%Tween for 5 minutes and Vectashield antifade mounting medium with DAPI was added for preservation. Dishes were then kept at 4 degrees C until imaged.

Table 2.2. ***IF antibodies.*** Dilution ratio for the primary and secondary antibodies used for IF.

Antibody	Dilution Ratio	Provider, catalogue n°
Phalloidin Alexa Fluor 555	1:300	Thermo Fisher, A34055
Phalloidin Alexa Fluor 647	1:300	Thermo Fisher, A22287
Anti-Mouse IgG Alexa Fluor 488	1:3000	Invitrogen, A21202
Anti-Mouse IgG Alexa Fluor 647	1:3000	Invitrogen, A28181
Mouse anti-human α5 integrin	1:250	BD Transduction Laboratories, 555651
Alexa Fluor 647 anti-human CD29 (β1 integrin)	1:250	BioLegend, 303018
Mouse anti-Fibronectin	1:250	BD Transduction Laboratories, 610077

2.5 Spheroids generation and Clearance assay

For the generation of spheroids the hanging drop method described in Bayarmagnai *et al.*, 2019 was used. 1/10 Ovcar3 cells, 1/20 A2780-Rab25 or DNA3 cells, from a confluent 10cm dish, were diluted in 2ml of media with methylcellulose (MTC), final concentration 4.8 mg/ml and 20µg/ml soluble collagen I for A2780 cells or 40µg/ml soluble collagen for Ovcar3 cells, ensuring spheroids are produced more reliably as it promotes cell aggregation and droplet

attachment to the petri dish. From this solution, 20µl droplets were formed on the lid of a 10cm petri dish. The dish was filled with PBS to avoid drying out due to media evaporation. The lid is then closed so that drops are hanging.

For embedding, spheroids were collected after 48 hours of incubation at 37 degrees C. Spheroids were then collected in an Eppendorf tube with media to remove the MTC solution by gently pipetting up and down. Spheroids were then allowed to set at the bottom of the tube and supernatant was removed. Spheroids were collected individually and embedded into 200µl of 4mg/ml rat tail collagen I and 4mg/ml GelTrex. The matrigel/collagen I mixture containing the spheroid was deposited into a 24 well glass bottom non adherent plate and placed in the incubator at 37 degrees C, 5% CO_2 for 30 minutes to allow polymerization. Finally, the matrix was covered with 1ml media. 50µM $\alpha 5$ inhibitor, ATN-161, was added to both the matrigel/collagen mixture and the media, water was used as control. Spheroids were imaged every day using an Olympus fluorescent microscope with a 4x objective. Analysis was performed in ImageJ (Schindelin et al., 2012), area of the core of the spheroid was measured at the different timepoints and subtracted to the total spheroid area, measured by drawing a region of interest around the invasive strands migrating from the spheroid, to obtaining the invasion area.

For clearance assays (figure 2.1) 35mm glass bottom dishes or 6 well plates were coated with 25µg/ml FN and incubated for polymerization for 1 hour, after which PBS was added and dishes/plates were kept at 4 degrees C overnight or until needed. After coating, MET-5a-GFP cells were seeded (1/5 from a 10cm dish) and incubated overnight to form a confluent monolayer of cells. A2780-Rab25 and DNA3 spheroids were collected after 48 hours hanging while Ovcar3 spheroids were collected after 72 hours. Spheroids were then placed in an Eppendorf tube with PBS to remove the MTC solution by gently pipetting up and down. Media was removed from the dishes with the monolayers and spheroids were then placed on top of

the monolayer by gently pipetting them on top. Gently, drop by drop, 1ml media was added on top avoiding moving the spheroids. Dishes were then kept at 37 degrees C, 5% CO_2 for 4 hours for A2780 cells and for 6 hours for Ovcar3 cells. A2780s/METs dishes were either imaged live with a Nikon W1 spinning disk microscope, 10x objective, every 2 hours for 16 hours or with an Olympus Fluorescence microscope, 4x objective at 0, 3 and 6 hours. Ovcar3/METs clearance were imaged at 0, 3, 6, 24, 48 hours using an Olympus Inverted Fluorescence microscope 4x objective. Clearance was assessed by measuring the area surrounding the spheroid in which MET-5a-GFP fluorescence was displaced either by A2780 or Ovcar3 cells.

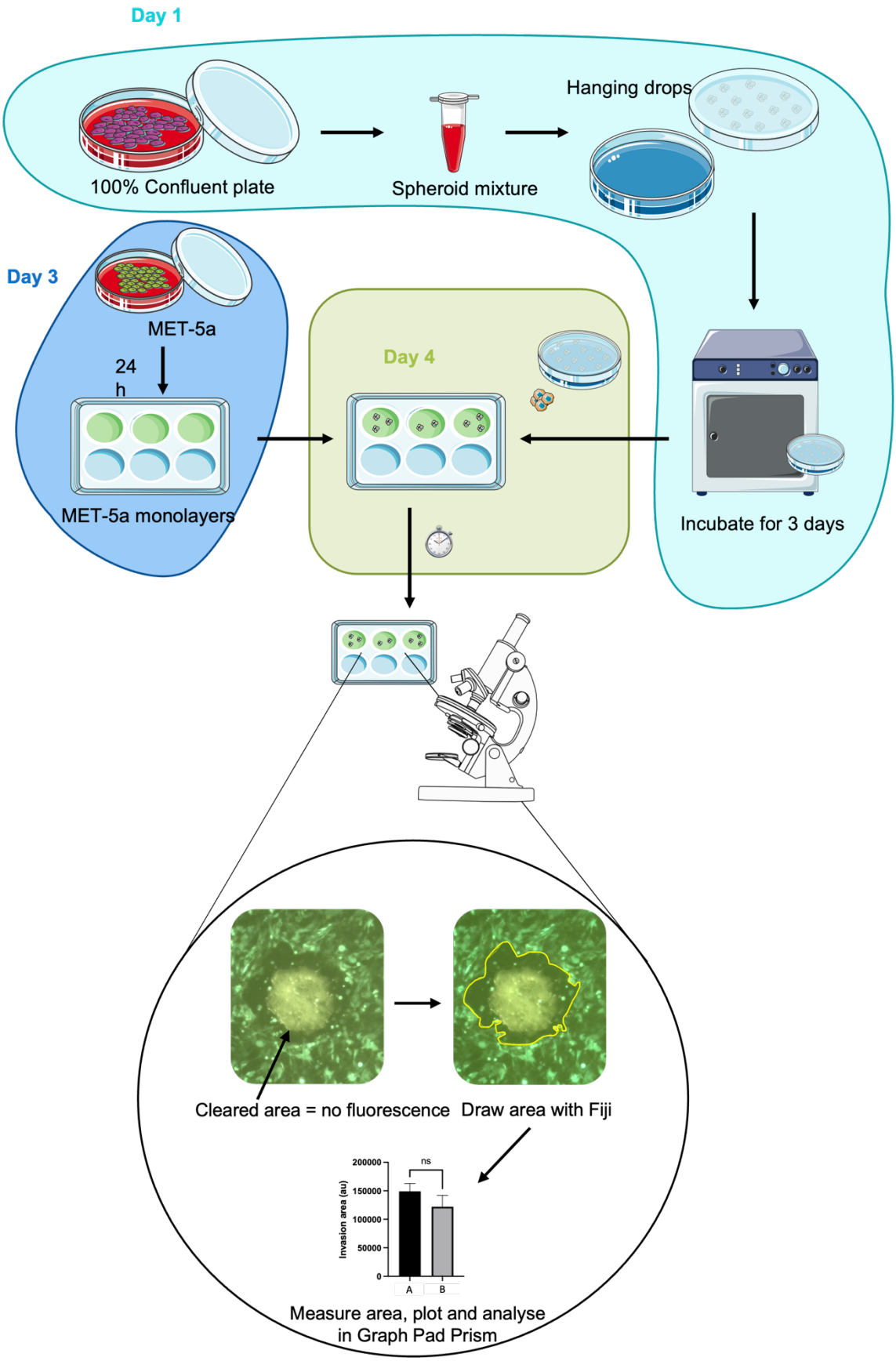

Figure 2.1: ***Clearance assay procedure***. Spheroids were generated on day 1, using the hanging drop method from a confluent plate of Ovcar3 cells and incubated for three days. One day before the spheroids are ready, MET-5a-GFP cells are seeded to obtain a confluent monolayer (day 3). Spheroids are then placed on top and imaged at

different timepoints on day 4. Timeline of the experiment is highlighted by different coloured areas. Analysis was then carried out by measuring the area cleared by the spheroid.

2.6 Western blotting

6-well plates were coated with 25µg/ml FN or 2mg/ml collagen I and left to polymerise for one hour at 37 degrees C, 5% CO_2, plastic was used as control. Cells were seeded and incubated for 24 hours to obtain a confluent monolayer.

For ADAMTS5 protein expression, cell media was changed after 6 hours from Dulbeecco's Modified Eagle Medium (DMEM) supplemented with 10% FBS or RPMI supplemented with 10% FBS to DMEM or RPMI with no FBS and kept at 37 degrees C, 5% CO_2 for three days. Cell media was collected, and the proteins were concentrated following a four-step centrifugation protocol, table 2.3 and figure 2.2.

For all western blot samples, cells were lysed in 100µl SDS-lysis buffer (50mM Tris pH7, 1%SDS in water). Lysates were collected into QiaShredder columns and centrifuged at RT for 5 minutes in a mini bench centrifuge. 4 x NuPAGE was mixed with dithiothreitol (DTT, final concentration 1mM) and proteins to a 4:1 ratio. 15µl to 20µl of samples were loaded into a Bio-Rad 4-15% Mini-PROTEAN precast polyacrylamide gel together with 3µl BioLabs protein ladder. Gels were run at 100V for 75 minutes in running buffer (25mM Tris base, 192mM glycine and 1% SDS in deionised water). Proteins were then transferred into FL-PVDF membrane in Towbin transfer buffer (25mM Tris, 192mM glycine, 20% methanol in deionised water) for 75 minutes at 100V. Immobilon transfer membranes were blocked for 1 hour in 5% BSA. Membranes were incubated with primary antibodies (table 2.4) in TBST (10mM Tris-HCl pH7.4, 150mM NaCl, 0.1% Tween-20 in deionised water) overnight at 4 degrees C. The next morning membranes were washed 3 times with TBST for 10 minutes with rocking. Secondary antibodies in TBST supplemented with 0.01% SDS were then added to the membrane for 1 hour at RT with rocking. Membranes were washed again 3 times with TBST

for 10 minutes with rocking and washed 3 times with deionised water before being imaged using a Licor Odyssey Sa system. Analysis was performed using ImageStudioLite. The bands intensity was quantified with Image Studio Lite and normalised to housekeeping protein intensity.

Table 2.3. ***Conditioned media sample collection***. 4-step centrifugation to obtain a concentrated sample of protein containing conditioned media.

Centrifuge speed (g)	Time
300 g	10 min
2000 g	10 min
max (5250) g	30 min
VivaSpin Centrifuge concentrator at 4000g Membrane 10000 MWCO	Until media drops to 250µl

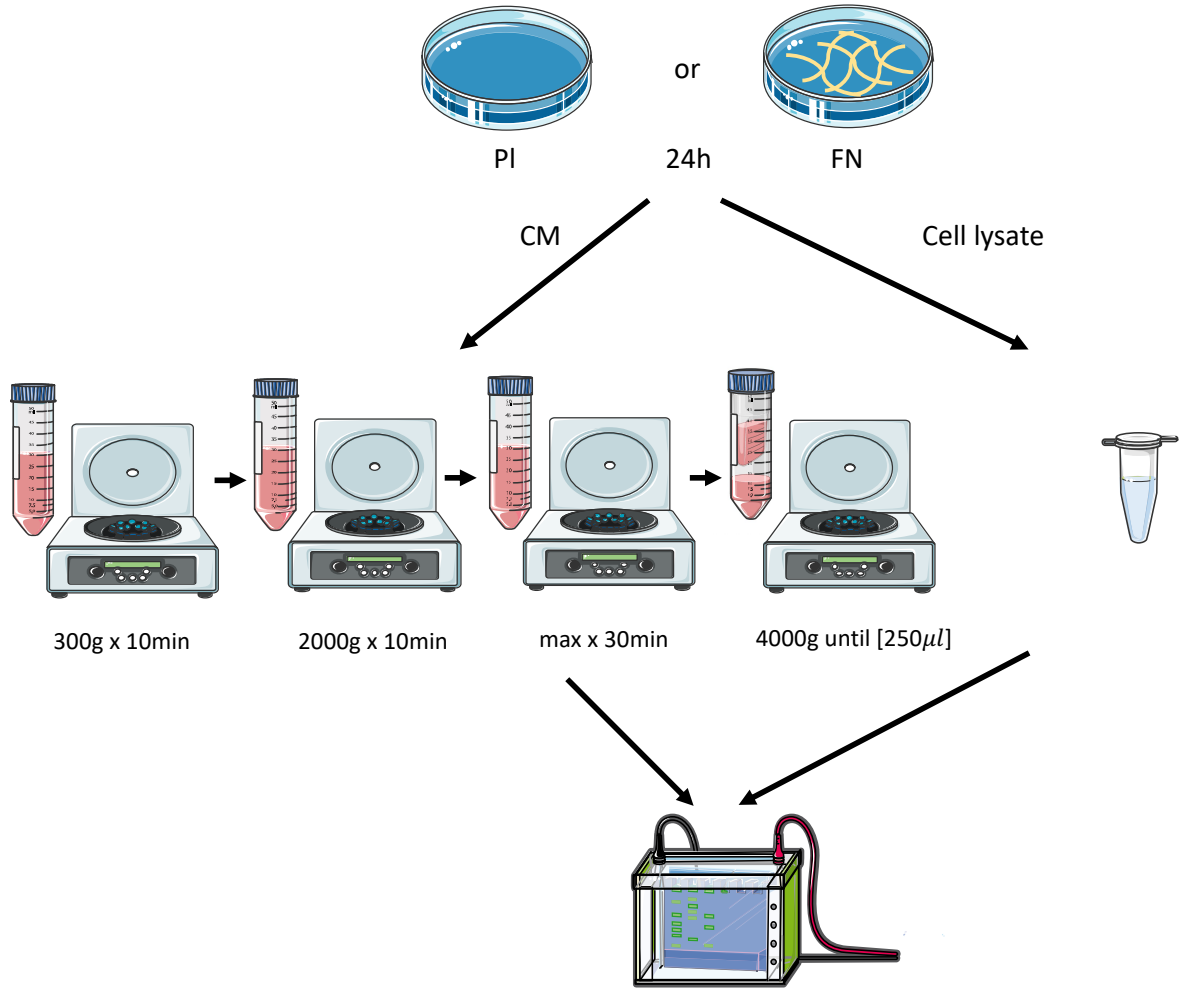

Figure 2.2. ***Centrifuge speed steps for protein concentration.*** 15 ml Falcon tubes were used during the first three steps. In the last Filter tube VivaSpin, 10K MWCO, was used to concentrate higher molecular weight proteins.

Table 2.4. ***Western blot antibodies.*** Primary and secondary antibodies used for western blot including the dilution ratio and supplier.

Antibodies	Dilution	Supplier, catalogue n°
Rabbit anti-Rab25	1:600	Proteintech, 13189-1-AP
Rabbit anti-ADAMTS5	1:250	Abcam, ab41037
Mouse anti-FN	1:1000	BD Transduction Laboratories, 610077
Mouse anti-CD29 (β1 integrin)	1:1000	BD Transduction Laboratories, 610467
Mouse anti-CD49b (α2 integrin)	1:1000	BD Transduction Laboratories, 611017
Rabbit anti-CD49e (α5 integrin)	1:2000	Proteintech, 84468-4-RR
Mouse anti-GAPDH	1:1000	Santa Cruz biotechnology, sc-477224
Mouse anti-Flag M2	1:5000	Sigma, F3165
Anti-mouse IgG IR-Dye 800 CW	1:30,000	Licor, 925-32210
Anti-rabbit IgG IR-Dye 680	1:20,000	Licor, 926-68071

2.7 Transformation of bacteria

Competent $DH5_{\alpha}$ cells were mixed with plasmid DNA (figure 2.3). Plasmids were integrated in bacteria via heat shock. Bacteria were allowed to grow at 37 degrees C overnight in 100μg/ml ampicillin or 100μg/ml ampicillin with 30μg/ml chloramphenicol agar plates, depending on the vector. DNA was obtained following GeneJet Plasmid Maxiprep kit protocol, as per manufacturer's instructions. DNA concentration was measured using a Nanodrop microvolume spectrophotometer. DNA was stored at -20 degrees until needed.

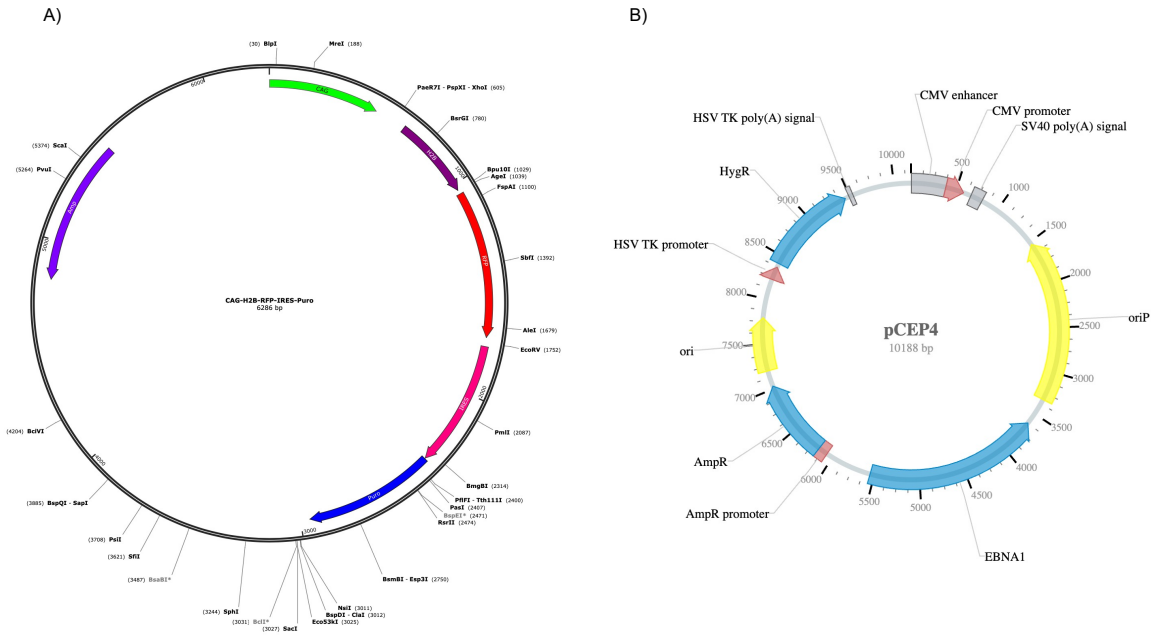

Figure 2.3. ***Plasmid maps.*** Plasmid map of the CAG-H2B-RFP-IRES-Puro plasmid (A) and pCEP4 backbone vector, ADAMTS5 with a FLAG-TAG at the C-terminus was inserted in it as described in Santamaria et al., 2019 (B).

2.8 Transfection of cancer cells

For transfection of DNA, 4x10^5 A2780-DNA3 were seeded overnight. On the following day, media was removed, 2.5µg ADAMTS5 DNA was added to 250µl RPMI FBS free media and 5µl Lipofectamine 2000 in 250µl RPMI FBS free media. Both solutions were mixed and incubated for 20 minutes at RT, after which they were added on the cells with additional 500µl RPMI FBS free media at 37 degrees C for 6 hours, after which media was changed to RPMI media with 10% FBS. To assess the transfection, cells were lysed as described above in section 2.5 Western blotting. ADAMTS5 expression was detected using an anti-FLAG antibody, as the construct contains a FLAG-TAG at the C-terminus.

For siRNA transfection, 4x10^5 cells were seeded in each well of a 6 well plate. 10µl of 5µM siRNA was mixed with 190µl Opti-MEM per well. At the same time, 2µl Dharmafect I was mixed with 198µl Opti-MEM. The two solutions were then mixed together and incubated for 20 minutes at RT. After which the solution was added to cells, that were incubated at 37 degrees

and 5% CO_2 for 24 hours before media was changed. Knocked down was assessed by qPCR, 1 day after transfection.

2.9 Stable cell line generation

For the generation of H2B-RFP stable cell lines, A2780s and Ovcar3 cells were seeded in 6 well plates to reach confluency on the next day. 5µl of Lipofectamine 2000 was added to 245µl Opti-MEM per transfection. In another Eppendorf tube 2.5µg H2B-RFP were mixed with 250µl Opti-MEM. The two solutions were then combined and incubated for 20 minutes at RT. 500µl of Lipofectamine/DNA/Opti-MEM mixture was added to each well, in the presence of additional 500µl of Opti-MEM. The cells were incubated at 37 degrees C for 6 hours before changing the media to RPMI with 10% FBS. On the next day, 25% of the optimal puromycin concentration for the cell line was added to the media. Each day the puromycin concentration was incremented to 50%, 75% and 100% of optimal concentration if cell were not less than 50% confluent. The optimal concentration was established by doing a kill curve, 1.5µg/ml was found to be optimal for A2780 cells and 1µg/ml was found to be optimal for Ovcar3 cells. Cells were grown in puromycin for a week and then puromycin was removed. To maintain high H2B-RFP expression cells were treated with 1.5µg/ml puromycin for one passage once a month.

2.10 Scratch/wound healing assays with matrix overlay

For scratches done manually (figure 2.4), A2780 (DNA and/or Rab25) or Ovcar3 cells were detached from a confluent 10cm dish using Trypsin EDTA and neutralised using 10% FBS containing media. Cells were seeded into a 12-well plate at a density of 1/12 and incubated overnight to achieve confluency. The next morning, 0.5 mg/ml matrigel or 0.5mg/ml matrigel plus 25µg/ml FN solutions in 10% FBS media were prepared for the overlay. Monolayers were scratched manually by doing a cross using the end of a 200µl pipette tip. Cells were either

covered by 300µl 10% FBS media, matrigel or matrigel plus FN and left in the incubator for 30 minutes to polymerise, after which wells were topped up with full media or media containing 10µM ADAMTS5 inhibitor or DMSO control. ADAMTS5 inhibitor is a thioxothiazolidinone compound that contains a Zn^{2+} chelating motif which inhibits ADAMTS-5 with higher selectivity over ADAMTS-4. Each branch of the scratches was imaged at 0h, 3h, 6h and 24h after adding the inhibitors using an Olympus Inverted Fluorescence Microscope. The area of the scratch was manually calculated by tracing the perimeter of the non-invaded area of the well using Image J.

For scratches imaged live, scratches were done as described above. After matrix polymerisation, plates were imaged live using the Nikon Widefield live-cell system (Nikon Ti eclipse with Oko-lab environmental control chamber) with a Plan Apo 10X objective. Each arm of the scratch was imaged, for a total of 4 images per well. Images were acquired for a total of 16h, 10-minute time frames. Cell migration was manually tracked using the manual tracking plug in Image J. Velocity and forward migration index (FMI) was calculated using the chemotaxis plug in Image J. FMI is defined as the efficacy of the cells to migrate forwards in relation to both axis, x and y. To properly interpret the data the expected effect needs to be perpendicular or parallel to the axis.

For scratches done with inserts (Ibidi, culture insert 2 well for self-insertion, catalogue number 80209), Ovcar3 or Ovcar3/MET-5a-GFP cells were detached from a 10cm dish using Trypsin EDTA and neutralised using 10% FBS media. Square inserts with two chambers were added to wells of a 12 well plate, cells at a density of 1/12 were added to 1 ml of media and mixed well before adding 70ul of mixture to each chamber. For coculture scratches, MET-5a-GFP and Ovcar3 cells were mixed at a 1:1 ratio into the 1ml media. 1 ml of PBS was added outside the chamber to avoid cell trying out and the plates were incubated overnight to form a monolayer. The next morning, 0.5 mg/ml matrigel or 0.5 mg/ml matrigel plus 25µg/ml FN

solutions were prepared for the overlay. Inserts were detached from the wells using tweezers. Cells were either covered by 300µl 10% FBS media, Matrigel, matrigel plus FN or Collagen I solutions and left in the incubator for 30 minutes to polymerise, after which wells were topped up with full media or media containing 10µM ADAMTS5 inhibitor or DMSO control. The scratches were imaged at 0h, 3h, 6h and 24h after adding the inhibitors using an Olympus Inverted Fluorescence Microscope. The area of the scratch was manually calculated by tracing the perimeter of the non-invaded area using Image J.

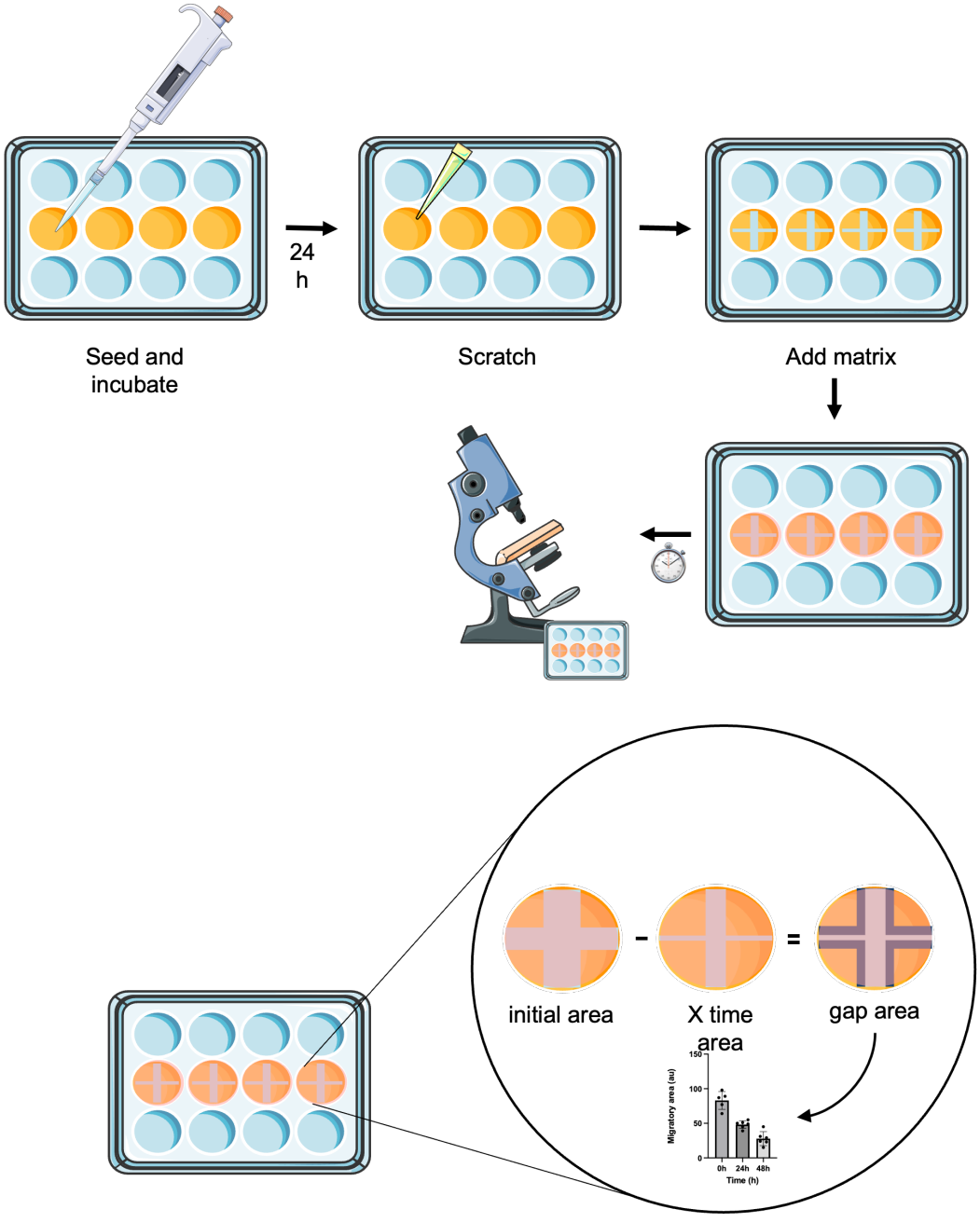

Figure 2.4. ***Scratch assay protocol.*** First cells are seeded and incubated overnight to achieve a confluent monolayer, then they were manually scratched forming a plus shape. Matrix was added on top and incubated for 30 min to polymerise. Finally, scratches were imaged at 0h, 3h, 6h and 24h. Migration was measured as the scratch area over time.

2.11 qPCR

1/12 A2780-Rab25 or A2780-DNA3 cells, 1/10 Ovcar3 and MEF, from a 10cm dish, were seeded into a 6-well plate precoated with FN at 25µg/ml or on plastic. Cells were then incubated for 24h at 37 degrees C before extracting the mRNA. Cells were detached using 0.25% trypsin-EDTA (for MEF) or TrypLE (for Rab25, DNA3 and Ovcar3) and neutralised after a 5-minute incubation at 37 degrees C with complete media. Cells were spun down at 1000rpm for 3 minutes and they were washed with PBS once after which they were spun down again. Supernatant was aspirated without disturbing the pellet and Eppendorfs were snap frozen at -80 degrees C. mRNA was extracted according to the manufacturer's protocol (RNeasy® Mini – Qiagen).

For one-step qPCR, Luna ® Universal One-Step RT-qPCR Kit was used. Samples were prepared by adding less than 1µg RNA, 5µl Luna Universal One-Step Reaction Mix, 0.5µl Luna WarmStart ® RT Enzyme Mix, 0.8µl mix forward and reverse primer and toped up with RNase free water for a total of 10µl.

For two-step qPCR, cDNA was first synthesised with High-Capacity cDNA Reverse Transcription Kit (Fisher). Afterward, loading master mix containing 5µl QuantiNova SYBR® Green PCR Kit (Qiagen) master mix, 1µl forward and reverse primer and 1µl RNase free water was prepped and mix with 3µl cDNA solution (5ng/µl).

Finally, for both one-step and two-step reactions, 10µl samples were loaded on a 324 well plate. Quantstudio 12K flex real-time PCR system was used as analyser in the SYBR ® mode, table 2.5 includes machine settings. Expression levels were calculated using the $2^{-\Delta\Delta}$Ct method

(Livak and Schmittgen, 2001). GAPDH was used as housekeeping gene. Each sample was tested in technical triplicates.

Table 2.5. ***Settings for the qPCR machine reactions.*** Table includes the time and temperature for the set-up of the qPCR reactions.

one-step qPCR							
	Hold stage		PCR Stage		Melt curve Stage		
Temperature (Degrees Celsius)		95	95	60	95	60	95
Time (min:sec)		2:00	0:10	0:30	0:15	1:00	0:15
Two-step qPCR							
	Hold stage		PCR Stage		Melt curve Stage		
Temperature (Degrees Celsius)	55	95	95	60	95	60	95
Time (min:sec)	10:00	1:00	0:10	1:00	0:15	1:00	0:15

2.12 FN fragments purification

2 bottles of 450ml 2YT autoinduction medium (table 2.6) in two 2L flasks were prepared and autoclaved in advance, together with 20x TBS (12.1g Tris pH7.5 and 87.7 g NaCl in 500ml water),1x TBS and 2YT agar.

Table 2.6. ***Bacteria growth medium recipe.*** List of the supplements needed to make the autoinduction media including final concentration needed.

2YT Medium Base (500ml)			
5g	Tryptone		
2.5g	Yeast extract		
450ml	H_2O		
Additives for auto-induction media (500ml)			
	Substance	Stock	Final Conc.
25ml	Na_2HPO_4	500mM	25mM
12.5ml	KH_2PO_4	1M	25mM
25ml	NH_4Cl	1M	50mM
2.5ml	Na_2SO_4	1M	5mM
1ml	$MgSO_4$	1M	2mM
1ml	$CaCl_2$ (add last)	1M	2mM
2.5ml	Glycerol (warm)		0.5%
0.25g	Glucose		0.05%
1g	Lactose		0.2%
0.5ml	Ampicillin	100mg/ml	

Transformed competent cells BLR:DE3 pLysS bacteria were mixed with H0 fragment plasmid (Makarem et al., 1994) or the 50K fragment plasmid (Danen et al., 1995). Plasmids were

integrated in bacteria via heat shock. Bacteria were allowed to grow at 37 degrees C overnight in 100µg/ml ampicillin and 30µg/ml CAP 2YT agar plates. The following day, one colony of bacteria for each plasmid was inoculated in 2x10ml 2YT media with 1000µg/ml Ampicillin and 30µg/ml CAP. Bacteria was put in incubator for approximately 8 hours. After, all the other components of the autoinduction media were added to a flask and it was inoculated with 0.5ml of the starter cultures. As $CaCl_2$ precipitates, it is important to add it at the end when the media is well mixed. After an overnight incubation at 37 degrees C in shaker incubator, the bacterial culture was divided into 4x 250ml centrifuge tubes, that were balanced with water. Cultures were then spun down at 5000rpm for 15min using an SLA-1500 rotor at 4 degrees C. The pellets were combined and resuspended in 40ml 1xTBS with 1/1000 complete protease inhibitor. Resuspended bacteria were then frozen in 50ml tube at -70 degrees C overnight. On the following day, bacteria were thawed in a beaker containing RT water to aid cells lysis. Bacteria were further sonicated six times for 30 seconds.

The two FN fragments were purified in different ways (figure 2.5). For the H0 fragment, 50µl of 10mg/ml DNase/Rnase was added to the lysate and incubated on ice for 30 minutes. While incubating, 3ml of glutathione magnetic beads were washed three times with 1x TBS. Cell debris were then pelleted by centrifugation using a JA25.50 rotor at 20,000 rpm for 30 minutes at 4 degrees C. Lysate was then added to the glutathione beads and incubated for 30 minutes at RT to allow binding. Beads were then washed five times using 25ml of ice-cold 1x TBS by leaving them in a rotator for 5 minutes each. Beads were then resuspended in 2ml 50mM Tris-HCl pH 8.0 with 10mM $CaCl_2$. 50U of thrombin were added to it and the mix was left for digestion for 4 hours at RT. Beads were removed from the solution using a magnet. Finally, eluted protein was passed through a 1ml benzamidine HiTrap column. Protein was aliquoted and stored at -20˚C. Protein was loaded on a Bis-Tris gel, to ensure correct elution. Gels were then stained with Coomassie stain to detect proteins.

For the 50K fragment, Buffer A and Buffer B were prepared in advance and diluted to have 1L of 1x Buffer A and Buffer B (table 2.7). While the cell debris were pelleted by centrifugation using a JA25.50 rotor at 20,000 rpm for 30 minutes at 4 degrees C, DEAE Sepharose™ fast flow, agarose, was packed into a 20cm x10mm column and equilibrated with 100ml of Buffer A at 7rpm flow rate. Clear lysate was then loaded in the column at 7rpm flow rate (if the lysate is not clear, it needs to be spun down again). It is important to keep some of the flow through and loaded sample for analysis. Column was then washed overnight at rate 3rpm with 100ml Buffer A. The proteins were then eluted from the column by running a gradient of 300ml Buffer A against Buffer B at rate 7rpm. Once eluted, profile was checked on a Bis-Tris gel, by loading 10µl sample mixed with 10µl SDS-PAGE buffer of every other fraction starting from fraction 8, including the original lysate and flow through as control. Gels were then stained with Coomassie stain and the fractions with the highest protein content were pooled together and concentrated down to 10ml using Vivaspin20, 3000 MWCO PES in a Mellor centrifuge at maximum speed. Proteins were then aliquoted and stored at -20˚C. Finally, the column was stripped with more than a 100ml high salt buffer and washed with more than 100ml low salt buffer before being stored away.

Table 2.7. ***Buffer A and Buffer B recipes.*** Amounts and ingredients of the high salt and low salt buffers needed for the protein concentration using the filter column and fraction collector.

20x Buffer A (500ml) Low Salt TBS		
	Substance	Stock
29.2g	NaCl	1M
28.2g	Tris, pH 6.0	400mM
500ml	H_2O	
20x Buffer B (500ml) High Salt TBS		
	Substance	Stock
73g	NaCl	2.5M
7.05g	Tris, pH 6.0	100mM
500ml	H_2O	

For both proteins, protein concentration was quantified using a BCA assay kit (Thermo Scientific, 18064090). BCA solution was prepared by diluting solution B with solution A using a 1:50 ratio, as per manufacturer's instructions. Eppendorf tubes containing 0, 2, 4, 8, 12, 16mg BSA standard (2mg/ml) and tubes with 2ul, 5ul, 10ul of the H0 and 50K fragments were prepared. To each tube, 1ml BCA solution was added. Solutions were then transferred into plastic cuvettes and incubated for 30 minutes at RT. After which, a spectrophotometer set at 562nm was used to measure the absorbance. BSA standard curve was produced using absorbance (y) against milligrams (x) using Excel. A trend line was added and with the equation generated the concentration of H0 and 50K protein elution was determined.

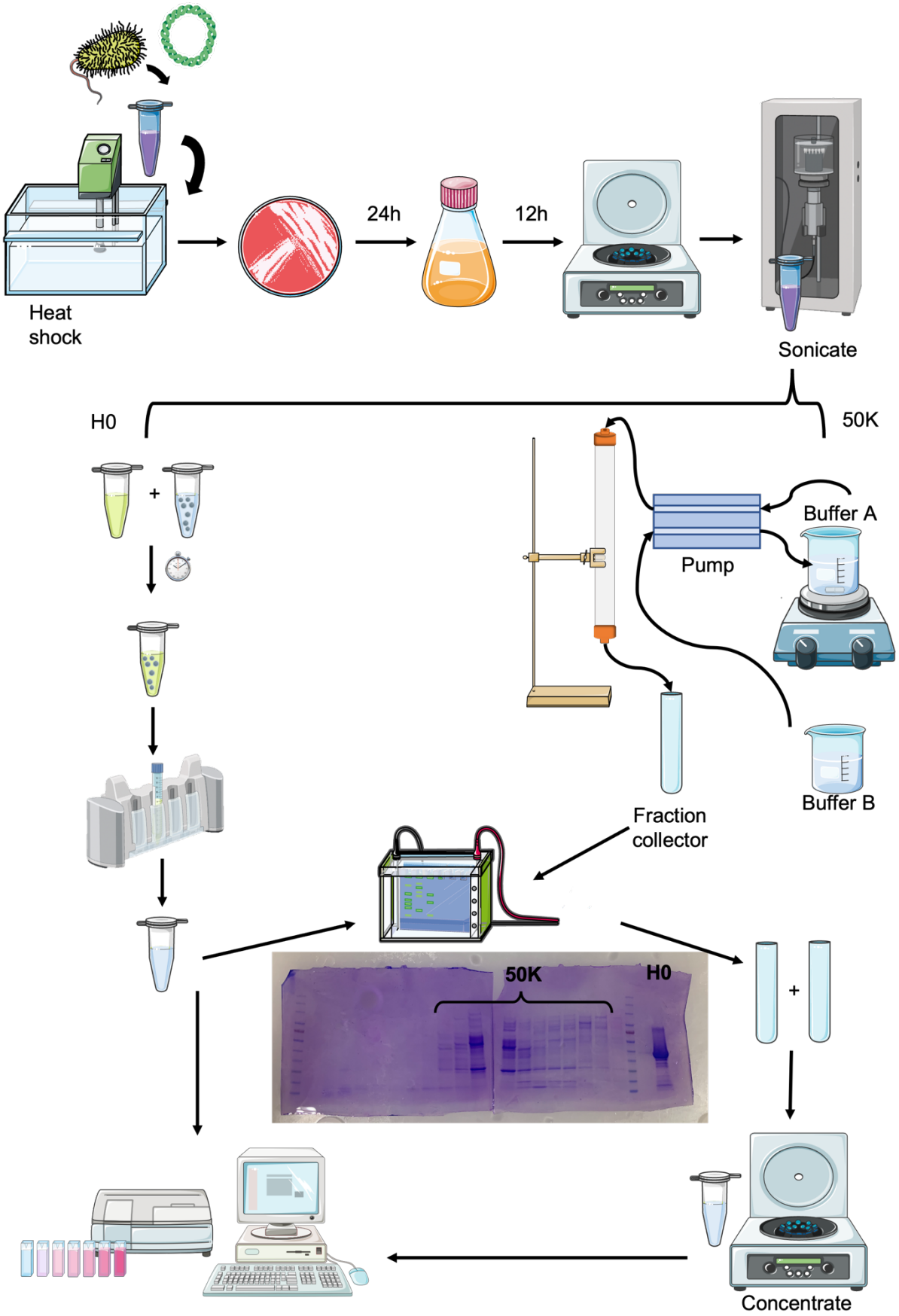

Figure 2.5. ***Illustration of the methodology followed to obtain FN fragments; 50K and H0.***

2.13 Zebrafish xenotransplants

A personal licence category B (I93771398) was obtained as per home office regulations covering modules L, E1, PIL A (theory and skills), K (theory and skills) and PIL B species zebrafish. All work was carried out under project licence PP8726269.

Adult fish, Nacre or Casper, were kept at 27–28.5 degrees C on a light–dark cycle. For mating, one male and one female were kept overnight in breeding tanks or tanks were marbled. Eggs were collected and sorted in petri dishes with E3 media and kept in a 28 degrees C incubator until day 2.5 post-fertilization.

Injection plates were prepared by melting 1.5% Agarose in E3 in the microwave for about 2 minutes and letting the agarose cool down in a thin layer over a petri dish plate. A2780 cells were detached using Trypsin and spun down at 1500 rpm for 3 min, supernatant was removed, and cells resuspended in 5 ml of PBS. Cells were counted and spun down again, ensuring all trypsin and media were removed. Cells were concentrated to $1x10^7$ cells in 1ml of PBS with 1% Polyvinylpyrrolidone (PVP).

Cells were kept on ice and 1 or 2.5-day post-fertilization (dpf) zebrafish embryos were anaesthetised with tricaine (figure 2.6). Cells were inserted in the microinjector and 2 embryos at the time were laid in the agar plate in the absence of E3 and microinjected using borosilicate capillaries with approximately 400 cancer cells in the brain ventricle (1dpf embryos) or cardiac cavity (2.5 dpf embryos). Embryos were then placed back in fresh E3 for recovery. 30min to 1-hour post-injection embryos were checked under a Leica fluorescent microscope to ensure cells were present and no cells were in the circulation. Embryos with no successful injection were culled. Embryos were then kept in a 34 degrees C incubator to ensure cell survival until they reach 4.5 to 10 dpf. 10 embryos from the anaesthetised plates were used as control and kept with the injected embryos in a 34 degrees C incubator. They were then imaged live using a Leica MZ10 F microscope or an Axio Zoom.V16 microscope.

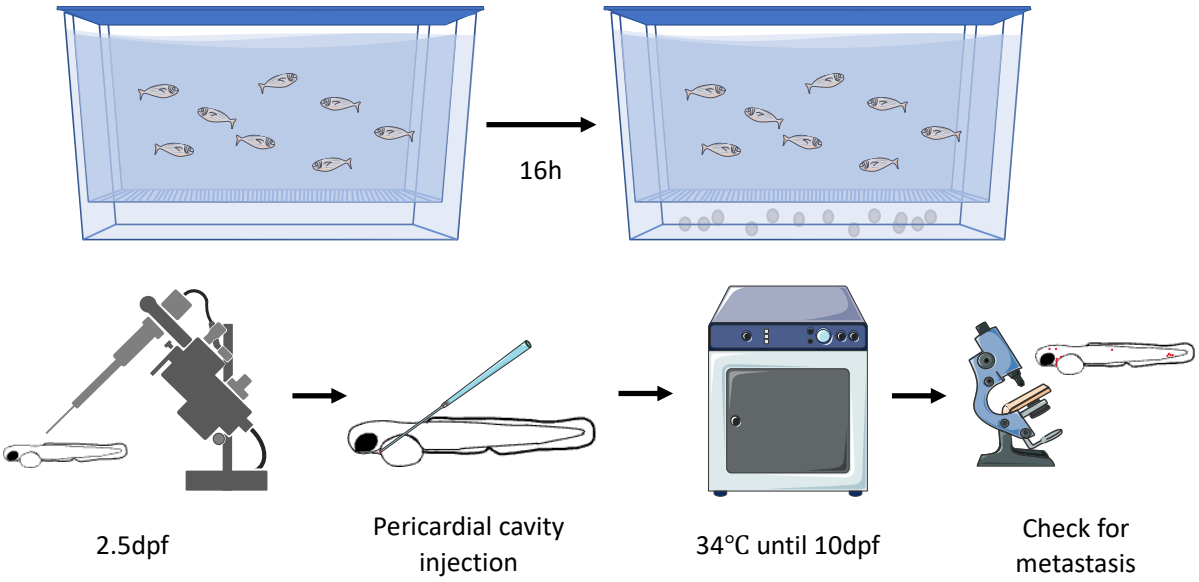

Figure 2.6. ***Zebrafish injection procedure.*** Embryos were collected and incubated at 28 degrees C until they reached 2.5dpf. Microinjector was set up and human cancer cells were injected in the pericardial cavity. Embryos were incubated at 34 degrees C up to 10dpf. Finally, embryos were imaged using a fluorescent microscope and checked for metastasis.

2.14 Statistical analysis

For each experiment, biological repeats were normalised to the control. Data were analysed and represented using GraphPad Prism 10.4.0. For experiments containing two unpaired data sets, non-parametric t tests were run (Mann-Whitney). In experiments with more than two unpaired datasets, one-way ANOVA with multiple comparisons, Kruskal-Wallis test, was performed. When having multiple variables, a two-way ANOVA with multiple comparisons was carried on. Parts of a whole graphs were used to plot percentages in observational analysis. Statistical significances were considered when the p value was less than 0.05. Super plots were generated as described in (Lord et al., 2020).

CHAPTER 3: Rab25 drives ADAMTS5 expression in a FN dependent manner via syndecan-4 in ovarian cancer cells.

3.1 Introduction:

Rab25 overexpression is observed in approximately half of ovarian cancers leading to higher aggressive state (Cheng et al., 2004; Jeong et al., 2018). In A2780 ovarian cancer cells Rab25 was found to promote migration on 3D matrices, characterised by the extension of long pseudopodia. Furthermore, direct interaction of Rab25 with ß1 integrin was discovered, which promoted α5ß1 recycling to the pseudopod tips (Caswell et al., 2007). Moreover, Rab25 was found to sort ligand-bound, active α5ß1 integrin to lysosomes. The lysosomal protein CLIC3 mediates the recycling of the integrins from the lysosome to the cell surface at the rear of the cell, activating Src which in turn promotes focal adhesion disassembly, allowing cells to move forward (Dozynkiewicz et al., 2012). Taken together, Rab25 appears to rapidly deliver inactive α5β1 integrin to the pseudopodia tip to form new adhesion, while active α5β1 integrin is sorted into CLIC3-positive lysosomes promoting disassembly of adhesions. In addition, ADAMTS5 was found upregulated in upon Rab25 overexpression when cells were cultured in 3D matrices compared to 2D matrices (Dozynkiewicz et al., 2012; Yuan et al., 2024). Additionally, we have demonstrated that Rab25 increases ADAMTS5 mRNA levels, and this was further promoted by the presence of fibroblast-generated cell derived matrix (CDM). Moreover, ADAMTS5 inhibition was found to significantly decrease pseudopod elongation and directional migration of Rab25 overexpressing cells when compared to control cells on CDM but not on plastic (Yuan et al., 2024).

FN, the ligand of α5ß1 integrin, is found in most connective/interstitial tissues. It is essential in different processes like wound healing and morphogenesis and regulates cell behaviours like adhesion, spreading and migration (Zollinger and Smith, 2017). FN interacts with different

ECM proteins, including glycosaminoglycans and cell surface receptors via specific domains. Collagen binds to domain type I 6 to 9 and domain type II 1 to 2, tenascin-C binds to different type III domains, growth factors share affinity with type II domains 12 to 14 similarly to glycosaminoglycans and proteoglycans containing heparin sulphate chains, like SDC4. This fragments are known as H0. Integrins bind FN via the RGD site located in the type III domain 10 and the PHSRN site located in type III domain 9, defined as 50K fragment (Pankov and Yamada, 2002) (Figure 3.1).

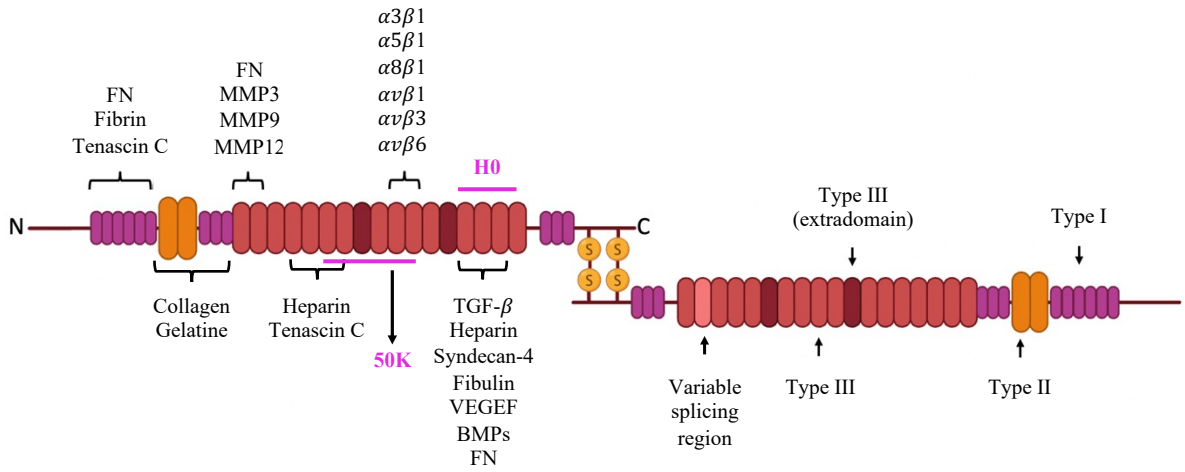

Figure 3.1. ***FN dimer structure.*** Schematic representation of the FN structure including the biding domains and binding partners. 50K FN polypeptide incorporates type III repeats 6 to 10 while H0 includes type III repeats 12 to 15.

FN is known to be highly expressed in ovarian cancer tissues, deposited by cancer associated fibroblasts or cancer cells themselves, being part of the tumour microenvironment. As FN is an abundant component of the fibroblast CDM (figure 3.2) and ADAMTS5 expression was increased when Rab25-overexpressing cells were seeded on CDM, we hypothesised that ovarian cancer cells binding to FN via α5ß1 led to the upregulation of ADAMTS5. In this chapter we found that both Rab25 and FN upregulate ADAMTS5 in ovarian cancer cells in a SDC4 dependent manner, but not in an α5ß1 dependent manner.

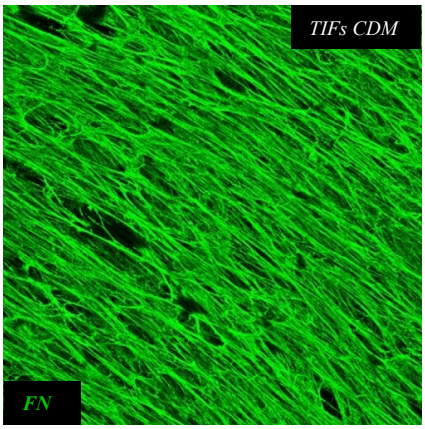

Figure 3.2. ***FN staining in CDM.*** CDM was produced by TIF cells and stained for FN (green). Image obtained from Rainero, E. (Unpublished).

3.2 Results:

3.2.1 Rab25 and Fibronectin promote ADAMTS5 upregulation:

We have recently found that the presence of fibroblast-generated matrices increased the expression levels of ADAMTS5 in A2780 cells overexpressing Rab25 (Yuan et al., 2024). As FN is one of the main ECM components of the premetastatic niche in the omentum and is highly enriched in fibroblast-generated matrices, we aimed to determine if FN leads to upregulation of ADAMTS5 in the presence of Rab25 overexpression, both at the mRNA and protein level. A2780 cells overexpressing Rab25 and control A2780 containing pcDNA3 vector control were cultured on plastic or FN (25μg/ml) coated plates for 24h and the mRNA was extracted. Similarly, protein expression was assessed by western blotting; cells were seeded, and media changed to FBS free after 6h before collecting the samples 72h after seeding. As ADAMTS5 is a secreted protein, both cell lysates and condition media were collected; the latter was concentrated by a 4-step centrifugation protocol (figure 3.3-A).

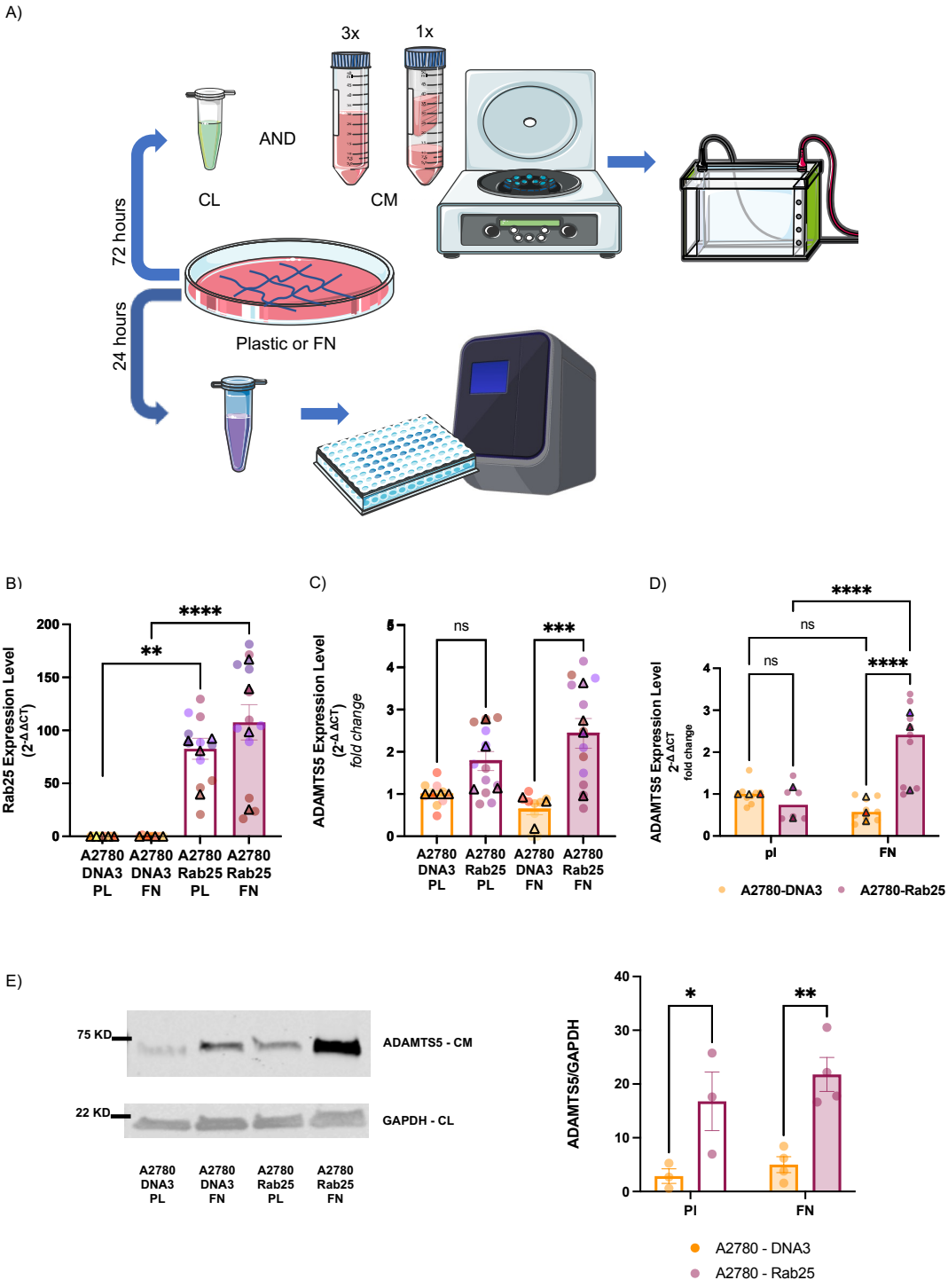

Figure 3.3. ***Rab25 overexpression drives ADAMTS5 expression.*** Schematic representation of the experimental plan (A). A2780-Rab25 and A2780-DNA3 cells were seeded on plastic (Pl) or 25µg/ml FN for 24h in media containing 10% FBS (B,C) or 1% FBS (D). RNA was extracted, and samples were loaded directly on a plate with LUNA one-step qPCR reagents following the kits instructions, to measure Rab25, ADAMTS5 and GAPDH (as housekeeping gene). Data represents normalised means (triangles) and individual data points (circles), ± SEM from N=4 independent experiments, **p=0.0013 and ****p<0.0001, Kruskal-Wallis test (B), ***p=0.0004, Kruskal-Wallis test (C), and ± SEM from N=3 independent experiments, **** p<0.0001, 2-Way ANOVA-Corrected Fisher's LSD (D). A2780-Rab25 and A2780-DNA3 cells were seeded on plastic (Pl) or 25µg/ml FN for 72 hours, media was changed 6h after seeding to serum free RPMI, cell lysate and conditioned media were collected, and conditioned media was concentrated. Samples were run through SDS-page gels, transferred to

FVDF membranes, and blotted for ADAMTS5 and GAPDH. Data represent individual data points, ± SEM from at least N=3 independent experiments, Šídák's multiple comparisons test, *p=0.0290 and **p=0.0043 (E). Image made using items from Servier medical Art and Biorender.

Rab25 overexpression was confirmed by qPCR, showing that A2780-Rab25 cells have higher Rab25 expression compared to DNA3 cells (figure 3.3-B). qPCR analysis shows a significant increase in the ADAMTS5 expression levels between DNA3 cells and Rab25 cells when seeded on FN (figure 3.3-C) for 24h, while there is a small, but not statistically significant increase in cells seeded on plastic. As the serum present in the media contains soluble FN, we reduced the serum levels to 1% to better assess the impact of matrix FN on ADAMTS5 expression. Under low serum conditions, ADAMTS5 mRNA levels were significantly increased when Rab25 overexpressing cells were seeded on FN compared to A2780-DNA3 cells, while there was no change when cells were plated on plastic (figure 3.3-D), indicating that Rab25 promoted ADAMTS5 expression only in the presence of FN. When looking at protein levels, A2780-Rab25 and DNA3 cells where seeded either on plastic or FN for 3 days before samples were collected on the contrary of qPCR experiments where cells were seeded for 24h. Western blot data show that there is a significant increase in ADAMTS5 protein levels in the conditioned media in Rab25-overexpressing cells compared to DNA3 cells. This increase is more pronounced when cells are seeded on FN, but it is also observed on plastic, despite the data being more variable potentially due to cell matrix deposition by cancer cells (figure 3.3-E).

To investigate the role of Rab25 in a more physiological context, the Ovcar3 cell line was used as it endogenously overexpresses Rab25, to a similar extent as the exogenous overexpression in A2780 cells (figure 3.4-A). Other highly used ovarian cancer cell lines were tested to investigate Rab25 expression, Ovcar4 and SKOV3, but no Rab25 protein expression was detected (figure 3.4-A). Consistent with our A2780 cell data, we observed a statistically significant increase in ADAMTS5 expression when Ovcar3 cells are seeded on FN compared

to plastic (figure 3.4-B,C). Overall, our finding indicate that FN promotes ADAMTS5 expression in Rab25 overexpressing ovarian cancer cells.

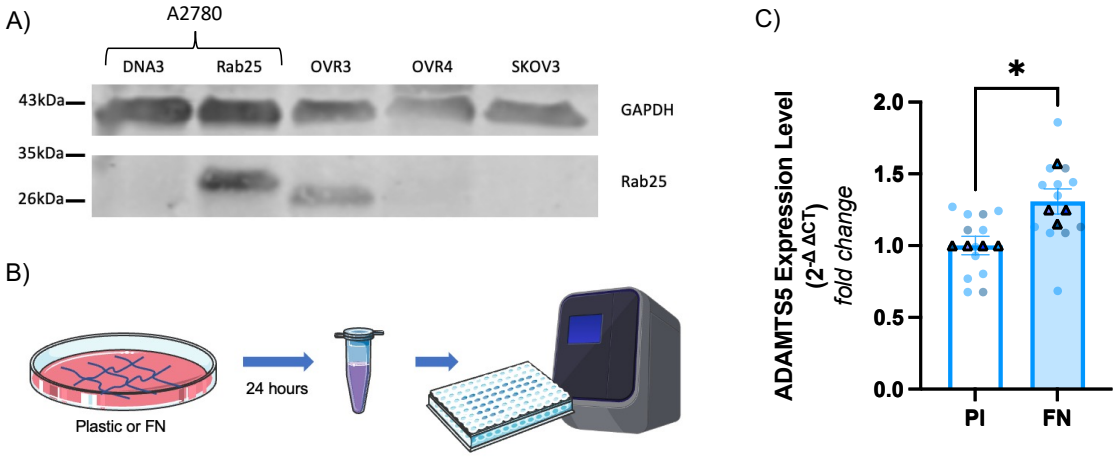

*Figure 3.4. **FN drives ADAMTS5 expression in Ovcar3 cells.*** A2780-DNA3, A2780-Rab25, Ovcar3, Ovcar4 and SKOV3 cells were lysed and the Rab25 and GAPDH protein levels were measured by Western Blotting (this figure is included in (Yuan et al., 2024) (A). Schematic representation of the experimental plan (B). Ovcar3 cells were seeded on plastic (Pl) or 25µg/ml FN for 24h. RNA was extracted, samples were then loaded directly on a plate with LUNA one-step qPCR reagents to measure Rab25, ADAMTS5 and GAPDH (as housekeeping gene). Data represents normalised mean and individual data points, ± SEM from N=4 independent experiments, *p=0.0137, Mann Whitney test (C).

3.2.2 α5β1 integrin expression and localisation differs between ovarian cancer cell lines:

Integrins are the major cellular ECM receptors, allowing cells to respond to ECM changes, adhere and migrate (Takada et al., 2007). α5ß1integrin is the typical FN receptor, mediating cell adhesion and migration (Hou et al., 2020). To assess if integrin α5ß1 could be mediating the upregulation of ADAMTS5 by binding to FN, we firstly characterised the expression of integrin α5, α2, β1 and FN in A2780 and Ovcar3 cells. A2780-DNA3, A2780-Rab25 and Ovcar3 cells were seeded on plastic for 24h, lysed and integrin expression was assessed by Western blotting. A2780 cells had significantly higher levels ofα5 and ß1integrin compared to Ovcar3 cells and in a Rab25-independent manner, as there was no significant difference between DNA3 and Rab25 cells, and Ovcar3 protein levels were two times lower than DNA3 cells. α2 integrin expression significantly higher in A2780-DNA3 cells compared to Ovcar3

cells while A2780-Rab25 cells had an intermediate level of α2 expression, but none of the differences were statistically significant, probably due to sample variability. Finally, A2780-DNA3 cells have almost a four times higher FN expression compared to Ovcar3 and A2780-Rab25 cells (Figure 3.5).

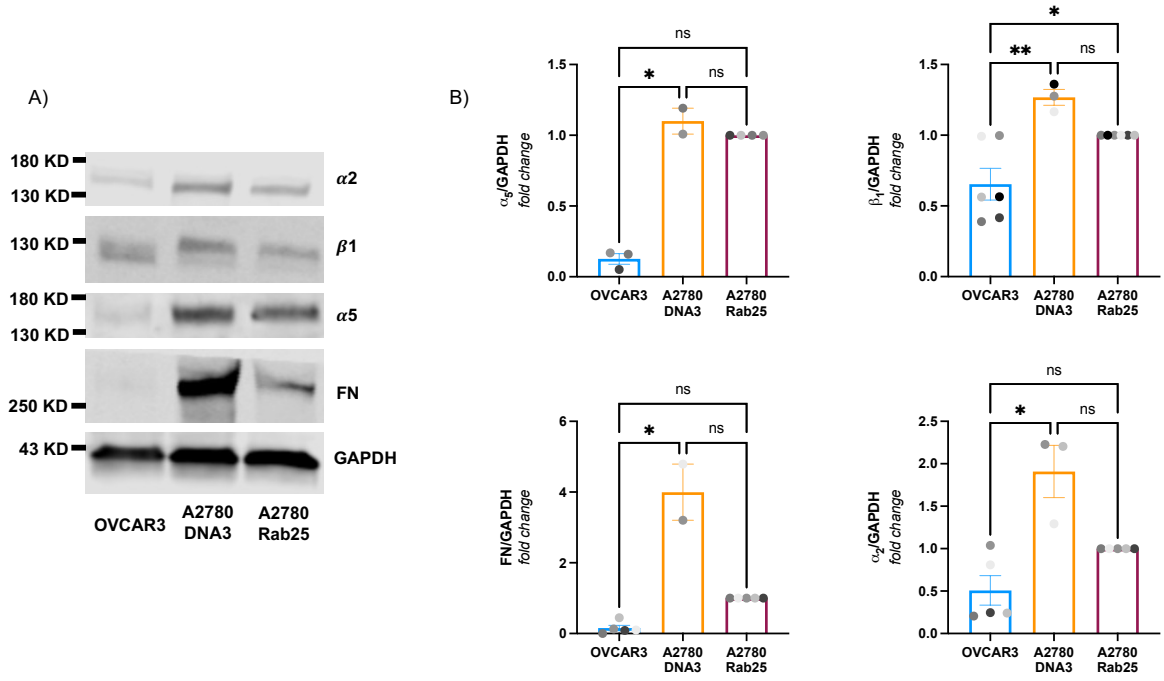

Figure 3.5. ***Integrin differential expression in ovarian cancer cells.*** A2780-DNA3, A2780-Rab25 and Ovcar3 cells were seeded on plastic for 24h. Cell lysates were collected, run, and blotted for integrin α2, α5, β1, FN and GAPPDH (A). Graphs represents normalised individual data points, ± SEM from N=5 independent experiments, Kruskal-Wallis test, *p=0.0198 α5 Ovcar3 vs DNA3, *p=0.0492 β1 Ovcar3 vs Rab25, **p=0.0018 β1 Ovcar3 vs DNA3, *p=0.0104 FN Ovcar3 vs DNA3 and α2 *p=0.0114 Ovcar3 vs DNA3 (B).

Previous research has shown that α5 integrin is located in focal adhesions and in fibrillar adhesions located under the nucleus when plated on FN coated dishes in Rab25 overexpressing A2780 cells, while it localises in focal adhesion in the absence of Rab25 expression (Rainero et al., 2015). We assessed the localisation of integrin α5 in both Rab25 overexpressing cells, A2780-Rab25 and Ovcar3, by seeding cells on glass-bottomed dishes precoated with FN (25ug/ml). Integrin α5 is mostly diffused in the cytoplasm of Ovcar3 cells, while in A2780-Rab25 cells it clearly accumulates in focal and fibrillar adhesions (figure 3.6). Overall, a

differential expression of integrins and FN was observed in ovarian cancer cell lines, showing higher levels of α5, α2, β1 and FN in A2780 compared to Ovcar3 cells.

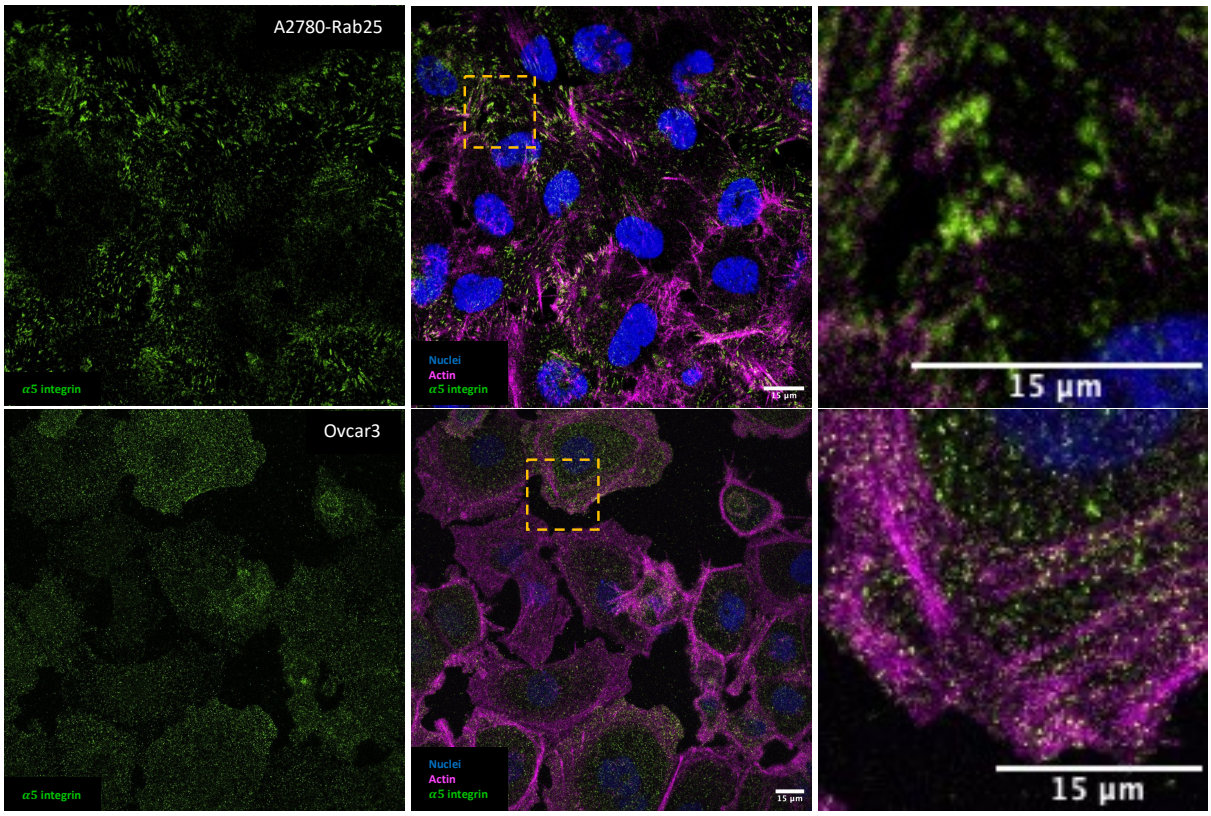

Figure 3.6. ***Integrins differential localization in ovarian cancer cells.*** Ovcar3 and A2780-Rab25 cells were seeded on a FN (25ug/ml) coated glass-bottomed dishes for 24h, fixed and stained for α5 integrin (green), actin (magenta) and nuclei (blue). Dishes were imaged using a Nikon A1 confocal microscope with a 60x objective.

3.2.3 α5β1 integrin binding to FN is not necessary for ADAMTS5 upregulation:

It is known that FN can engage with the cells via interactions with integrins, like α5ß1, and cell surface proteoglycans, such as SDC1 and 4, that have been found to form cooperative pairs to modulate different cellular responses to extracellular stimuli (Morgan et al., 2007). Moreover, Rab25 overexpression is linked to higher recycling of integrin α5ß1 to the plasma membrane, particularly to the leading edge of migrating cells (Caswell et al., 2007). We wanted to investigate whether the interaction between FN and its receptors integrin α5ß1 and/or SDC4 was required for FN-dependent ADAMTS5 expression (figure 3.7-A). Firstly, FN fragments were purified as previously described in (Danen et al., 1995; Sharma et al., 1999). Two different

fragments, one containing the RGD integrin binding domain (50K) and one containing the heparin binding domain (H0), binding to SDC4, were synthetised (figure 2.4). A2780-DNA3, A2780-Rab25 and Ovcar3 cells were seeded on glass-bottomed dishes precoated with 50K, H0 or full-length FN for 24 hours and mRNA was extracted (figure 3.7-B).

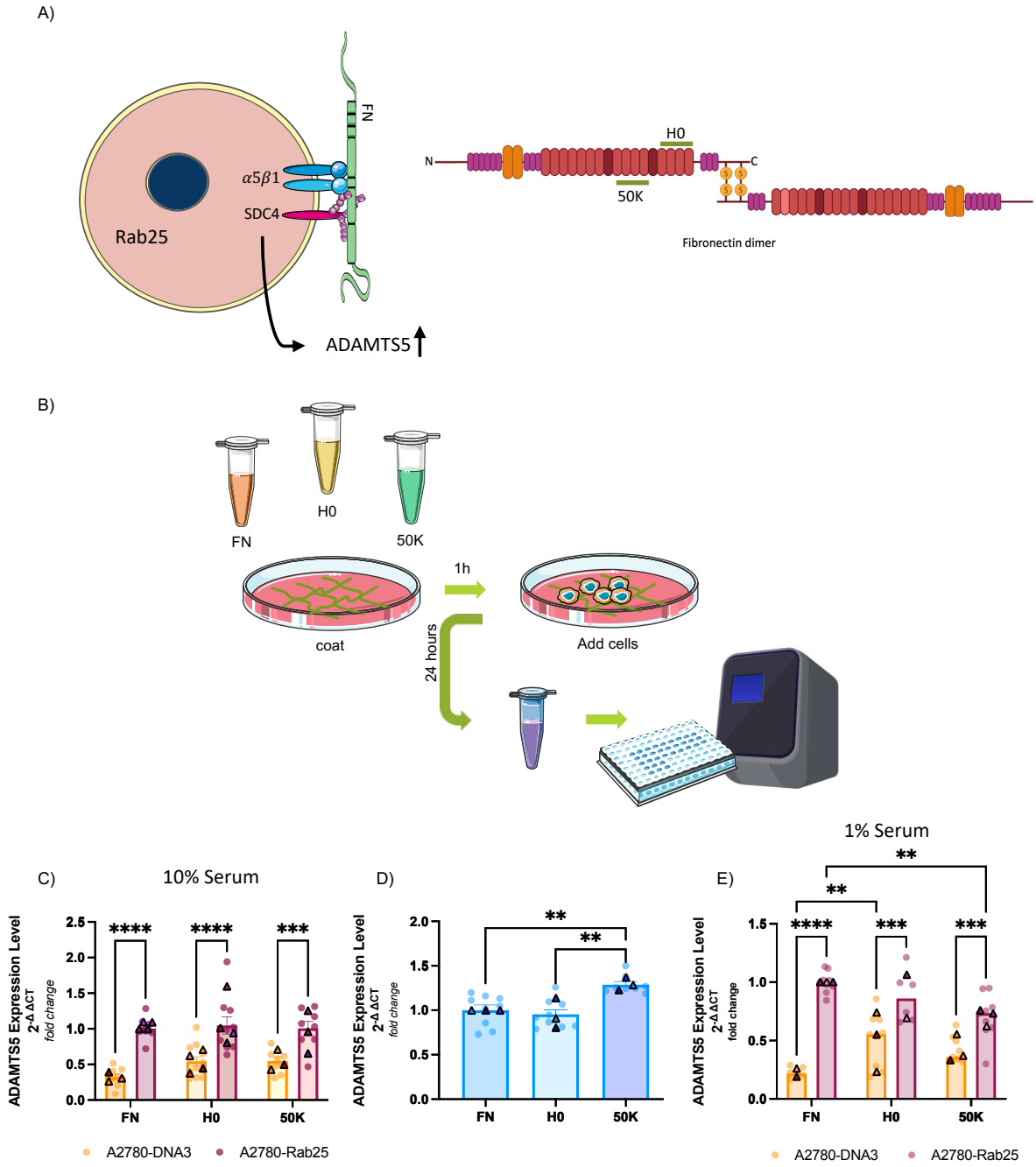

Figure 3.7. ***Both H0 and 50K FN fragments promote ADAMTS5 upregulation in ovarian cancer cells.*** Diagram showing the hypothesis tested and the FN fragments binding sites (A). qPCR samples were generated by seeding A2780 or Ovcar3 cells on full length FN, H0 or 50K FN fragments for 24h in 10% FBS media (C,D) or 1% FBS media (E). RNA was extracted, samples were then loaded directly on a plate with LUNA one-step qPCR reagents (B). Data represents normalised mean and individual data points ± SEM from N=4 independent experiments, **** p<0.0001, Šídák's multiple comparisons test (C), ± SEM from N=3 independent experiments, **p=0.0064 FN vs 50K and **p=0.0025 H0 vs 50K, Kruskal-Wallis test (D) and data represents normalised mean and individual

data points ± SEM from N=3 independent experiments, **p=0.0015 Rab25 FN vs 50K, **p=0.0072 DNA3 FN vs H0, ***p=0.0007 50K DNA3 vs Rab25, *p=0.0001 H0 DNA3 vs Rab25 and ****p<0.0001, Šídák's multiple comparisons test (E). Image made using items from Servier medical Art and Biorender and adapted from (Morwood et al., 2023).

qPCR results show that ADAMTS5 expression levels were significantly increased in Rab25-overexpressing cells when compared to DNA3 cells on both FN fragments, to the same extent of full-length FN (figure 3.7-C). In Ovcar3 cells, we detected a small, but statistically significant, increase in ADAMTS5 expression in cells seeded on the 50K fragment, containing the integrin binding site (figure 3.7-D). As serum full length FN might confound the results, qPCR experiments were repeated using 1% FBS supplemented media, to reduce the amount of plasma FN. Although we detected an increase in ADAMTS5 expression in Rab25 cells on all fragments when compared to DNA3, the 50K fragment led to a statistically significant reduction in ADAMTS5 expression levels compared to full length FN, while there was no significant difference between the H0 fragment and the full-length FN. Interestingly, the H0 fragment led to increased ADAMTS5 expression in DNA3 cells when compared to full length FN (figure 3.7-E). These experiments suggest that both α5β1 integrin and SDC4 might be required for ADAMTS5 expression, as this was not reduced to DNA3 cell levels with either of the FN fragments. To test whether α5β1 integrin was required for ADAMTS5 expression, A2780 cells were seeded on full length FN overnight in the presence of either an α5 integrin inhibitor (ATN-161) or anti-ß1 blocking antibody (AIIB2). ATN-161 is a non-competitive inhibitor of the FN PHSRN sequence, located close to the RGD binding site. It was shown to inhibits integrin signalling without affecting integrin-dependent adhesion (Cianfrocca et al., 2006). A2780-DNA3 and A2780-Rab25 cells were firstly seeded on FN (25µg/ml) for 6hr to allow them to adhere, then ATN-161 (50mM), DMSO control, and AIIB2 (2ug/ml) or IgG1 control were added to the media. Cells were then incubated overnight before samples were collected for qPCR. Consistent with previous data, ADAMTS5 expression was increased in

A2780-Rab25 compared to DNA3 cells, in both DMSO and α5 inhibitor treated cells (figure 3.8-A). Similarly, the treatment with an anti- ß1 blocking antibody (AIIB2) or a control antibody (IgG1) did not prevent Rab25-induced ADAMTS5 over-expression in cells seeded on FN (figure 3.8-B). Overall, our data suggests that binding to α5ß1 integrin is not needed to upregulate ADAMTS5 expression in the presence of FN.

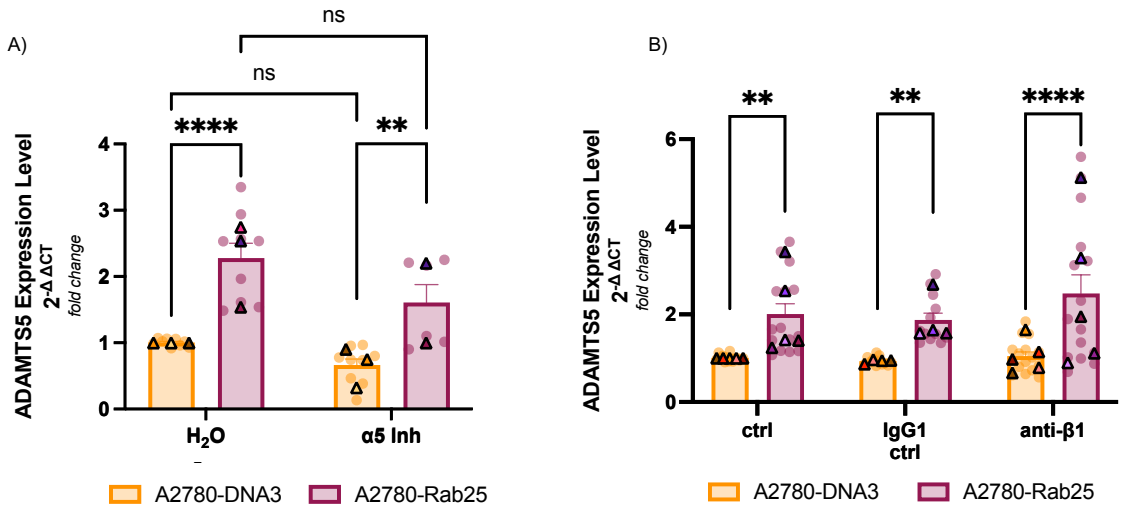

Figure 3.8. ***FN biding to α5β1 is not needed for the upregulation of ADAMTS5 induced by Rab25.*** A2780-DNA3 and A2780-Rab25 cells were seeded on FN (25µg/ml) for 6hr and kept overnight in the presence of either the α5 inhibitor ATN-161 (50mM) or DMSO (A) or anti-ß1 blocking antibody (AIIB2) (2ug/ml) or an IgG1 control (B). RNA was extracted, samples were then loaded directly on a plate with LUNA one-step qPCR reagents to measure ADAMTS5 and GAPDH levels. Data represents normalised mean and individual data points, ± SEM from N=3, **p=0.0038 and ****p<0.0001, Šídák's multiple comparisons test (A) and N=5 independent experiments, **p=0.0014 Cntr DNA3 vs Rab25, **p=0.0075 IgG Cntr DNA3 vs Rab25 and ****p<0.0001, Šídák's multiple comparisons test (B).

3.2.4 Syndecan-4 drives ADAMTS5 upregulation:

Since integrin α5ß1 was not involved in the upregulation of ADAMTS5, we wanted to investigate the role of SDC4 binding to FN, as SDC4 is a coreceptor of integrin α5ß1 during focal adhesion formation. Interestingly, it was found that SDC4 regulated ADAMTS5 activation via upregulation of MMPs in a mouse model of osteoarthritis (Echtermeyer et al., 2009). We firstly used mouse embryonic fibroblasts (MEFs) from either wild type or SDC4-KO mice (Bass et al., 2007), seeded either in Pl or FN (25µg/ml) for 24h, to see if any detectable differences in ADAMTS5 expression were observed when SDC4 was not expressed before

moving to our ovarian cancer cell lines. We found that in wild type MEFs there was an increase in ADAMTS5 expression when cells were seeded on FN, and this increase was completely blocked in the SDC4-KO MEFs (figure 3.9). As a decreased in ADAMTS5 expression was observed in MEFs, we then tested ADATMS5 mRNA levels in A2780-DNA3 and A2780-Rab25 cells transfected with an siRNA targeting SDC4 or a non-targeting control and seeded on 25µg/ml FN. Consistently, ADAMTS5 expression levels were higher in A2780-Rab25 cells compared to DNA3 in the presence of a non-targeting siRNA, but this increase was strongly reduced when SDC4 was knocked down (KD) (figure 3.10-A). Similarly, SDC4 KD resulted in a small but statistically significant reduction in ADAMTS5 expression in Ovcar3 cells (figure 3.10-B). qPCR analysis confirmed a 64% reduction in SDC4 expression upon KD in both cell lines (figure 3.10-C,D). Interestingly, Rab25-overexpression resulted in a small but statistically significant increase in SDC4 levels in A2780 cells seeded on FN (figure 3.10-C). Similarly, in Ovcar3 cells, SDC4 expression was higher when cells were seeded on FN compared to plastic (figure 3.11). These data suggest that SDC4 regulates ADAMTS5 expression in Rab25 overexpressing cells seeded on FN, while SDC4 expression is increased in Rab25 overexpressing cells seeded on FN.

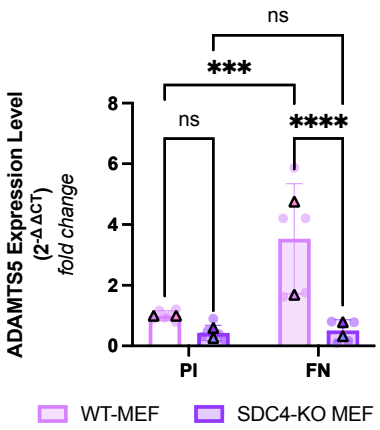

Figure 3.9. ***SDC4 regulates ADAMTS5 expression in MEF.*** WT and SDC4 KO MEF were seeded on plastic (Pl) or FN (25µg/ml) for 24h. RNA was extracted, samples were loaded directly on a plate with LUNA one-step qPCR reagents. ADAMTS5 and GAPDH mRNA levels were measured, data represents normalised mean and individual data points, ± SEM from N=2 independent experiments, ***p=0.0002 and ****p<0.0001, 2way ANOVA-Uncorrected Fisher's LSD.

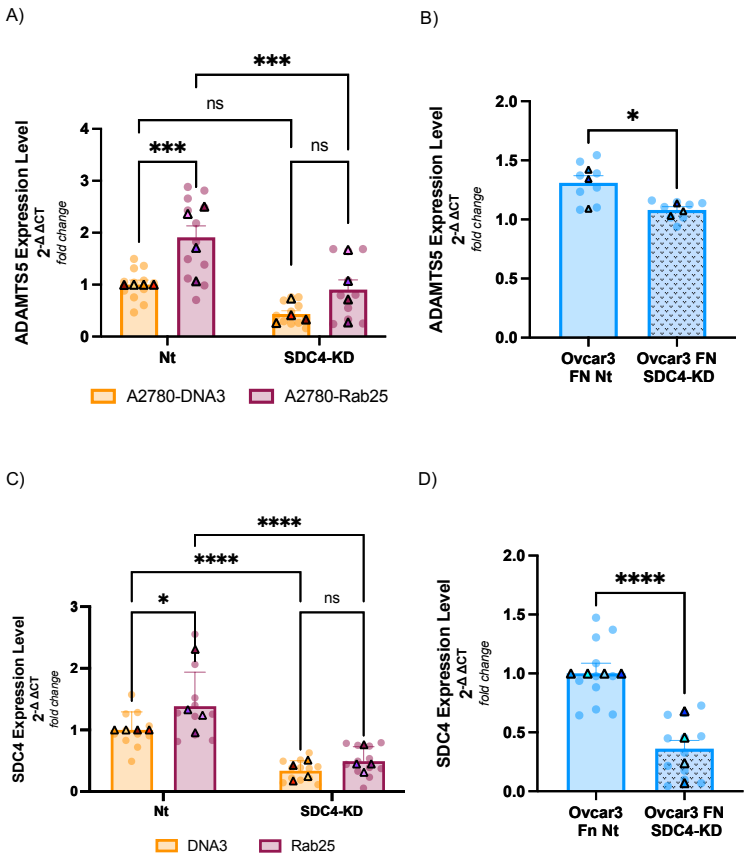

Figure 3.10. ***SDC4 regulates ADAMTS5 expression in ovarian cancer cells.*** A2780-DNA3 and A2780-Rab25 cells were transfected with an siRNA against SDC4 (SDC4 KD) or non-targeting siRNA (Nt) and seeded on FN for 24h, mRNA was extracted and ADAMTS5 and GAPDH levels were measured by qPCR, data represents normalised mean and individual data points, ± SEM from N=4 independent experiments, ***p=0.0002 Rab25 Nt vs SDC4-KD and ***p=0.0005 Nt DNA3 vs Rab25, Šídák's multiple comparisons test (A); Ovcar3 cells were transfected with siRNA against SDC4 (SDC4 KD) or non-targeting siRNA (Nt) and seeded on FN for 24h, mRNA was extracted and ADAMTS5 and GAPDH levels were measured by qPCR, data represents normalised mean and individual data points, ± SEM from N=3 independent experiments, *p=0.0207, Mann Whitney test (B); efficiency of SDC4 KD in A2780-DNA3 and A2780-Rab25 cells were measured by qPCR, data represents normalised mean and individual data points, ± SEM from N=4 independent experiments, *p=0.0110 and ****p<0.0001, 2way ANOVA-Uncorrected Fisher's LSD (C); efficiency of SDC4 KD in Ovcar3 cells were measured by qPCR, data represents normalised mean and individual data points, ± SEM from N=3 independent experiments ****p<0.0001, Mann Whitney test (D).

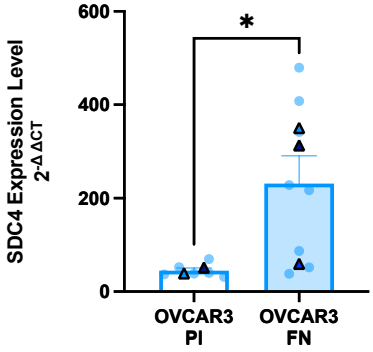

Figure 3.11. ***SDC4 expression increases on FN in Ovcar3 cells.*** Ovcar3 cells were seeded on plastic (Pl) or FN (25µg/ml) for 24h, mRNA was extracted and SDC4 levels were measured by qPCR, data represents normalised mean and individual data points, ± SEM from N=3 independent experiments, *p=0.0200, Mann Whitney test.

SDC4 signalling is primarily mediated by the activation of protein kinase C (PKC) (Murakami et al., 2002). To determine whether PKC was required for SDC4-mediated ADAMTS5 upregulation in Rab25 expressing cells, we used a reversable PKC inhibitor, BIM. A2780-DNA3 and A2780-Rab25 cells were seeded on FN and BIM or DMSO were added after 6h, samples were collected for qPCR after 24h. As shown in figure 3.12, the presence of BIM did not affect the expression of ADAMTS5 in Rab25-overexpressing cells, as we detected a similar increase in ADAMTS5 expression in A2780-Rab25 compared to DNA3 cells in the presence of both DMSO and BIM. Overall, these results suggest that the binding of FN to SDC4 is needed for upregulation of ADAMTS5, but this process does not seem to be mediated by PKC activation.

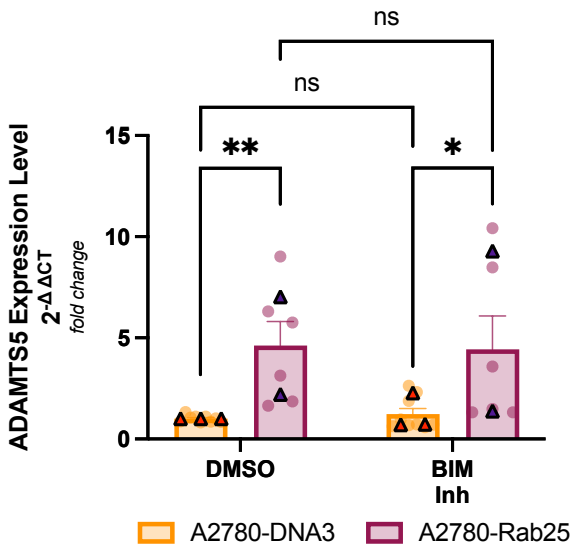

Figure 3.12. ***PKC inhibition does not alter ADAMTS5 expression.*** A2780-DNA3 and A2780-Rab25 cells were seeded on FN (25µg/ml) for 6h, BIM (100nM) or DMSO were added and incubated for 24h. RNA was extracted, samples were loaded directly on a plate with LUNA one-step qPCR reagents and ADAMTS5 and GAPDH levels were measured. Data represents normalised mean and individual data points, ± SEM from at least N=2 independent experiments, ** p=0.0048, *p=0.0113, Fisher's LSD.

3.3 Discussion:

In this chapter, we found that ADAMTS5 expression is promoted by FN and SDC4, downstream of Rab25. The small GTPase Rab25 has been found to function as an oncogene in different cancer types, including ovarian cancer, where it was linked with aggressiveness (Cheng et al., 2004). Since we demonstrated that presence CDM increased ADAMTS5 expression in Rab25 overexpressing cells (Yuan et al., 2024) and CDM has high levels of FN, we wanted to investigate if FN was promoting ADAMTS5 expression. When cells were seeded

on FN coated plates or plastic in 10% FBS-containing media, no significant differences in ADAMTS5 mRNA levels were observed. FBS contains plasma FN that, even if it differs structurally and functionally from cellular FN, can be used by cancer cells and rearranged, affecting both cell motility and metastatic capacities (Humphries et al., 1986). The presence of plasma FN could be the reason why no significant differences in ADAMTS5 mRNA levels are observed between plastic and FN in A2780-Rab25. We then reduced FBS to 1%, which did not affect cell morphology and viability (not shown). A significant difference between plastic and FN was now observed, indicating that FN regulates the expression of ADAMTS5 in Rab25 overexpressing cells. However, in Ovcar3 cells we detected a significant increase in ADAMTS5 expression in the presence of 10% FBS. Ovcar3 cells have been previously reported to not discriminate between cellular or plasma FN, adhering at similar rates to both FN types when compared to plastic (Zand et al., 2003). We were not able to grow Ovcar3 cells with 1% FBS as we observed reduced viability in low FBS conditions which led to insufficient cells to obtain RNA for qPCR. This could mean that we might potentially underestimate the FN-dependent increase in ADAMTS5 expression in Ovcar3 cells. Despite this, the effect observed from the ECM presence, in this case FN, was smaller in Ovcar3 cells compared to A2780-Rab25 cells, consistent with our previous findings in the presence of CDM (Yuan et al., 2024). Ovcar3 cells express Rab25 at relatively high levels which are comparable to those found in A2780 cells when Rab25 is exogenously overexpress, cell expression differences could be also due to the different origin of the cells. Further controls could have been carried out like using Ovcar4 cancer cells which have similar cell origin as Ovcar3, as they were established from ascitic fluid of patients, but do not express Rab25, as seen in figure 3.4. This could have given further confirmation of the need of Rab25 expression for ADAMTS5 upregulation. Furthermore, Ovcar3 Rab25-KD were carried out by our lab which led to no

changes in ADAMTS5 expression when cells were seeded on CDM (Yuan et al., 2024), but a repeat of the experiment can be done of FN as further control.

ADAMTS5 protein levels were also found to be increased in Rab25 overexpressing cells when comparing to DNA3 cells. In agreement with our previous results, FN led to an increase in ADAMTS5 compared to plastic, but the difference was not statistically significant. The relatively high ADAMTS5 protein levels observed on plastic could be due to the fact that A2780 cells might secrete their own ECM, containing FN, as cells were cultured for 72 hours. In this instance there was no FBS in the media as after adhesion (6h) the media was changed to serum free. Media was changed to serum free as ADAMTS5 is mainly found in the conditioned media (CM), due to the protein being secreted. Proteins from the FBS can increase background in the western blots, so it is common practice to remove or reduce FBS in the media when detecting low abundance proteins (Rashid and Coombs, 2019). Multiple studies have shown a differential impact on signalling pathway response by cancer cells when in serum-free conditions. Among these, a proteomic study has shown divergent responses on various signalling pathways, including Akt and EGFR/MAPK, when high grade glioma and seven different adenocarcinoma cell lines where serum starved (0.5% FBS added to culture media) (Levin et al., 2010). The secretome has also been shown to be affected by serum availability. Interestingly, increase secretion of MMPs was found in the presence of serum compared to the absence of serum, in a glioblastoma cell line, potentially due to cells responding to serum availability (Shin et al., 2019). No other ECM enzymes have been identified to be differentially expressed in this research, and our results show similar trends independently of serum presence. We were not able to investigate ADAMTS5 protein expression in Ovcar3 cells, because new batches of the antibody previously used for A2780 cells failed to detect the protein, and currently available antibodies are not reliable or unspecific.

As Rab25 is known to recycle α5β1 integrin to the plasma membrane, we hypothesised that a crosstalk between α5β1 integrin and its ligand FN was needed to promote ADAMTS5 expression. We started by investigating integrin expression in A2780s and Ovcar3 cells. Interestingly, A2780-Rab25 cells had higher levels of α5 and of ß1integrin compared to Ovcar3 cells. Lower expression of α5ß1integrin (Cannistra et al., 1995) and high α3, α6 and αv integrin expression (Ahmed et al., 2005) has been previously reported by others in Ovcar3 cells, suggesting that Ovcar3 cells are less associated with FN binding compared to other ovarian cancer cell lines, such as CAOV-3 or SKOV-3 (Cannistra et al., 1995). Contrarily to the literature (Bao et al., 2021), we found lower FN protein expression in Ovcar3 cells compered to A2780 cells. This could potentially be due to increased α5β1 and FN lysosomal degradation. According to the protein atlas, CLIC3 is undetectable at the protein level and very low at the mRNA level in Ovcar3 cells. This suggests that the expression of Rab25 might drive FN-bound integrin lysosomal delivery, followed by degradation due to the lack of CLIC3-dependent recycling. Therefore, further investigation of ligand-dependent α5β1 integrin ubiquitination and degradation is still needed (Rainero and Norman, 2013). Alternatively, Ovcar3 cells could secrete and organise FN as an insoluble matrix, that will not be extracted by the cell lysis buffer used in these experiments.

We used two different approaches to determine if α5β1 integrin was required for FN-dependent ADAMTS5 expression: 1) FN fragments which specifically bind to either integrins (50K) or syndecans (H0) and 2) α5 integrin inhibitor (ATN-161) or anti- ß1 blocking antibody (AIIB2). Overall, our data suggest that α5ß1 integrin is not the major regulator of ADAMTS5 expression downstream of Rab25, although we cannot rule out the fact that α5β1 might still partially contribute to ADAMTS5 expression. When cells were seeded on FN fragments in the presence of 1% FBS, we detected a small but statistically significant reduction in ADAMTS5 expression when cells were seeded on the 50K fragment when compared to full length FN. Interestingly,

there was no difference between the full length and the H0 fragment, suggesting that this FN portion was sufficient to promote ADAMTS5 expression. Furthermore, the HO fragment was able to increase ADAMTS5 expression in DNA3 cells, potentially to allow cancer cells to remodel the ECM after increased adhesion to the matrix. The H0 fragment binds to SDC4 via the heparan binding domain, suggesting that SDC4 might control ADAMTS5 levels downstream of Rab25. SDC4 is a coreceptor of α5ß1integrin that has been found to reduce cell avidity to FN, regulate cell surface availability of α5ß1integrin and trigger caveolin-dependent endocytosis of integrin complexes (Bass et al., 2011). Consistently, we found that knocking down SDC4 reduced completely abrogated the increase in ADAMTS5 mRNA levels induced by Rab25 overexpression in A2780 cells. Similarly, a smaller but statistically significant decrease of ADAMTS5 expression was also observed in Ovcar3 cells upon SDC4 knock down. In osteoarthritis, SDC4 was also found to promote the aggrecanase activity of ADAMTS5 by regulating the expression of MMP3, in an ERK1/2-dependent manner (Echtermeyer et al., 2009). However, it is not clear how SDC4 could modulate ADAMTS5 mRNA levels. Finally, we also observed an increase in SDC4 expression levels in Rab25 overexpressing cells compared to DNA3. A 10-fold increase in SDC4 RNA expression (nTPM) was reported in Ovcar3 cells compared to wild type A2780 cells, data available in the human protein atlas (proteinatlas.org). Two new NF-κB biding sites have been identified in the SDC4 promoter region, that have been reported to be responsible for the effects of TNF-α upregulation of SDC4 in vascular endothelium (Okuyama et al., 2013). Furthermore, we recently showed that NF-κB levels are higher in A2780-Rab25 when compared to DNA3 cells. Moreover, Rab25 knockdown in Ovcar3 resulted in a similar reduction in NF-κB levels. Furthermore, we found that Rab25 overexpression led to a significant increase in the mRNA levels of the NF-κB target gene CXCL8; while Rab25 downregulation reduced CXCL8 expression (Yuan et al., 2024).

Therefore, this suggests that Rab25 might promote SDC4 expression through NF-κB activation.

To conclude, we found that Rab25 overexpression led to upregulation of ADAMTS5 in ovarian cancer cells, in a FN-dependent manner. This appears to not be dependent on α5ß1integrin, but to require the expression of SDC4, that is slightly increased in Rab25 overexpressing cells.

CHAPTER 4: ADAMTS5 is required for ovarian cancer cells migration

4.1 Introduction:

Cancer cells need to become motile to be able to migrate, invade and metastasise. To do this cancer cells activate molecular processes where they change their cell surface proteins, they activate transcription factors, reorganise their cytoskeleton and produce ECM degrading enzymes, among other changes (Kalluri and Weinberg, 2009). This process is called Epithelial-Mesenchymal Transition (EMT). There are different ways in which cancer cells can migrate: collectively, where a group of cells is still connected together via adhesion molecules or junctions; or individually, where individual cells invade the surrounding tissue; in addition, these cells can adopt two different migratory mechanisms: mesenchymal migration or ameboid like migration (Krakhmal et al., 2015).

In ovarian cancer different types of migration have been observed. As ovarian cancer originates from epithelial cells, the most common transition that occurs is EMT, allowing ovarian cancer cells to acquire mesenchymal properties and invade into neighbouring tissues. This process is mediated by Wnt and Notch signalling pathways and the presence of cytokines, together with matrix metalloproteinases and growth factors (Śliwa et al., 2024). In some cases, ameboid like migration can occur. This process is integrin independent, and it is promoted by the Rho/ROCK signalling pathway. Cells are more contractile, lack cell adhesions and there are weak cell-ECM contacts (Śliwa et al., 2024).

Rab25, whose expression is restricted to epithelial cells, was found to contribute to the aggressiveness of ovarian cancer and breast cancer (Cheng et al., 2004). We have previously demonstrated that Rab25 overexpressing cells significantly increase their pseudopod length and directional migration when seeded on fibroblast-generated cell-derived matrix (CDM). More importantly, both pharmacological inhibitors, blocking ADAMTS5 protease activity, and siRNA mediated ADAMTS5 downregulation reduced pseudopod elongation and directional

cell migration on CDM in Rab25 cells without affecting DNA3 cells. Importantly, ADAMT5 inhibition did not affect cell migration on plastic (Yuan et al., 2024). To further characterise the role of secreted ADAMTS5, conditioned media from Rab25 cells was added on DNA3 cells, leading to increased pseudopodial length and increased directional migration. This was not observed when using conditioned media from ADAMTS5 knockdown Rab25 cells, indicating that ADAMTS5 secreted in the media by Rab25 overexpressing cells is sufficient to drive migration on CDM (Yuan et al., 2024). Furthermore, overexpression of ADAMTS5 in DNA3 cells was sufficient to drive pseudopod elongation, directional cell migration and velocity, figure 4.1 (Yuan et al., 2025 – in press).

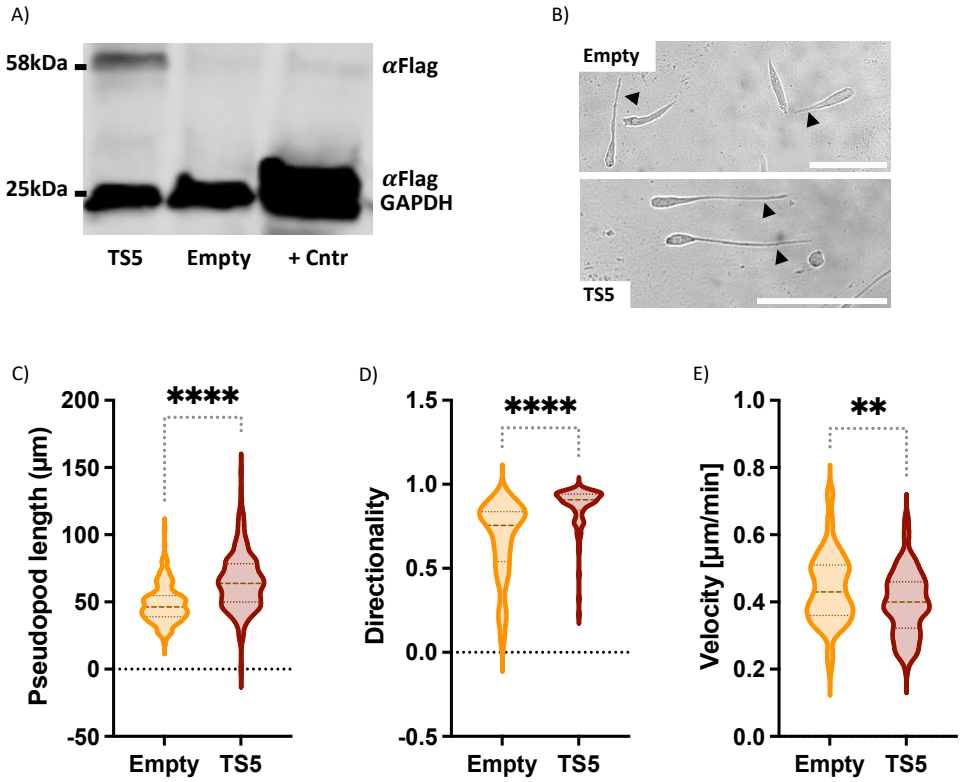

Figure 4.1. ***ADAMTS5 overexpression increased A2780-DNA3 pseudopod elongation and directional migration on CDM.*** A2780-DNA3 cells were seeded on plastic and transfected with ADAMTS5-flag (ADAMTS5-Flag-pCEP4 vector), empty vector (p3xFLAG-CMV-10) and positive control vector, + Cntr, (ZWINT1-FLAG-pCMV3). 24h after cell lysates were collected and analysed by western blotting. Membranes were stained for. FLAG tag and GAPDH (A). Cells were transfected as in A, seeded on CDM for 4h and imaged live with a Nikon widefield live-cell system (Nikon Ti eclipse with Oko-lab environmental control chamber) with a 10X objective for 16h. Black arrowheads point to the elongated pseudopods. Scale bar: 200µm (B). The pseudopod length (µm) (C), directionality (D) and average velocity [µm/min], (E) of cell migration were measured in ImageJ, N=3 independent experiments. The graph shows a Violin plot with median and quartiles. **p=0.0069, **** p<0.0001, Mann-Whitney test. Data from Yuan et al., 2025, in press.

While it is well established that Rab25 is required for mesenchymal cell migration and invasion (Caswell et al., 2007) and ADAMTS5 plays a key role in this process (Yuan et al., 2024), little is known about the role of ADAMTS5 in collective cell migration. In this chapter, we therefore aimed to investigate the role of ADAMTS5 in Rab25 overexpressing ovarian cancer cell collective migration/invasion in FN rich substrates.

4.2. Results:

4.2.1. Does ADAMTS5 regulate FN-dependent Rab25 overexpressing ovarian cancer cell migration?

While it was previously shown that Rab25 promoted FN-dependent migration of ovarian cancer cells in 3D environments (Caswell et al., 2007), we wanted investigate the role of ADAMTS5 in FN-driven collective cell migration.

We firstly tested the effect of FN on the migration of Ovcar3 cells, endogenously overexpressing Rab25. Ovcar3 cells were seeded in 12 well plates for 24h until a monolayer was achieved. The monolayer was then scratched in a cross pattern and cells were overlayed with 0.5mg/ml matrigel or 0.5mg/ml matrigel supplemented with 25ug/ml FN. ECM was polymerised for 30 minutes, after which each arm of the scratch was imaged every 24 hours. As shown in figure 4.2, Ovcar3 cells migrated into the wound area in the presence of matrigel, but they were not able to fully close the gap after 48h. On the contrary, the presence of FN in the matrigel strongly increased cell migration, as the scratch was almost completely closed after 48h. Quantification of the scratch area showed that, after 24h, the presence of FN resulted in a small but statistically significant reduction in the scratch area (23.5% decrease), while at 48h the scratch was 88% smaller in the presence of FN compared to matrigel only.

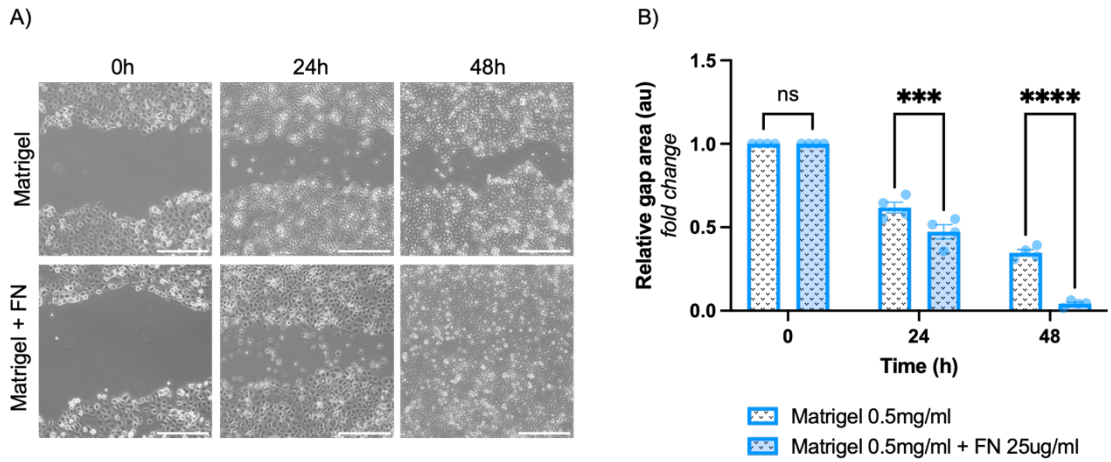

Figure 4.2. ***FN promoted Ovcar3 cell migration.*** Ovcar3 cells were seeded in 12 well plates, after 24h cells were scratched, 0.5mg/ml matrigel or 0.5mg/ml matrigel containing 25ug/ml FN was added on top and allowed to polymerise for 30 min. Scratches were imaged every 24h using an Olympus fluorescent microscope with a 4x objective, scale bar 250µm (A). Gap area was quantified with ImageJ and normalised to time 0. Graph shows the normalised mean of the relative gap area ± SEM from N=1 independent experiment, Tukey's multiple comparisons test, ***p=0.0004 and ****p<0.0001 (B).

To assess the role of ADATMS5 in FN-driven collective cell migration, Ovcar3 cells were scratched, overlayed with matrigel supplemented with FN and allowed to migrate in the presence of 10µM ADAMTS5 inhibitor, see material and methods 2.10, or DMSO control. In the presence of DMSO, Ovcar3 cells migrated into the scratch area, resulting in ~50% closure by 48h. Cell migration was inhibited in the presence of ADAMTS5 inhibitor. The difference between the gap in the presence and absence of ADAMTS5 inhibitor was small but statistically significant, resulting in 30.6% increase when the inhibitor was added (figure 4.3). To summarise, FN promoted collective cell migration while ADMTS5 inhibitor reduced it in Ovcar3 cells.

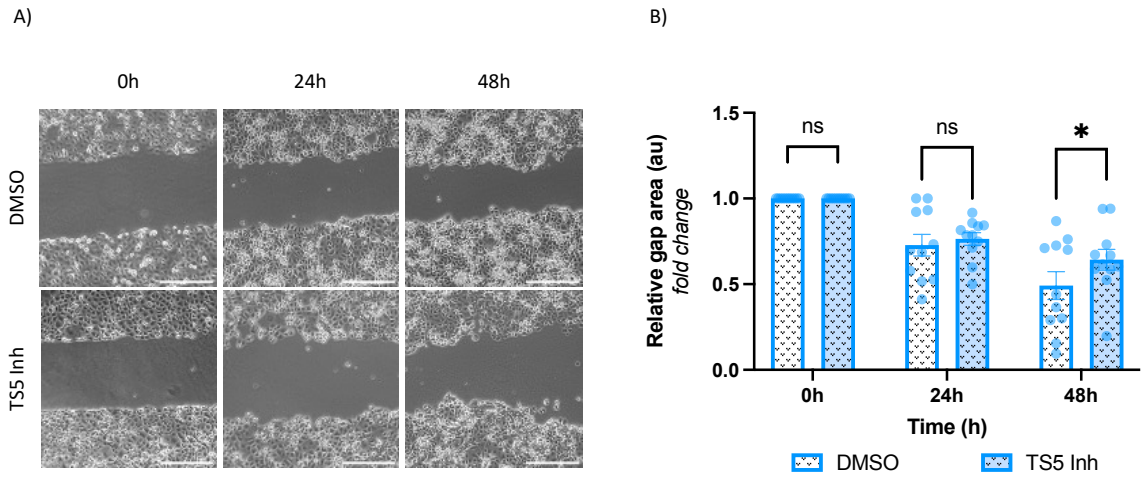

Figure 4.3. ***ADAMTS5 inhibition reduced cell migration in the presence of FN.*** Ovcar3 cells were seeded in 12 well plates, after 24h cells were scratched and 0.5mg/ml matrigel with FN 25ug/ml was added on top. Either DMSO or ADAMTS5 inhibitor (10µM) was added to the matrigel and the media. Scratches were imaged every 24h using an Olympus fluorescent microscope with an objective 4x, scale bar 250µm (A). Gap area was quantified with ImageJ and normalised to time 0. Graph shows the normalised mean of the relative gap area, ± SEM from N=3 independent experiments, Šídák's multiple comparisons test, *p=0.0412.

4.2.2. Ovarian cancer cell coculture with mesothelial cells; increasing physiological relevance.

Next, we wanted to improve our migration model by making it more physiological relevant to the ovarian metastasis microenvironment. When ovarian cancer cells metastasise, they reach secondary organs mainly by passive migration. Once they reach the new organ they need to 'breach through' a layer of mesothelial cells and migrate to colonise the new location. Previous studies recently summarised in Mogi et al., 2021, reported that mesothelial cells can become cancer associated fibroblasts and aid in proliferation, migration and invasion during peritoneal metastasis, by secreting ECM components like FN and vitronectin. We firstly confirmed the secretion/arrangement of FN by mesothelial cells (MET-5a-GFP) and then cocultured MET-5a-GFP cells with Ovcar3 cells to assess their organization. After 24h of incubation of MET-5a-GFP cells on a FN precoated glass-bottom dishes, it was possible to observe rearrangement of the FN fibrils. As MET-5a cells formed a confluent monolayer, FN started to accumulate in between and on top of the cells, forming a network that extends across multiple cells (figure 4.4).

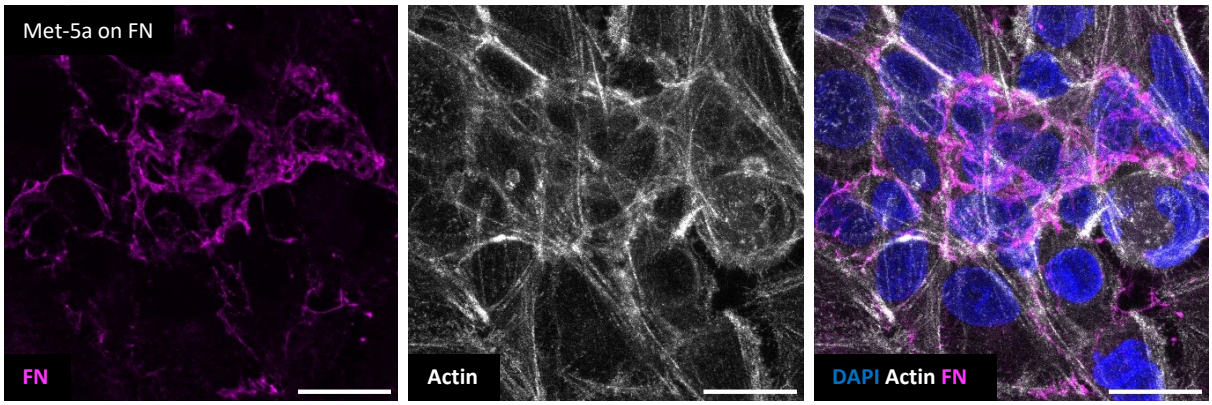

Figure 4.4. ***Mesothelial cells FN organisation.*** Mesothelial cells (MET-5a) were seeded on glass bottom dishes coated with 25µg/ml FN, incubated for 24h, fixed, stained for FN (magenta), actin (white) and nuclei (blue). Cells were imaged using a Nikon A1 confocal microscope with a 60x magnification objective. Z stacks were acquired and presented as a maximum projection, scale bar 22µm.

Afterwards, MET-5a-GFP were cocultured with Ovcar3 cells for 14 days on 25µg/ml FN coated glass bottom dishes. FN was added to improve adhesion to the dish and media was changed once after 7 days of incubation, to avoid altering any secreted factors. Mesothelial and Ovcar3 cells organised in the dish. Mesothelial cells, located closer to the ovarian cancer cells, changed shape from a more epithelial shape to a fibroblast-like shape. Furthermore, Ovcar3 cells formed a monolayer of one cell width thickness that sit in between MET-5a cells looking like 'valleys', while MET-5a cells grew in hight, forming thicker 3D structures that appear like 'mountains' (figure 4.5). FN is again located mostly on top and around mesothelial cells.

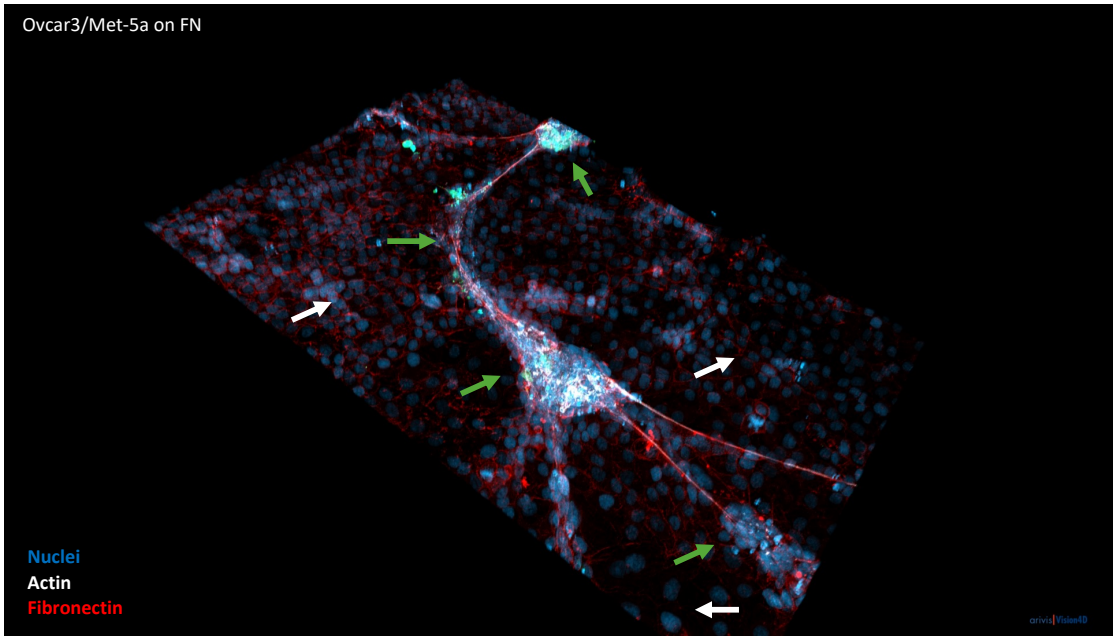

Figure 4.5. ***Mesothelial and Ovcar3 cells 3D reconstruction.*** Mesothelial cells (MET-5a) (green arrows) and Ovcar3 (white arrows) cells, ratio 1:1, were seeded on glass bottom dishes coated with 25µg/ml FN. They were incubated for 14 days, fixed, stained for FN (red), actin (white) and nuclei (blue) and imaged using a Zeiss Airy Scan microscope. Images are representative of N=3 independent experiments. 3D reconstruction was generated by stitching a 3x2 stack images, that were then denoised and reconstructed by Avaris vision 4D software.

We then assess more closely FN and $\beta 1$ integrin distribution in Ovcar3/Met5a cocultures (figure 4.6). Mesothelial cells are delimited with a green line, defined using the GFP signal, which was removed from the images to better appreciate the distribution of the stained proteins. FN was mostly deposited on top and in between mesothelial cells, nicely aligning with the actin cytoskeleton, but almost no FN was observed in the Ovcar3 cell area (figure 4.6-A). In the close-up images, Ovcar3 cells appear to have ventral stress fibres, but there is no FN located under them. In figure 4.6-B, integrin $\beta 1$ was stained in magenta, its location matches with FN deposition in mesothelial cells, accumulating at the plasma membrane of mesothelial cells. In addition, a weak $\beta 1$ integrin staining is present at the plasma membrane in Ovcar3 cells, while FN was not present at all. Mesothelial cells have higher levels of $\beta 1$ integrin that appear to be along the actin filaments. Actin filaments from one mesothelial cell were almost forming a continuous filament with the neighbouring cell, giving rise to a continuous network of actin filaments. All considered, our data indicate that MET-5a cells secrete and assemble FN, while Ovcar3 cells appear not to do so.

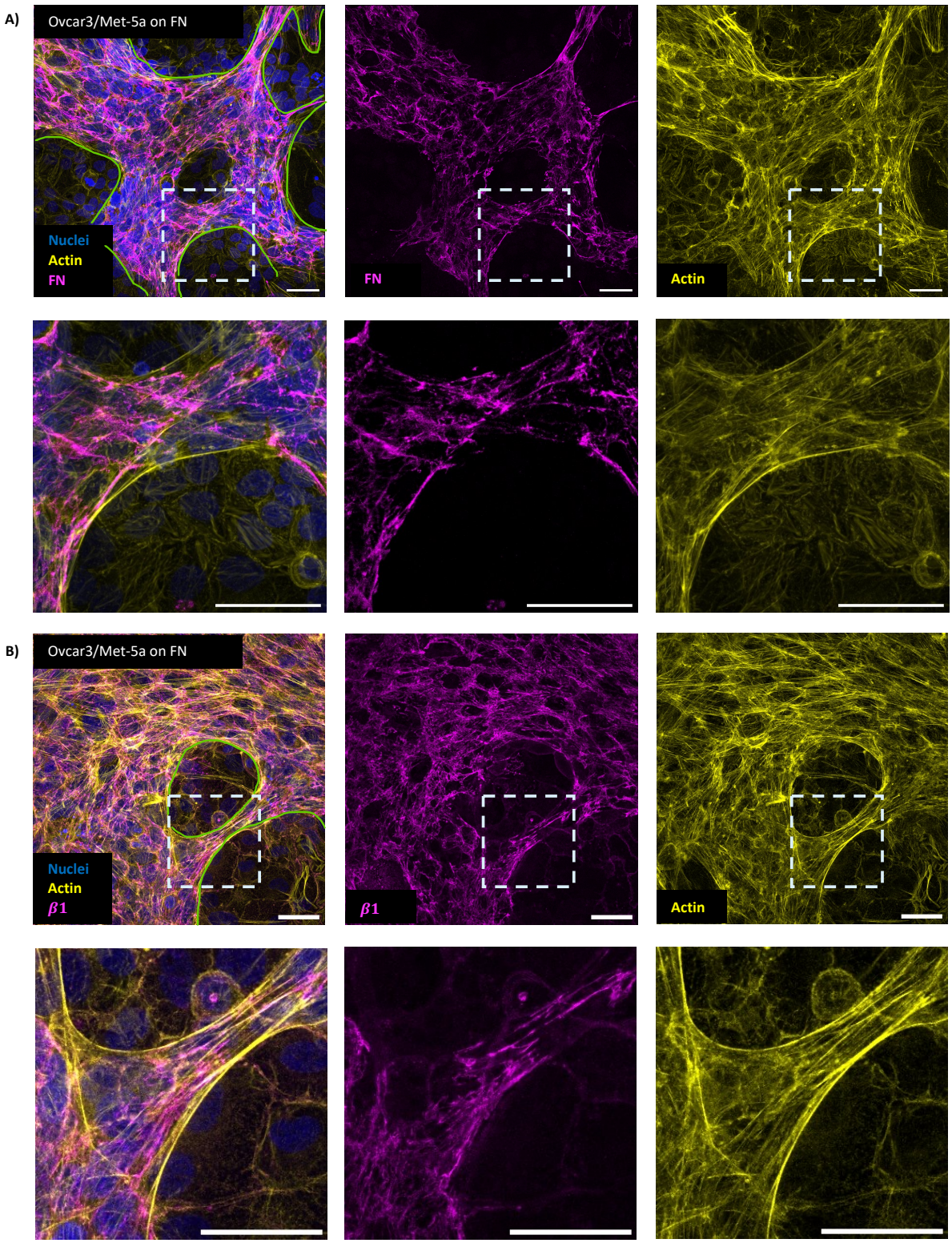

Figure 4.6. ***FN and β1 integrin distribution in mesothelial and Ovcar3 cells coculture.*** Mesothelial cells (MET-5a) and Ovcar3 cells, ratio 1:1, were seeded on glass bottom dishes coated with 25µg/ml FN, incubated for 14 days, fixed, stained for FN or integrin β1 (magenta), actin (yellow) and nuclei (blue) and imaged using a Nikon A1 confocal microscope. The green line delimits the mesothelial cell area. Scale bar, 45µm (A, B). Images are representative of N=2 independent experiments.

Once we established the ratio of MET-5a-GFP and Ovcar3 cell needed for them to survive in coculture and the numbers of days needed for the re-organisation to happen, we assessed cell migration. Firstly, we wanted to determine if FN increased migration in Ovcar3 cells cocultured with MET-5a-GFP cells. Due to the fragility of the monolayers formed, sticky inserts were used to create a scratch. MET-5a-GFP were cocultured with Ovcar3 in the insert chambers for 4 days, inserts were then removed, an overlay of matrigel or matrigel with FN was added on top and allowed to polymerise for 30min. Scratches were then imaged every 3h. A mixture of the two cell lines can be seen in the monolayers around the scratch, organised in distinct areas as in the immunofluorescence experiments described above. As mesothelial cells are GFP tagged, cells can be identified in the green channel images. Both cell lines were migrating into the scratched area, no differences were observed between matrigel and matrigel with FN at any of the timepoints images and at 24h the scratches were almost closed (figure 4.7). Ovcar3 cocultured with MET-5a moved faster than when migrating alone, as in previous experiments (figure 4.2) it took Ovcar3 cells 48h to almost close the gap. This suggests that mesothelial cells are promoting ovarian cancer cells migration, in an exogenous FN-independent manner.

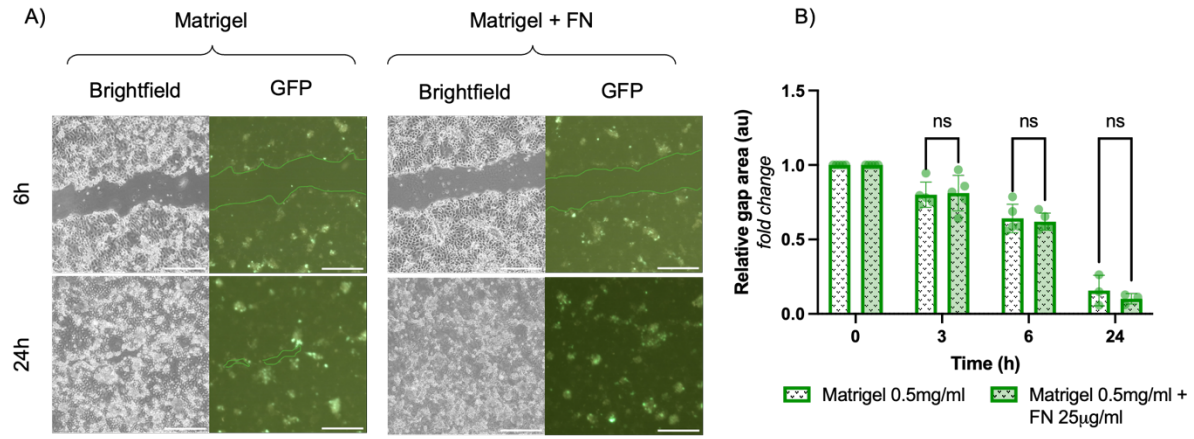

Figure 5.7. ***FN supplementation did not affect MET-5a-GFP/Ovcar3 cell coculture migration.*** Ovcar3 and MET-5a-GFP (1:1 ratio) cells were seeded in inserts chambers in 12 well plates, after 4 days inserts were removed. 0.5mg/ml matrigel or 0.5mg/ml matrigel with 25µg/ml FN was added on top and allowed to polymerise for 30 min. Scratches were imaged for 24h using an Olympus fluorescent microscope. Wound margins are marked by green line in the GFP images. Scale bar, 250µm (A). Gap area was quantified with ImageJ and normalised to time 0. Graph shows the normalised mean of the relative gap area, ± SEM from N=3 independent experiments. Šídák's multiple comparisons test (B).

We next assessed if ADAMTS5 affected cell migration in the coculture system. Met5a-GFP and Ovcar3 cocultures were scratched and overlayed with FN-containing matrigel, then either DMSO or ADAMTS5 inhibitor was added to the matrigel plus FN mix and to the media. Scratches were then imaged for a total of 48 hours. At 0h the scratches were the same size, as inserts were used; at 24h, the cocultured cells migrated into the scratch, covering approximately half of the area, both in the presence and absence of ADAMTS5 inhibitor. By 48h the scratches were almost closed, with no difference between DMSO and ADAMTS5 inhibitor (figure 4.8). Overall MET-5a coculture promoted Ovcar3 cell migration, but this is independent on the supplementation of FN or the activity of ADAMTS5.

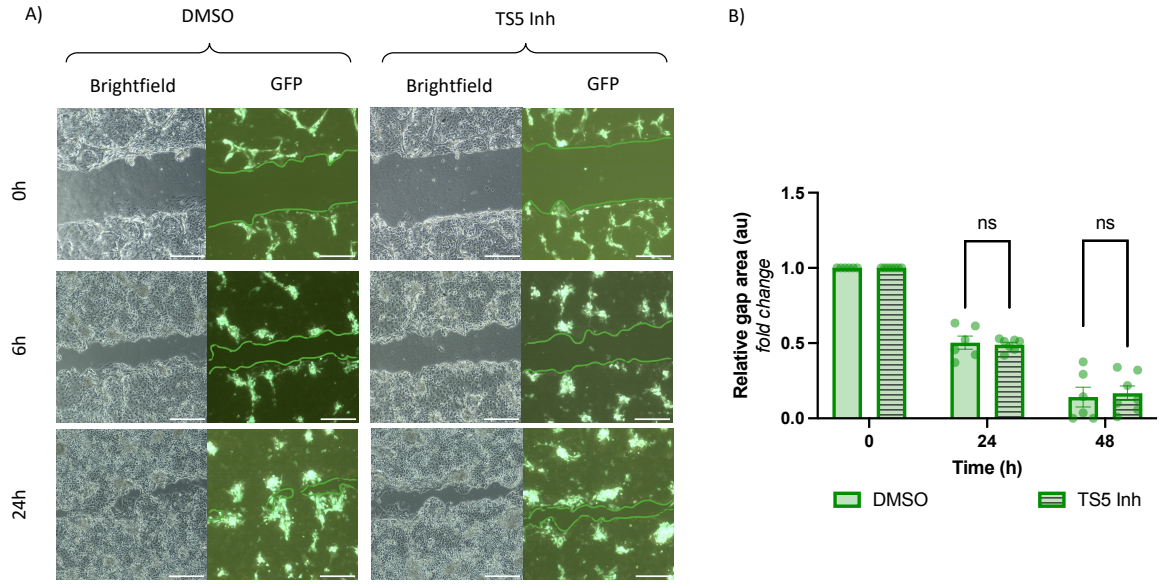

Figure 4.8. ***ADAMTS5 inhibitor did not affect the migration of MET-5a-GFP and Ovcar3 coculture in FN supplemented matrix.*** Ovcar3 and MET-5a-GFP cells, 1:1 ratio, were seeded in inserts chambers in 12 well plates, after 4 days inserts were removed. 0.5mg/ml matrigel with 25ug/ml FN was added on top with DMSO of ADAMTS5 inhibitor (10µM). Scratches were imaged for 48h using an Olympus fluorescence microscope, 4x objective. Wound margins are marked by green line in the GFP images. Scale bar, 250µm (A). Gap area was quantified with ImageJ and normalised to time 0. Graph shows the normalised mean of the relative gap area, ± SEM from N=3 independent experiments. Šídák's multiple comparisons test, (B).

4.2.3. ADAMTS5 was not required for scratch closure in A2780 cells

To elucidate the role of Rab25 in collective cell migration and confirm the contribution of ADAMTS5, A2780-DNA3 and Rab25 cells were seeded in a 12 well plate, scratched after 24h and overlayed with FN-supplemented matrigel. ADAMTS5 inhibitor or DMSO were added to

the matrigel mix during polymerization and to the media. Our hypothesis was that Rab25-induced increase cell migration would be prevented by ADAMTS5 inhibition. However, no difference in scratch closure was observed either in the presence or in the absence of ADAMTS5 inhibitor between A2780-Rab25 and A2780-DNA3 cells (figure 4.9). A2780 cells migrated into the scratch area faster than Ovcar3 cells. At 3h after scratching, both DNA3 and Rab25 migrated to a similar extent, regardless of the presence of ADAMTS5 inhibitor. Finally, at 6h, more than half of the scratch was covered by both DNA3 and Rab25 cells, with a relative gap area mean of 0.45 and 0.44 respectively. On the contrary to what hypothesised, when ADAMTS5 inhibitor was added both DNA3 and Rab25 cells closed the scratch slightly more than in the presence of DMSO, with a relative gap area 0.36 and 0.39, respectively. Overall, no significant differences in migration were observed in A2780s cells, as the variability between experiments was quite high.

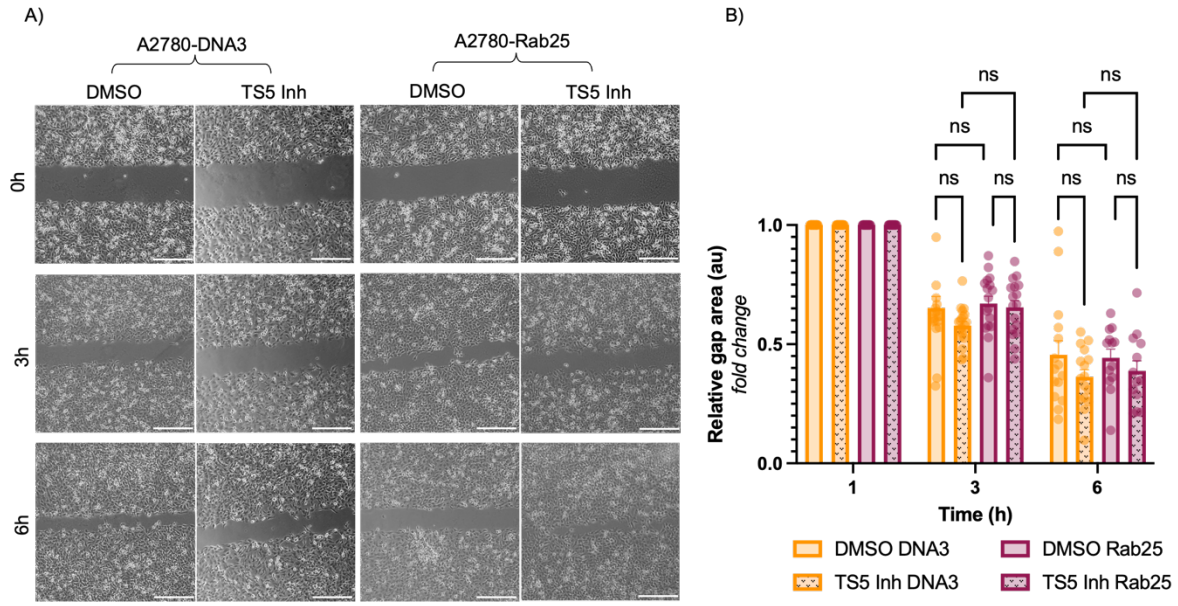

Figure 4.9. ***ADAMTS5 inhibitor did not affect A2780 cell collective migration.*** A2780-DNA3 and A2780-Rab25 cells were seeded in 12 well plates, after 24h cells were scratched and 0.5mg/ml matrigel with 25µg/ml FN was added on top. Either DMSO or ADAMTS5 inhibitor (10µM) was added to the ECM mix and to the media. Scratches were imaged every 3h using an Olympus fluorescence microscope. Scale bar, 250µm (A). Gap area was quantified with ImageJ and normalised to time 0. Graph shows the normalised mean of the relative gap area, ± SEM from N=3 independent experiments Tukey's multiple comparisons test (B).

4.2.4. FN did not affect the velocity and directionality of collective cell migration in A2780 cells

Since A2780 cells migrated faster than Ovcar3 cells, with full wound closure happening overnight, scratch experiments were repeated using live cell microscopy, to be able to track individual cell migration. A2780-DNA3 and Rab25 cells were seeded in a 12 well plate, after 24h the wells were scratched and overlayed with FN-supplemented matrigel or matrigel only before imaging. Scratches closed in approximately 12h (figure 4.10). Both cell lines were covering more or less the same area of scratch up to 6h, at that point DNA3 cells moved further into the wound when FN was present than only matrigel, but both scratches were fully closed by 12h. In Rab25 cells, scratches were closing equally at all time points. Overall, there is a small but not statistically significant increase in DNA3 cell velocity in the presence of FN-supplemented matrigel compared to matrigel only. Rab25 cell velocity was significantly higher than DNA3 in the absence, but not in the presence, of FN. Moreover, FN did not affect Rab25 cell migration velocity. As it was previously shown that Rab25 increased directionally of cell migration in 3D matrices, we quantified the forward migration index (FMI), which measures the efficacy of forward migration of the cells in relation to both axis, hypothesising that Rab25 cells would migrate more directionally towards the middle of the scratch in matrigel supplemented with FN. However, we only detected a small, and not statistically significant, difference in the FMI between DNA3 and Rab25 cells, in the presence and absence of FN. These data suggest that Rab25 expression and the presence of FN do not affect directional cell migration in A2780 cells.

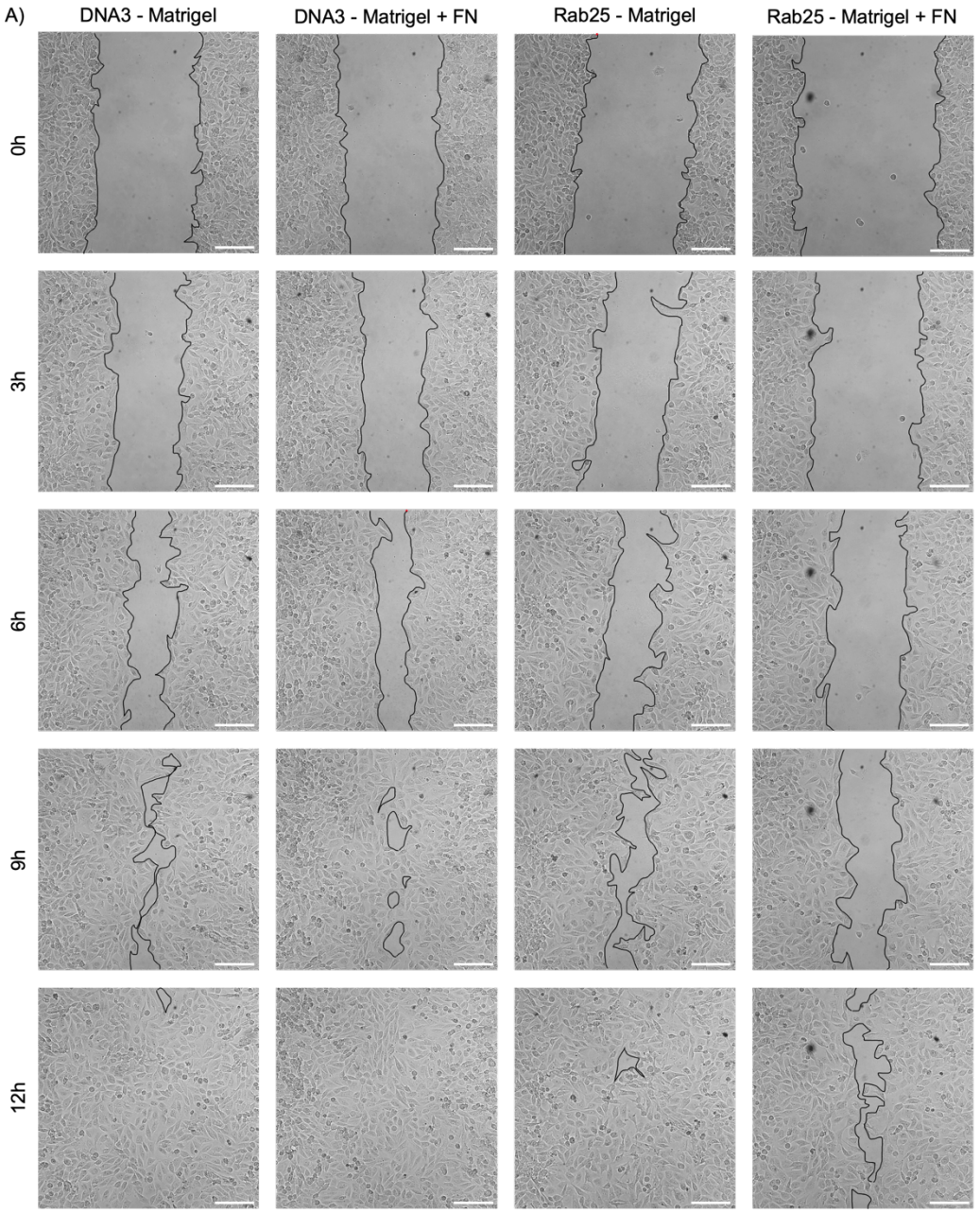
A)
DNA3 - Matrigel
DNA3 - Matrigel + FN
Rab25 - Matrigel
Rab25 - Matrigel + FN
0h
3h
6h
9h
12h

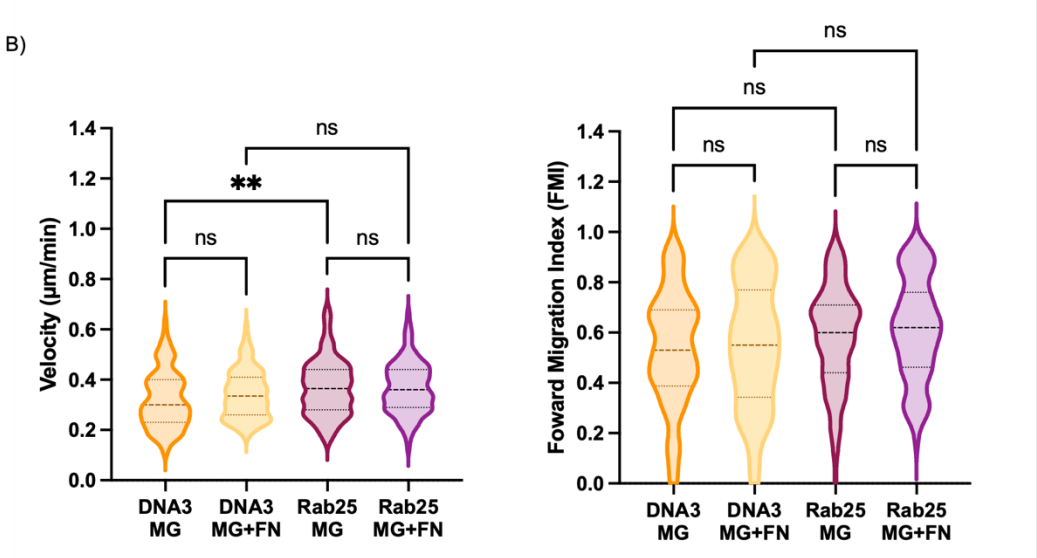
B)
Velocity (µm/min)
1.4
1.2
1.0
0.8
0.6
0.4
0.2
0.0
**
ns
ns
ns
DNA3 MG
DNA3 MG+FN
Rab25 MG
Rab25 MG+FN
Foward Migration Index (FMI)
1.4
1.2
1.0
0.8
0.6
0.4
0.2
0.0
ns
ns
ns
ns
DNA3 MG
DNA3 MG+FN
Rab25 MG
Rab25 MG+FN

Figure 4.10. ***FN increases FMI in A2780 cells.*** A2780-DNA3 and Rab25 cells were seeded in 12 well plates, after 24h cells were scratched and 0.5mg/ml matrigel or 0.5mg/ml matrigel with 25µg/ml FN was added on top. Cells were imaged live as soon as matrigel was polymerised every 10min for 16h, using a Nikon Widefield Live-Cell System (Nikon Ti eclipse with Oko-lab environmental control chamber) with a 10x objective. Scale bar, 150µm (A). Cells were manually tracked and velocity (µm/min) and forward migration index (FMI) were quantified using ImageJ. Graph shows violin plot with median and quartiles from N=3 independent experiments, Kruskal-Wallis test, ** p=0.0037 (B).

4.2.5. ADAMTS5 was required for directional collective cell migration in A2780 cells overexpressing Rab25

We then wanted to assess the role of ADAMTS5 in FN-driven collective cell migration. For this, A2780-DNA3 and A2780-Rab25 cells were scratched, overlayed with matrigel supplemented with FN and imaged live in the presence of 10µM ADAMTS5 inhibitor or DMSO control. As shown in figure 4.11, in the presence of DMSO, both DNA3 cells and Rab25 cells covered approximately half of the scratch area by 6h and fully closed the gap in 12h. Rab25 cells seemed to form a slightly patchier monolayer at 12h compared to DNA3 cells, which appeared more compact. On the other hand, when ADAMTS5 inhibitor was added both DNA3 and Rab25 cells cover less area of the scratch, images appear similar up to 6h of wound closure when ADAMTS5 inhibited cells start to leave bigger gaps. No difference in migration velocity was detected between DMSO and ADAMTS5 inhibitor in either DNA3 or Rab25 cells. However, here we detected a significant increase in directionality of cell migration in Rab25 cells compared to DNA3, which was completely abrogated by ADAMTS5 pharmacological inhibition (figure 4.11-B).

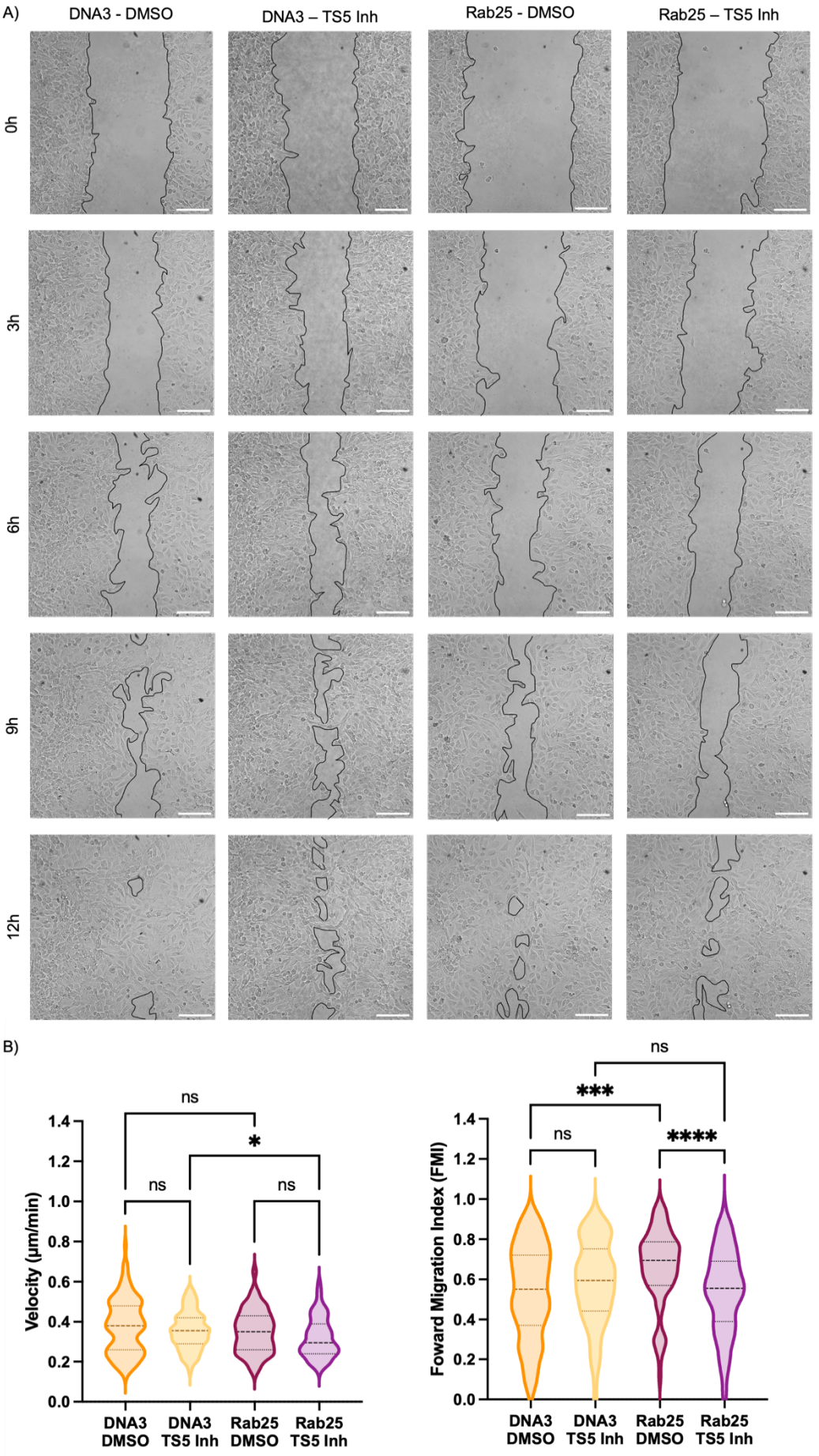
A)
DNA3 - DMSO
DNA3 – TS5 Inh
Rab25 - DMSO
Rab25 – TS5 Inh
0h
3h
6h
9h
12h
B)
Velocity (µm/min)
ns
*
ns
ns
DNA3 DMSO
DNA3 TS5 Inh
Rab25 DMSO
Rab25 TS5 Inh
Foward Migration Index (FMI)
ns
***
ns
****

Figure 4.11. ***ADAMTS5 was required for directional cell migration in A2780 cells.*** A2780-DNA3 and Rab25 cells were seeded in 12 well plates, after 24h cells were scratched and 0.5mg/ml matrigel with 25µg/ml FN was added on top. Either DMSO or ADAMTS5 inhibitor (10µM) was added to the ECM mix and to the media. Cells were imaged live as soon as matrigel was polymerised every 10min for 16h, using a Nikon Widefield Live-Cell System (Nikon Ti eclipse with Oko-lab environmental control chamber) with a 10X objective. Scale bar, 150µm (A). Cells were manually tracked and migration velocity (µm/min) and forward migration index (FMI) were quantified using ImageJ. Graph shows violin plot with median and quartiles from N=3 independent experiments, Kruskal-Wallis test, * p=0.0473, *** p=0.0001, ****p<0.0001 (B).

To confirm the role of ADAMTS5 in collective cell migration, we used siRNAs to downregulate its expression. As we have previously established that SDC4 was required for Rab25-dependent ADAMTS5 expression, we also knocked down SDC4. A2780-Rab25 cells were transfected with siRNAs targeting SDC4, ADAMTS5 or a non-targeting siRNA control. Cells were seeded in a 12 well plate, after 6h the wells were scratched and overlayed with 0.5mg/ml matrigel with 25µg/ml FN. After matrix polymerization, cells were imaged live. As shown in figure 4.12, that scratches were fully closed after approximately 12h. At the beginning the scratches were approximately the same size in the three conditions, after 3h a small portion of the wounds were covered and by 6h half the wound areas were covered in all conditions. In all three conditions there is a consistent coverage of the wound area that is fully closed by 12h. Single cell tracking showed no difference in velocity between control and ADAMTS5-KD or SDC4-KD. On the other hand, ADAMTS5-KD resulted in a small, but statistically significant, reduction in directionally of cell migration, while no differences in FMI were observed between upon SDC4 downregulation. qPCR analysis, confirmed the knocked down efficiency for both ADAMTS5 and SDC4. Indeed, transfection with ADAMTS5 siRNA resulted in an 83% decrease in ADAMTS5 expression, while SDC4 siRNA caused a 68% decrease in SDC4 expression (figure 4.13). Together, these data indicate that ADAMTS5 is required for directional collective cell migration, while SDC4 does not seem to play a role.

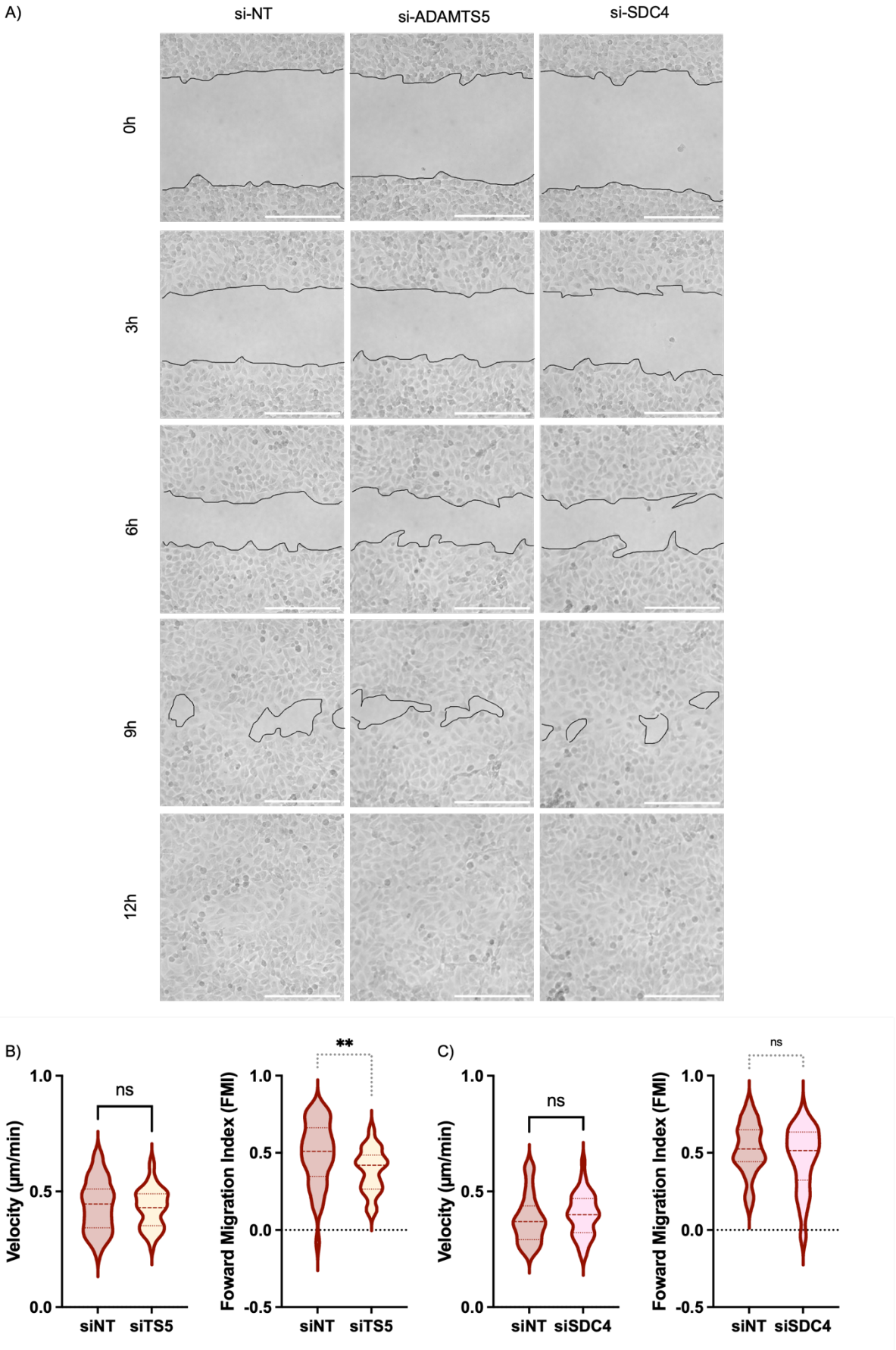
A)
si-NT
si-ADAMTS5
si-SDC4
0h
3h
6h
9h
12h
B)
Velocity (µm/min)
1.0
0.5
0.0
ns
siNT
siTS5
Foward Migration Index (FMI)
1.0
0.5
0.0
-0.5
**
siNT
siTS5
C)
Velocity (µm/min)
1.0
0.5
0.0
ns
siNT
siSDC4
Foward Migration Index (FMI)
1.0
0.5
0.0
-0.5
ns
siNT
siSDC4

*Figure 4.12. **ADAMTS5 knock down decreased directional migration in A2780-Rab225 cells.** **A2780-Rab25*** cells were transfected with an siRNA targeting ADAMTS5 (siTS5), an siRNA targeting SDC4 (siSDC4) or a non-targeting siRNA control (siNT) and incubated for 3 days. Cells were seeded in 12 well plates, after 24h cells were scratched and 0.5mg/ml matrigel with 25µg/ml FN was added on top. Cells were imaged live as soon as matrigel was polymerised every 10min for 16h, using a Nikon Widefield Live-Cell System (Nikon Ti eclipse with Oko-lab environmental control chamber) with a 10X objective. Scale bar, 250µm (A). Individual cells were manually tracked and velocity (µm/min) and forward migration index (FMI) were quantified using ImageJ. Graph shows violin plot with median and quartiles from N=1 independent experiments, Mann Whitney test, ** p=0.0047

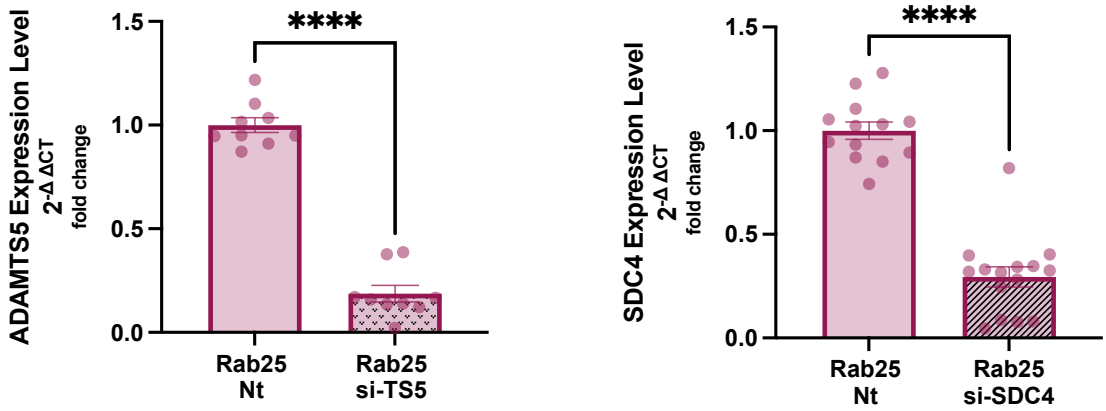

*Figure 4.13. **ADAMTS5 and SDC4 knock down efficacy.*** Cells were transfected with an siRNA targeting ADAMTS5 (si-TS5), an siRNA targeting SDC4 (si-SDC4) or a non-targeting siRNA control (NT) and incubated for 1 days before samples were collected for qPCR. One-step qPCR was run by extracting RNA from the cell lysate following kits instruction and loading a qPCR plate with RNA and Luna kit reagents. Graph shows Graph shows the normalised mean, ±SEM from N=3 (ADAMTS5) and N=4 (SDC4) independent experiments, Mann Whitney test, **** p<0.0001

4.3 Discussion:

In this chapter, we showed that FN promotes collective cell migration in ovarian cancer cells and ADAMTS5 is required for this. Caswell, et at., 2007 have shown that Rab25 promotes α5β1-FN-Dependent invasion of A2780 cells in 3D environments. Moreover, we have previously shown that overexpression of Rab25 increased pseudopod elongation and directional migration in ovarian cancer cells, in a ADAMTS5 dependent manner when single cells were seeded on CDM (Yuan et al., 2024). Here, we wanted to investigate if ADAMTS5 was also required for collective cell migration in FN-containing matrices. In Ovcar3 cells, that endogenously overexpress Rab25, the addition of FN strongly promoted cell migration compared to matrigel only, supporting previous literature (Caswell et al., 2007; Yousif, 2014). Interestingly. ADMATS5 inhibition resulted in a reduction in migration, in agreement our

findings that FN promotes ADAMTS5 upregulation in Rab25 overexpressing cells. An issue we encountered was the variability in Ovcar3 migration, apparent from the comparison of figure 4.2 and 4.3. In figure 4.2, cells supplemented with FN covered a total area of 95.8% since the start of the experiment, but in figure 4.3, cells in the presence of FN only covered 50.8% of the scratch area since the beginning of the experiment, closer to what Ovcar3 cells migrated when on matrigel only in figure 4.2, 65.29%. A key difference between the 2 sets of experiments was the presence of DMSO in figure 4.3. DMSO has been found to affect migration, at higher concentrations (2.5% DMSO) compared low (0.1%-1%), which was the concentration used (0.1%) in our experiments, in prostate cancer cells (Khurana et al., 2022), to reduce ovarian cancer cell growth (Grunt et al., 1991), and to increase cytotoxicity of tumour cells of antineoplastic agents (Pommler et al., 1988). Alternatively, it is possible that the discrepancy in the results was caused by cell-cell variability, cells getting older (even if morphological changes where not appreciated and splitting behaviour was not altered between experiments) or FN batches variability.

Ovarian cancer cell metastasis is characterised by cancer cell interactions with mesothelial cells, which facilitate metastasis in the omentum and peritoneum (Lengyel, 2010). Mesothelial cells were considered a layer of cells with low motility, but it had been demonstrated that they can be reprogrammed by the tumour microenvironment and adquire invasive/migratory capacities, aiding in peritoneal dissemination (Del Rio et al., 2021; Mogi et al., 2021; Rynne-Vidal et al., 2015). To produce a more physiologically relevant migration model, we cocoltured Ovcar3 cells with MET-5a-GFP, to assess if migration was improved in FN-rich matrices and if migration could be slowed down by ADAMTS5 inhibition, as previously observed. We firstly examined different cell ratios to ensure that both cell populations were surviving, and assess their behaviour. We established that the best ratio was 1:1, and we observed that MET-5a cell were depositing FN on top and around the cells, forming a FN network, while Ovcar3

cells did not have any FN located around them, after 14 days of coculture. We then performed scratch assays to assess migration. One of the first issues we had was the fragility of the monolayers. After a 3-day coculture, the monolayers peeled away during the scratch or the scratches were too big to be imaged. This was probably due to the fact that mesothelial cells secreted their own matrix on top of the monolayers, increasing the cell cohesion. To avoid this issue, we used two chambered sticky inserts that were added to the centre of the wells, allowing to create a gap without damaging the cells. This method also allowed us to increase the coculture time to a total of 4 days. At 4-day coculture we could observe the beginning of cell reorganisation, as MET-5a cells were rearrainging around the Ovcar3 cells, but there was no 3D structure formation, due to the limited growth area - leaving them longer could led to peeling of the stucture when washing or overlaying with the matrigel. This time incubation differences between the immunofluorescence coculture and the scratch coculture could lead to cell behaviour differences. MET-5a coculture increased Ovcar3 cell migration, but we did not detect differences in cell migration in the presence and absence of FN. This could be due to MET-5a cells secreating and arranging their own FN, as shown in figure 4.4 and by others (Mutsaers and Wilkosz, 2007). When ADAMTS5 inhibitor was added, no changes in migration were observed in the coculture model. Interestingly migration of the coculture cells led to faster closure of the scratch than when Ovcar3 cells were cultured alone, as full wound closure was observed in 24h instead of 48h. In the migrated area it was possible to observe both mesothelial cells and ovarian cancer cells. This suggests that MET-5a cells can drive Ovcar3 cell migration in an ADAMTS5 independent manner. Further experiments assessing mesothelial cell migration on their own could be performed to determine if the coculture model also leads to an increase in MET-5a motility.

Additionally, we wanted to confirm the results obtained with the Ovcar3 cells in A2780 cells, to assess the role of Rab25 in collective cell migration. No difference was observed between

A2780 cells migrating on matrigel with FN compared to matrigel only. Furthermore, differences in migration between Ovcar3 cells and A2780s were observed, the first migrated more slowly and in a more cohesive way in comparison to the latter. A2780-Rab25 cells have been previously reported to migrate more randomly than A2780-DNA3 cells on plastic and more directionally on CDM (Caswell et al., 2008; Rainero et al., 2015). Due to these differences, we decided to assess individual cell migration and repeated the scratches using a Nikon widefield live cell system, to track live migration. Interestingly, FN only increased directional cell migration in Rab25-overexpressing cells in one set of experiments, but not in the other, making it difficult to determine the role Rab25 in FN-dependent collective cell migration. Nevertheless, the addition of ADAMTS5 inhibitor led to ~ 30% decrease in directional migration only in Rab25 overexpressing cells, while no changes were observed in A2780-DNA3. A similar reduction in FMI, ~20%, was observed when A2780-Rab25 cells were transfected with ADAMTS5 si-RNA. compared to non-targeting siRNA. Interestingly, no significant changes were observed when SDC4 was knocked down. However, this experiment was only carried out once, so further experiments are needed to confirm the trend. It is important to note that the difference in the way in which cells move upon ADAMTS5 inhibition does not seem to affect their ability to close the wound. Overall, we can conclude that when ADAMTS5 is inhibited or knocked down in A2780-Rab25 cells directionality of cell migration is reduced and in Ovcar3 cells ADAMTS5 inhibition reduces migration. On the other side, the role of SDC4 in regulating migration needs to be further elucidated. Moreover, the addition of mesothelial cells to the culture of Ovcar3 cells promoted Ovcar3 cell migration, in an ADAMTS5-independent manner.

CHAPTER 5: ADAMTS5 is required for ovarian cancer cell clearance of mesothelial monolayers

5.1 Introduction:

Ovarian cancer is the fifth cause of cancer related death in women as there is no definitive screening tools and symptoms can be confused with other non-malignant problems. This means that a high percentage of women (75%) present with metastasis when diagnosed with ovarian cancer, dropping the 5-year survival rate to 25% from 90% if diagnosed at stage I (Lengyel, 2010; Stewart et al., 2019). Ovarian cancer cells mostly metastasize in a passive way. As the ovaries have no physical barriers surrounding them when cancer cells dethatch from the primary tumour, either as single cells or clusters, they can be carried around by the movement of peritoneal fluid to other parts of the abdomen like the omentum or the peritoneum, a membrane that covers the organs in the abdominal cavity (Lengyel, 2010). Clinical observations suggest that the mesothelium covering he abdominal organs is the "soil" of ovarian cancer metastasis, as patients who had shunts implanted, which implied draining the peritoneal cavity into their jugular vein, to alleviate pain from ascitic fluid build-up, did not develop distant disseminated hematogenous metastases even if malignant tumour cells were directly infused in the circulation (Tarin et al., 1984).

The current understanding of the metastatic switch in ovarian cancer can be summarised as follows (Lengyel, 2010); epithelial cancer cells lose E-cadherin allowing them to undergo EMT (Huber et al., 2005). Cells gain a fibroblast like phenotype, becoming more invasive and being able to survive better in hypoxic conditions (Imai et al., 2003). Matrix metalloproteinases are induced, which mediate the cleavage of ECM and cell-cell adhesions, allowing cells to shed from the primary tumour into the ascitic fluid (Symowicz et al., 2007). The physical movement of the fluid allows the spread of cancer cells to other organs. As ovarian cancer cells have lost

E-cadherin expression, it was shown that in response they upregulate adhesion receptors like α5β1 integrin via increased phosphorylation of FAK and ERK (Sawada et al., 2008), facilitating adhesion to the ECM. Cancer cells also express FN on their surface, facilitating cell-cell adhesion in the ascitic fluid (Burleson et al., 2004; Casey et al., 2001). Moreover, FN had been found as one of the most prominent extracellular protein in ascites and the mesothelium covering the omentum and peritoneum, together with laminin and type IV collagen (Lengyel, 2010; Wilhelm et al., n.d.). Once at the secondary location, carcinoma cells bind to the mesothelial monolayer via integrins and CD44, a major receptor for hyaluronic acid. Matrix metalloproteinases are upregulated. For instance, MMP2 was found to cleave FN and vitronectin into smaller fragments increasing ovarian cancer cell adhesion to mesothelial cells via α5β1 integrin (Kenny et al., 2008). Similarly, cleavage of laminin by MMP2 was found to promote migration of breast cancer cells (Giannelli et al., 1997). However, further investigation on why ECM proteins fragments improve cancer cell engagement with mesothelial cells, when compared to full length proteins, is still needed. Spheroids have also been reported to bind vitronectin, laminin and collagen I and IV, in addition to FN in a cell specific manner (Buczek-Thomas et al., 1998; Burleson et al., 2004; Cannistra et al., 1995; Casey et al., 2001; Fishman et al., 1999). Once adhesion is established, cancer cells start invading the mesothelium.

Different *in-vitro* 3D ovarian cancer models have been established to recapitulate the ovarian cancer metastatic process (Erin et al., 2014). Developing models in 3D allows the study of an array of processes in a more physiologically relevant way than utilising 2D cell culture on plastic. 3D models allow the incorporation of multiple cell types and ECM, allowing to study the interactions among different cells, the contribution of the stroma, adhesion, migration, and invasion. In the 1970s one of the first 3D cultures were made using soft agar, where similarities between cancer cells growing in tumours and in 3D conditions were observed (Hamburger and

Salmon, 1977). The complexity of 3D cell cultures can vary from using scaffolds, gel-like substances such as matrigel or growing cells in suspension to more complex models like organoids, organ on chip or 3D bio-printed cultures (Barbolina et al., 2007; Kenny et al., 2007; King et al., 2011; Levanon et al., 2010; Loessner et al., 2010). In this chapter we utilised a 3D culturing method that allows to assess mesothelial cell invasion, called clearance assay, which mimics early steps of ovarian cancer metastasis (Davidowitz et al., 2012). A monolayer of mesothelial cells is formed in a dish, to which ovarian cancer cell spheroids are added, mimicking tumour spheroids shedding from the primary tumour and attaching to the mesothelium of the omentum or peritoneum. This model can be made more complex by adding ECM to the bottom of the dishes, producing spheroids with cocultures, or adding fibroblasts under the mesothelial cells. Ability of different ovarian cancer cell spheroids to clear mesothelial cells has been previously assessed. A2780 and Ovcar3 cells were found to be able to clear monolayers, together with other 9 cell lines, including ES2, HEYC2 and OV207, while 6 cell lines were found to not clear, including PE06, CAOV3 and MCAS. Research suggested that cells able to clear had enriched EMT signature genes (SNAI1, ZEB1 and TWIST1) (Davidowitz et al., 2014). Interestingly, protein atlas data indicates similar ADAMTS5 and SNAI1 RNA levels in A2780 and Ovcar3 cells (proteinatlas.org). Here, we assessed the role of Rab25, SDC4 and ADAMTS5 in mesothelial cell clearance and invasion by ovarian cancer cells. The hypothesis was that Rab25 overexpressing cells clear faster than control, in an ADAMTS5- and SDC4-dependent manner. Consistently, we found that Rab25 overexpression led to faster clearance of mesothelial cells. In addition, clearance was dependent on SDC4 and ADAMTS5 expression, as well as ADAMTS5 proteolytic activity.

5.2. Results:

5.2.1 Rab25 overexpression leads to faster mesothelial cell clearance:

It has been previously reported that α5β1 integrin and FN are needed for ovarian cancer spheroid adhesion to mesothelial cells (Kenny et al., 2014). Moreover FN has also been found to contribute to formation, adhesion and disaggregation of ovarian cancer spheroids (Burleson et al., 2004; Mitra et al., 2011; Zand et al., 2003). We firstly investigated if Rab25 overexpressing ovarian cancer spheroids cleared mesothelial cells faster than the control DNA3 cells, as Rab25-overexpressing cells have increased invasive abilities. Cell-tracker Red labelled A2780-DNA3 and Rab25 cells were mixed with soluble collagen and methylcellulose to form spheroids using the hanging drop method for 72h. 24 hours before the spheroids were ready, mesothelial cells (MET-5a-GFP) were seeded on a FN precoated 35mm glass bottom dishes. Spheroids were then added to the monolayer and left in the incubator for 6 hours to allow spheroids to adhere and were imaged live using a Nikon spinning disc microscope for 16h. As shown in figure 5.1, A2780-Rab25 cells cleared mesothelial cells faster than control A2780-DNA3 cells. Initially both cell lines were clearing out the mesothelial monolayer at a similar rate, from hour 0 to 6, at that point Rab25 overexpressing cells started to clear more area than the DNA3 cells progressively increasing over time. By hour 12, the difference in cleared area became statistically significant. Images show a single z plane where the spheroid was seen to invade into the mesothelial monolayer. As mesothelial cells are in different focal planes, the monolayer may appear patchy in some areas. Figure 5.1-B shows the brightfield maximum projection of the z stack, which allows to see a continuous monolayer of MET-5a-GFP.

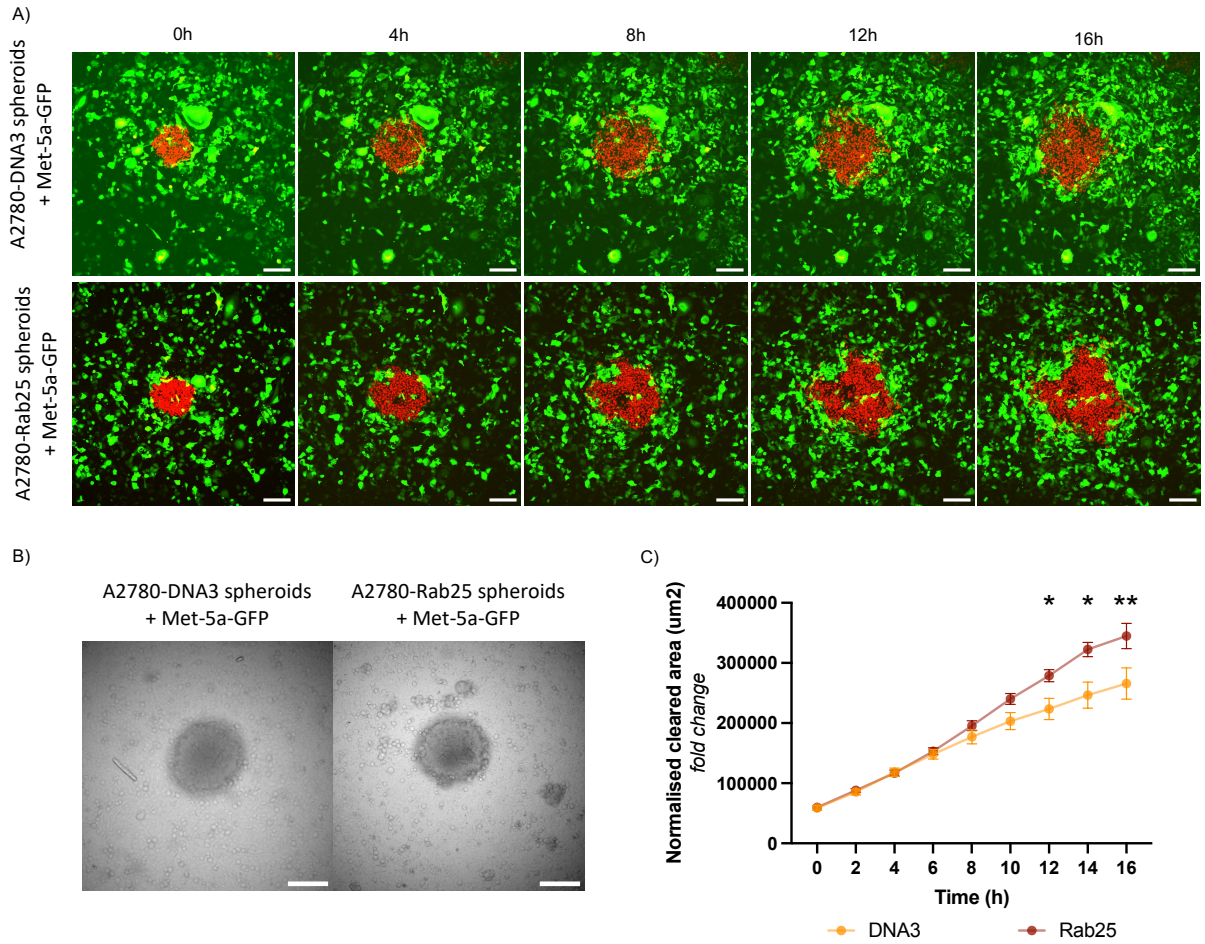

Figure 5.1. ***Rab25 overexpression promoted mesothelial cell monolayer clearance***. A2780-DNA3 and A2780-Rab25 cells were labelled with Cell-Tracker Red, and spheroids were generated using the hanging drop method for 3 days. Spheroids were then added to a monolayer of mesothelial cells (MET-5a-GFP) seeded on 25μg/ml FN. Cells were imaged every 2h for 16h live on a Nikon spinning disc microscope, 10x objective. Images were acquired as a z stack, only the slice containing the brightest MET-5a-GFP signal was used for analysis. Scale bar, 175 μm (A). Brightfield maximum projection of z stack acquired at 0h (C). Clearance was assessed by quantifying the displacement of mesothelial cells by A2780 cells with Fiji/Image J, data are presented as mean ± SEM from N=3 independent experiments. Šídák's multiple comparisons test, *p=0.0150 DNA3 vs Rab25 12h, *p=0.0104 DNA3 vs Rab25 14h and ** p=0.0087 DNA3 vs Rab25 16h (C).

We then assessed the ability of Ovcar3 cells, endogenously overexpressing Rab25, to clear mesothelial cell monolayers. Ovcar3 spheroids were generated with the hanging drop method, seeded on a monolayer of GFP-tagged mesothelial cells and imaged after 4h, 24h or 48h. In agreement with published observations (Trelford et al., 2024; Zhang et al., 2021), Ovcar3 spheroids progressively invaded into the mesothelial monolayer. Spheroids firstly adhered to the monolayer and started to "push away" mesothelial cells from under the area of adhesion. From the brightfield images, mesothelial cells appear to be compressed together by the Ovcar3

cell migrating out of the spheroid. MET-5a-GFP cells appeared to be more elongated when in close proximity to Ovcar3 cells, encapsulating the invading Ovcar3 cells. From the green channel it is possible to observe that the fluorescence intensity of the area underneath the spheroid was decreasing over time, suggesting there was no MET-5a-GFP cells located in the area, while on some occasions individual mesothelial cells left behind in the invasion area that appear as a bright green dots, highlighted by the arrowhead (figure 5.2).

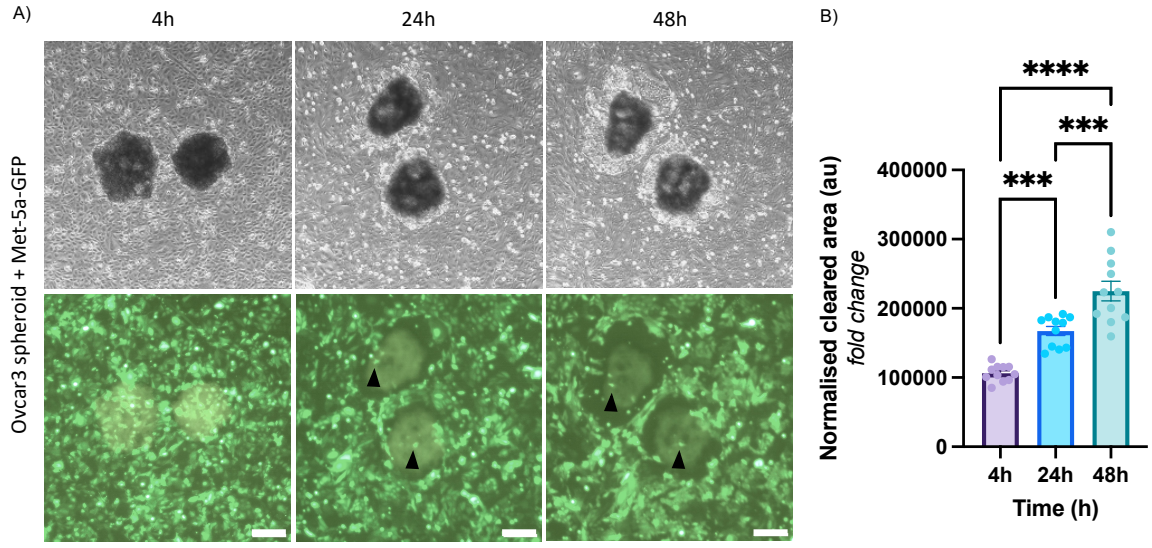

Figure 5.2. ***Ovcar3 cells cleared mesothelial cell monolayers.*** Ovcar3 spheroids were generated using the hanging drop method for 3 days, spheroids were then added to a monolayer of mesothelial cells (MET-5a-GFP) seeded on 25μg/ml FN. Cells were imaged for 48h every 24h on Olympus fluorescence microscope, 4x objective, scale bar is 150μm (A). Clearance was assessed by measuring the displacement of mesothelial cells by Ovcar3 cells with Fiji/Image J. Data are presented as mean ± SEM from N=1 independent experiment. Tukey's multiple comparisons test, ***p=0.002 4h vs 24h, ***p=0.0004 4h vs 48h and **** p< 0.0001 (B).

5.2.2 ADAMTS5 is required for ovarian cancer cell mesothelial clearance:

We have previously shown that ADAMTS5 is required for ovarian cancer cells to invade in 3D environments. A2780-Rab25 spheroids were embedded in a mix of GelTrex, collagen I and FN, treated with ADAMTS5 inhibitor and invasion was assessed over the course of 2 days. We found that treatment with ADAMTS5 inhibitor reduced invasion in a dose-dependent manner. Similarly, ADAMTS5 knockdown significantly reduced A2780-Rab25 spheroid invasion (Yuan et al., 2024). This demonstrated that ADAMTS5 is required for Rab25 overexpressing

cell invasion in 3D matrices. As during metastasis spheroids located in the ascitic fluid first interact with mesothelial cells, we wanted to investigate if ADAMTS5 was needed for mesothelial cell clearance. Ovcar3 spheroids were generated by the hanging drop method and seeded on top of a monolayer of MET-5a-GFP cells. Either 10μM of ADAMTS5 inhibitor or DMSO control were added to the media and clearance by ovarian cancer cells was assessed by imaging the spheroids every 24h using an Olympus fluorescence microscope. The brightfield images show that at 0h Ovcar3 spheroids were located on top of the mesothelial cells that are forming a confluent monolayer under the spheroid and in the surrounding area independently of the ADAMTS5 inhibitor presence. In the presence of DMSO control, as times passes ovarian cancer cells moved out from the spheroid into the mesothelial cell monolayer clearing the area around the spheroid and growing/invading in a compact manner. Mesothelial cells that have been pushed away assumed a more elongated morphology in the area around the spheroid, where the cancer cells were invading. The green channel images show a non-fluorescent area where mesothelial cells were replaced by Ovcar3 cells. Conversely, spheroids that were treated with ADAMTS5 inhibitor only cleared a small portion of mesothelial cells located directly underneath the spheroid. Indeed, no clear empty rim of fluorescence was detected in the green channel image (figure 5.3-A). Image analysis shows that Ovcar3 cells spheroids cleared significantly less area when ADAMTS5 inhibitor was added to the media compared to DMSO (figure 5.3-B).

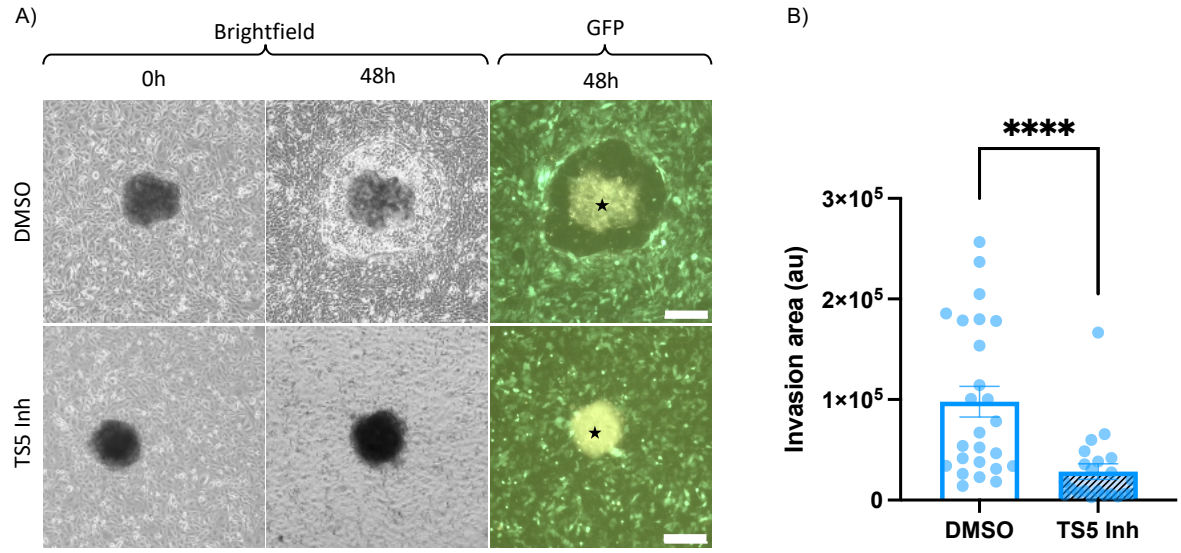

Figure 5.3. ***ADAMTS5 was required for mesothelial cell clearance by Ovcar3 spheroids***. Ovcar3-RFP cell spheroids were generated using the hanging drop method for 3 days, spheroids were then added to a monolayer of mesothelial cells (MET-5a-GFP) seeded on 25μg/ml FN, ADAMTS5 inhibitor (10µM) or DMSO were added to the media at the same time. Cells were imaged for 48h every 24h with an Olympus fluorescence microscope, 4x objective, scale bar 150μm. * Starred area represents the Ovcar3 spheroids, as cells were RFP ladled, some of the fluorescence bled into the green-fluorescence channel, giving the yellow signal (A). Clearance was assessed by measuring the displacement of mesothelial cells by Ovcar3 cells with Image J. Data are presented as mean ± SEM from N=3 independent experiments. Tukey's multiple comparisons test **** p> 0.0001 (B).

Similarly, when A2780-Rab25 spheroids were added to the monolayer of mesothelial cells in the presence of DMSO, a non-fluorescent area can be seen under the spheroids, with a thick invasion rim surrounding the spheroid and invading into the mesothelial cells, clearly visible in the brightfield image. This effect was significantly reduced when ADAMTS5 inhibitor was added. A smaller invasion edge can be observed around the spheroid and more GFP-fluorescence is present under the spheroid, suggesting the presence of more mesothelial cells compared to DMSO (figure 5.4-A). Consistently, the quantification shows that A2780-Rab25 cell spheroids invasion area was significantly reduced when ADAMTS5 inhibitor was added (figure 5.4-B).

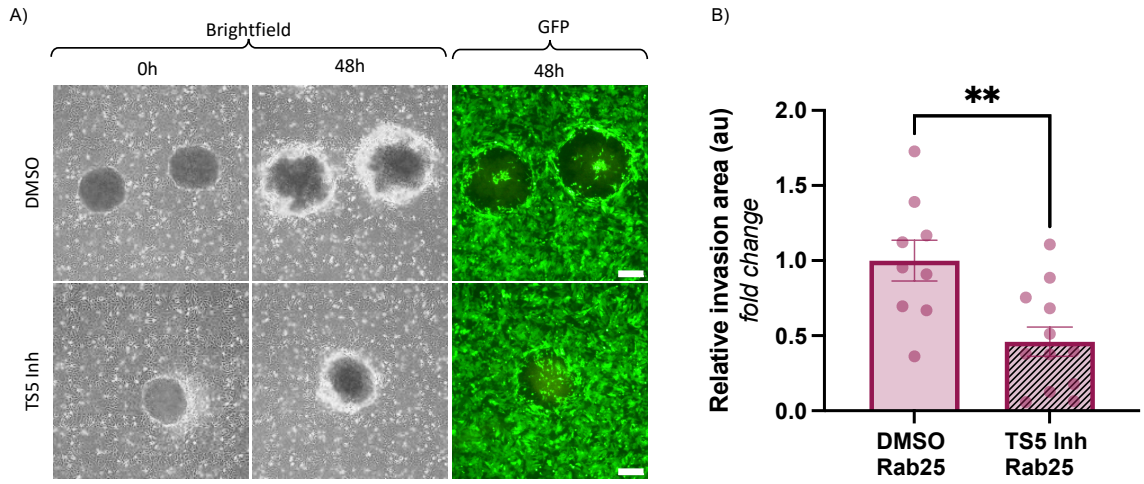

Figure 5.4. ***ADAMTS5 was required for mesothelial cell clearance by A2780-Rab25 spheroids***. A2780-Rab25 cell spheroids were generated using the hanging drop method for 3 days, spheroids were then added to a monolayer of mesothelial cells (MET-5a-GFP) seeded on 25μg/ml FN, ADAMTS5 inhibitor (10µM) or DMSO were added to the media at the same time. Cells were imaged for 48h every 24h with an Olympus fluorescence microscope, 4x objective, scale bar 150μm. (A). Clearance was assessed by measuring the displacement of mesothelial cells by Ovcar3 cells with Image J. Data are presented as mean ± SEM from N=2 independent experiments. Mann Whitney test ** p=0.0073 (B).

Finally, we wanted to determine if ovarian cancer cells were the source of ADAMTS5 that led promoted mesothelial cell clearance. MET-5a were tested by qPCR to elucidate if they also expressed ADAMTS5. Figure 5.5 shows that MET-5a expressed ADAMTS5, but its expression was not affected by the presence of FN.

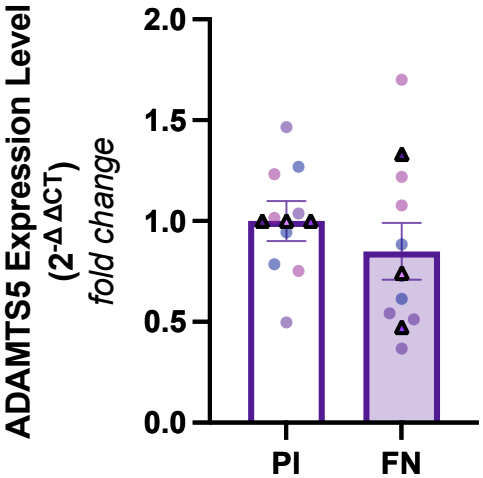

Figure 5.5. ***Mesothelial cell expression of ADAMTS5***. MET-5a-GFP cells were seeded on plastic (Pl) or 25µg/ml FN for 24h. RNA was extracted and ADAMTS5 and GAPDH (as housekeeping gene) expression was measured. Data represents normalised mean and individual data points, ± SEM from N=3 independent experiments, p=0.2973, Mann Whitney test.

As mesothelial cells also expressed ADAMTS5, we wanted to investigate the contribution of ADAMTS5 expressed by ovarian cancer cells in clearance. Our hypothesis is that ovarian cancer cell spheroid interacts with FN located on the cell surface of MET-5a, driving ADAMTS5 expression, that in turns leads to mesothelial cell clearance by ovarian cancer cells. To investigate this, ADAMTS5 was knocked down in A2780-Rab25 cells and clearance assays were performed. Transfected cells were used to generate spheroids, which were then added on top of the monolayer of MET-5a-GFP cells. Consistent with the pharmacological inhibitor results, knocking down ADAMTS5 in A2780-Rab25 cells significantly reduced the capacity of the cancer cells to clear the mesothelial monolayer. In the presence of the control non-targeting si-RNA, under the A2780-Rab25 spheroid there was a clear area lacking green fluorescence signal, where no mesothelial cells were present. Conversely, in ADAMTS5 knockdown spheroids, mesothelial cells are still located underneath in an almost intact monolayer (figure 5.6). We have previously established that SDC4 is required for FN induced ADAMTS5 expression, we therefore wanted to investigate if SDC4 was also required for mesothelial cell clearance. A2780-Rab25 cells were transfected with SDC4 si-RNA or a non-targeting siRNA control. Spheroids were then generated and added on the mesothelial cell monolayer. As shown in figure 5.6, that the invasion area cleared by A2780-Rab25 with SDC4 knocked down was significantly smaller than non-targeted si-RNA and had a similar effect than the use of ADAMTS5 si-RNA. Both SDC4 and ADAMTS5 knockdowns led to the attachment of the spheroid to the monolayer but almost no displacement of mesothelial cells nor invasion of ovarian cancer cells into the monolayer occurred, while it was possible to observe a cleared area of mesothelial cells, where no fluorescence was detected, underneath the non-targeting si-RNA spheroid.

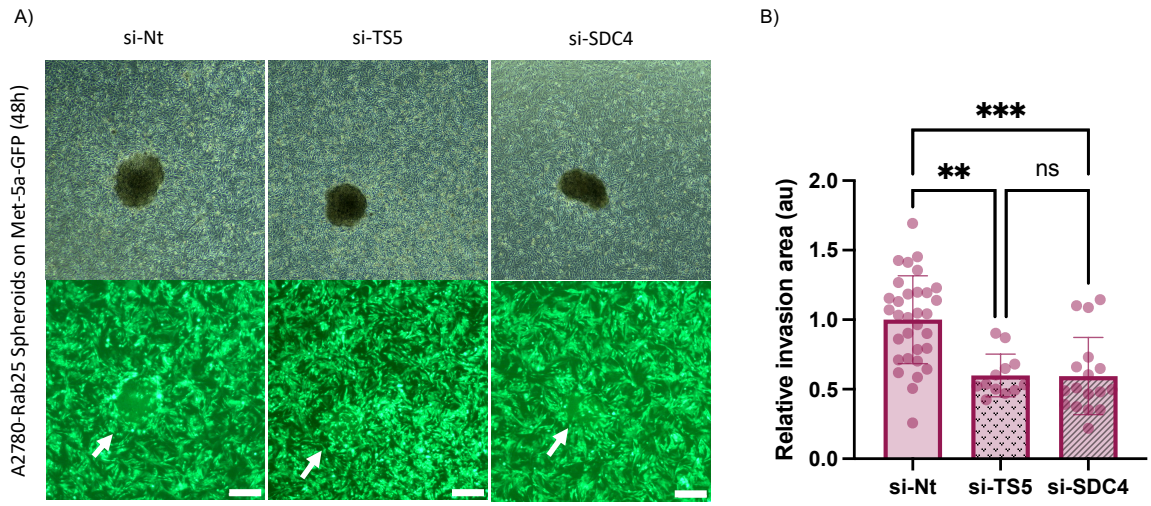

*Figure 5.6. **ADAMTS5 and SDC4 were required for A2780-Rab25 cell mesothelial clearance.*** A2780-Rab25 cells were transfected with an siRNA targeting ADAMTS5 (si-TS5), an siRNA targeting SDC4 (si-SDC4) or a non-targeting siRNA control (si-nt). Spheroids were generated using the hanging drop method for 3 days and added to a monolayer of mesothelial cells (MET-5a-GFP) seeded on 25μg/ml FN. Cells were imaged for 48h every 24h with an Olympus fluorescence microscope, 4x objective, scale 150 μm. White arrows point at the area where the spheroid is attached (A). Clearance was assessed by measuring at the displacement of mesothelial cells by A2780-Rab25 spheroids with Image J. Data are presented as mean ± SEM from N=2 independent experiments. Kruskal-Wallis test, ** p=0.0016 and *** p=0.0001 (B).

α5 integrin has been previously involved in promoting clearance of ovarian cancer spheroids by increasing adhesion of spheroids to mesothelial monolayers (Kenny et al., 2014). We then wanted to confirm that A2780-Rab25 spheroid clearance of mesothelial cells was mediated by α5 integrin. Treatment of the spheroids with an inhibitor for α5 (ATN161) resulted in a small decrease in clearance, which was not statistically significant, when compared to the vehicle control (H_2O). Both conditions showed a reduction in green fluorescence under the spheroid suggesting that the majority of MET-5a-GFP have been pushed aside, while clear dots of individual cells can be seen in both conditions. A small, fluorescence free, ring can be observed in the control which suggest invasion of cells into the mesothelial monolayer, that is not present when the α5 inhibitor was added. This difference is reflected in the statistical analysis, as a decrease in relative invasion area is observed in the α5 inhibitor condition when compared to water but, it is not statistically significant, probably due to the two spheroids that did not clear well in the control condition (figure 5.7). In this chapter, we have shown that both SDC4 and

ADAMTS, and to a lesser extent α5 integrin, are required for ovarian cancer cell clearance of mesothelial cells.

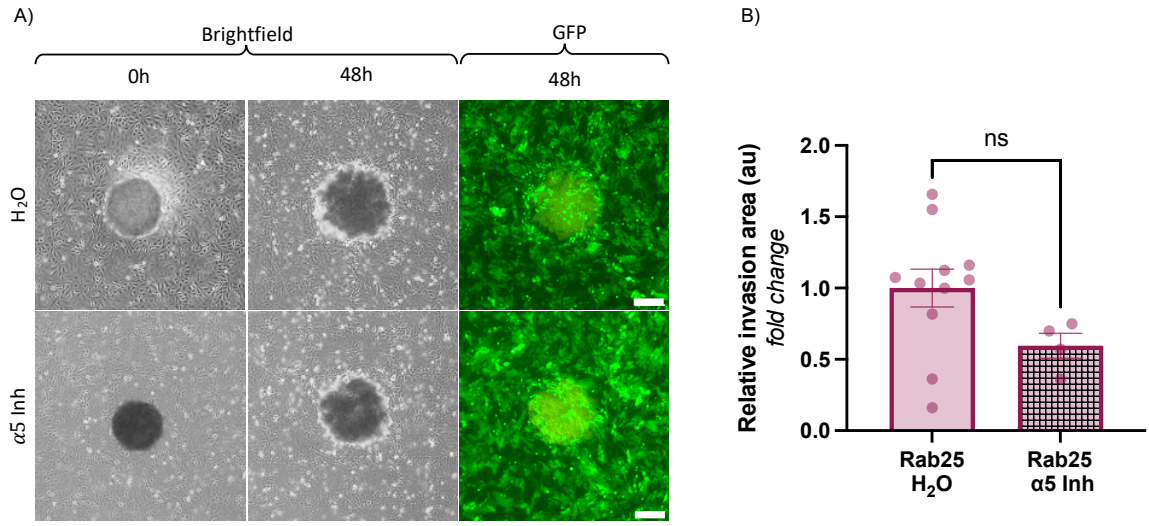

Figure 5.7. ***α5 inhibition has a modest effect on mesothelial cell clearance in Rab25 overexpressing cells.*** A2780-Rab25-RFP cell spheroids were generated using the hanging drop method for 3 days, spheroids were then added to a monolayer of mesothelial cells (MET-5a-GFP) seeded on 25μg/ml FN, α5 inhibitor (50μM) or H_2O were added to the media at the same time. Cells were imaged for 48h every 24h with an Olympus fluorescence microscope, 4x objective, scale bar 150μm. (A). Clearance was assessed by measuring the displacement of mesothelial cells by Ovcar3 cells with Image J. Data are presented as mean ± SEM from N=2 independent experiments. Mann Whitney test p=0.0557 (B).

5.3. Discussion:

In this chapter we have shown that Rab25 overexpressing spheroids cleared mesothelial cell monolayers faster than cells lacking Rab25 expression. Data presented further suggest that ADAMTS5 and SDC4 are required for this process.

Due to the passive way ovarian cancer metastasises, mesothelium attachment and invasion is the first step ovarian cancer cells are required to do to undergo metastasis. Therefore, mesothelium clearance assays are commonly used to study this process in vitro in a physiologically relevant manner. Experiments carried out using ascitic spheroids form ovarian cancer patients demonstrated spheroid binding to ECM components and mesothelial cells monolayers (Burleson et al., 2006; Casey et al., 2001; Iwanicki et al., 2011). Inspired by this work, we investigated mesothelial cell clearance using GFP labelled mesothelial cells and

ovarian cancer cell spheroids produced using the hanging drop method, that allowed us to make spheroids with consistent cell number in a reproducible manner. Previous research has examined patient ascitic fluid (stage III and IV) and investigated the multicellular aggregates located in it. Sized ranged from 50 to 750 μm, patient samples contained a mix a spheroid sizes and the range varied in a patient-specific manner (Casey et al., 2001). The authors generated physiologically relevant aggregates by liquid overlay technique using between 5,000 and 50,000 cells per ml of media, while we produced spheroids ranging from 150 to 350 μm via the hanging drop method using approximately 2000 cells per spheroid, generating spheroids of physiologically relevant size.

Interestingly differential behaviour on the clearing mechanism was found among the cell lines used. On the one hand, A2780 cells, independently of the overexpression of Rab25, cleared mesothelial monolayers in two ways; by pushing MET-5a cells apart and intercalating with them and by crawling on top of the mesothelial cells before intercalating. On the other hand, Ovcar3 cells pushed mesothelial cells from the bottom of the spheroid, with Ovcar3 cells remaining compact in the spheroid and slowly expanding the invasion area from underneath after breaching the monolayer. Interestingly, a similar behaviour to A2780 cells was seen in other ovarian cancer cell lines and multicellular aggregates that expressed N-cadherin (N-cad), as these cells migrated laterally before penetrating into 3D collagen gels, adhering to mesothelial cells, extending, and intercalating protrusions within the mesothelial monolayer without major disruptions. These cells only retained some cell-cell junctions, while cells that express E-cadherin (E-cad) only or hybrid E-cad/N-cad were not associated to multicellular streaming, migratory behaviour characterised by loosely adherent cells that migrate following the same path (Klymenko et al., 2017). E-cad and N-cad levels have been previously tested in A2780 and Ovcar3 cells, showing that both cells lines express N-cad, A2780 cells express lower levels of E-cad while Ovcar3 cells express 10 times more (Kielbik et al., 2021). This

differences in behaviour could also be due to the fact that A2780 cells were established from an ovarian endometroid adenocarcinoma, while Ovcar3 were isolated from a malignant ascites of a patient with progressive adenocarcinoma (atcc.org).

Rab25 overexpression in A2780 ovarian cancer cells has been previously found to increase migration in 3D matrices characterised by the extension of long pseudopodia, and linked to the association of Rab25 with α5β1 integrin promoting its recycling to the pseudopodial tips located at the cell front (Caswell et al., 2007; Dozynkiewicz et al., 2012). Our results show that Rab25 overexpressing spheroids cleared the mesothelial monolayer faster than control spheroids lacking Rab25 expression. This could be due to the increased recycling of integrin α5β1 in Rab25 overexpressing cells. This hypothesis is supported by other research that suggested that integrin α5β1, talin I and myosin II are required for mesothelial clearance, as cancer spheroids use the FN present on the mesothelial cells to exert force via the actomyosin contractility machinery to move mesothelial cells (Iwanicki et al., 2011). Moreover, β1 has been implicated in the regulation of the adhesion of ovarian cancer cell spheroids to the ECM present at sites of secondary tumour growth (Casey et al., 2001).

Furthermore, our lab has previously found that when Rab25 overexpressing cells were cultured as spheroids inhibition of ADAMTS5 reduced invasion capacity in the surrounding ECM both in monoculture and when cocultured with cancer associated fibroblasts (Yuan et al., 2024). Here we assessed ADAMTS5 requirement to clear mesothelial monolayers. In previous chapters we have established that ADAMTS5 expression is increased in Rab25 cells and further increased on FN matrices. In our assays, mesothelial cells were seeded on precoated FN dishes. We and others (Kenny et al., 2014) have shown that FN is rearranged by mesothelial cells and displayed on their surface. We, therefore, hypothesised that binding of Rab25 overexpressing ovarian cancer spheroids to FN located on mesothelial cells would upregulate ADAMTS5 expression that led to mesothelial cell clearance. Our results show that both inhibition and

knock down of ADAMTS5 in Ovcar3 and A2780-Rab25 spheroids led to reduction of mesothelial cell clearance. A 71% reduction in clearance was observed in Ovcar3 spheroids when ADAMTS5 inhibitor was present while A2780-Rab25 cells showed a smaller reduction of 54%. This could be a cell specific variation as ADAMTS5 knockdown in A2780-Rab25 cells led to a similar reduction of clearance, 40.1%. Overall ADAMTS5 expression levels are higher in Ovcar3 cell compared to A2780 cells, which could explain why inhibiting ADAMTS5 leads to a bigger effect in Ovcar3 cells compared to A2780. This suggests that ADAMTS5 might be one of the main drivers of mesothelial cell clearance by Ovcar3, while other mechanisms may also be involved in promoting A2780 cell clearance, such as $\alpha 5\beta 1$ integrin recycling.

Furthermore, a 40.5% reduction in clearance was observed when SDC4 was knocked down, almost exactly the same reduction observed when ADAMTS5 expression was targeted. Further experiments knocking down SDC4 in Ovcar3 cells are needed, to confirm its role in mesothelial cell clearance. SDC4 has been found to interact with ADAMTS5 via heparan sulphate side chains, that led to activation of ADAMTS5 increasing matrix degradation (Wang et al., 2011). Activation of ADAMTS5 by SDC4 could be modulating mesothelial cell clearance, in addition to controlling its expression. Further testing on ADAMTS5 protein function is needed as currently only mRNA upregulation was tested upon SDC4 knockdown. In addition, ADAMTS5 inhibitor can affect both MET-5a and Ovcar3 cells in our clearance assays since both cell types express ADAMTS5. To determine if cancer cells are the main source of ADAMTS5 impacting clearance, we performed knockdown experiments targeting ADAMTS5 in cancer cells. However, but further studies are required to assess if MET-5a cells can compensate for the loss of ADAMTS5 expression, as only a partial reduction in clearance was observed upon ADAMTS5 downregulation in cancer cells.

To summarise, we have shown that ADAMTS5 and SDC4 are required for mesothelial cell clearance by Rab25-overexpressing ovarian cancer cell spheroids.

CHAPTER 6: Establishment of an in vivo *Zebrafish model for ovarian cancer cell metastasis*

6.1 Introduction:

Danio Rerio (zebrafish), is a small tropical freshwater fish naturally found in southern Asia. 70% of its genome is shared with humans and 80% of disease causing protein-coding genes are conserved, being a great tool to capture disease initiation, progression and resolution (Patton et al., 2021).

Zebrafish have been used for decades in the field of biomedical research. Its use as a biomedical animal model was firstly suggested by George Streisinger and colleagues at the University of Oregon (Streisinger et al., 1981). Zebrafish have multiple advantages over other animal models, including a fully sequenced genome, short generation time, high fecundity leading to hundreds of eggs per breading, rapid embryonic development (24h) reaching larval stage in 72h post-fertilization (hpf), and external fertilization (Teame et al., 2019). In addition, they are transparent at early stages of development, can be genetically modified to establish multiple zebrafish lines that are optically transparent throughout development and adulthood, enabling visualization of fluorescently labelled tissues in transgenic fish, or cells in transplants (Patton et al., 2021).

Zebrafish has also been used in cancer research to model cancer occurrence, progression, and drug response. Thanks to the rapid development of the fish, cancer can be studied through the animal life. By exposing zebrafish to mutagens, spontaneous cancers develop that are histologically similar to human cancer. These models can be used to carry out chemical and genetic screens (White et al., 2013). Moreover, allo- or xenotransplants experiments can be performed for the *in vivo* imaging of cancer cells during initiation, progression, and metastasis (White et al., 2013). Transplantation or grafting of tumour cells from a donor, either from the

same species (allograft) or from another species (xenograft), into zebrafish has become a popular resource, due to its greater ease and cost effectiveness when compared to mice, making it a more advantageous approach. Some of the advantages are that zebrafish lacks an adaptive immune system until 30dpf, which allows the xenotransplantation of human cancer cells avoiding immune rejection, without the need of immunosuppressant drugs or variants (Gamble et al., 2021). Furthermore, due to their small size, Zebrafish can be easily grown in petri dishes at early stages and xenografts only require a few hundred cells, while mouse experiments need higher number of cells and larger living spaces, limiting the amount of manageable transplantations (Lal et al., 2012). Different cancer cells with various metastatic potential have been shown to migrate and metastasise in zebrafish, including breast, colon, prostate, and pancreatic cancer cells (Teng et al., 2013), when injected in the perivitelline space. Other cancer cells, such as non-small cell lung cancer cells (Fan et al., 2021) and glioblastoma cells (Yang et al., 2013), have been shown to metastasise to the zebrafish brain when injected into the perivitelline space or to the tail when injected in the yolk sac, respectively. Studies using A2780 ovarian cancer cells have also been published, showing high invasion to the tail and trunk of the fish when cells were injected into the yolk sac (Begum et al., 2024). Furthermore, it was shown that increased α5β1 recycling promoted A2780 ovarian cancer cells and H1299 mutant p53 non-small cell lung cancer cells invasion into the jaw region of zebrafish (Paul et al., 2015). We, therefore, wanted to investigate the role of Rab25 and ADAMTS5 in promoting ovarian cancer cell invasion *in vivo*, eventually to establish if ADAMTS5 can be considered a target to prevent metastasis of ovarian cancer cells. To achieve this, we firstly established a zebrafish model where we injected ovarian cancer cells in the pericardial cavity of the zebrafish at 2.5dpf and assessed cancer cell migration at 10dpf. Multiple injection sites have been used to inject cancer cells for xenografts (Bhargava et al., 2022), figure 6.1. After testing different sites, we decided to inject cancer cells into the pericardial cavity, as it better mimics ovarian cancer cell

microenvironment. Indeed, the pericardial cavity of the zebrafish is a fluid filled area containing the heart, similar to the abdominal cavity filled with ascitic fluid in ovarian cancer patients (Paatero et al., 2018). For cancer cells to migrate, either entrance in the blood circulation, via the heart, or breach through the pericardial cavity wall is needed, similar to breach of the mesothelium or entrance in the blood circulation by intravasation observed in ovarian cancer (in both mouse models and patients).

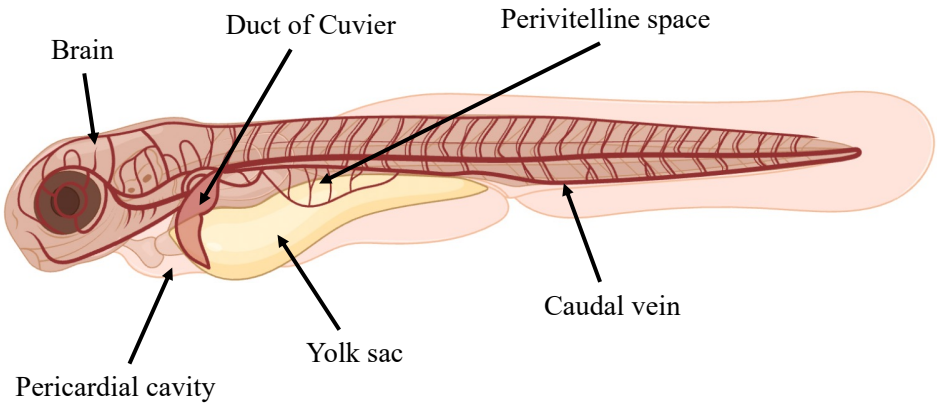

Figure 6.1. ***Xenograft injection sites in zebrafish.*** Diagram showing the most common injection sites in zebrafish for cancer cell xenotransplant models. Zebrafish outline, overlayed with the outline of the vasculature. Image made using BioRender.

6.2 Results:

6.2.1 Xenograft optimisation in zebrafish embryos

To fully understand the role of Rab25 and ADAMTS5 in ovarian cancer progression and metastasis, it was necessary to establish in an *in-vivo* model. Ovarian cancer zebrafish xenografts have been previously carried out to asses cancer cell migration and response to chemotherapy (Paul et al., 2015), therefore we decided to establish this cancer model in our lab.

First, we started by assessing cancer cell survival after injection, to optimise the cell number needed for the injections. To start with, GFP-MDA-MB-231 cells were used, as this breast cancer cell line has been reported in zebrafish xenograft models in the literature (Eguiara et al.,

2011; Guo et al., 2020; Xiao et al., 2022). Cells were detached using trypsin, spun down and resuspended to contain 10 million cells in 500µl of PBS. Cells were maintained on ice to avoid lysis and the microinjector was set up as described in the methods 2.13. About 100 GFP-MDA-MB-231 cells were injected in the ventricle of the developing brain of 1dpf *nacre* zebrafish. The chorion was removed from the embryos, which were placed on an agarose coated dish without E3 medium to avoid fish sliding. Fish were anesthetised with tricane and injected using a microneedle, preloaded with the cancer cells in suspension, after which they were placed in a new dish with fresh media. Fish were then incubated at 30-32 degrees C until 5dpf. Cells were tracked each day to assess survival and migration (figure 6.2). Approximately 1h after injection, cancer cells were mostly dispersed as individual cells in the ventricle, without forming a tumour mass (figure 6.2-A,B). When the fish reached 3dfp, we observed two different phenotypes. On the one hand, no tumour mass was present, and some cells appeared to have moved out of the area of injection towards the yolk sack (figure 6.2-C). On the other hand, a small tumour mass was present in the ventricle, and some cells appeared to have migrated, but cells were only detected in the tissues surrounding the injection site (figure 6.2-D). However, there seemed to be an overall reduction in the numbers of cancer cells in the embryos by 3dpf, suggesting a reduction in cell viability after injection.

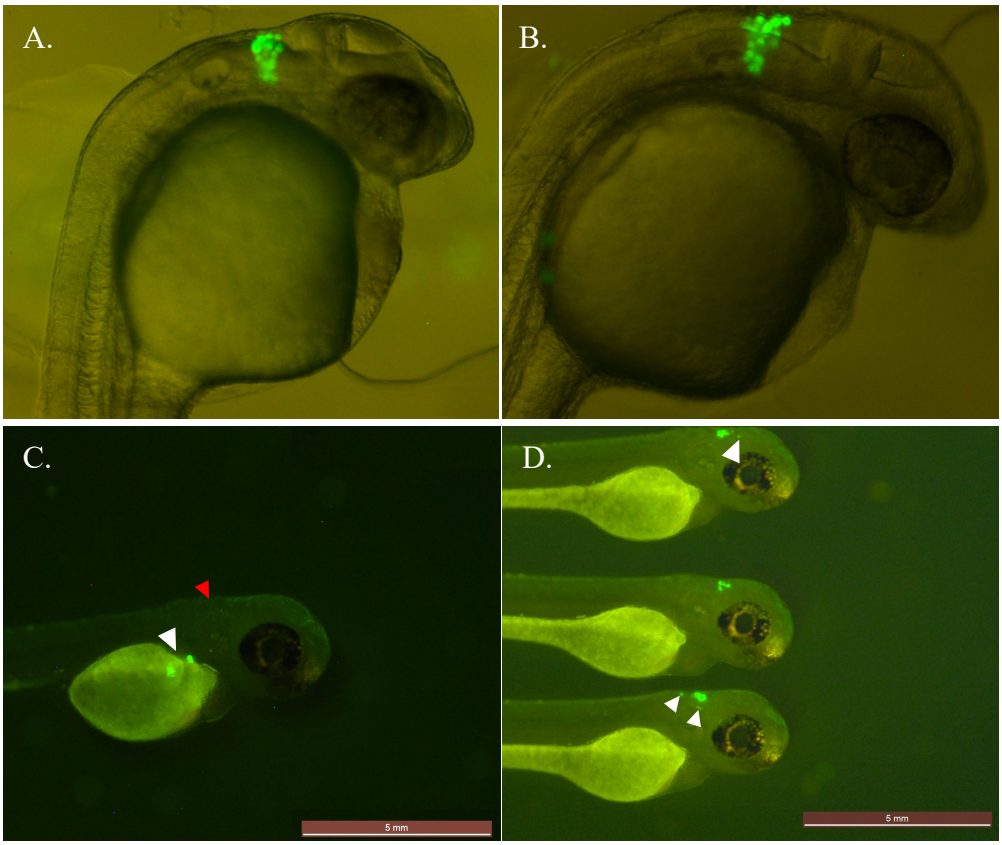

Figure 6.2. ***MDA-MB-231 cancer cells injected in zebrafish ventricle.*** ~100 GFP-MDA-MB-231 cells (green) were injected in the brain ventricle of 1dpf zebrafish embryos, which were kept at 32ºC. Embryos were imaged 1hr (A,B) after injection or at 3dpf (C,D) using a Leica M205 FCA microscope, scale bar 5mm. White arrowheads point at cells out of the injection area, while the red arrowhead points at an empty injection site. N=23 fish from 3 independent experiments.

To try and prevent the loss of cells, we injected increased cell numbers and changed the temperature of the fish incubation from 30-32 degrees C to 34 degrees C, as it is closer to the optimal temperature for growing human cancer cells (37 degrees C) and it has been shown not to damage the embryos. However, we still did not detect cells invasion in a consistent pattern and cell loss was still high (data not shown).

One of the reasons behind the cell loss could be that not enough cells were injected to sustain tumour formation. We realised that during injections cells mostly remained in the microneedle and only a small portion of cells were being pushed by the PBS they were suspended with. We firstly modified the width of the microneedle to obtain thicker or thinner needles. We then broke the needles at different sizes to facilitate cell flow, but the use of thicker needles damaged the embryos, resulting in cancer cells being pushed out of the injury wound (not shown). To

facilitate tumour formation in the embryo, we produced MDA-MB-231 cancer cell spheroids and injected the cells as aggregates. Multiple attempts were made to produce small aggregates, stating from 1000 cells/spheroid, but the spheroids were too big to be delivered via microinjections. We then generated smaller aggregates using 50 and 25 cells/spheroids. Aggregates were much smaller in size but when passed through a needle they were deformed and cells seemed damaged, which could affect the fish after injection (figure 6.3).

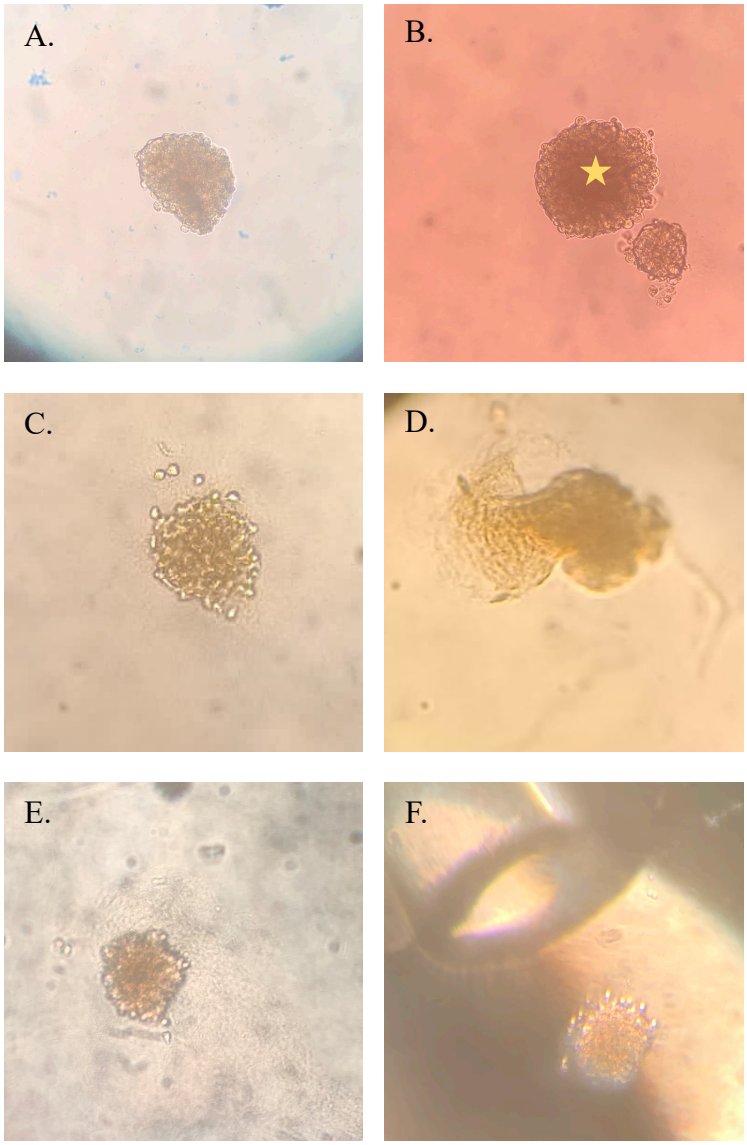

Figure 6.3. ***Cancer cells spheroid production for cell delivery in zebrafish xenograft.*** MDA-MB-231 spheroids were generated using the hanging drop method, 1000 cells (A); 1000 cells (star) or 50 cells (B). 50 cell spheroids were imaged before (C) and after (D) passing them though the microloader Eppendorf tip. 25 cell spheroids were imaged alone (E) or next to the microloader Eppendorf tip (F). Images were taken using an Olympus fluorescence microscope, 20x objective.

To improve the survival and delivery of the cells, we tested a method defined in Johnson, 2021. We mixed 1% polyvinylpyrrolidone (PVP) with PBS increasing the viscosity of the PBS, and we changed site of injection to the pericardial cavity (figure 6.4). The pericardial cavity is a small fluid filled cavity that contains the heart. By injecting approximately 500 GFP-MDA-MB-231 cells in the pericardial cavity of 2.5dpf *nacre* zebrafish embryos (figure 6.4-A), we were now able to image more compact tumour masses both at 3dpf (figure 6.4-B) and 4pdf (figure 6.4-C). Even if a clear tumour mass was present in the fish, we did not detect any sign of cancer cell invasion outside the injection area.

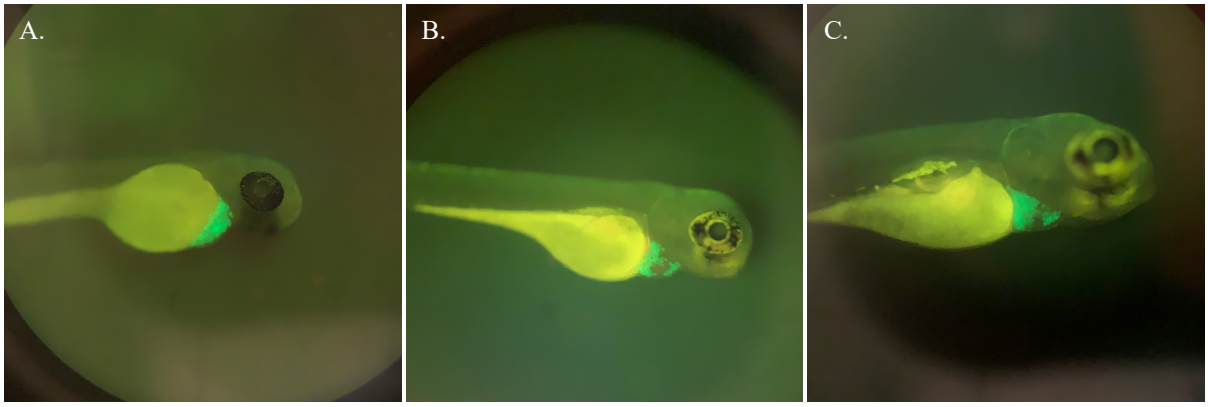

Figure 6.4. ***Pericardial cavity injection site in zebrafish.*** Approximately 500 GFP-MDA-MB-231 cells (green) were injected in the pericardial cavity of a 2.5dpf zebrafish embryo. Embryos were kept at 34ºC, anesthetised, and imaged every 24hr. Fish were imaged at 1h post injection (A), 3dpf (B) and 4dpf (C). Images taken using a Leica M205 FCA microscope. N=85 fish from 5 independent experiments.

Having optimised the cell injection, we started to investigate ovarian cancer cell lines, using A2780-Rab25 cells. To be able to perform live cell imaging and avoid fish autofluorescence in the GFP channel, we generated A2780 cells stably expressing RPF-H2B (referred to as RFP-A2780 cells). RFP-A2780-Rab25 cells injected using 1%PVP in PBS into the pericardial cavity of 2.5dpf *nacre* zebrafish embryos were found to form tumour masses. Some cells seemed to be spread on the surroundings of the main mass (black arrows), but they overall looked close to the cardiac wall (figure 6.5), suggesting that more time might be needed to detect cancer cell invasion through the embryo. Moreover, lots of autofluorescence from the fish was

encountered during imaging, making harder to differentiate between invading cancer cells autofluorecent embryo components.

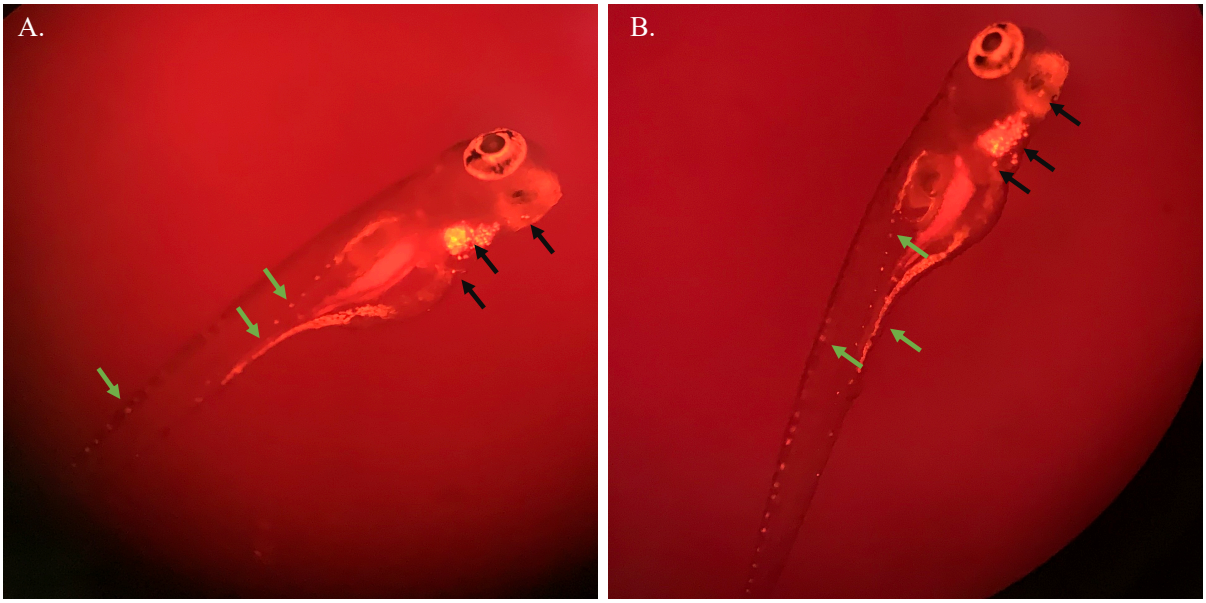

*Figure 6.5. **A2780-Rab25 cancer cell invasion in zebrafish.*** Approximately 500 RFP-A2780-Rab25 cells injected in the pericardial cavity of a 2.5dpf zebrafish embryo and embryos were kept at 34ºC up to 5dpf. Images taken with a Leica MZ10 F microscope. 2 representative embryos are shown. Cells that appear to have migrated from the primary tumour are marked with black arrows, while green arrows indicate potential fish autofluorescence. N=40 fish from 3 independent experiments.

Zebrafish have three different types of pigment cells, known as chromatophores (figure 6.6-A). Melanophores derive from the neural crest, that during development segregate from the neural tube and migrate to the periphery of the zebrafish embryo. They then differentiate into different cell types including pigment cells, which appear at approximately 24hpf in the trunk and head (Douarin and Kalcheim, 1999; Kimmel et al., 1995). At around 42hpf xanthophores develop, containing pigment that gives rise to a pale-yellow coloration to the dorsal aspect of the head. Finally, iridophores, another pigmented cell type, develop around 42hpf and contain reflective platelets made of purine, located around the eye and dorsal midline of the tail (Lister et al., 1999). *Nacre* zebrafish have a mutation in the gene that encodes for a basic helix-loop-helix/leucine zipper transcription factor related to microphthalmia. Mutants do not develop melanophores, but have an increased number of iridophores (Lister et al., 1999). We firstly used *nacre* for our xenograft model, as zebrafish larvae do not develop melanophores having a

transparent appearance that allowed us to track the tagged ovarian cancer cells. However, xanthophores (Miyadai et al., 2023) and iridophores (Higdon et al., 2013) have been reported to show autofluorescence. We, therefore, improved imaging of the xenografts by using *casper* zebrafish (figure 6.6-B,C), which was developed by inbreeding two recessive pigment mutant, *nacre* and *roy orbison*, resulting in fish lacking reflective iridophores (D'Agati et al., 2017).

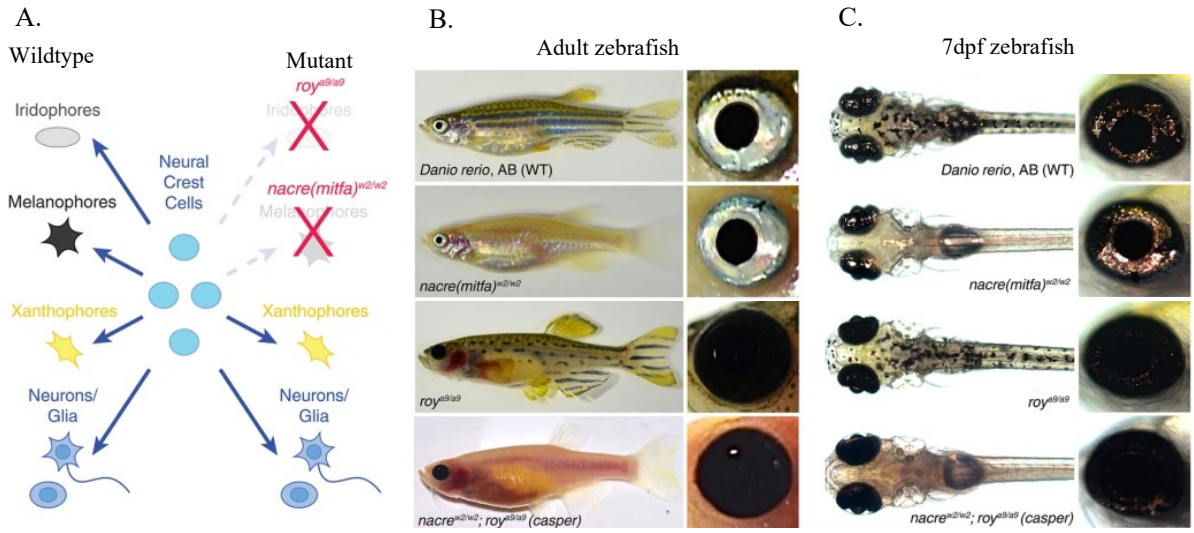

Figure 6.6. ***Pigmented cells in zebrafish.*** Schematic diagram with the different pigmented cells found in zebrafish and the progenitor cells, neural crest cells. Wildtype is shown on the left and mutants on the right (A). Pigmentation pattern seen in wildtype, *nacre*, *roy* and *casper* in zebrafish adults (B) and in 7dpf larvae (C). Image adapted from (Antinucci and Hindges, 2016).

We therefore injected RFP-A2780-Rab25 cells in *casper* 2.5dpf embryos and imaged them at end point at 10dpf. The RFP channel in figure 6.7 shows the main tumour mass, which looks compacted and located close to the heart, with a few cells on the periphery. The brightfield channel shows the fish structures, helping to identify potential autofluorescence. In the merged image, it is possible to appreciate that the primary tumour lays in the pericardial cavity and cells have migrated out of the mass into surrounding tissues, marked with a black arrow, close to the ears and into the jaw area. We did now have a good number of injected cells, good cell survival in the fish, and it was possible to better visualize the injected cells. Despite some autofluorescence remaining, especially around the yolk sack area and the dorsal midline of the tail, we considered this as the final optimized model (figure 6.7).

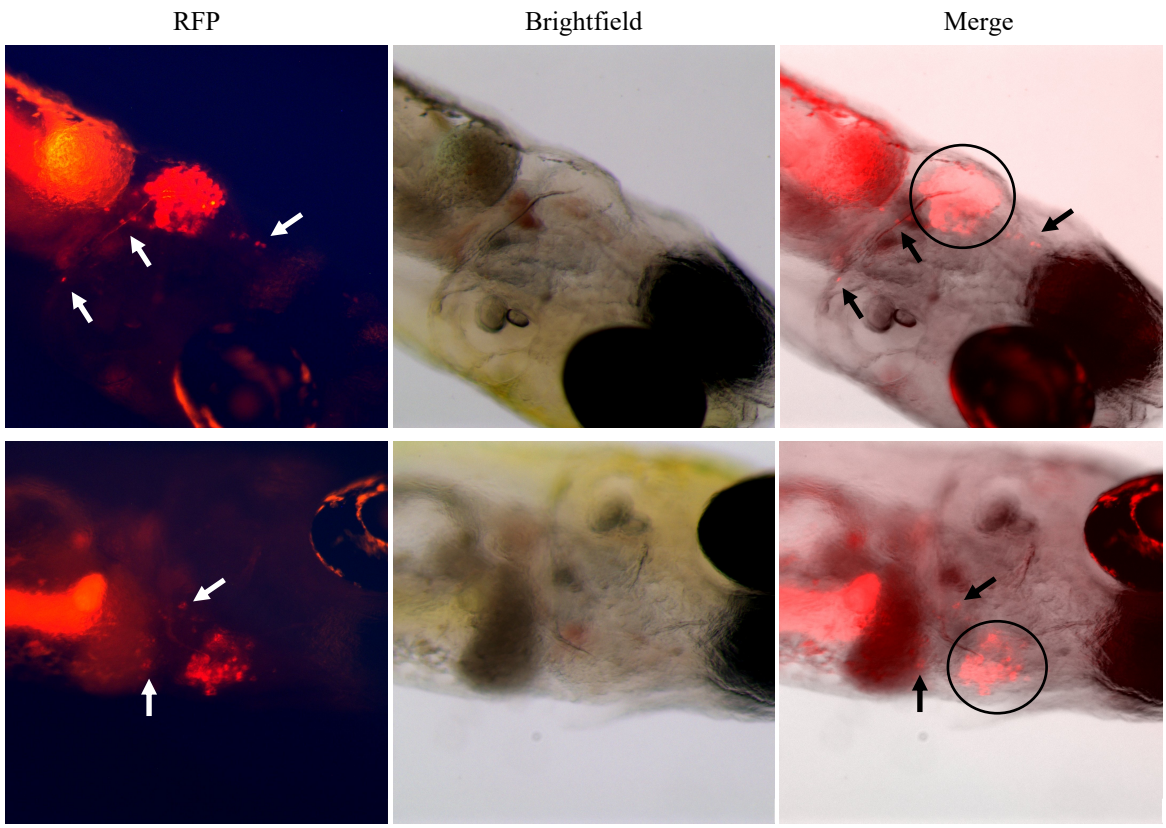

Figure 6.7. ***A2780-Rab25 cell injection in casper zebrafish.*** Approximately 500 RFP-A2780-Rab25 cells were injected in the pericardial cavity of a 2.5dpf *casper* zebrafish embryo. Fish were maintained at 34ºC and only assessed at endpoint, 10dpf. Fish were fed and water was changed every day from when fish reached 5dpf. Larvae were imaged with a Axio Zoom.V16 microscope. 2 representative images are presented, white or black arrows indicate invading cancer cells. N=75 fish from 5 independent experiments.

6.2.2 Rab25 expression promotes metastasis formation in vivo

Once the *in vivo* model was optimized, we investigated the role of Rab25 in promoting ovarian cancer cell invasion. Our hypothesis was that Rab25 overexpression would promote ovarian cancer cell invasion and metastasis, potentially due to the upregulation of ADAMTS5. RFP-A2780-DNA3 and RFP-A2780-Rab25 cells were injected in *casper* zebrafish embryos at 2.5dpf. Embryos were incubated at 34 degrees C. Once embryos reached 5dpf, they were fed once a day and water was changed 1h after feeding. At 10dpf, zebrafish were assessed for cell invasion and metastasis (figure 6.8). Cells were considered to have invaded if they migrated out of the area of injection, independently of the location found. On the one hand, in fish injected with A2780-DNA3 cells, invasion was observed in 10 out of 15 fish. Invading cells

tended to be localized in the head trunk area of the fish, in proximity of the primary tumour with no metastasis present in the tail portion of the fish. The primary tumours looked less compact compared to Rab25 tumours, with cells scattered in the pericardial cavity. On the other hand, A2780-Rab25 cells invaded out of the primary tumour in 18 zebrafish out of 19. Invasion occurred mainly in the head and trunk of the fish, with 15% of the embryos presenting cells in the tail. Moreover, we quantified the primary tumour mass by measuring the fluorescence intensity of the area that englobes the tumours (figure 6.8-B). We found that there was no significant difference between the primary tumour intensity in the presence and absence of Rab25, with a trend towards smaller tumours in zebrafish injected with Rab25-overexpressing cells, suggesting that both cells can efficiently form tumours and the differences in metastasis formation is not a consequence of faster A2780-Rab25 primary tumour growth. Overall, our data suggests that Rab25 promotes metastasis *in vivo*.

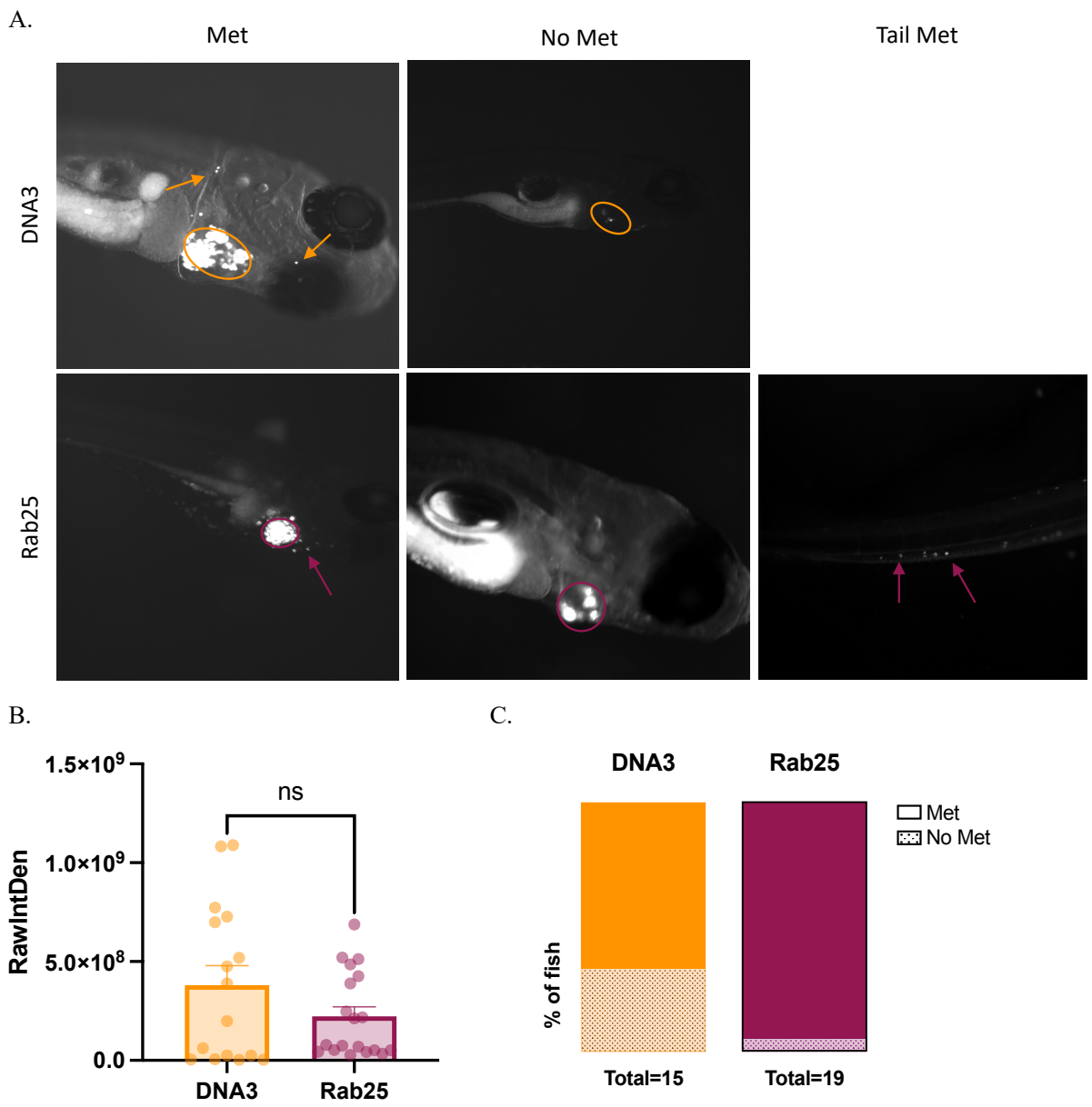

Figure 6.8. ***Rab25 overexpression promoted metastasis formation in vivo.*** Approximately 500 RFP-A2780-DNA3 or RFP-A2780-Rab25 cells were injected in the pericardiac cavity of 2.5dpf *casper* zebrafish embryos which were then incubated at 34 degrees C until 10dpf, fish were fed once a day from when they reached 5dpf. The circles mark the primary tumour mass, and the arrows point to cells that have invaded into the tissue. Images taken with an Axio Zoom.V16 microscope (A). Raw integrated density of the primary tumour was measured with Image J, p=0.8573 Mann Whitney test (B). Parts of a whole graph representing the percentage of fish presenting or not presenting metastasis. Metastasis was defined as presence of cells that have migrated out of the injected area (C). N=34 fish from 2 independent experiments.

6.3. Discussion:

In this chapter, we developed an ovarian cancer cell metastasis model in zebrafish embryos. The cardiac ECM is mainly composed of albumin, collagen, fibronectin, laminin,

proteoglycans (like versican), glycosaminoglycans (like hyaluronic acid) and elastin, Moreover MMPs, ADAMs, ADAMTSs and hyaluronidases have been reported to be expressed, to ensure proper modification and degradation of the ECM throughout heart development (Derrick and Noël, 2021). Similarly, in the mammalian peritoneal cavity, collagens, laminin and fibronectin are present underneath the mesothelium (Witz et al., 2001), while during ovarian cancer progression higher levels of fibronectin, proteoglycans (like versican) and hyaluronic acid are present, around the cancer cells and the mesothelium; furthermore, proteases are also upregulated (Brown et al., 2023). Overall, the ECM components are similar in both compartments. Moreover, the cardiac cavity, a fluid-filled space surrounding the heart, mimics the surroundings of the ovarian cancer tumours, as during tumour development there is build-up of ascitic fluid in the abdominal cavity, in which cells will float allowing them to be displaced. This implies that similar to ovarian cancer metastasis in humans, cancer cells in our model have to adhere and breach through a layer of cells, the pericardium, to be able to migrate. Both the ECM location and the cavity structure explains why in most of the zebrafish xenografts we can see a tumour mass forming around the heart, which when observed live under the microscope can be seen beating together with the heart, suggesting that it is anchored to the heart surface.

In the literature, different injection sites have been used to investigate tumour growth and metastasis in zebrafish. For example, in neuroblastoma, GFP labelled patient-derived cancer cells have been injected into the midbrain of a 1dpf zebrafish, after which fish were treated with inhibitors and tumour growth was assessed (Almstedt et al., 2020). In prostate cancer studies, Qtracker 525-labelled prostate cancer cells were injected into the sinus venosus (caudal portion of the heart that collects all ducts of Cuvier) of 2dpf zebrafish, resulting in metastases to multiple locations in the tail of the fish and head area (Xu et al., 2018). One of the most used injection site is the yolk. This was used to test ovarian cancer cisplatin response, where ovarian

cancer cells were injected in the yolk of a 2dpf embryos, which were treated with cisplatin. Untreated fish showed metastasis to the tail of the embryo from 24h post injection which was increased by 48h post injection (Latifi et al., 2011). Glioma (Yang et al., 2013) and melanoma (Hill et al., 2018) cells were also injected in the yolk of a 2dpf zebrafish which developed micrometastases in the trunk and tail of the fish 2 and 3 days post injection respectively. We also attempted yolk injections, but cells did not appear to migrate outside the yolk in the 2 days post injection like others have observed and primary tumour masses were not visible, appearing like a RFP-positive blurred area in the yolk (data not shown). Primary tumours similar to the ones we obtained were observed when approximately 400 melanoma cells were injected into the pericardial cavity of a 2dpf embryo (Paatero et al., 2018), with migration of cancer cells in the surrounding area of the cavity achieved 4 days post injection, showing a similar timeline as A2780 cells.

Zebrafish ovarian cancer models have been established to test chemoresistance and tumour metastasis. Two different cell lines, one carboplatin resistant (OVCAR8 cells) and one sensitive (A2780 cells) were injected into mice to produce tumours, which were then disaggregated and injected into 2dpf zebrafish into the perivitelline space. After a 3 days treatment with carboplatin A2780 tumour growth and metastatic spread was reduced when compared to OVCAR8 cells, which predicted the differential response observed in the human cells lines to carboplatin treatment (Song et al., 2025). The authors also injected patients-derived cells in 2dpf zebrafish, which showed consistent tumour growth among different experimental repeats being also able to accurately mimic metastasis. Treatment of the patient cells xenografted zebrafish with carboplatin showed similar responses to therapy than the respective patient outcome (Song et al., 2025), which suggests that zebrafish can be used as an animal model to predict therapeutic efficiency.

Interestingly, we found that Rab25 overexpression promoted metastasis formation in vivo, as we detected approximately 30% more metastasis in A2780-Rab25 cell injected embryos compare to A27800-DNA3 cells, suggesting that Rab25 overexpression promotes cell invasion in an *in vivo* environment. Rab25 overexpression was found to increase cancer cell proliferation and block apoptosis. Use of RNA interference against Rab25 in ovarian cancer cells significantly inhibited tumour growth in nude mice which developed smaller and lesser tumour than non-transfected control, supporting the hypothesis that Rab25 plays a role in tumour progression and aggressiveness (Yang et al., 2006). Moreover, Rab25 overexpression was also found to increase tumour volume and lung metastasis in injected mice with SKOV-3 cells transfected with Rab25 vector when compared to control vector (Jeong et al., 2018). Moreover, it was previously shown, that A2780 and H1299 cells are capable to form tumour masses in xenograft zebrafish but barley disseminated to surrounding tissues (Paul et al., 2015), consistent with our results. The authors further showed that addition of cRGDfV or expression of mutant p53 increased invasion into the jaw region, which we also observed in A2780-Rab25 injected cells. cRGDfV or mutant p53 expression are known to promote Rab coupling protein (RCP)- dependent α5β1 trafficking, due to inhibition of αvβ3 in FN rich matrices (Caswell et al., 2008; Muller et al., 2009; Rainero et al., 2012). RCP is a Rab11 interacting protein that promotes the recycling of α5β1 integrin from the Rab11 positive perinuclear recycling compartment to the plasma membrane. Inhibition of Rab4-dependent αvβ3 recycling to the plasma membrane leads to increased recycling of α5β1 integrin mediated by RCP, which promotes migration and invasion in FN rich matrices.

We also wanted to determine whether ADAMTS5 was required for the invasion of Rab25-overexpressing cells *in vivo*. We, therefore, injected RFP-A2780-Rab25 cells in which ADAMTS5 was transiently knockdown and compared with non-targeted siRNA transfected cells. However, the knockdown efficiency could not be confirmed at 10dpf and no changes in

invasion were detected, as both control and ADAMTS5 knockdown cells were still able to invade the surrounding tissues to a similar extent (data not shown). This experiment was only carried out once, therefore further repeats are needed to confirm the results. Production of a stable knockdown cell line using and shRNA for ADAMTS5 will help clarifying ADAMTS5's role, as the effects of the transient knockdown might not be maintained throughout the experiment. Furthermore, ADAMTS5 was shown to have an anti-tumorigenic effect, independently of its catalytic activity, by sequestering VEGF, resulting in inhibited tumour angiogenesis and progression (Kumar et al., 2012b). This could explain why knocking down ADAMTS5 did not lead to reduction of metastasis in our zebrafish xenotransplant model. To support this, VEGF was found to drive hypoxia mediated metastasis by increasing tumour cell (mice tumour cell line T241) invasion and dissemination under hypoxic conditions in the head and trunk of zebrafish (Lee et al., 2009). Moreover, it will be important to test pharmacological inhibitors of ADAMTS5 in our zebrafish model, to determine if ADAMTS5 catalytic activity is needed for tumour progression.

Future work to confirm the involvement of Rab25 overexpression in *in vivo* ovarian cancer metastasis is also required, including the repetition of the experiment using different cells lines, such as Ovcar3 cells, with and without Rab25 knocked down. Additionally, to better understand the *in vivo* metastatic differences between Rab25 overexpressing ovarian cancer cells and non-overexpressing cells, a GFP-vasculature labelled zebrafish (*Tg(kdrl):EGFP*) can be used, allowing us to differentiate between "passive" migration or hematogenous spread.

In addition, the imaging approach needs to be improved, as difficulties to image some of our experiments were encounter. The problems included: 1) positioning of the fish for optimal imaging of the grafted cells; 2) thickness of the fish compromising focus on the cells; and 3) autofluorescence. Most reports in the literature rely on confocal microscopy to obtain high resolution imaging of zebrafish larvae, allowing a more precise identification invasion,

migration and micrometastases formation (Marques et al., 2009; Tulotta et al., 2016). Moreover, light-sheet fluorescence imaging has also been used to assess tumour proliferation in glioblastoma zebrafish xenotransplants (Vargas-Patron et al., 2019). Autofluorescence reduction of the zebrafish was already achieved by changing from *nacre* to *casper* embryos. In the future, imaging can be further improved by using a spinning disc microscope, which would allow faster imaging of the fish without compromising the resolution. This would enable us to quickly image the fish before reaching the experimental endpoint.

Quantification of zebrafish xenotransplants is affected by image resolution, as migrating cells may be hard to observe. Analyses carried out in this chapter were done manually by drawing an area around the primary tumour mass and assessing fluorescence intensity, which correlates with cells number, while invasion/metastasis were assessed as any cell that was seen outside the injection area. This method does not distinguish between distant or proximal metastasis, nor accounts for different number of cells that have migrated. A semi-automatic technique has been reported (Köpke et al., 2024), which utilises Cellpose to segment and python scripts to quantify human cancer cells in zebrafish xenotransplants, providing a more unbiased and reliable method. Currently, several parameters have been quantified in the literature, including cell fluorescence changes (Hill et al., 2018), observational/qualitative analysis (Marques et al., 2009) and disseminating capacity by measuring the cumulative distance travelled by cells from the primary tumour to the metastatic site (Ghotra et al., 2012).

To conclude, Rab25 overexpression increased metastatic potential of A2780 ovarian cancer cells, but further experiments are needed to validate the results.

CHAPTER 7: Discussion

7.1 Summary: Key findings and working model.

Cancer is one of the leading mortality causes worldwide, being the reason why laborious work on deciphering signalling pathways and events that take place during cancer initiation and progression has been put. The interplay between malignant cancer cells and the tumour stroma, that forms the TME, still represents one of the major challenges in cancer research (Kessenbrock et al., 2010). Multiple studies, over the last decades, have shown the importance of matrix degrading enzymes in altering the TME during cancer progression leading to the remodelling of ECM due to proteolytic cleavage (Gialeli et al., 2011; Kessenbrock et al., 2010). MMP, zinc-dependent endopeptidases, ADAM and AMDATS, zinc-requiring proteases, have been found to degrade the ECM and shed membrane-bond receptor in several pathologies (Bacchetti et al., 2024; Egeblad and Werb, 2002; Rowan et al., 2008). In this thesis, we investigated the crosstalk between ADAMTS5 and ECM receptors in ovarian cancer cell migration and invasion. We have shown that cell-matrix interaction promotes ADAMTS5 expression, leading to in ovarian cancer migration and invasion.

We found that Rab25 overexpression led to ADAMTS5 upregulation in a FN-dependent manner in ovarian cancer cells (Chapter 3). This process appears to be regulated by SDC4 and not by $\alpha5\beta1$ integrin. FN fragments were used to determine if $\alpha5\beta1$integrin binding to FN was needed for ADAMTS5 upregulation. The 50K FN fragment, containing the integrin binding motif, failed to upregulate ADAMTS5 to the same extent than full length FN, while the H0 fragment, that binds to SDC4, upregulated the protease expression to the same extent as the full length. Consistent with this, the pharmacological inhibition of $\alpha5\beta1$ integrin did not affect ADAMTS5 expression in cells seeded on FN. On the contrary, SDC4 knock down in Rab25 overexpressing cells led to a statistically significant reduction of ADAMTS5 expression. Interestingly, we detected a small but statistically significant increase in SDC4 expression in

Rab25-overexpressing cells. This suggests that Rab25 overexpression might upregulate SDC4. which in turn could lead to ADAMTS5 upregulation. We have recently shown that NF-κB is required for Rab25-dependent ADAMTS5 expression when cells are seeded on fibroblast-generated cell-derived matrices. Moreover, we found that the knock down of Rab25 led to a reduction in NF-κB protein levels and a downregulation of the expression of an NF-κB target gene (Yuan et al., 2024). Interestingly, SDC4 has been reported to be upregulated by NF-κB during intervertebral disc degeneration (Wang et al., 2011), indicating that Rab25 might promote SDC4 expression through the activation of the NF-κB pathway. Moreover, SDC4 has been shown to promote ADAMTS5 mediated aggrecan degradation in intervertebral disc degeneration (Wang et al., 2011). Alternatively, SDC4 could also act upstream of NF-κB, through the activation of Rac1-dependent signalling pathways. SDC4 has been found to promote Rac1 activation in a PKCα dependent manner (Bass et al., 2007); furthermore SDC4 has been found to regulate and stabilise availability of $\alpha 5\beta 1$ integrin in the cell membrane (Bass et al., 2011). We, therefore, wanted to test if ADAMTS5 upregulation depended on PKCα activation, by using bisindolylmaleimide-1 (BIM-1) that has been shown to inhibit PKCα downstream of SDC4 (Brooks et al., 2024), and found that inhibition of PKCα did not affect ADAMTS5 expression in Rab25 overexpressing cells. This suggested that ADAMTS5 upregulation via SDC4 was not dependent on PKCα. SDC4 has been shown to directly regulate Rac1 activity by binding to the Rac GEF Tiam1 (Keller-Pinter et al., 2017). Moreover, the Rac1-PAK-p38 axis has been found to activate NF-κB in oncogenic Ras expressing cancer cells (Norris and Baldwin, 1999). As we have also found that NF-κB upregulation is not dependant on PI3K/AKT and MAPK/ERK activation in Rab25 overexpressing ovarian cancer cells (Yuan et al., 2024), our current working model is: 1) SDC4 senses FN in the ECM, 2) Rab25 overexpression, potentially by driving α5β1 integrin recycling, promotes SDC4 expression and downstream Rac1-PAK-p38 signalling axis, resulting in NF-κB activation, 3)

NF-κB promotes ADAMTS5 expression, stimulating the migration and invasion in ovarian cancer cells (figure 7.1). This signalling pathway can then be stabilised by 4) a positive feedback loop whereby NF-κB further promotes SDC4 expression. Further elucidation of the mechanism is needed to fully comprehend the complexity behind Rab25-mediated upregulation of ADAMTS5.

We found that ADAMTS5 was required for Rab25-dependent ovarian cancer collective cell migration, as both pharmacological inhibition and knock down of ADAMTS5 led to decreased migration (Chapter 4). Consistently, ADAMTS5 inhibition and knock down led to decreased clearance of mesothelial cells by Rab25-overexpressing ovarian cancer cells. Furthermore, SDC4 knock down in A2780-Rab25 cells led to a similar decrease in clearance, while inhibition of $\alpha 5\beta 1$ integrin resulted in a small and not statistically significant inhibition (Chapter 5).

In summary, Rab25 overexpression led to upregulation of ADAMTS5 via SDC4, which promoted invasion and migration in FN rich matrices. A deeper understanding of the molecular mechanism(s) behind SDC4-dependent upregulation of ADAMTS5 in Rab25 overexpressing cells is essential to fully define ADAMTS5 tumour promoting role in ovarian cancer.

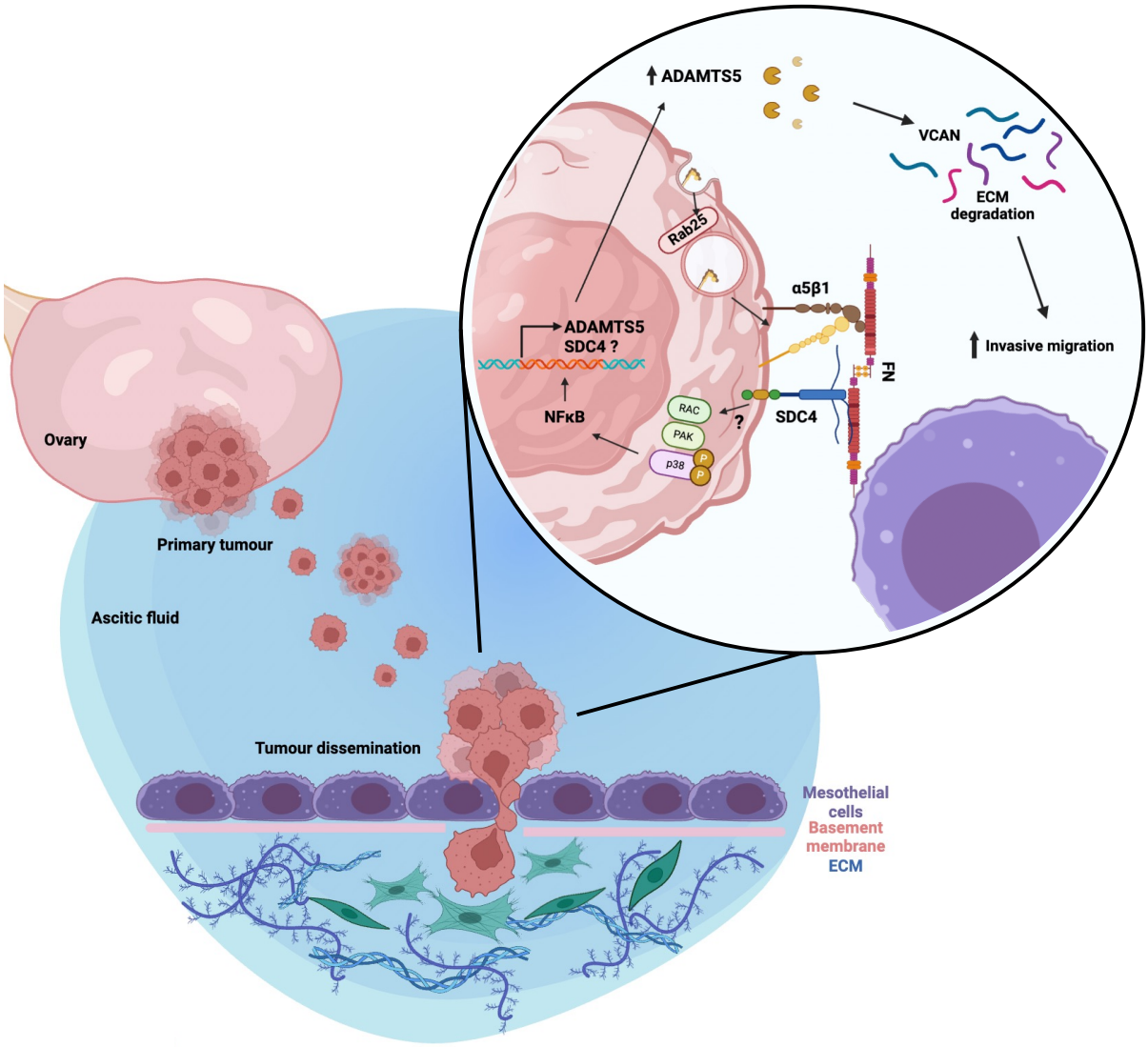

Figure 7.1: **Working model**. FN binding to SDC4, and potentially $\alpha 5\beta 1$, activates Rac-PAK-p38 signalling, leading to NFκB activation that in turns upregulates ADAMTS5 expression and potentially creates a positive feedback loop by also stimulating SDC4 expression. This leads to increased ASDAMTS5 expression and activation. ADAMTS5-mediated ECM cleavage allows Rab25-overexpressing ovarian cancer cells to clear mesothelial monolayers and migrate, eventually leading to the formation of peritoneal metastasis.

7.2 Mesothelial cells; cell-cell and cell-matrix interactions relevance during ovarian cancer trans-mesothelial invasion.

The role of mesothelial cells in peritoneal dissemination is still unclear, but they are believed to play a fundamental role in ovarian cancer tumour progression (Mikuła-Pietrasik et al., 2014). Multiple studies have shown that the interaction of ovarian cancer cells with mesothelial cells in the peritoneum induces mesothelial to mesenchymal transition. This process is driven by

TGF-β, which promotes the conversion of mesothelial cells into cancer-associated mesothelial cells (CAM), characterised by morphological changes and α-smooth muscle actin upregulation (Fujikake et al., 2018; Rynne-Vidal et al., 2017; Sandoval et al., 2013).

We have shown that ovarian cancer cells overexpressing Rab25 attach to, clear, and invade mesothelial monolayers in an ADAMTS5-dependent manner. The principal components of the ECM that play an important role in ovarian cancer adhesion to the mesothelium are FN, vitronectin, laminin, collagen I and collagen IV (Casey et al., 2003). FN is highly expressed by CAMs and has been reported to promote ovarian cancer spheroids adhesion (Burleson et al., 2004; Kenny et al., 2014), supporting our data that FN is needed to promote invasion and migration of ovarian cancer cells. We propose that ovarian cancer cell spheroids, travelling in the ascitic fluid, anchor to the FN displayed on mesothelial cells via $\alpha 5\beta 1$ integrin, that when stabilised by SDC4 leads to the upregulation of ADAMTS5, promoting clearance of the monolayer. Multiple studies have demonstrated that $\beta 1$ integrin promotes spheroid binding to the mesothelium (Burleson et al., 2004; Casey et al., 2001; Iwanicki et al., 2011). Two main theories on how ovarian cancer cells infiltrate the sub-mesothelium are in place. On the one hand, it has been reported that mesothelial cell apoptosis by tumour associated immune cells can induce ovarian cancer cell peritoneal invasion (Steitz et al., 2023). On the other hand, similarly to our results, researchers have shown that mesothelial cells have lateral mobility (Nagai et al., 2013). This can be accentuated by the presence of tumour cells, creating gaps in between mesothelial cells where tumour cells can infiltrate and invade. It has been suggested that filopodia are needed for trans-mesothelial migration (Yoshihara et al., 2020) and that ovarian cancer cells exhert myosin-generated force on mesothelial cells via $\alpha 5\beta 1$-talin I (Iwanicki et al., 2011). We show mesothelial cells being “pushed away”, changing shape by getting more elongated around invading ovarian cancer cells, while this invasion process was significantly reduced by ADAMTS5 inhibition. Interestingly, mesothelial cells secrete

proteoglycans, glycosaminoglycans and surfactants to repel cell adhesion, allowing abdominal organs to glide (Mutsaers, 2004). Furthermore, multiple MMPs have been found to be implicated in ovarian cancer cell invasion, specifically the collagenolytic subset (MMP1, MMP8 and MMP13) (Sodek et al., 2012). MMP1 mRNA has been found to be cargo of extracellular vesicles that led to MET-5a cell apoptosis in mouse models, increasing peritoneal metastasis (Yokoi et al., 2017). It was suggested that extracellular vesicles transferred the MMP1 mRNA into mesothelial cells, increasing their total mRNA levels leading to apoptosis, but further verification of the hypothesis is needed. MMP2 has also been involved in increasing adhesion of spheroids to the mesothelium by cleaving fibronectin and vitronectin to improve substratum binding for integrins (Kenny et al., 2008). This could suggest that ADAMTS5, also a matrix degrading enzyme, could increase clearance of mesothelial cells by cleaving the proteoglycans located on the surface.

Moreover, ADAMTS5 could be only important in early steps of ovarian cancer dissemination, to clear the monolayer for invasion to occur. At later stages of invasion activation of mesothelial cells may aid further migration and colonization independently of ADAMTS5 expression.

7.3 ECM dysregulation: ADAMTS5 could promote migration via versican degradation

The ECM plays a fundamental role in cancer progression, whereby the increased or decreased secretion of its components, and the remodelling by tumour cells forms a pro-tumorigenic microenvironment that will ultimately promote tumour cell survival, migration and chemo-resistance (Cho et al., 2015). Proteoglycans help increase compressive resistance and hydration in tissues (Varki et al., 1999). Aggrecan, versican and brevican are substrates of ADAMTS5 (Santamaria, 2020). Since we have shown that ADAMTS5 catalytic activity is needed for Rab25 overexpressing cells to migrate and clear mesothelial cells, we hypothesise that ADAMTS5 might promote cancer cell invasion through the cleavage of one of its substrates.

Versican is known to regulate different processes of folliculogenesis and it is enriched in the remodelling matrix during ovulation (Russell et al., 2003). Not surprisingly, it was found to be upregulated in epithelial ovarian cancers, correlated with increased levels of hyaluronan that lead to increased tumour cell survival and spread (Voutilainen et al., 2003). Furthermore, versican overexpression was identified in ovarian cancer tumour stroma, where the V1 isoform was found to be the most expressed one. In addition, versican immunolocalization showed that patients with high versican expression in the tumour stroma had lower overall survival and lower progression-free survival than patients with low levels (Ghosh et al., 2010). ADAMTS5 was found to be upregulated in glioblastomas, where it mediated brevican cleavage to promote glioma cells invasion (Viapiano et al., 2008). Multiple studies have shown that degradation of brevican by ADAMTS4 and ADAMTS5 (Nakada et al., 2005; Nakamura et al., 2000) led to the generation of G1-ESE fragments (Matthews et al., 2000) similar to the ones formed when ADAMTSs degrade aggrecan (G1-EGE) and versican (G1-DPEAAE) (Kintakas and McCulloch, 2011). ADAMTS5 is known to cleave V1 isoform of versican at the Glu^{441}-Ala^{442} site forming a G1-DPEAAE fragment, versikine, known to be biologically active (Longpré et al., 2009; McCulloch et al., 2009). Due to similarities between the fragments, it would be possible to suggest that versican fragment versikine can promote invasive phenotypes like brevican fragments do in gliomas (Viapiano et al., 2008). Further investigation on the role of ADAMTS5 in versican cleavage and versikine production in ovarian cancer migration and invasion is needed.

At the same time, versican has also been found to interact with FN (Wu et al., 2005). V0 and V1 versican was found to be secreted by prostate fibroblasts, being found at high levels in the conditioned media, leading to reduced adhesion of prostate cancer cells to fibronectin substrates (Sakko et al., 2003). Furthermore, it was suggested that versican can bind to fibronectin via the RGD domain, sequestering the protein from cancer cells, which in turn

inhibits adhesion (Sakko et al., 2003; Wu et al., 2005). Versican G3, binding to fibronectin and integrin $\beta 1$, has been linked to cancer cell proliferation, resistance to apoptosis and migration (Keire et al., 2017). ADAMTS5-mediated versican cleavage could therefore promote FN availability, allowing ovarian cancer cell spheroids to adhere to the mesothelium, but further investigation is needed to establish whether this is the case.

7.4 Peritoneal metastasis and other cancer types

Peritoneal metastasis does not only occur in ovarian cancer. It is also common in colorectal and gastric cancers, while other gastrointestinal, reproductive and genitourinary cancers, such as pancreatic, small intestine, endometrium, appendix and prostate, show peritoneal metastasis with less frequency (Desai and Moustarah, 2025). Moreover, Rab25 overexpression has been demonstrated to increase integrin $\beta 1$ level promoting gastric cancer cell invasiveness (Jeong et al., 2018). Multiple MMPs have been found upregulated in gastric cancer. For instance, activation of MMP9 downstream of STAT3 via miR-93-5p inhibition of IFNAR1, an interferon α and β receptor, promoted migration, invasion and proliferation of gastric cancer cells, both in vitro and in vivo, promoting intraperitoneal metastasis formation (Ma et al., 2017). Additionally, the overexpression of HIF-2α upregulated both MMP2 and MMP9, promoting invasion, migration and metastasis in gastric cancer (Tong et al., 2015). The expression of several members of the ADAMTS family was found enhanced in gastric cancer. ADAMTS16 upregulation was found to promote cancer cell proliferation and invasion (T. Li et al., 2022), ADAMTS2 overexpression in gastric tumour cells and stroma led to poor prognosis (Jiang et al., 2019), ADAMTS12 was found to promote angiogenesis and chemo-resistance (Jiang et al., 2023) and ADAMTS7 enhanced gastric cancer growth and metastasis in vivo in nude mice (Chen et al., 2025). In addition, data from the protein atlas show that ADAMTS5 mean transcripts per million is of 1.3 in gastric cancer and 0.5 in ovarian cancer ("Expression of ADAMTS5 in cancer - Summary - The Human Protein Atlas," n.d.), showing a similar ratio

between gastric and ovarian cancer Rab25 transcripts per million mean (96.7 and 55.7 respectively). As expression levels are similar and both cancers are known to overexpress Rab25, it suggests that ADAMTS5 could be mediating peritoneal metastasis in gastric cancer as well. Further studies are required to elucidate the importance of ADAMTS5 mediated migration and invasion in gastric cancer cells. The experiments performed in this thesis could be repeated using NCC-StC-K140 cell line, stomach carcinoma cell line from patient with metastatic stomach adenocarcinoma, which overexpresses both Rab25 and ADAMTS5.

In colorectal cancer, high expression of ADAMTS12 has been linked to poor prognosis and to increased cell proliferation and migration via activation of the Wnt signalling pathway (Li et al., 2020). In addition, a study investigated ADAMTS expression patterns in colorectal cancer tissues compared to normal, as increased levels of versican are observed in cancerous colon and rectum (Mukaratirwa et al., 2004; Tsara et al., 2002). In this context, overexpression of ADAMTS5 could promote proteoglycans degradation, that can result in the release of active fragments, known to boost migration (Longpré et al., 2009). It was found that ADAMTS5 and 4 are overexpressed in colorectal cancer tissues, mainly in the stroma at early stages and mostly in malignant cells at later stages of the disease. Moreover, high levels of ADAMTS5 mRNA were related to more aggressive cells lines than ADAMTS4 (Filou et al., 2015). However, colorectal cancer has decreased Rab25 expression independently of the cancer stage, contrary to other epithelial cancers that overexpress Rab25 in more aggressive states (Goldenring and Nam, 2011).

Rab25 tumour-promoting function has been linked to integrin $\alpha 5\beta 1$ recycling to the cell surface, but this is not the only pathway that can lead to promotion of integrin recycling. It was shown that the expression of gain-of-function mutant of the tumour suppressor p53 promoted the recycling of $\alpha 5\beta 1$ integrin and EGFR in breast and lung cancer cells, promoting cell migration and invasion (Muller et al., 2009). My preliminary data indicate that the expression

of mutant p53 in the lung cancer cell line H1299 promoted ADAMTS5 expression, when compared to p53-null H1299 control cells. This suggests that recycling of the integrin $\alpha 5\beta 1$ to the cell membrane may be the key event leading to the upregulation of ADAMTS5, independently on the upstream regulator. Further investigation is needed to clarify the cascade of events leading to ADAMTS5 upregulation and how it promotes cancer cell invasion.

7.5 Therapeutic opportunities

As we showed that ADAMTS5 catalytic activity is required for the migration and invasion of ovarian cancer cells, this protease might represent a therapeutical target for small molecule inhibitors. Matrix degrading enzymes like MMPs, and ADAM have already been explored as drug targets in cancer, due to the significant evidence involving their activity in cancer progression. Multiple MMP inhibitors were generated to target the Zn-binding site. Tanomastat, a MMP2, MMP3 and MMP9 inhibitor was found to have antiangiogenic and antimetastatic properties in vivo and was used in a phase III clinical trial for ovarian cancer. Overall the inhibitor was well tolerated, but it did not improve patients survival (Hirte et al., 2006). SB-3CT, a small molecule inhibitor designed to bind the active site of MMP2 and MMP9 was is shown to be antimetastatic and antiangiogenic in in vitro and in vivo studies (Bonfil et al., 2006), NCC405020, a novel small molecule inhibitor, blocks PEX activity, which in turn modulates MT1-MMP. It was shown to impair tumour growth and collagen I cleavage, but further studies are needed to confirm its efficacy in the clinic (Remacle et al., 2012). In addition, multiple broad-spectrum MMP inhibitors have failed in clinical trials, due to unspecific inhibition and low substrate selectivity (Piperigkou et al., 2021). At the moment, no ADAMTS inhibitor is being investigated in clinical trials to as anti-cancer agent, even if evidence of ADAMTS involvement in cancer is expanding, as reviewed in Bacchetti et al., 2024 and Cal and López-Otín, 2015). ADAMTS5 has been extensively studied in osteoarthritis where a small molecule inhibitor, GLLPG1972/S201086, has shown promising results in

mouse models, where it partially prevented the occurrence of cartilage degradation (Brebion et al., 2021). Moreover, this inhibitor has been tested in clinical trials, but it did not meet its primary end-points and it was suggested that the patient sample was not adequate (Latourte and Richette, 2022; Schnitzer et al., 2023). Another inhibitor for ADAMTS5, M6495, has been considered for clinical trials, as phase-I studies showed a good safety profile and inhibited release of the ARGS aggrecan fragment (Bihlet et al., 2024). Targeting ADAMTS5 appears to be an effective and promising way to reduce cartilage degradation and, based on our findings, these drugs could be repurposed to limit ovarian cancer progression and metastasis. Producing inhibitors specific for ADAMTS5 is highly challenging as it shares structural and functional similarities with ADAMTS4. Current ADAMTS5 inhibitors use a zinc binding group molecule to chelate the catalytic zinc domain decreasing selectivity as they could also bind other metalloproteases. Compounds that do not bind to the active site are being synthesised and tested to improve specificity. For instance, compound 4b was found to effectively inhibit aggrecan proteolysis by interacting with K532 and K533 in the Dis domain located next to the active site cleft, which is highly variable among family members (Santamaria et al., 2021). Interestingly, we found that 4b inhibits ovarian cancer cell invasion to a similar extent to the ADAMTS5 inhibitor used in this thesis (Yuan et al., 2024).

Another potential therapeutic target to prevent the upregulation of ADAMATS5 in ovarian cancer cells could be SDC4. SDC1 antibodies have been developed to target SCD1 in melanoma, triple negative breast cancer and myeloma, showing efficacy both in in vitro and in vivo studies in reducing cancer progression (Karamanos et al., 2018). Not many inhibitors have been tested against SDC4; recently, bufalin, a small molecule SDC4 inhibitor, was shown to decrease cell invasion, proliferation, and angiogenesis in hepatocellular carcinoma, suggesting that SDC4 could be a druggable target (Yang et al., 2021).

7.6 Conclusions and future work

In this thesis, we have demonstrated that Rab25 overexpression promotes FN- and SDC4-dependent ADAMTS5 expression, thus promoting ovarian cancer cell migration and invasion. Nevertheless, several questions remain unanswered, and the following points outline that in the future it would be important to:

* Investigate if Rab25 overexpression leads to the co-recycling of SDC4 with $\alpha5\beta1$ integrin. Syntenin was found to interact with SDC2 promoting the recycling of endosomes to the plasma membrane in a Arf6-dependent manner. Interestingly, Rab11 was also found in endosomal compartments which contained SDC2 and syntenin. Therefore, we could assess whether syntenin binds to SDC4, co-localises with Rab25 and whether SDC4 is recycled in a syntenin- and Rab25-dependent manner.
* Elucidate the role of $\alpha5\beta1$ integrin/FN interaction in the upregulation of ADAMTS5. We found that inhibitors against $\alpha5\beta1$ integrin did partially reduce ADAMST5 expression, but the difference was not statistically significant. Moreover, we detected a small upregulation of ADAMTS5 levels in Rab25-expressing cells seeded on the RGD-containing FN fragment. Is SDC4-mediated stabilisation of $\alpha5\beta1$ integrin needed for signalling activation? Knocking down α5β1 integrin in Rab25-overexpressing cells could help better elucidate its role in controlling ADAMTS5 expression.
* Characterise SDC4 downstream signalling pathways, leading to ADAMTS5 expression. We have hypothesised that the activation of RAC-PAK-p38 axis by SDC4 could promote the activation of NFκB, which in turn upregulates both ADAMTS5 and SDC4. This can be investigated by inhibiting RAC, PAK or p38 in Rab25 expressing ovarian cancer cells and assessing NFκB expression and activation, as well as ADAMTS5 and SDC4 expression.
* Define the mechanisms through which ADAMTS5 promotes cancer cell migration and invasion. To investigate whether this is mediated by versican cleavage, the levels of

intact and cleaved versican could be monitored by western blotting. In addition, we could investigate the role of recombinant versikine in Rab25-overexpressing cell migration and mesothelial cell clearance. In particular, it would be interesting to assess whether recombinant versikine rescues ADAMTS5 inhibition.

* It would be interesting to elucidate if versican cleavage by ADATMS5 is required for ovarian cancer spheroids attachment to mesothelial monolayers. Our preliminary observations suggest that ADAMTS5 inhibition might prevent/delay spheroid adhesion to mesothelial cells. Therefore, we could block versican cleavage with a cleavage site specific antibody (Foulcer et al., 2014) and assess the ability of ovarian cancer cell spheroids to adhere and clear mesothelial cell monolayers.

To summarise, this thesis shows that Rab25 overexpression in ovarian cancer cells leads to the upregulation of ADAMTS5 in a FN-dependent manner. We also revealed that SDC4 binding to FN, but not $\alpha 5\beta 1$ integrin binding, leads to ADAMTS5 upregulation, downstream of Rab25. Moreover, we found that inhibition and knock down of ADAMTS5 in ovarian cancer cells, leads to decrease cell migration in FN supplemented matrices, and clearance of mesothelial monolayers. Similarly, SDC4 was also required for ovarian cancer cell clearance of mesothelial cells. Due to ADAMTS5 and SDC4 role in regulating migration and clearance in ovarian cancer cells, they could be considered as potential therapeutic targets to prevent ovarian cancer metastasis.

References

Abbink, K., Zusterzeel, P.L., Geurts-Moespot, A.J., Herwaarden, A.E. van, Pijnenborg, J.M., Sweep, F.C., Massuger, L.F., 2018. HE4 is superior to CA125 in the detection of recurrent disease in high-risk endometrial cancer patients. Tumour Biol 40, 1010428318757103. https://doi.org/10.1177/1010428318757103

Adur, J., Pelegati, V.B., de Thomaz, A.A., Baratti, M.O., Andrade, L.A.L.A., Carvalho, H.F., Bottcher-Luiz, F., Cesar, C.L., 2014. Second harmonic generation microscopy as a powerful diagnostic imaging modality for human ovarian cancer. Journal of Biophotonics 7, 37–48. https://doi.org/10.1002/jbio.201200108

Agarwal, R., Kaye, S.B., 2003. Ovarian cancer: strategies for overcoming resistance to chemotherapy. Nat Rev Cancer 3, 502–516. https://doi.org/10.1038/nrc1123

Ahmed, N., Riley, C., Rice, G., Quinn, M., 2005. Role of Integrin Receptors for Fibronectin, Collagen and Laminin in the Regulation of Ovarian Carcinoma Functions in Response to a Matrix Microenvironment. Clin Exp Metastasis 22, 391–402. https://doi.org/10.1007/s10585-005-1262-y

Al-Alem, L., Curry, T.E., 2015. OVARIAN CANCER: INVOLVEMENT OF THE MATRIX METALLOPROTEINASES. Reproduction 150, R55–R64. https://doi.org/10.1530/REP-14-0546

Alberts, B., Johnson, A., Lewis, J., Raff, M., Roberts, K., Walter, P., 2002. Integrins, in: Molecular Biology of the Cell. 4th Edition. Garland Science.

Alim, L.F., Keane, C., Souza-Fonseca-Guimaraes, F., 2024. Molecular mechanisms of tumour necrosis factor signalling via TNF receptor 1 and TNF receptor 2 in the tumour microenvironment. Current Opinion in Immunology 86, 102409. https://doi.org/10.1016/j.coi.2023.102409

Almstedt, E., Elgendy, R., Hekmati, N., Rosén, E., Wärn, C., Olsen, T.K., Dyberg, C., Doroszko, M., Larsson, I., Sundström, A., Arsenian Henriksson, M., Påhlman, S., Bexell, D., Vanlandewijck, M., Kogner, P., Jörnsten, R., Krona, C., Nelander, S., 2020. Integrative discovery of treatments for high-risk neuroblastoma. Nat Commun 11, 71. https://doi.org/10.1038/s41467-019-13817-8

Amankwah, E.K., Wang, Q., Schildkraut, J.M., Tsai, Y.-Y., Ramus, S.J., Fridley, B.L., Beesley, J., Johnatty, S.E., Webb, P.M., Chenevix-Trench, G., Group, A.O.C.S., Dale, L.C., Lambrechts, D., Amant, F., Despierre, E., Vergote, I., Gayther, S.A., Gentry-Maharaj, A., Menon, U., Chang-Claude, J., Wang-Gohrke, S., Anton-Culver, H., Ziogas, A., Dörk, T., Dürst, M., Antonenkova, N., Bogdanova, N., Brown, R., Flanagan, J.M., Kaye, S.B., Paul, J., Bützow, R., Nevanlinna, H., Campbell, I., Eccles, D.M., Karlan, B.Y., Gross, J., Walsh, C., Pharoah, P.D.P., Song, H., Kjær, S.K., Høgdall, E., Høgdall, C., Lundvall, L., Nedergaard, L., Kiemeney, L.A.L.M., Massuger, L.F.A.G., Altena, A.M. van, Vermeulen, S.H.H.M., Le, N.D., Brooks-Wilson, A., Cook, L.S., Phelan, C.M., Cunningham, J.M., Vachon, C.M., Vierkant, R.A., Iversen, E.S., Berchuck, A., Goode, E.L., Sellers, T.A., Kelemen, L.E., 2011.

Polymorphisms in Stromal Genes and Susceptibility to Serous Epithelial Ovarian Cancer: A Report from the Ovarian Cancer Association Consortium. PLOS ONE 6, e19642. https://doi.org/10.1371/journal.pone.0019642

Antinucci, P., Hindges, R., 2016. A crystal-clear zebrafish for in vivo imaging. Sci Rep 6, 29490. https://doi.org/10.1038/srep29490

Apte, S.S., 2009. A disintegrin-like and metalloprotease (reprolysin-type) with thrombospondin type 1 motif (ADAMTS) superfamily: functions and mechanisms. J Biol Chem 284, 31493–31497. https://doi.org/10.1074/jbc.R109.052340

Armstrong, D.K., Bundy, B., Wenzel, L., Huang, H.Q., Baergen, R., Lele, S., Copeland, L.J., Walker, J.L., Burger, R.A., Gynecologic Oncology Group, 2006. Intraperitoneal cisplatin and paclitaxel in ovarian cancer. N Engl J Med 354, 34–43. https://doi.org/10.1056/NEJMoa052985

Aspberg, A., 2012. The Different Roles of Aggrecan Interaction Domains. J Histochem Cytochem. 60, 987–996. https://doi.org/10.1369/0022155412464376

Attenuon, 2007. A Dose-Ranging, Phase II, Open Label Study of ATN 161 in Advanced Renal Cell Cancer (Clinical trial registration No. NCT00131651). clinicaltrials.gov.

Aumailley, M., 2013. The laminin family. Cell Adh Migr 7, 48–55. https://doi.org/10.4161/cam.22826

Bacchetti, R., Yuan, S., Rainero, E., 2024. ADAMTS Proteases: Their Multifaceted Role in the Regulation of Cancer Metastasis. Dis Res 4, 40–52. https://doi.org/10.54457/DR.202401004

Balkwill, F., 2004. Cancer and the chemokine network. Nat Rev Cancer 4, 540–550. https://doi.org/10.1038/nrc1388

Bao, H., Huo, Q., Yuan, Q., Xu, C., 2021. Fibronectin 1: A Potential Biomarker for Ovarian Cancer. Disease Markers 2021, 5561651. https://doi.org/10.1155/2021/5561651

Barbareschi, M., Maisonneuve, P., Aldovini, D., Cangi, M.G., Pecciarini, L., Angelo Mauri, F., Veronese, S., Caffo, O., Lucenti, A., Palma, P.D., Galligioni, E., Doglioni, C., 2003. High syndecan-1 expression in breast carcinoma is related to an aggressive phenotype and to poorer prognosis. Cancer 98, 474–483. https://doi.org/10.1002/cncr.11515

Barbolina, M.V., Adley, B.P., Ariztia, E.V., Liu, Y., Stack, M.S., 2007. Microenvironmental Regulation of Membrane Type 1 Matrix Metalloproteinase Activity in Ovarian Carcinoma Cells via Collagen-induced EGR1 Expression*. Journal of Biological Chemistry 282, 4924–4931. https://doi.org/10.1074/jbc.M608428200

Bass, M.D., Morgan, M.R., Humphries, M.J., 2007. Integrins and syndecan-4 make distinct, but critical, contributions to adhesion contact formation. Soft Matter 3, 372–376. https://doi.org/10.1039/B614610D

Bass, M.D., Williamson, R.C., Nunan, R.D., Humphries, J.D., Byron, A., Morgan, M.R.,

Martin, P., Humphries, M.J., 2011. A Syndecan-4 Hair Trigger Initiates Wound Healing through Caveolin- and RhoG-Regulated Integrin Endocytosis. Developmental Cell 21, 681–693. https://doi.org/10.1016/j.devcel.2011.08.007

Begum, S., Irvin, S.D., Cox, C.K., Huang, Z., Wilson, J.J., Monroe, J.D., Gibert, Y., 2024. Anti-ovarian cancer migration and toxicity characteristics of a platinum(IV) pro-drug with axial HDAC inhibitor ligands in zebrafish models. Invest New Drugs 42, 644–654. https://doi.org/10.1007/s10637-024-01479-3

Bell, D., Berchuck, A., Birrer, M., Chien, J., Cramer, D.W., Dao, F., Dhir, R., DiSaia, P., Gabra, H., Glenn, P., Godwin, A.K., Gross, J., Hartmann, L., Huang, M., Huntsman, D.G., Iacocca, M., Imielinski, M., Kalloger, S., Karlan, B.Y., Levine, D.A., Mills, G.B., Morrison, C., Mutch, D., Olvera, N., Orsulic, S., Park, K., Petrelli, N., Rabeno, B., Rader, J.S., Sikic, B.I., Smith-McCune, K., Sood, A.K., Bowtell, D., Penny, R., Testa, J.R., Chang, K., Creighton, C.J., Dinh, H.H., Drummond, J.A., Fowler, G., Gunaratne, P., Hawes, A.C., Kovar, C.L., Lewis, L.R., Morgan, M.B., Newsham, I.F., Santibanez, J., Reid, J.G., Trevino, L.R., Wu, Y.-Q., Wang, M., Muzny, D.M., Wheeler, D.A., Gibbs, R.A., Getz, G., Lawrence, M.S., Cibulskis, K., Sivachenko, A.Y., Sougnez, C., Voet, D., Wilkinson, J., Bloom, T., Ardlie, K., Fennell, T., Baldwin, J., Nichol, R., Fisher, S., Gabriel, S., Lander, E.S., Ding, L., Fulton, R.S., Koboldt, D.C., McLellan, M.D., Wylie, T., Walker, J., O'Laughlin, M., Dooling, D.J., Fulton, L., Abbott, R., Dees, N.D., Zhang, Q., Kandoth, C., Wendl, M., Schierding, W., Shen, D., Harris, C.C., Schmidt, H., Kalicki, J., Delehaunty, K.D., Fronick, C.C., Demeter, R., Cook, L., Wallis, J.W., Lin, L., Magrini, V.J., Hodges, J.S., Eldred, J.M., Smith, S.M., Pohl, C.S., Vandin, F., Upfal, E., Raphael, B.J., Weinstock, G.M., Mardis, E.R., Wilson, R.K., Meyerson, M., Winckler, W., Getz, G., Verhaak, R.G.W., Carter, S.L., Mermel, C.H., Saksena, G., Nguyen, H., Onofrio, R.C., Lawrence, M.S., Hubbard, D., Gupta, S., Crenshaw, A., Ramos, A.H., Ardlie, K., Chin, L., Protopopov, A., Zhang, Juinhua, Kim, T.M., Perna, I., Xiao, Y., Zhang, H., Ren, G., Sathiamoorthy, N., Park, R.W., Lee, E., Park, P.J., Kucherlapati, R., Absher, D.M., Waite, L., Sherlock, G., Brooks, J.D., Li, J.Z., Xu, J., Myers, R.M., Laird, P.W., Cope, L., Herman, J.G., Shen, H., Weisenberger, D.J., Noushmehr, H., Pan, F., Triche Jr, T., Berman, B.P., Van Den Berg, D.J., Buckley, J., Baylin, S.B., Spellman, P.T., Purdom, E., Neuvial, P., Bengtsson, H., Jakkula, L.R., Durinck, S., Han, J., Dorton, S., Marr, H., Choi, Y.G., Wang, V., Wang, N.J., Ngai, J., Conboy, J.G., Parvin, B., Feiler, H.S., Speed, T.P., Gray, J.W., Levine, D.A., Socci, N.D., Liang, Y., Taylor, B.S., Schultz, N., Borsu, L., Lash, A.E., Brennan, C., Viale, A., Sander, C., Ladanyi, M., Hoadley, K.A., Meng, S., Du, Y., Shi, Y., Li, L., Turman, Y.J., Zang, D., Helms, E.B., Balu, S., Zhou, X., Wu, J., Topal, M.D., Hayes, D.N., Perou, C.M., Getz, G., Voet, D., Saksena, G., Zhang, Junihua, Zhang, H., Wu, C.J., Shukla, S., Cibulskis, K., Lawrence, M.S., Sivachenko, A., Jing, R., Park, R.W., Liu, Y., Park, P.J., Noble, M., Chin, L., Carter, H., Kim, D., Samayoa, J., Karchin, R., Spellman, P.T., Purdom, E., Neuvial, P., Bengtsson, H., Durinck, S., Han, J., Korkola, J.E., Heiser, L.M., Cho, R.J., Hu, Z., Parvin, B., Speed, T.P., Gray, J.W., Schultz, N., Cerami, E., Taylor, B.S., Olshen, A., Reva, B., Antipin, Y., Shen, R., Mankoo, P., Sheridan, R., Ciriello, G., Chang, W.K., Bernanke, J.A., Borsu, L., Levine, D.A., Ladanyi, M., Sander, C., Haussler, D., Benz, C.C., Stuart, J.M., Benz, S.C., Sanborn, J.Z., Vaske, C.J., Zhu, J., Szeto, C., Scott, G.K., Yau, C., Hoadley, K.A., Du, Y., Balu, S., Hayes, D.N., Perou, C.M., Wilkerson, M.D., Zhang, N., Akbani, R., Baggerly, K.A.,

Yung, W.K., Mills, G.B., Weinstein, J.N., Penny, R., Shelton, T., Grimm, D., Hatfield, M., Morris, S., Yena, P., Rhodes, P., Sherman, M., Paulauskis, J., Millis, S., Kahn, A., Greene, J.M., The Cancer Genome Atlas Research Network, (Participants are arranged by area of contribution and then by institution.), Disease working group and tissue source sites, Genome sequencing centres: Baylor College of Medicine, Broad Institute, Washington University in St Louis, Cancer genome characterization centres: Broad Institute/Dana-Farber Cancer Institute, Harvard Medical School, HudsonAlpha Institute/Stanford University, University of Southern California/Johns Hopkins University, Lawrence Berkeley National Laboratory, Memorial Sloan-Kettering Cancer Center, University of North Carolina at Chapel Hill, Genome data analysis centres: Broad Institute, Johns Hopkins University, University of California Santa Cruz/Buck Institute, The University of Texas MD Anderson Cancer Center, Biospecimen core resource, Data coordination centre, 2011. Integrated genomic analyses of ovarian carcinoma. Nature 474, 609–615. https://doi.org/10.1038/nature10166

Berek, J.S., Renz, M., Kehoe, S., Kumar, L., Friedlander, M., 2021. Cancer of the ovary, fallopian tube, and peritoneum: 2021 update. International Journal of Gynecology & Obstetrics 155, 61–85. https://doi.org/10.1002/ijgo.13878

Bergers, G., Brekken, R., McMahon, G., Vu, T.H., Itoh, T., Tamaki, K., Tanzawa, K., Thorpe, P., Itohara, S., Werb, Z., Hanahan, D., 2000. Matrix metalloproteinase-9 triggers the angiogenic switch during carcinogenesis. Nat Cell Biol 2, 737–744. https://doi.org/10.1038/35036374

Bharadwaj, D., Mandal, M., 2024. Tumor microenvironment: A playground for cells from multiple diverse origins. Biochimica et Biophysica Acta (BBA) - Reviews on Cancer 1879, 189158. https://doi.org/10.1016/j.bbcan.2024.189158

Bhargava, A., Pullaguri, N., Bhargava, Y., 2022. Zebrafish as a Xenotransplantation Model for Studying Cancer Biology and Cancer Drug Discovery, in: Bhandari, P.R., Bharani, K.K., Khurana, A. (Eds.), Zebrafish Model for Biomedical Research. Springer Nature, Singapore, pp. 43–59. https://doi.org/10.1007/978-981-16-5217-2_3

Bhuin, T., Roy, J.K., 2014. Rab proteins: the key regulators of intracellular vesicle transport. Exp Cell Res 328, 1–19. https://doi.org/10.1016/j.yexcr.2014.07.027

Bieging, K.T., Mello, S.S., Attardi, L.D., 2014. Unravelling mechanisms of p53-mediated tumour suppression. Nat Rev Cancer 14, 359–370. https://doi.org/10.1038/nrc3711

Bihlet, A.R., Balchen, T., Goteti, K., Sonne, J., Ladel, C., Karsdal, M.A., Ona, V., Moreau, F., Waterhouse, R., Bay-Jensen, A.-C., Guehring, H., 2024. Safety, Tolerability, and Pharmacodynamics of the ADAMTS-5 Nanobody M6495: Two Phase 1, Single-Center, Double-Blind, Randomized, Placebo-Controlled Studies in Healthy Subjects and Patients With Osteoarthritis. ACR Open Rheumatology 6, 205–213. https://doi.org/10.1002/acr2.11610

Birkedal-Hansen, H., Moore, W.G., Bodden, M.K., Windsor, L.J., Birkedal-Hansen, B., DeCarlo, A., Engler, J.A., 1993. Matrix metalloproteinases: a review. Crit Rev Oral Biol Med 4, 197–250. https://doi.org/10.1177/10454411930040020401

Blagden, S.P., 2015. Harnessing Pandemonium: The Clinical Implications of Tumor Heterogeneity in Ovarian Cancer. Front. Oncol. 5. https://doi.org/10.3389/fonc.2015.00149

Boire, A., Burke, K., Cox, T., Guise, T., Jamal-Hanjani, M., Janowitz, T., Kaplan, R., Lee, R., Swanton, C., Heiden, M.G.V., Sahai, E., 2024. Roadmap: Why do patients with cancer die? Nat Rev Cancer 24, 578–589. https://doi.org/10.1038/s41568-024-00708-4

Boire, A., Covic, L., Agarwal, A., Jacques, S., Sherifi, S., Kuliopulos, A., 2005. PAR1 is a matrix metalloprotease-1 receptor that promotes invasion and tumorigenesis of breast cancer cells. Cell 120, 303–313. https://doi.org/10.1016/j.cell.2004.12.018

Bonfil, R.D., Sabbota, A., Nabha, S., Bernardo, M.M., Dong, Z., Meng, H., Yamamoto, H., Chinni, S.R., Lim, I.T., Chang, M., Filetti, L.C., Mobashery, S., Cher, M.L., Fridman, R., 2006. Inhibition of human prostate cancer growth, osteolysis and angiogenesis in a bone metastasis model by a novel mechanism-based selective gelatinase inhibitor. International Journal of Cancer 118, 2721–2726. https://doi.org/10.1002/ijc.21645

Bray, F., Laversanne, M., Sung, H., Ferlay, J., Siegel, R.L., Soerjomataram, I., Jemal, A., 2024. Global cancer statistics 2022: GLOBOCAN estimates of incidence and mortality worldwide for 36 cancers in 185 countries. CA: A Cancer Journal for Clinicians 74, 229–263. https://doi.org/10.3322/caac.21834

Brebion, F., Gosmini, R., Deprez, P., Varin, M., Peixoto, C., Alvey, L., Jary, H., Bienvenu, N., Triballeau, N., Blanque, R., Cottereaux, C., Christophe, T., Vandervoort, N., Mollat, P., Touitou, R., Leonard, P., Ceuninck, F.D., Botez, I., Monjardet, A., van der Aar, E., Amantini, D., 2021. Discovery of GLPG1972/S201086, a Potent, Selective, and Orally Bioavailable ADAMTS-5 Inhibitor for the Treatment of Osteoarthritis. J. Med. Chem. 64, 2937–2952. https://doi.org/10.1021/acs.jmedchem.0c02008

Brooks, R., Wei, X., Lei, M.L., Cid, F.C., Roper, J.A., Williamson, R.C., Bass, M.D., 2024. Inhibition of EphA2 by syndecan-4 in wounded skin regulates clustering of fibroblasts. Journal of Molecular Cell Biology mjae054. https://doi.org/10.1093/jmcb/mjae054

Brown, Y., Hua, S., Tanwar, P.S., 2023. Extracellular matrix in high-grade serous ovarian cancer: Advances in understanding of carcinogenesis and cancer biology. Matrix Biology 118, 16–46. https://doi.org/10.1016/j.matbio.2023.02.004

Brun, J.-L., Cortez, A., Commo, F., Uzan, S., Rouzier, R., Daraï, E., 2008. Serous and mucinous ovarian tumors express different profiles of MMP-2, -7, -9, MT1-MMP, and TIMP-1 and -2. Int J Oncol 33, 1239–1246.

Bruney, L., Conley, K.C., Moss, N.M., Liu, Y., Stack, M.S., 2014. Membrane-type I matrix metalloproteinase-dependent ectodomain shedding of mucin16/ CA-125 on ovarian cancer cells modulates adhesion and invasion of peritoneal mesothelium. Biological Chemistry 395, 1221–1231. https://doi.org/10.1515/hsz-2014-0155

Buchanan, P.C., Boylan, K.L.M., Walcheck, B., Heinze, R., Geller, M.A., Argenta, P.A., Skubitz, A.P.N., 2017. Ectodomain shedding of the cell adhesion molecule Nectin-4 in ovarian cancer is mediated by ADAM10 and ADAM17. Journal of Biological Chemistry 292, 6339–

6351. https://doi.org/10.1074/jbc.M116.746859

Buczek-Thomas, J.A., Chen, N., Hasan, T., 1998. Integrin-Mediated Adhesion and Signalling in Ovarian Cancer Cells. Cellular Signalling 10, 55–63. https://doi.org/10.1016/S0898-6568(97)00074-0

Burleson, K.M., Boente, M.P., Pambuccian, S.E., Skubitz, A.P., 2006. Disaggregation and invasion of ovarian carcinoma ascites spheroids. Journal of Translational Medicine 4, 6. https://doi.org/10.1186/1479-5876-4-6

Burleson, K.M., Casey, R.C., Skubitz, K.M., Pambuccian, S.E., Oegema, T.R., Skubitz, A.P.N., 2004. Ovarian carcinoma ascites spheroids adhere to extracellular matrix components and mesothelial cell monolayers. Gynecologic Oncology 93, 170–181. https://doi.org/10.1016/j.ygyno.2003.12.034

Burleson, K.M., Hansen, L.K., Skubitz, A.P.N., 2005. Ovarian carcinoma spheroids disaggregate on type I collagen and invade live human mesothelial cell monolayers. Clin Exp Metastasis 21, 685–697. https://doi.org/10.1007/s10585-004-5768-5

Buys, S.S., Partridge, E., Black, A., Johnson, C.C., Lamerato, L., Isaacs, C., Reding, D.J., Greenlee, R.T., Yokochi, L.A., Kessel, B., Crawford, E.D., Church, T.R., Andriole, G.L., Weissfeld, J.L., Fouad, M.N., Chia, D., O'Brien, B., Ragard, L.R., Clapp, J.D., Rathmell, J.M., Riley, T.L., Hartge, P., Pinsky, P.F., Zhu, C.S., Izmirlian, G., Kramer, B.S., Miller, A.B., Xu, J.-L., Prorok, P.C., Gohagan, J.K., Berg, C.D., PLCO Project Team, for the, 2011. Effect of Screening on Ovarian Cancer Mortality: The Prostate, Lung, Colorectal and Ovarian (PLCO) Cancer Screening Randomized Controlled Trial. JAMA 305, 2295–2303. https://doi.org/10.1001/jama.2011.766

Byers, L.J., Osborne, J.L., Carson, L.F., Carter, J.R., Haney, A.F., Weinberg, J.B., Ramakrishnan, S., 1995. Increased levels of laminin in ascitic fluid of patients with ovarian cancer. Cancer Letters 88, 67–72. https://doi.org/10.1016/0304-3835(94)03625-S

Cal, S., López-Otín, C., 2015. ADAMTS proteases and cancer. Matrix Biology, Metalloproteinases in Extracellular Matrix Biology 44–46, 77–85. https://doi.org/10.1016/j.matbio.2015.01.013

Calderwood, D.A., Fujioka, Y., de Pereda, J.M., García-Alvarez, B., Nakamoto, T., Margolis, B., McGlade, C.J., Liddington, R.C., Ginsberg, M.H., 2003. Integrin beta cytoplasmic domain interactions with phosphotyrosine-binding domains: a structural prototype for diversity in integrin signaling. Proc Natl Acad Sci U S A 100, 2272–2277. https://doi.org/10.1073/pnas.262791999

Campo, E., Merino, M.J., Tavassoli, F.A., Charonis, A.S., Stetler-Stevenson, W.G., Liotta, L.A., 1992. Evaluation of basement membrane components and the 72 kDa type IV collagenase in serous tumors of the ovary. Am J Surg Pathol 16, 500–507. https://doi.org/10.1097/00000478-199205000-00009

Cannistra, S.A., Ottensmeier, C., Niloff, J., Orta, B., DiCarlo, J., 1995. Expression and Function of β1 and αvβ3 Integrins in Ovarian Cancer. Gynecologic Oncology 58, 216–225.

https://doi.org/10.1006/gyno.1995.1214

Casey, R.C., Burleson, K.M., Skubitz, K.M., Pambuccian, S.E., Oegema, T.R., Ruff, L.E., Skubitz, A.P.N., 2001. β1-Integrins Regulate the Formation and Adhesion of Ovarian Carcinoma Multicellular Spheroids. The American Journal of Pathology 159, 2071–2080. https://doi.org/10.1016/S0002-9440(10)63058-1

Casey, R.C., Oegema, T.R., Skubitz, K.M., Pambuccian, S.E., Grindle, S.M., Skubitz, A.P.N., 2003. Cell membrane glycosylation mediates the adhesion, migration, and invasion of ovarian carcinoma cells. Clin Exp Metastasis 20, 143–152. https://doi.org/10.1023/A:1022670501667

Casey, R.C., Skubitz, A.P.N., 2000. CD44 and β1 integrins mediate ovarian carcinoma cell migration toward extracellular matrix proteins. Clin Exp Metastasis 18, 67–75. https://doi.org/10.1023/A:1026519016213

Caswell, P.T., Chan, M., Lindsay, A.J., McCaffrey, M.W., Boettiger, D., Norman, J.C., 2008. Rab-coupling protein coordinates recycling of α5β1 integrin and EGFR1 to promote cell migration in 3D microenvironments. Journal of Cell Biology 183, 143–155. https://doi.org/10.1083/jcb.200804140

Caswell, P.T., Spence, H.J., Parsons, M., White, D.P., Clark, K., Cheng, K.W., Mills, G.B., Humphries, M.J., Messent, A.J., Anderson, K.I., McCaffrey, M.W., Ozanne, B.W., Norman, J.C., 2007. Rab25 Associates with α5β1 Integrin to Promote Invasive Migration in 3D Microenvironments. Developmental Cell 13, 496–510. https://doi.org/10.1016/j.devcel.2007.08.012

Catterall, J.B., Jones, L.M., Turner, G.A., 1999. Membrane protein glycosylation and CD44 content in the adhesion of human ovarian cancer cells to hyaluronan. Clin Exp Metastasis 17, 583–591. https://doi.org/10.1023/a:1006756518500

Chan, K.K.L., Chen, C.-A., Nam, J.-H., Ochiai, K., Wilailak, S., Choon, A.-T., Sabaratnam, S., Hebbar, S., Sickan, J., Schodin, B.A., Sumpaico, W.W., 2013. The use of HE4 in the prediction of ovarian cancer in Asian women with a pelvic mass. Gynecologic Oncology 128, 239–244. https://doi.org/10.1016/j.ygyno.2012.09.034

Chang, J., Chaudhuri, O., 2019. Beyond proteases: Basement membrane mechanics and cancer invasion. J Cell Biol 218, 2456–2469. https://doi.org/10.1083/jcb.201903066

Chen, F., 2021. Rab 25: Oncogenes and Tumor Suppressive of Cancer. E3S Web Conf. 245, 03050. https://doi.org/10.1051/e3sconf/202124503050

Chen, S., He, J., Gao, H., Gao, X., Dai, L., Chen, J., Sha, Z., 2025. ADAMTS7 Enhances Gastric Cancer Growth and Metastasis by Triggering the NF-κB Signaling Pathway. J. Cancer 16, 1008–1019. https://doi.org/10.7150/jca.103093

Cheng, K.W., Lahad, J.P., Kuo, W., Lapuk, A., Yamada, K., Auersperg, N., Liu, J., Smith-McCune, K., Lu, K.H., Fishman, D., Gray, J.W., Mills, G.B., 2004. The RAB25 small GTPase determines aggressiveness of ovarian and breast cancers. Nat Med 10, 1251–1256. https://doi.org/10.1038/nm1125

Cheon, D.-J., Tong, Y., Sim, M.-S., Dering, J., Berel, D., Cui, X., Lester, J., Beach, J.A., Tighiouart, M., Walts, A.E., Karlan, B.Y., Orsulic, S., 2014. A Collagen-Remodeling Gene Signature Regulated by TGF-β Signaling Is Associated with Metastasis and Poor Survival in Serous Ovarian Cancer. Clinical Cancer Research 20, 711–723. https://doi.org/10.1158/1078-0432.CCR-13-1256

Chiarugi, P., 2013. Cancer-associated fibroblasts and macrophages: Friendly conspirators for malignancy. OncoImmunology 2, e25563. https://doi.org/10.4161/onci.25563

Cho, A., Howell, V.M., Colvin, E.K., 2015. The Extracellular Matrix in Epithelial Ovarian Cancer – A Piece of a Puzzle. Front Oncol 5, 245. https://doi.org/10.3389/fonc.2015.00245

Cho, S.J., Jeong, B.Y., Yoon, S.-H., Park, C.G., Lee, H.Y., 2024. Rab25 suppresses colon cancer cell invasion through upregulating claudin-7 expression. Oncology Reports 51, 1–11. https://doi.org/10.3892/or.2023.8685

Chung, H., Multhaupt, H.A.B., Oh, E.-S., Couchman, J.R., 2016. Minireview: Syndecans and their crucial roles during tissue regeneration. FEBS Letters 590, 2408–2417. https://doi.org/10.1002/1873-3468.12280

Cianfrocca, M.E., Kimmel, K.A., Gallo, J., Cardoso, T., Brown, M.M., Hudes, G., Lewis, N., Weiner, L., Lam, G.N., Brown, S.C., Shaw, D.E., Mazar, A.P., Cohen, R.B., 2006. Phase 1 trial of the antiangiogenic peptide ATN-161 (Ac-PHSCN-NH2), a beta integrin antagonist, in patients with solid tumours. Br J Cancer 94, 1621–1626. https://doi.org/10.1038/sj.bjc.6603171

Cirri, P., Chiarugi, P., 2011. Cancer associated fibroblasts: the dark side of the coin. Am J Cancer Res 1, 482–497.

Clark, E.A., Brugge, J.S., 1995. Integrins and Signal Transduction Pathways: the Road Taken. Science 268, 233–239. https://doi.org/10.1126/science.7716514

Colognato, H., Yurchenco, P.D., 2000. Form and function: The laminin family of heterotrimers. Developmental Dynamics 218, 213–234. https://doi.org/10.1002/(SICI)1097-0177(200006)218:2<213::AID-DVDY1>3.0.CO;2-R

Cornelius, L.A., Nehring, L.C., Harding, E., Bolanowski, M., Welgus, H.G., Kobayashi, D.K., Pierce, R.A., Shapiro, S.D., 1998. Matrix Metalloproteinases Generate Angiostatin: Effects on Neovascularization1. The Journal of Immunology 161, 6845–6852. https://doi.org/10.4049/jimmunol.161.12.6845

Couchman, J.R., Pataki, C.A., 2012. An Introduction to Proteoglycans and Their Localization. J Histochem Cytochem 60, 885–897. https://doi.org/10.1369/0022155412464638

Cross, N. a., Chandrasekharan, S., Jokonya, N., Fowles, A., Hamdy, F. c., Buttle, D. j., Eaton, C. l., 2005. The expression and regulation of ADAMTS-1, -4, -5, -9, and -15, and TIMP-3 by TGFβ1 in prostate cells: relevance to the accumulation of versican. The Prostate 63, 269–275. https://doi.org/10.1002/pros.20182

Cuatrecasas, M., Villanueva, A., Matias-Guiu, X., Prat, J., 1997. K-ras mutations in mucinous ovarian tumors. Cancer 79, 1581–1586. https://doi.org/10.1002/(SICI)1097-

0142(19970415)79:8<1581::AID-CNCR21>3.0.CO;2-T

Cui, N., Hu, M., Khalil, R.A., 2017. Biochemical and Biological Attributes of Matrix Metalloproteinases. Prog Mol Biol Transl Sci 147, 1–73. https://doi.org/10.1016/bs.pmbts.2017.02.005

Cukierman, E., Bassi, D.E., 2010. Physico-mechanical aspects of extracellular matrix influences on tumorigenic behaviors. Semin Cancer Biol 20, 139–145. https://doi.org/10.1016/j.semcancer.2010.04.004

Czarnowski, D., 2021. Syndecans in cancer: A review of function, expression, prognostic value, and therapeutic significance. Cancer Treatment and Research Communications 27, 100312. https://doi.org/10.1016/j.ctarc.2021.100312

D'Agati, G., Beltre, R., Sessa, A., Burger, A., Zhou, Y., Mosimann, C., White, R.M., 2017. A defect in the mitochondrial protein Mpv17 underlies the transparent *casper* zebrafish. Developmental Biology 430, 11–17. https://doi.org/10.1016/j.ydbio.2017.07.017

Danen, E.H.J., Aota, S., Kraats, A.A. van, Yamada, K.M., Ruiter, D.J., Muijen, G.N.P. van, 1995. Requirement for the Synergy Site for Cell Adhesion to Fibronectin Depends on the Activation State of Integrin α5β1 (∗). Journal of Biological Chemistry 270, 21612–21618. https://doi.org/10.1074/jbc.270.37.21612

Davidowitz, R.A., Iwanicki, M.P., Brugge, J.S., 2012. In vitro Mesothelial Clearance Assay that Models the Early Steps of Ovarian Cancer Metastasis. J Vis Exp 3888. https://doi.org/10.3791/3888

Davidowitz, R.A., Selfors, L.M., Iwanicki, M.P., Elias, K.M., Karst, A., Piao, H., Ince, T.A., Drage, M.G., Dering, J., Konecny, G.E., Matulonis, U., Mills, G.B., Slamon, D.J., Drapkin, R., Brugge, J.S., 2014. Mesenchymal gene program–expressing ovarian cancer spheroids exhibit enhanced mesothelial clearance. J Clin Invest 124, 2611–2625. https://doi.org/10.1172/JCI69815

Davies, E.J., Blackhall, F.H., Shanks, J.H., David, G., McGown, A.T., Swindell, R., Slade, R.J., Martin-Hirsch, P., Gallagher, J.T., Jayson, G.C., 2004. Distribution and Clinical Significance of Heparan Sulfate Proteoglycans in Ovarian Cancer. Clinical Cancer Research 10, 5178–5186. https://doi.org/10.1158/1078-0432.CCR-03-0103

De Franceschi, N., Hamidi, H., Alanko, J., Sahgal, P., Ivaska, J., 2015. Integrin traffic – the update. J Cell Sci 128, 839–852. https://doi.org/10.1242/jcs.161653

de Visser, K.E., Joyce, J.A., 2023. The evolving tumor microenvironment: From cancer initiation to metastatic outgrowth. Cancer Cell 41, 374–403. https://doi.org/10.1016/j.ccell.2023.02.016

Del Rio, D., Masi, I., Caprara, V., Spadaro, F., Ottavi, F., Strippoli, R., Sandoval, P., López-Cabrera, M., Sainz de la Cuesta, R., Bagnato, A., Rosanò, L., 2021. Ovarian Cancer-Driven Mesothelial-to-Mesenchymal Transition is Triggered by the Endothelin-1/β-arr1 Axis. Front Cell Dev Biol 9, 764375. https://doi.org/10.3389/fcell.2021.764375

Demircan, K., Gunduz, E., Gunduz, M., Beder, L.B., Hirohata, S., Nagatsuka, H., Cengiz, B., Cilek, M.Z., Yamanaka, N., Shimizu, K., Ninomiya, Y., 2009. Increased mRNA expression of ADAMTS metalloproteinases in metastatic foci of head and neck cancer. Head Neck 31, 793–801. https://doi.org/10.1002/hed.21045

Derrick, C.J., Noël, E.S., 2021. The ECM as a driver of heart development and repair. Development 148, dev191320. https://doi.org/10.1242/dev.191320

Deryugina, E.I., Quigley, J.P., 2006. Matrix metalloproteinases and tumor metastasis. Cancer Metastasis Rev 25, 9–34. https://doi.org/10.1007/s10555-006-7886-9

Desai, J.P., Moustarah, F., 2025. Peritoneal Metastasis, in: StatPearls. StatPearls Publishing, Treasure Island (FL).

Desjardins, M., Xie, J., Gurler, H., Muralidhar, G.G., Sacks, J.D., Burdette, J.E., Barbolina, M.V., 2014. Versican regulates metastasis of epithelial ovarian carcinoma cells and spheroids. Journal of Ovarian Research 7, 70. https://doi.org/10.1186/1757-2215-7-70

Deying, W., Feng, G., Shumei, L., Hui, Z., Ming, L., Hongqing, W., 2017. CAF-derived HGF promotes cell proliferation and drug resistance by up-regulating the c-Met/PI3K/Akt and GRP78 signalling in ovarian cancer cells. Biosci Rep 37, BSR20160470. https://doi.org/10.1042/BSR20160470

Dick, G., Akslen-Hoel, L.K., Grøndahl, F., Kjos, I., Prydz, K., 2012. Proteoglycan Synthesis and Golgi Organization in Polarized Epithelial Cells. J Histochem Cytochem 60, 926–935. https://doi.org/10.1369/0022155412461256

Ding, B., Cui, B., Gao, M., Li, Z., Gao, C., Fan, S., He, W., 2017. Knockdown of Ras-Related Protein 25 (Rab25) Inhibits the In Vitro Cytotoxicity and In Vivo Antitumor Activity of Human Glioblastoma Multiforme Cells. OR 25, 331–340. https://doi.org/10.3727/096504016X14736286083065

Dolinschek, R., Hingerl, J., Benge, A., Zafiu, C., Schüren, E., Ehmoser, E.-K., Lössner, D., Reuning, U., 2021. Constitutive activation of integrin αvβ3 contributes to anoikis resistance of ovarian cancer cells. Molecular Oncology 15, 503–522. https://doi.org/10.1002/1878-0261.12845

Dötzer, K., Schlüter, F., Koch, F.E. von, Brambs, C.E., Anthuber, S., Frangini, S., Czogalla, B., Burges, A., Werner, J., Mahner, S., Mayer, B., 2021. Integrin α2β1 Represents a Prognostic and Predictive Biomarker in Primary Ovarian Cancer. Biomedicines 9, 289. https://doi.org/10.3390/biomedicines9030289

Douarin, N.L., Kalcheim, C., 1999. The Neural Crest. Cambridge University Press.

Dozynkiewicz, M.A., Jamieson, N.B., MacPherson, I., Grindlay, J., van den Berghe, P.V.E., von Thun, A., Morton, J.P., Gourley, C., Timpson, P., Nixon, C., McKay, C.J., Carter, R., Strachan, D., Anderson, K., Sansom, O.J., Caswell, P.T., Norman, J.C., 2012. Rab25 and CLIC3 Collaborate to Promote Integrin Recycling from Late Endosomes/Lysosomes and Drive Cancer Progression. Dev Cell 22, 131–145. https://doi.org/10.1016/j.devcel.2011.11.008

Drapkin, R., von Horsten, H.H., Lin, Y., Mok, S.C., Crum, C.P., Welch, W.R., Hecht, J.L., 2005. Human Epididymis Protein 4 (HE4) Is a Secreted Glycoprotein that Is Overexpressed by Serous and Endometrioid Ovarian Carcinomas. Cancer Research 65, 2162–2169. https://doi.org/10.1158/0008-5472.CAN-04-3924

Dunton, C.J., Hutchcraft, M.L., Bullock, R.G., Northrop, L.E., Ueland, F.R., 2021. Salvaging Detection of Early-Stage Ovarian Malignancies When CA125 Is Not Informative. Diagnostics 11, 1440. https://doi.org/10.3390/diagnostics11081440

Echtermeyer, F., Bertrand, J., Dreier, R., Meinecke, I., Neugebauer, K., Fuerst, M., Lee, Y.J., Song, Y.W., Herzog, C., Theilmeier, G., Pap, T., 2009. Syndecan-4 regulates ADAMTS-5 activation and cartilage breakdown in osteoarthritis. Nat Med 15, 1072–1076. https://doi.org/10.1038/nm.1998

Edwards, D.R., Handsley, M.M., Pennington, C.J., 2008. The ADAM metalloproteinases. Molecular Aspects of Medicine, Metzincin Metalloproteinases 29, 258–289. https://doi.org/10.1016/j.mam.2008.08.001

Edwards, I.J., 2012. Proteoglycans in prostate cancer. Nat Rev Urol 9, 196–206. https://doi.org/10.1038/nrurol.2012.19

Egeblad, M., Werb, Z., 2002. New functions for the matrix metalloproteinases in cancer progression. Nat Rev Cancer 2, 161–174. https://doi.org/10.1038/nrc745

Eguiara, A., Holgado, O., Beloqui, I., Abalde, L., Sanchez, Y., Callol, C., Martin, A.G., 2011. Xenografts in zebrafish embryos as a rapid functional assay for breast cancer stem-like cell identification. Cell Cycle 10, 3751–3757. https://doi.org/10.4161/cc.10.21.17921

Erin, W., Hilary, K., Ernst, L., 2014. Three-dimensional modeling of ovarian cancer. Adv Drug Deliv Rev 0, 184–192. https://doi.org/10.1016/j.addr.2014.07.003

Evanko, S.P., Tammi, M.I., Tammi, R.H., Wight, T.N., 2007. Hyaluronan-Dependent Pericellular Matrix. Adv Drug Deliv Rev 59, 1351–1365. https://doi.org/10.1016/j.addr.2007.08.008

Evans, J.P., 2001. Fertilin beta and other ADAMs as integrin ligands: insights into cell adhesion and fertilization. Bioessays 23, 628–639. https://doi.org/10.1002/bies.1088

Expression of ADAMTS5 in cancer - Summary - The Human Protein Atlas [WWW Document], n.d. URL https://www.proteinatlas.org/ENSG00000154736-ADAMTS5/cancer (accessed 1.28.25).

Fan, R.-Y., Wu, J.-Q., Liu, Y.-Y., Liu, X.-Y., Qian, S.-T., Li, C.-Y., Wei, P., Song, Z., He, M.-F., 2021. Zebrafish xenograft model for studying mechanism and treatment of non-small cell lung cancer brain metastasis. Journal of Experimental & Clinical Cancer Research 40, 371. https://doi.org/10.1186/s13046-021-02173-5

Fang, X., Schummer, M., Mao, M., Yu, S., Tabassam, F.H., Swaby, R., Hasegawa, Y., Tanyi, J.L., LaPushin, R., Eder, A., Jaffe, R., Erickson, J., Mills, G.B., 2002. Lysophosphatidic acid is a bioactive mediator in ovarian cancer. Biochimica et Biophysica Acta (BBA) - Molecular

and Cell Biology of Lipids, Lysolipid Mediators in Cell Signalling and Disease 1582, 257–264. https://doi.org/10.1016/S1388-1981(02)00179-8

Filou, S., Korpetinou, A., Kyriakopoulou, D., Bounias, D., Stavropoulos, M., Ravazoula, P., Papachristou, D.J., Theocharis, A.D., Vynios, D.H., 2015. ADAMTS Expression in Colorectal Cancer. PLOS ONE 10, e0121209. https://doi.org/10.1371/journal.pone.0121209

Fishman, D.A., Kearns, A., Chilukuri, K., Bafetti, L.M., O'Toole, E.A., Georgacopoulos, J., Ravosa, M.J., Stack, M.S., 1999. Metastatic Dissemination of Human Ovarian Epithelial Carcinoma Is Promoted by α2β1-Integrin-Mediated Interaction with Type I Collagen. Invasion and Metastasis 18, 15–26. https://doi.org/10.1159/000024495

Fontanil, T., Álvarez-Teijeiro, S., Villaronga, M.Á., Mohamedi, Y., Solares, L., Moncada-Pazos, A., Vega, J.A., García-Suárez, O., Pérez-Basterrechea, M., García-Pedrero, J.M., Obaya, A.J., Cal, S., 2017. Cleavage of Fibulin-2 by the aggrecanases ADAMTS-4 and ADAMTS-5 contributes to the tumorigenic potential of breast cancer cells. Oncotarget 8, 13716–13729. https://doi.org/10.18632/oncotarget.14627

Foulcer, S.J., Nelson, C.M., Quintero, M.V., Kuberan, B., Larkin, J., Dours-Zimmermann, M.T., Zimmermann, D.R., Apte, S.S., 2014. Determinants of Versican-V1 Proteoglycan Processing by the Metalloproteinase ADAMTS5. J Biol Chem 289, 27859–27873. https://doi.org/10.1074/jbc.M114.573287

Franke, F.E., Von Georgi, R., Zygmunt, M., Münstedt, K., 2003. Association between fibronectin expression and prognosis in ovarian carcinoma. Anticancer Res 23, 4261–4267.

Frantz, C., Stewart, K.M., Weaver, V.M., 2010. The extracellular matrix at a glance. Journal of Cell Science 123, 4195–4200. https://doi.org/10.1242/jcs.023820

Freedman, R.S., Deavers, M., Liu, J., Wang, E., 2004. Peritoneal inflammation - A microenvironment for Epithelial Ovarian Cancer (EOC). J Transl Med 2, 23. https://doi.org/10.1186/1479-5876-2-23

Fujikake, K., Kajiyama, H., Yoshihara, M., Nishino, K., Yoshikawa, N., Utsumi, F., Suzuki, S., Niimi, K., Sakata, J., Mitsui, H., Shibata, K., Senga, T., Kikkawa, F., 2018. A novel mechanism of neovascularization in peritoneal dissemination via cancer-associated mesothelial cells affected by TGF-β derived from ovarian cancer. Oncology Reports 39, 193–200. https://doi.org/10.3892/or.2017.6104

Gamble, J.T., Elson, D.J., Greenwood, J.A., Tanguay, R.L., Kolluri, S.K., 2021. The Zebrafish Xenograft Models for Investigating Cancer and Cancer Therapeutics. Biology (Basel) 10, 252. https://doi.org/10.3390/biology10040252

Gao, Y., Foster, R., Yang, X., Feng, Y., Shen, J.K., Mankin, H.J., Hornicek, F.J., Amiji, M.M., Duan, Z., 2015. Up-regulation of CD44 in the development of metastasis, recurrence and drug resistance of ovarian cancer. Oncotarget 6, 9313–9326. https://doi.org/10.18632/oncotarget.3220

Gardner, M.J., Catterall, J.B., Jones, L.M.H., Turner, G.A., 1996. Human ovarian tumour cells

can bind hyaluronic acid via membrane CD44: a possible step in peritoneal metastasis. Clin Exp Metast 14, 325–334. https://doi.org/10.1007/BF00123391

Geiger, B., Yamada, K.M., 2011. Molecular Architecture and Function of Matrix Adhesions. Cold Spring Harb Perspect Biol 3, a005033. https://doi.org/10.1101/cshperspect.a005033

Geng, D., Zhao, W., Feng, Y., Liu, J., 2016. Overexpression of Rab25 promotes hepatocellular carcinoma cell proliferation and invasion. Tumor Biol. 37, 7713–7718. https://doi.org/10.1007/s13277-015-4606-5

George, E.L., Georges-Labouesse, E.N., Patel-King, R.S., Rayburn, H., Hynes, R.O., 1993. Defects in mesoderm, neural tube and vascular development in mouse embryos lacking fibronectin. Development 119, 1079–1091. https://doi.org/10.1242/dev.119.4.1079

Ghosh, S., Albitar, L., LeBaron, R., Welch, W.R., Samimi, G., Birrer, M.J., Berkowitz, R.S., Mok, S.C., 2010. Up-regulation of stromal versican expression in advanced stage serous ovarian cancer. Gynecologic Oncology 119, 114–120. https://doi.org/10.1016/j.ygyno.2010.05.029

Ghotra, V.P.S., He, S., Bont, H. de, Ent, W. van der, Spaink, H.P., Water, B. van de, Snaar-Jagalska, B.E., Danen, E.H.J., 2012. Automated Whole Animal Bio-Imaging Assay for Human Cancer Dissemination. PLOS ONE 7, e31281. https://doi.org/10.1371/journal.pone.0031281

Gialeli, C., Theocharis, A.D., Karamanos, N.K., 2011. Roles of matrix metalloproteinases in cancer progression and their pharmacological targeting. The FEBS Journal 278, 16–27. https://doi.org/10.1111/j.1742-4658.2010.07919.x

Giannelli, G., Falk-Marzillier, J., Schiraldi, O., Stetler-Stevenson, W.G., Quaranta, V., 1997. Induction of Cell Migration by Matrix Metalloprotease-2 Cleavage of Laminin-5. Science 277, 225–228. https://doi.org/10.1126/science.277.5323.225

Goldenring, J.R., Nam, K.T., 2011. Rab25 as a tumour suppressor in colon carcinogenesis. Br J Cancer 104, 33–36. https://doi.org/10.1038/sj.bjc.6605983

Gomez-Roman, N., Sahasrabudhe, N.M., McGregor, F., Chalmers, A.J., Cassidy, J., Plumb, J., 2016. Hypoxia-inducible factor 1 alpha is required for the tumourigenic and aggressive phenotype associated with Rab25 expression in ovarian cancer. Oncotarget 7, 22650–22664. https://doi.org/10.18632/oncotarget.7998

Gomis-Rüth, F.X., 2009. Catalytic domain architecture of metzincin metalloproteases. J Biol Chem 284, 15353–15357. https://doi.org/10.1074/jbc.R800069200

Goody, R.S., Rak, A., Alexandrov, K., 2005. The structural and mechanistic basis for recycling of Rab proteins between membrane compartments. Cell Mol Life Sci 62, 1657–1670. https://doi.org/10.1007/s00018-005-4486-8

Grigore, A.D., Jolly, M.K., Jia, D., Farach-Carson, M.C., Levine, H., 2016. Tumor Budding: The Name is EMT. Partial EMT. Journal of Clinical Medicine 5, 51. https://doi.org/10.3390/jcm5050051

Grunt, T.W., Somay, C., Pavelka, M., Ellinger, A., Dittrich, E., Dittrich, C., 1991. The effects of dimethyl sulfoxide and retinoic acid on the cell growth and the phenotype of ovarian cancer cells. J Cell Sci 100 (Pt 3), 657–666. https://doi.org/10.1242/jcs.100.3.657

Gu, J., Chen, J., Feng, J., Liu, Y., Xue, Q., Mao, G., Gai, L., Lu, X., Zhang, R., Cheng, J., Hu, Y., Shao, M., Shen, H., Huang, J., 2016. Overexpression of ADAMTS5 can regulate the migration and invasion of non-small cell lung cancer. Tumor Biol. 37, 8681–8689. https://doi.org/10.1007/s13277-015-4573-x

Guo, Y., Fan, Y., Pei, X., 2020. Fangjihuangqi Decoction inhibits MDA-MB-231 cell invasion in vitro and decreases tumor growth and metastasis in triple-negative breast cancer xenografts tumor zebrafish model. Cancer Medicine 9, 2564–2578. https://doi.org/10.1002/cam4.2894

Gurler, H., Yu, Y., Choi, J., Kajdacsy-Balla, A.A., Barbolina, M.V., 2015. Three-dimensional collagen type I matrix up-regulates nuclear isoforms of the microtubule associated protein tau implicated in resistance to paclitaxel therapy in ovarian carcinoma. Int J Mol Sci 16, 3419–3433. https://doi.org/10.3390/ijms16023419

Győrffy, B., 2023. Discovery and ranking of the most robust prognostic biomarkers in serous ovarian cancer. Geroscience 45, 1889–1898. https://doi.org/10.1007/s11357-023-00742-4

Gyorffy, B., Lánczky, A., Szállási, Z., 2012. Implementing an online tool for genome-wide validation of survival-associated biomarkers in ovarian-cancer using microarray data from 1287 patients. Endocr Relat Cancer 19, 197–208. https://doi.org/10.1530/ERC-11-0329

Hamano, Y., Zeisberg, M., Sugimoto, H., Lively, J.C., Maeshima, Y., Yang, C., Hynes, R.O., Werb, Z., Sudhakar, A., Kalluri, R., 2003. Physiological levels of tumstatin, a fragment of collagen IV α3 chain, are generated by MMP-9 proteolysis and suppress angiogenesis via αVβ3 integrin. Cancer Cell 3, 589–601. https://doi.org/10.1016/S1535-6108(03)00133-8

Hamburger, A.W., Salmon, S.E., 1977. Primary Bioassay of Human Tumor Stem Cells. Science. https://doi.org/10.1126/science.560061

Hamidi, H., Ivaska, J., 2018. Every step of the way: integrins in cancer progression and metastasis. Nat Rev Cancer 18, 533–548. https://doi.org/10.1038/s41568-018-0038-z

Hanahan, D., 2022. Hallmarks of Cancer: New Dimensions. Cancer Discov 12, 31–46. https://doi.org/10.1158/2159-8290.CD-21-1059

Hanahan, D., Weinberg, R.A., 2011. Hallmarks of Cancer: The Next Generation. Cell 144, 646–674. https://doi.org/10.1016/j.cell.2011.02.013

Hantke, B., Harbeck, N., Schmalfeldt, B., Claes, I., Hiller, O., Luther, M.-O., Welk, A., Kuhn, W., Schmitt, M., Tschesche, H., Muehlenweg, B., 2003. Clinical Relevance of Matrix Metalloproteinase-13 Determined with a New Highly Specific and Sensitive ELISA in Ascitic Fluid of Advanced Ovarian Carcinoma Patients 384, 1247–1251. https://doi.org/10.1515/BC.2003.137

Haraguchi, N., Ohara, N., Koseki, J., Takahashi, H., Nishimura, J., Hata, T., Mizushima, T., Yamamoto, H., Ishii, H., Doki, Y., Mori, M., 2017. High expression of ADAMTS5 is a potent

marker for lymphatic invasion and lymph node metastasis in colorectal cancer. Mol Clin Oncol 6, 130–134. https://doi.org/10.3892/mco.2016.1088

Hedemann, N., Herz, A., Schiepanski, J.H., Dittrich, J., Sebens, S., Dempfle, A., Feuerborn, J., Rogmans, C., Tribian, N., Flörkemeier, I., Weimer, J., Krüger, S., Maass, N., Bauerschlag, D.O., 2021. ADAM17 Inhibition Increases the Impact of Cisplatin Treatment in Ovarian Cancer Spheroids. Cancers (Basel) 13, 2039. https://doi.org/10.3390/cancers13092039

Held-Feindt, J., Paredes, E.B., Blömer, U., Seidenbecher, C., Stark, A.M., Mehdorn, H.M., Mentlein, R., 2006. Matrix-degrading proteases ADAMTS4 and ADAMTS5 (disintegrins and metalloproteinases with thrombospondin motifs 4 and 5) are expressed in human glioblastomas. International Journal of Cancer 118, 55–61. https://doi.org/10.1002/ijc.21258

Hibbs, K., Skubitz, K.M., Pambuccian, S.E., Casey, R.C., Burleson, K.M., Oegema, T.R., Thiele, J.J., Grindle, S.M., Bliss, R.L., Skubitz, A.P.N., 2004. Differential Gene Expression in Ovarian Carcinoma. Am J Pathol 165, 397–414.

Higdon, C.W., Mitra, R.D., Johnson, S.L., 2013. Gene Expression Analysis of Zebrafish Melanocytes, Iridophores, and Retinal Pigmented Epithelium Reveals Indicators of Biological Function and Developmental Origin. PLoS One 8, e67801. https://doi.org/10.1371/journal.pone.0067801

Hill, D., Chen, L., Snaar-Jagalska, E., Chaudhry, B., 2018. Embryonic zebrafish xenograft assay of human cancer metastasis. F1000Res 7, 1682. https://doi.org/10.12688/f1000research.16659.2

Hiltunen, E.L.J., Anttila, M., Kultti, A., Ropponen, K., Penttinen, J., Yliskoski, M., Kuronen, A.T., Juhola, M., Tammi, R., Tammi, M., Kosma, V.-M., 2002. Elevated Hyaluronan Concentration without Hyaluronidase Activation in Malignant Epithelial Ovarian Tumors1. Cancer Research 62, 6410–6413.

Hirte, H., Vergote, I.B., Jeffrey, J.R., Grimshaw, R.N., Coppieters, S., Schwartz, B., Tu, D., Sadura, A., Brundage, M., Seymour, L., 2006. A phase III randomized trial of BAY 12-9566 (tanomastat) as maintenance therapy in patients with advanced ovarian cancer responsive to primary surgery and paclitaxel/platinum containing chemotherapy: A National Cancer Institute of Canada Clinical Trials Group Study. Gynecologic Oncology 102, 300–308. https://doi.org/10.1016/j.ygyno.2005.12.020

Holle, A.W., Govindan Kutty Devi, N., Clar, K., Fan, A., Saif, T., Kemkemer, R., Spatz, J.P., 2019. Cancer Cells Invade Confined Microchannels via a Self-Directed Mesenchymal-to-Amoeboid Transition. Nano Lett. 19, 2280–2290. https://doi.org/10.1021/acs.nanolett.8b04720

Hopkins, D.R., Keles, S., Greenspan, D.S., 2007. The Bone Morphogenetic Protein 1/Tolloid-like Metalloproteinases. Matrix Biol 26, 508–523. https://doi.org/10.1016/j.matbio.2007.05.004

Horiuchi, K., Weskamp, G., Lum, L., Hammes, H.-P., Cai, H., Brodie, T.A., Ludwig, T., Chiusaroli, R., Baron, R., Preissner, K.T., Manova, K., Blobel, C.P., 2003. Potential role for

ADAM15 in pathological neovascularization in mice. Mol Cell Biol 23, 5614–5624. https://doi.org/10.1128/MCB.23.16.5614-5624.2003

Hou, J., Yan, D., Liu, Y., Huang, P., Cui, H., 2020. The Roles of Integrin α5β1 in Human Cancer. Onco Targets Ther 13, 13329–13344. https://doi.org/10.2147/OTT.S273803

Hrabar, D., Aralica, G., Gomerčić, M., Ljubičić, N., Krušlin, B., Tomas, D., 2010. Epithelial and Stromal Expression of Syndecan-2 in Pancreatic Carcinoma. Anticancer Research 30, 2749–2753.

Hua, R., Yu, J., Yan, X., Ni, Q., Zhi, X., Li, X., Jiang, B., Zhu, J., 2020. Syndecan-2 in colorectal cancer plays oncogenic role *via* epithelial-mesenchymal transition and MAPK pathway. Biomedicine & Pharmacotherapy 121, 109630. https://doi.org/10.1016/j.biopha.2019.109630

Huang, J., Sun, Y., Chen, H., Liao, Y., Li, S., Chen, C., Yang, Z., 2019. ADAMTS5 acts as a tumor suppressor by inhibiting migration, invasion and angiogenesis in human gastric cancer. Gastric Cancer 22, 287–301. https://doi.org/10.1007/s10120-018-0866-2

Huang, Qingyun, Wu, L., Wang, Y., Kong, X., Xiao, X., Huang, Qiyuan, Li, M., Zhai, Y., Shi, F., Zhao, R., Zhong, J., Xiong, L., 2022. Caveolin-1-deficient fibroblasts promote migration, invasion, and stemness via activating the TGF-β/Smad signaling pathway in breast cancer cells. Acta Biochim Biophys Sin (Shanghai) 54, 1587–1598. https://doi.org/10.3724/abbs.2022150

Huang, Y.-L., Liang, C.-Y., Ritz, D., Coelho, R., Septiadi, D., Estermann, M., Cumin, C., Rimmer, N., Schötzau, A., Núñez López, M., Fedier, A., Konantz, M., Vlajnic, T., Calabrese, D., Lengerke, C., David, L., Rothen-Rutishauser, B., Jacob, F., Heinzelmann-Schwarz, V., 2020. Collagen-rich omentum is a premetastatic niche for integrin α2-mediated peritoneal metastasis. eLife 9, e59442. https://doi.org/10.7554/eLife.59442

Huber, M.A., Kraut, N., Beug, H., 2005. Molecular requirements for epithelial–mesenchymal transition during tumor progression. Current Opinion in Cell Biology, Cell-to-cell contact and extracellular matrix 17, 548–558. https://doi.org/10.1016/j.ceb.2005.08.001

Hughes, P.E., Diaz-Gonzalez, F., Leong, L., Wu, C., McDonald, J.A., Shattil, S.J., Ginsberg, M.H., 1996. Breaking the integrin hinge. A defined structural constraint regulates integrin signaling. J Biol Chem 271, 6571–6574. https://doi.org/10.1074/jbc.271.12.6571

Humphries, M.J., Akiyama, S.K., Komoriya, A., Olden, K., Yamada, K.M., 1986. Identification of an alternatively spliced site in human plasma fibronectin that mediates cell type-specific adhesion. Journal of Cell Biology 103, 2637–2647. https://doi.org/10.1083/jcb.103.6.2637

Hynes, R.O., 2002. Integrins: bidirectional, allosteric signaling machines. Cell 110, 673–687. https://doi.org/10.1016/s0092-8674(02)00971-6

Hynes, R.O., 1990. Interactions of Fibronectins, in: Hynes, R.O. (Ed.), Fibronectins. Springer, New York, NY, pp. 84–112. https://doi.org/10.1007/978-1-4612-3264-3_5

Hynes, R.O., Naba, A., 2012. Overview of the Matrisome—An Inventory of Extracellular

Matrix Constituents and Functions. Cold Spring Harb Perspect Biol 4, a004903. https://doi.org/10.1101/cshperspect.a004903

Hynes, R.O., Yamada, K.M., 1982. Fibronectins: multifunctional modular glycoproteins. J Cell Biol 95, 369–377.

Iba, K., Albrechtsen, R., Gilpin, B., Fröhlich, C., Loechel, F., Zolkiewska, A., Ishiguro, K., Kojima, T., Liu, W., Langford, J.K., Sanderson, R.D., Brakebusch, C., Fässler, R., Wewer, U.M., 2000. The Cysteine-Rich Domain of Human Adam 12 Supports Cell Adhesion through Syndecans and Triggers Signaling Events That Lead to β1 Integrin–Dependent Cell Spreading. J Cell Biol 149, 1143–1156.

Ibrahim, S.A., Gadalla, R., El-Ghonaimy, E.A., Samir, O., Mohamed, H.T., Hassan, H., Greve, B., El-Shinawi, M., Mohamed, M.M., Götte, M., 2017. Syndecan-1 is a novel molecular marker for triple negative inflammatory breast cancer and modulates the cancer stem cell phenotype via the IL-6/STAT3, Notch and EGFR signaling pathways. Mol Cancer 16, 57. https://doi.org/10.1186/s12943-017-0621-z

Imai, T., Horiuchi, A., Wang, C., Oka, K., Ohira, S., Nikaido, T., Konishi, I., 2003. Hypoxia Attenuates the Expression of E-Cadherin via Up-Regulation of SNAIL in Ovarian Carcinoma Cells. The American Journal of Pathology 163, 1437–1447. https://doi.org/10.1016/S0002-9440(10)63501-8

Iwanicki, M.P., Davidowitz, R.A., Ng, M.R., Besser, A., Muranen, T., Merritt, M., Danuser, G., Ince, T., Brugge, J.S., 2011. Ovarian cancer spheroids use myosin-generated force to clear the mesothelium. Cancer Discov 1, 144–157. https://doi.org/10.1158/2159-8274.CD-11-0010

Jacobs, I.J., Menon, U., Ryan, A., Gentry-Maharaj, A., Burnell, M., Kalsi, J.K., Amso, N.N., Apostolidou, S., Benjamin, E., Cruickshank, D., Crump, D.N., Davies, S.K., Dawnay, A., Dobbs, S., Fletcher, G., Ford, J., Godfrey, K., Gunu, R., Habib, M., Hallett, R., Herod, J., Jenkins, H., Karpinskyj, C., Leeson, S., Lewis, S.J., Liston, W.R., Lopes, A., Mould, T., Murdoch, J., Oram, D., Rabideau, D.J., Reynolds, K., Scott, I., Seif, M.W., Sharma, A., Singh, N., Taylor, J., Warburton, F., Widschwendter, M., Williamson, K., Woolas, R., Fallowfield, L., McGuire, A.J., Campbell, S., Parmar, M., Skates, S.J., 2016. Ovarian cancer screening and mortality in the UK Collaborative Trial of Ovarian Cancer Screening (UKCTOCS): a randomised controlled trial. The Lancet 387, 945–956. https://doi.org/10.1016/S0140-6736(15)01224-6

Jacobs, I.J., Skates, S.J., MacDonald, N., Menon, U., Rosenthal, A.N., Davies, A.P., Woolas, R., Jeyarajah, A.R., Sibley, K., Lowe, D.G., Oram, D.H., 1999. Screening for ovarian cancer: a pilot randomised controlled trial. The Lancet 353, 1207–1210. https://doi.org/10.1016/S0140-6736(98)10261-1

Jagoe, W.N., Lindsay, A.J., Read, R.J., McCoy, A.J., McCaffrey, M.W., Khan, A.R., 2006. Crystal Structure of Rab11 in Complex with Rab11 Family Interacting Protein 2. Structure 14, 1273–1283. https://doi.org/10.1016/j.str.2006.06.010

Jelinic, P., Mueller, J.J., Olvera, N., Dao, F., Scott, S.N., Shah, R., Gao, J., Schultz, N., Gonen,

M., Soslow, R.A., Berger, M.F., Levine, D.A., 2014. Recurrent SMARCA4 mutations in small cell carcinoma of the ovary. Nat Genet 46, 424–426. https://doi.org/10.1038/ng.2922

Jeong, B.Y., Cho, K.H., Jeong, K.J., Park, Y.-Y., Kim, J.M., Rha, S.Y., Park, C.G., Mills, G.B., Cheong, J.-H., Lee, H.Y., 2018. Rab25 augments cancer cell invasiveness through a β1 integrin/EGFR/VEGF-A/Snail signaling axis and expression of fascin. Exp Mol Med 50, e435–e435. https://doi.org/10.1038/emm.2017.248

Jiang, C., Zhou, Y., Huang, Y., Wang, Y., Wang, W., Kuai, X., 2019. Overexpression of ADAMTS-2 in tumor cells and stroma is predictive of poor clinical prognosis in gastric cancer. Human Pathology 84, 44–51. https://doi.org/10.1016/j.humpath.2018.08.030

Jiang, Y., Huang, J., Huang, Z., Li, W., Tan, R., Li, T., Chen, Z., Tang, X., Zhao, Y., Qiu, J., Li, C., Chen, H., Yang, Z., 2023. ADAMTS12 promotes oxaliplatin chemoresistance and angiogenesis in gastric cancer through VEGF upregulation. Cellular Signalling 111, 110866. https://doi.org/10.1016/j.cellsig.2023.110866

Johansson, N., Airola, K., Grénman, R., Kariniemi, A.L., Saarialho-Kere, U., Kähäri, V.M., 1997. Expression of collagenase-3 (matrix metalloproteinase-13) in squamous cell carcinomas of the head and neck. Am J Pathol 151, 499–508.

Johansson, N., Vaalamo, M., Grénman, S., Hietanen, S., Klemi, P., Saarialho-Kere, U., Kähäri, V.-M., 1999. Collagenase-3 (MMP-13) is Expressed by Tumor Cells in Invasive Vulvar Squamous Cell Carcinomas. Am J Pathol 154, 469–480.

Johnson, G., 2021. THE P-REX2 AND FLII SIGNALLING AXIS IN MELANOMA. Division of Immunology, Immunity to Infection and Respiratory Medicine, The University of Manchester.

Jones, L.M.H., Gardner, M.J., Catterall, J.B., Turner, G.A., 1995. Hyaluronic acid secreted by mesothelial cells: a natural barrier to ovarian cancer cell adhesion. Clin Exp Metast 13, 373–380. https://doi.org/10.1007/BF00121913

Joshi, R.S., Kanugula, S.S., Sudhir, S., Pereira, M.P., Jain, S., Aghi, M.K., 2021. The Role of Cancer-Associated Fibroblasts in Tumor Progression. Cancers (Basel) 13, 1399. https://doi.org/10.3390/cancers13061399

Kalluri, R., Weinberg, R.A., 2009. The basics of epithelial-mesenchymal transition. The Journal of Clinical Investigation 119, 1420. https://doi.org/10.1172/JCI39104

Kalluri, R., Zeisberg, M., 2006. Fibroblasts in cancer. Nat Rev Cancer 6, 392–401. https://doi.org/10.1038/nrc1877

Kaplan, R.N., Riba, R.D., Zacharoulis, S., Bramley, A.H., Vincent, L., Costa, C., MacDonald, D.D., Jin, D.K., Shido, K., Kerns, S.A., Zhu, Z., Hicklin, D., Wu, Y., Port, J.L., Altorki, N., Port, E.R., Ruggero, D., Shmelkov, S.V., Jensen, K.K., Rafii, S., Lyden, D., 2005. VEGFR1-positive haematopoietic bone marrow progenitors initiate the pre-metastatic niche. Nature 438, 820–827. https://doi.org/10.1038/nature04186

Karamanos, N.K., Piperigkou, Z., Theocharis, A.D., Watanabe, H., Franchi, M., Baud, S.,

Brézillon, S., Götte, M., Passi, A., Vigetti, D., Ricard-Blum, S., Sanderson, R.D., Neill, T., Iozzo, R.V., 2018. Proteoglycan Chemical Diversity Drives Multifunctional Cell Regulation and Therapeutics. Chem. Rev. 118, 9152–9232. https://doi.org/10.1021/acs.chemrev.8b00354

Kartalou, M., Essigmann, J.M., 2001. Recognition of cisplatin adducts by cellular proteins. Mutation Research/Fundamental and Molecular Mechanisms of Mutagenesis 478, 1–21. https://doi.org/10.1016/S0027-5107(01)00142-7

Katsumata, N., Yasuda, M., Takahashi, F., Isonishi, S., Jobo, T., Aoki, D., Tsuda, H., Sugiyama, T., Kodama, S., Kimura, E., Ochiai, K., Noda, K., Japanese Gynecologic Oncology Group, 2009. Dose-dense paclitaxel once a week in combination with carboplatin every 3 weeks for advanced ovarian cancer: a phase 3, open-label, randomised controlled trial. Lancet 374, 1331–1338. https://doi.org/10.1016/S0140-6736(09)61157-0

Keire, P.A., Kang, I., Wight, T.N., 2017. Versican: Role in Cancer Tumorigenesis, in: Brekken, R.A., Stupack, D. (Eds.), Extracellular Matrix in Tumor Biology. Springer International Publishing, Cham, pp. 51–74. https://doi.org/10.1007/978-3-319-60907-2_4

Keller-Pinter, A., Ughy, B., Domoki, M., Pettko-Szandtner, A., Letoha, T., Tovari, J., Timar, J., Szilak, L., 2017. The phosphomimetic mutation of syndecan-4 binds and inhibits Tiam1 modulating Rac1 activity in PDZ interaction–dependent manner. PLOS ONE 12, e0187094. https://doi.org/10.1371/journal.pone.0187094

Kelley, L.C., Lohmer, L.L., Hagedorn, E.J., Sherwood, D.R., 2014. Traversing the basement membrane in vivo: A diversity of strategies. Journal of Cell Biology 204, 291–302. https://doi.org/10.1083/jcb.201311112

Kelwick, R., Desanlis, I., Wheeler, G.N., Edwards, D.R., 2015. The ADAMTS (A Disintegrin and Metalloproteinase with Thrombospondin motifs) family. Genome Biology 16, 113. https://doi.org/10.1186/s13059-015-0676-3

Kenny, H.A., Chiang, C.-Y., White, E.A., Schryver, E.M., Habis, M., Romero, I.L., Ladanyi, A., Penicka, C.V., George, J., Matlin, K., Montag, A., Wroblewski, K., Yamada, S.D., Mazar, A.P., Bowtell, D., Lengyel, E., 2014. Mesothelial cells promote early ovarian cancer metastasis through fibronectin secretion. J Clin Invest 124, 4614–4628. https://doi.org/10.1172/JCI74778

Kenny, H.A., Kaur, S., Coussens, L.M., Lengyel, E., 2008. The initial steps of ovarian cancer cell metastasis are mediated by MMP-2 cleavage of vitronectin and fibronectin. J Clin Invest 118, 1367–1379. https://doi.org/10.1172/JCI33775

Kenny, H.A., Krausz, T., Yamada, S.D., Lengyel, E., 2007. Use of a novel 3D culture model to elucidate the role of mesothelial cells, fibroblasts and extra-cellular matrices on adhesion and invasion of ovarian cancer cells to the omentum. International Journal of Cancer 121, 1463–1472. https://doi.org/10.1002/ijc.22874

Kessenbrock, K., Plaks, V., Werb, Z., 2010. Matrix Metalloproteinases: Regulators of the Tumor Microenvironment. Cell 141, 52–67. https://doi.org/10.1016/j.cell.2010.03.015

Kessler, D., Gruen, G.-C., Heider, D., Morgner, J., Reis, H., Schmid, K.W., Jendrossek, V.,

2012. The Action of Small GTPases Rab11 and Rab25 in Vesicle Trafficking During Cell Migration. CPB 29, 647–656. https://doi.org/10.1159/000295249

Khurana, N., Kim, H., Khan, T., Kahhal, S., Bukvic, A., Abdel-Mageed, A.B., Sikka, S.C., Mondal, D., 2022. Abstract 2446: Low dose dimethyl sulfoxide (DMSO) downregulates the expression of androgen receptor (AR) and AR-variant 7 (AR-v7) in castration resistant prostate cancer (CRPC) cells. Cancer Research 82, 2446. https://doi.org/10.1158/1538-7445.AM2022-2446

Kielbik, M., Szulc-Kielbik, I., Klink, M., 2021. Impact of Selected Signaling Proteins on SNAIL 1 and SNAIL 2 Expression in Ovarian Cancer Cell Lines in Relation to Cells' Cisplatin Resistance and EMT Markers Level. International Journal of Molecular Sciences 22, 980. https://doi.org/10.3390/ijms22020980

Kim, J.H., Park, J., 2014. Prognostic significance of heme oxygenase-1, S100 calcium-binding protein A4, and syndecan-1 expression in primary non–muscle-invasive bladder cancer. Human Pathology 45, 1830–1838. https://doi.org/10.1016/j.humpath.2014.04.020

Kim, M.-S., Ha, S.-E., Wu, M., Zogg, H., Ronkon, C.F., Lee, M.-Y., Ro, S., 2021. Extracellular Matrix Biomarkers in Colorectal Cancer. Int J Mol Sci 22, 9185. https://doi.org/10.3390/ijms22179185

Kim, S., Han, Y., Kim, S.I., Lee, J., Jo, H., Wang, W., Cho, U., Park, W.-Y., Rando, T.A., Dhanasekaran, D.N., Song, Y.S., 2021. Computational modeling of malignant ascites reveals CCL5-SDC4 interaction in the immune microenvironment of ovarian cancer. Mol Carcinog 60, 297–312. https://doi.org/10.1002/mc.23289

Kim, Y.-H., Lee, H.C., Kim, S.-Y., Yeom, Y.I., Ryu, K.J., Min, B.-H., Kim, D.-H., Son, H.J., Rhee, P.-L., Kim, J.J., Rhee, J.C., Kim, H.C., Chun, H.-K., Grady, W.M., Kim, Y.S., 2011. Epigenomic Analysis of Aberrantly Methylated Genes in Colorectal Cancer Identifies Genes Commonly Affected by Epigenetic Alterations. Ann Surg Oncol 18, 2338–2347. https://doi.org/10.1245/s10434-011-1573-y

Kimmel, C.B., Ballard, W.W., Kimmel, S.R., Ullmann, B., Schilling, T.F., 1995. Stages of embryonic development of the zebrafish. Developmental Dynamics 203, 253–310. https://doi.org/10.1002/aja.1002030302

King, S.M., Quartuccio, S., Hilliard, T.S., Inoue, K., Burdette, J.E., King, S.M., Quartuccio, S., 2011. Alginate Hydrogels for Three-Dimensional Organ Culture of Ovaries and Oviducts. Journal of Visualized Experiments (JoVE) e2804. https://doi.org/10.3791/2804

Kintakas, C., McCulloch, D.R., 2011. Emerging roles for ADAMTS5 during development and disease. Matrix Biology 30, 311–317. https://doi.org/10.1016/j.matbio.2011.05.004

Klass, C.M., Couchman, J.R., Woods, A., 2000. Control of extracellular matrix assembly by syndecan-2 proteoglycan. J Cell Sci 113 (Pt 3), 493–506. https://doi.org/10.1242/jcs.113.3.493

Klymenko, Y., Kim, O., Loughran, E., Yang, J., Lombard, R., Alber, M., Stack, M.S., 2017. Cadherin composition and multicellular aggregate invasion in organotypic models of epithelial

ovarian cancer intraperitoneal metastasis. Oncogene 36, 5840–5851. https://doi.org/10.1038/onc.2017.171

Köbel, M., Kang, E.Y., 2022. The Evolution of Ovarian Carcinoma Subclassification. Cancers (Basel) 14, 416. https://doi.org/10.3390/cancers14020416

Koike, T., Kimura, N., Miyazaki, K., Yabuta, T., Kumamoto, K., Takenoshita, S., Chen, J., Kobayashi, M., Hosokawa, M., Taniguchi, A., Kojima, T., Ishida, N., Kawakita, M., Yamamoto, H., Takematsu, H., Suzuki, A., Kozutsumi, Y., Kanangi, R., 2004. Hypoxia induces adhesion molecules on cancer cells: A missing link between Warburg effect and induction of selectin-ligand carbohydrates. Proceedings of the National Academy of Sciences 101, 8132–8137. https://doi.org/10.1073/pnas.0402088101

Koo, B.-H., Longpré, J.-M., Somerville, R.P.T., Alexander, J.P., Leduc, R., Apte, S.S., 2007. Regulation of ADAMTS9 secretion and enzymatic activity by its propeptide. J Biol Chem 282, 16146–16154. https://doi.org/10.1074/jbc.M610161200

Köpke, K., Lembke, C.-S., Oosterhof, N., Dijkstra, E.S.C., Paridaen, J.T.M.L., 2024. Protocol for quantifying xenografted human cancer cells in zebrafish larvae using Cellpose. STAR Protocols 5, 103479. https://doi.org/10.1016/j.xpro.2024.103479

Krakhmal, N.V., Zavyalova, M.V., Denisov, E.V., Vtorushin, S.V., Perelmuter, V.M., 2015. Cancer Invasion: Patterns and Mechanisms. Acta Naturae 7, 17–28.

Krishnan, M., Lapierre, L.A., Knowles, B.C., Goldenring, J.R., 2013. Rab25 regulates integrin expression in polarized colonic epithelial cells. MBoC 24, 818–831. https://doi.org/10.1091/mbc.e12-10-0745

Kulbe, H., Otto, R., Darb-Esfahani, S., Lammert, H., Abobaker, S., Welsch, G., Chekerov, R., Schäfer, R., Dragun, D., Hummel, M., Leser, U., Sehouli, J., Braicu, E.I., 2019. Discovery and Validation of Novel Biomarkers for Detection of Epithelial Ovarian Cancer. Cells 8, 713. https://doi.org/10.3390/cells8070713

Kumar, S., Rao, N., Ge, R., 2012a. Emerging Roles of ADAMTSs in Angiogenesis and Cancer. Cancers (Basel) 4, 1252–1299. https://doi.org/10.3390/cancers4041252

Kumar, S., Sharghi-Namini, S., Rao, N., Ge, R., 2012b. ADAMTS5 functions as an anti-angiogenic and anti-tumorigenic protein independent of its proteoglycanase activity. Am J Pathol 181, 1056–1068. https://doi.org/10.1016/j.ajpath.2012.05.022

Kuo, K.-T., Mao, T.-L., Jones, S., Veras, E., Ayhan, A., Wang, T.-L., Glas, R., Slamon, D., Velculescu, V.E., Kuman, R.J., Shih, I.-M., 2009. Frequent Activating Mutations of *PIK3CA* in Ovarian Clear Cell Carcinoma. The American Journal of Pathology 174, 1597–1601. https://doi.org/10.2353/ajpath.2009.081000

Kusumoto, T., Kodama, J., Seki, N., Nakamura, K., Hongo, A., Hiramatsu, Y., 2010. Clinical significance of syndecan-1 and versican expression in human epithelial ovarian cancer. Oncology Reports 23, 917–925. https://doi.org/10.3892/or_00000715

Kveiborg, M., Fröhlich, C., Albrechtsen, R., Tischler, V., Dietrich, N., Holck, P., Kronqvist,

P., Rank, F., Mercurio, A.M., Wewer, U.M., 2005. A role for ADAM12 in breast tumor progression and stromal cell apoptosis. Cancer Res 65, 4754–4761. https://doi.org/10.1158/0008-5472.CAN-05-0262

Kwon, M.J., 2023. Matrix metalloproteinases as therapeutic targets in breast cancer. Front Oncol 12, 1108695. https://doi.org/10.3389/fonc.2022.1108695

Lal, S., La Du, J., Tanguay, R.L., Greenwood, J.A., 2012. Calpain 2 is required for the invasion of glioblastoma cells in the zebrafish brain microenvironment. Journal of Neuroscience Research 90, 769–781. https://doi.org/10.1002/jnr.22794

Lambrecht, B.N., Vanderkerken, M., Hammad, H., 2018. The emerging role of ADAM metalloproteinases in immunity. Nat Rev Immunol 18, 745–758. https://doi.org/10.1038/s41577-018-0068-5

Latifi, A., Abubaker, K., Castrechini, N., Ward, A.C., Liongue, C., Dobill, F., Kumar, J., Thompson, E.W., Quinn, M.A., Findlay, J.K., Ahmed, N., 2011. Cisplatin treatment of primary and metastatic epithelial ovarian carcinomas generates residual cells with mesenchymal stem cell-like profile. Journal of Cellular Biochemistry 112, 2850–2864. https://doi.org/10.1002/jcb.23199

Latourte, A., Richette, P., 2022. Inhibition of ADAMTS-5: the right target for osteoarthritis? Osteoarthritis and Cartilage 30, 175–177. https://doi.org/10.1016/j.joca.2021.09.012

Ledermann, J.A., Luvero, D., Shafer, A., O'Connor, D., Mangili, G., Friedlander, M., Pfisterer, J., Mirza, M.R., Kim, J.-W., Alexandre, J., Amit, O., Brown, J., 2014. Gynecologic Cancer InterGroup (GCIG) Consensus Review for Mucinous Ovarian Carcinoma. International Journal of Gynecological Cancer 24, S14–S19. https://doi.org/10.1097/IGC.0000000000000296

Lee, S.L.C., Rouhi, P., Jensen, L.D., Zhang, D., Ji, H., Hauptmann, G., Ingham, P., Cao, Y., 2009. Hypoxia-induced pathological angiogenesis mediates tumor cell dissemination, invasion, and metastasis in a zebrafish tumor model. Proceedings of the National Academy of Sciences 106, 19485–19490. https://doi.org/10.1073/pnas.0909228106

Lemmon, C.A., Ohashi, T., Erickson, H.P., 2011. Probing the Folded State of Fibronectin Type III Domains in Stretched Fibrils by Measuring Buried Cysteine Accessibility *. Journal of Biological Chemistry 286, 26375–26382. https://doi.org/10.1074/jbc.M111.240028

Lendorf, M.E., Manon-Jensen, T., Kronqvist, P., Multhaupt, H.A.B., Couchman, J.R., 2011. Syndecan-1 and Syndecan-4 Are Independent Indicators in Breast Carcinoma. J Histochem Cytochem 59, 615–629. https://doi.org/10.1369/0022155411405057

Lengyel, E., 2010. Ovarian Cancer Development and Metastasis. Am J Pathol 177, 1053–1064. https://doi.org/10.2353/ajpath.2010.100105

Lessan, K., Aguiar, D.J., Oegema, T., Siebenson, L., Skubitz, A.P.N., 1999. CD44 and β1 Integrin Mediate Ovarian Carcinoma Cell Adhesion to Peritoneal Mesothelial Cells. Am J Pathol 154, 1525–1537.

Levanon, K., Ng, V., Piao, H.Y., Zhang, Y., Chang, M.C., Roh, M.H., Kindelberger, D.W., Hirsch, M.S., Crum, C.P., Marto, J.A., Drapkin, R., 2010. Primary ex vivo cultures of human fallopian tube epithelium as a model for serous ovarian carcinogenesis. Oncogene 29, 1103–1113. https://doi.org/10.1038/onc.2009.402

Levin, V.A., Panchabhai, S.C., Shen, L., Kornblau, S.M., Qiu, Y., Baggerly, K.A., 2010. Different Changes in Protein and Phosphoprotein Levels Result from Serum Starvation of High-Grade Glioma and Adenocarcinoma Cell Lines. J. Proteome Res. 9, 179–191. https://doi.org/10.1021/pr900392b

Lheureux, S., Braunstein, M., Oza, A.M., 2019. Epithelial ovarian cancer: Evolution of management in the era of precision medicine. CA: A Cancer Journal for Clinicians 69, 280–304. https://doi.org/10.3322/caac.21559

Li, C., Luo, X., Huang, B., Wang, X., Deng, Y., Zhong, Z., 2020. ADAMTS12 acts as a cancer promoter in colorectal cancer via activating the Wnt/β-catenin signaling pathway in vitro. Ann Transl Med 8, 301. https://doi.org/10.21037/atm.2020.02.154

Li, C., Xiong, Y., Yang, X., Wang, L., Zhang, S., Dai, N., Li, M., Ren, T., Yang, Y., Zhou, S.-F., Gan, L., Wang, D., 2015. Lost expression of ADAMTS5 protein associates with progression and poor prognosis of hepatocellular carcinoma. Drug Des Devel Ther 9, 1773–1783. https://doi.org/10.2147/DDDT.S77069

Li, H., Zeng, C., Shu, C., Cao, Y., Shao, W., Zhang, M., Cao, H., Zhao, S., 2022. Laminins in tumor-derived exosomes upregulated by ETS1 reprogram omental macrophages to promote omental metastasis of ovarian cancer. Cell Death Dis 13, 1028. https://doi.org/10.1038/s41419-022-05472-7

Li, Q., Park, P.W., Wilson, C.L., Parks, W.C., 2002. Matrilysin shedding of syndecan-1 regulates chemokine mobilization and transepithelial efflux of neutrophils in acute lung injury. Cell 111, 635–646. https://doi.org/10.1016/s0092-8674(02)01079-6

Li, S., Sampson, C., Liu, C., Piao, H., Liu, H.-X., 2023. Integrin signaling in cancer: bidirectional mechanisms and therapeutic opportunities. Cell Communication and Signaling 21, 266. https://doi.org/10.1186/s12964-023-01264-4

Li, T., Zhou, J., Jiang, Y., Zhao, Y., Huang, J., Li, W., Huang, Z., Chen, Z., Tang, X., Chen, H., Yang, Z., 2022. The Novel Protein ADAMTS16 Promotes Gastric Carcinogenesis by Targeting IFI27 through the NF-κb Signaling Pathway. Int J Mol Sci 23, 11022. https://doi.org/10.3390/ijms231911022

Li, Y., Jia, Q., Zhang, Q., Wan, Y., 2015. Rab25 upregulation correlates with the proliferation, migration, and invasion of renal cell carcinoma. Biochemical and Biophysical Research Communications 458, 745–750. https://doi.org/10.1016/j.bbrc.2015.01.144

Liddington, R.C., Ginsberg, M.H., 2002. Integrin activation takes shape. J Cell Biol 158, 833–839. https://doi.org/10.1083/jcb.200206011

Lima, M.A., Santos, L. dos, Turri, J.A., Nonogaki, S., Buim, M., Lima, J.F., Pinheiro, J. de

J.V., Osório, C.A.B. de T., Soares, F.A., Freitas, V.M., 2016. Prognostic Value of ADAMTS Proteases and Their Substrates in Epithelial Ovarian Cancer. PAT 83, 316–326. https://doi.org/10.1159/000446244

Lin, H.-W., Fu, C.-F., Chang, M.-C., Lu, T.-P., Lin, H.-P., Chiang, Y.-C., Chen, C.-A., Cheng, W.-F., 2018. CDH1, DLEC1 and SFRP5 Methylation Panel As a Prognostic Marker for Advanced Epithelial Ovarian Cancer. Epigenomics 10, 1397–1413. https://doi.org/10.2217/epi-2018-0035

Lin, J., Ding, D., 2017. The prognostic role of the cancer stem cell marker CD44 in ovarian cancer: a meta-analysis. Cancer Cell International 17, 8. https://doi.org/10.1186/s12935-016-0376-4

Lindahl, G., Fjellander, S., Selvaraj, K., Vildeval, M., Ali, Z., Almter, R., Erkstam, A., Rodriguez, G.V., Abrahamsson, A., Kersley, Å.R., Fahlgren, A., Kjølhede, P., Linder, S., Dabrosin, C., Jensen, L., 2024. Zebrafish tumour xenograft models: a prognostic approach to epithelial ovarian cancer. npj Precis. Onc. 8, 1–11. https://doi.org/10.1038/s41698-024-00550-9

Lister, J.A., Robertson, C.P., Lepage, T., Johnson, S.L., Raible, D.W., 1999. nacre encodes a zebrafish microphthalmia-related protein that regulates neural-crest-derived pigment cell fate. Development 126, 3757–3767. https://doi.org/10.1242/dev.126.17.3757

Liu, Y., Zhang, X., Gu, W., Su, H., Wang, Xin, Wang, Xu, Zhang, J., Xu, M., Sheng, W., 2024. Unlocking the crucial role of cancer-associated fibroblasts in tumor metastasis: Mechanisms and therapeutic prospects. Journal of Advanced Research. https://doi.org/10.1016/j.jare.2024.05.031

Livak, K.J., Schmittgen, T.D., 2001. Analysis of relative gene expression data using real-time quantitative PCR and the 2(-Delta Delta C(T)) Method. Methods 25, 402–408. https://doi.org/10.1006/meth.2001.1262

Lochter, A., Galosy, S., Muschler, J., Freedman, N., Werb, Z., Bissell, M.J., 1997. Matrix metalloproteinase stromelysin-1 triggers a cascade of molecular alterations that leads to stable epithelial-to-mesenchymal conversion and a premalignant phenotype in mammary epithelial cells. J Cell Biol 139, 1861–1872. https://doi.org/10.1083/jcb.139.7.1861

Loessner, D., Stok, K.S., Lutolf, M.P., Hutmacher, D.W., Clements, J.A., Rizzi, S.C., 2010. Bioengineered 3D platform to explore cell–ECM interactions and drug resistance of epithelial ovarian cancer cells. Biomaterials 31, 8494–8506. https://doi.org/10.1016/j.biomaterials.2010.07.064

Löffek, S., Schilling, O., Franzke, C.-W., 2011. Biological role of matrix metalloproteinases: a critical balance. European Respiratory Journal 38, 191–208. https://doi.org/10.1183/09031936.00146510

Longpré, J.-M., McCulloch, D.R., Koo, B.-H., Alexander, J.P., Apte, S.S., Leduc, R., 2009. Characterization of proADAMTS5 processing by proprotein convertases. The International Journal of Biochemistry & Cell Biology 41, 1116–1126.

https://doi.org/10.1016/j.biocel.2008.10.008

Lord, S.J., Velle, K.B., Mullins, R.D., Fritz-Laylin, L.K., 2020. SuperPlots: Communicating reproducibility and variability in cell biology. Journal of Cell Biology 219, e202001064. https://doi.org/10.1083/jcb.202001064

Lou, X., Han, X., Jin, C., Tian, W., Yu, W., Ding, D., Cheng, L., Huang, B., Jiang, H., Lin, B., 2013. SOX2 Targets Fibronectin 1 to Promote Cell Migration and Invasion in Ovarian Cancer: New Molecular Leads for Therapeutic Intervention. OMICS: A Journal of Integrative Biology 17, 510–518. https://doi.org/10.1089/omi.2013.0058

Louault, K., Li, R.-R., DeClerck, Y.A., 2020. Cancer-Associated Fibroblasts: Understanding Their Heterogeneity. Cancers (Basel) 12, 3108. https://doi.org/10.3390/cancers12113108

Luque, A., Carpizo, D.R., Iruela-Arispe, M.L., 2003. ADAMTS1/METH1 Inhibits Endothelial Cell Proliferation by Direct Binding and Sequestration of VEGF165*. Journal of Biological Chemistry 278, 23656–23665. https://doi.org/10.1074/jbc.M212964200

Lv, Z.-D., Na, D., Ma, X.-Y., Zhao, C., Zhao, W.-J., Xu, H.-M., 2011. Human peritoneal mesothelial cell transformation into myofibroblasts in response to TGF-ß1 in vitro. Int J Mol Med 27, 187–193. https://doi.org/10.3892/ijmm.2010.574

Ma, D.-H., Li, B.-S., Liu, J.-J., Xiao, Y.-F., Yong, X., Wang, S.-M., Wu, Y.-Y., Zhu, H.-B., Wang, D.-X., Yang, S.-M., 2017. miR-93-5p/IFNAR1 axis promotes gastric cancer metastasis through activating the STAT3 signaling pathway. Cancer Letters 408, 23–32. https://doi.org/10.1016/j.canlet.2017.08.017

Ma, R., Tang, Z., Sun, kunkun, Ye, X., Cheng, H., Chang, X., Cui, H., 2018. Low levels of ADAM23 expression in epithelial ovarian cancer are associated with poor survival. Pathology - Research and Practice 214, 1115–1122. https://doi.org/10.1016/j.prp.2018.06.007

Madsen, D.H., Bugge, T.H., 2015. The source of matrix-degrading enzymes in human cancer: Problems of research reproducibility and possible solutions. J Cell Biol 209, 195–198. https://doi.org/10.1083/jcb.201501034

Majerus, E.M., Zheng, X., Tuley, E.A., Sadler, J.E., 2003. Cleavage of the ADAMTS13 propeptide is not required for protease activity. J Biol Chem 278, 46643–46648. https://doi.org/10.1074/jbc.M309872200

Makarem, R., Newham, P., Askari, J.A., Green, L.J., Clements, J., Edwards, M., Humphries, M.J., Mould, A.P., 1994. Competitive binding of vascular cell adhesion molecule-1 and the HepII/IIICS domain of fibronectin to the integrin alpha 4 beta 1. Journal of Biological Chemistry 269, 4005–4011. https://doi.org/10.1016/S0021-9258(17)41734-0

Malik, R., Lelkes, P.I., Cukierman, E., 2015. Biomechanical and biochemical remodeling of stromal extracellular matrix in cancer. Trends in Biotechnology 33, 230–236. https://doi.org/10.1016/j.tibtech.2015.01.004

Marques, I.J., Weiss, F.U., Vlecken, D.H., Nitsche, C., Bakkers, J., Lagendijk, A.K., Partecke, L.I., Heidecke, C.-D., Lerch, M.M., Bagowski, C.P., 2009. Metastatic behaviour of primary

human tumours in a zebrafish xenotransplantation model. BMC Cancer 9, 128. https://doi.org/10.1186/1471-2407-9-128

Matthews, R.T., Gary, S.C., Zerillo, C., Pratta, M., Solomon, K., Arner, E.C., Hockfield, S., 2000. Brain-enriched Hyaluronan Binding (BEHAB)/Brevican Cleavage in a Glioma Cell Line Is Mediated by a Disintegrin and Metalloproteinase with Thrombospondin Motifs (ADAMTS) Family Member *. Journal of Biological Chemistry 275, 22695–22703. https://doi.org/10.1074/jbc.M909764199

Mazzocca, A., Coppari, R., De Franco, R., Cho, J.-Y., Libermann, T.A., Pinzani, M., Toker, A., 2005. A secreted form of ADAM9 promotes carcinoma invasion through tumor-stromal interactions. Cancer Res 65, 4728–4738. https://doi.org/10.1158/0008-5472.CAN-04-4449

McCulloch, D.R., Goff, C.L., Bhatt, S., Dixon, L.J., Sandy, J.D., Apte, S.S., 2009. *Adamts5*, the gene encoding a proteoglycan-degrading metalloprotease, is expressed by specific cell lineages during mouse embryonic development and in adult tissues. Gene Expression Patterns 9, 314–323. https://doi.org/10.1016/j.gep.2009.02.006

Meen, A.J., Øynebråten, I., Reine, T.M., Duelli, A., Svennevig, K., Pejler, G., Jenssen, T., Kolset, S.O., 2011. Serglycin Is a Major Proteoglycan in Polarized Human Endothelial Cells and Is Implicated in the Secretion of the Chemokine GROα/CXCL1 *. Journal of Biological Chemistry 286, 2636–2647. https://doi.org/10.1074/jbc.M110.151944

Mikuła-Pietrasik, J., Sosińska, P., Kucińska, M., Murias, M., Maksin, K., Malińska, A., Ziółkowska, A., Piotrowska, H., Woźniak, A., Książek, K., 2014. Peritoneal mesothelium promotes the progression of ovarian cancer cells *in vitro* and in a mice xenograft model *in vivo*. Cancer Letters 355, 310–315. https://doi.org/10.1016/j.canlet.2014.09.041

Mitra, A., Sawada, K., Tiwari, P., Mui, K., Gwin, K., Lengyel, E., 2011. Ligand independent activation of c-Met by fibronectin and α5β1-integrin regulates ovarian cancer invasion and metastasis. Oncogene 30, 1566–1576. https://doi.org/10.1038/onc.2010.532

Mitra, S., Cheng, K.W., Mills, G.B., 2012. Rab25 in Cancer: A brief update. Biochem Soc Trans 40, 1404–1408. https://doi.org/10.1042/BST20120249

Miyadai, M., Takada, H., Shiraishi, A., Kimura, T., Watakabe, I., Kobayashi, H., Nagao, Y., Naruse, K., Higashijima, S., Shimizu, T., Kelsh, R.N., Hibi, M., Hashimoto, H., 2023. A gene regulatory network combining Pax3/7, Sox10 and Mitf generates diverse pigment cell types in medaka and zebrafish. Development 150, dev202114. https://doi.org/10.1242/dev.202114

Mogi, K., Yoshihara, M., Iyoshi, S., Kitami, K., Uno, K., Tano, S., Koya, Y., Sugiyama, M., Yamakita, Y., Nawa, A., Tomita, H., Kajiyama, H., 2021. Ovarian Cancer-Associated Mesothelial Cells: Transdifferentiation to Minions of Cancer and Orchestrate Developing Peritoneal Dissemination. Cancers (Basel) 13, 1352. https://doi.org/10.3390/cancers13061352

Moore, R.G., McMeekin, D.S., Brown, A.K., DiSilvestro, P., Miller, M.C., Allard, W.J., Gajewski, W., Kurman, R., Bast, R.C., Skates, S.J., 2009. A novel multiple marker bioassay utilizing HE4 and CA125 for the prediction of ovarian cancer in patients with a pelvic mass. Gynecologic Oncology 112, 40–46. https://doi.org/10.1016/j.ygyno.2008.08.031

Moreno-Layseca, P., Icha, J., Hamidi, H., Ivaska, J., 2019. Integrin trafficking in cells and tissues. Nat Cell Biol 21, 122–132. https://doi.org/10.1038/s41556-018-0223-z

Morgan, M.R., Humphries, M.J., Bass, M.D., 2007. Synergistic control of cell adhesion by integrins and syndecans. Nat Rev Mol Cell Biol 8, 957–969. https://doi.org/10.1038/nrm2289

Morla, A., Ruoslahti, E., 1992. A fibronectin self-assembly site involved in fibronectin matrix assembly: reconstruction in a synthetic peptide. J Cell Biol 118, 421–429. https://doi.org/10.1083/jcb.118.2.421

Morrissey, M.A., Hagedorn, E.J., Sherwood, D.R., 2013. Cell invasion through basement membrane. Worm 2, e26169. https://doi.org/10.4161/worm.26169

Morwood, A.J., El-Karim, I.A., Clarke, S.A., Lundy, F.T., 2023. The Role of Extracellular Matrix (ECM) Adhesion Motifs in Functionalised Hydrogels. Molecules 28, 4616. https://doi.org/10.3390/molecules28124616

Moser, T.L., Young, T.N., Rodriguez, G.C., Pizzo, S.V., Bast Jr, R.C., Stack, M.S., 1994. Secretion of extracellular matrix-degrading proteinases is increased in epithelial ovarian carcinoma. International Journal of Cancer 56, 552–559. https://doi.org/10.1002/ijc.2910560415

Mukaratirwa, S., van Ederen, A.M., Gruys, E., Nederbragt, H., 2004. Versican and Hyaluronan Expression in Canine Colonic Adenomas and Carcinomas: Relation to Malignancy and Depth of Tumour Invasion. Journal of Comparative Pathology 131, 259–270. https://doi.org/10.1016/j.jcpa.2004.04.007

Muller, D., Wolf, C., Abecassis, J., Millon, R., Engelmann, A., Bronner, G., Rouyer, N., Rio, M.C., Eber, M., Methlin, G., 1993. Increased stromelysin 3 gene expression is associated with increased local invasiveness in head and neck squamous cell carcinomas. Cancer Res 53, 165–169.

Muller, P.A.J., Caswell, P.T., Doyle, B., Iwanicki, M.P., Tan, E.H., Karim, S., Lukashchuk, N., Gillespie, D.A., Ludwig, R.L., Gosselin, P., Cromer, A., Brugge, J.S., Sansom, O.J., Norman, J.C., Vousden, K.H., 2009. Mutant p53 Drives Invasion by Promoting Integrin Recycling. Cell 139, 1327–1341. https://doi.org/10.1016/j.cell.2009.11.026

Murakami, M., Horowitz, A., Tang, S., Ware, J.A., Simons, M., 2002. Protein Kinase C (PKC) δ Regulates PKCα Activity in a Syndecan-4-dependent Manner*. Journal of Biological Chemistry 277, 20367–20371. https://doi.org/10.1074/jbc.M202501200

Murphy, G., 2011. Tissue inhibitors of metalloproteinases. Genome Biol 12, 233. https://doi.org/10.1186/gb-2011-12-11-233

Mutsaers, S.E., 2004. The mesothelial cell. The International Journal of Biochemistry & Cell Biology 36, 9–16. https://doi.org/10.1016/S1357-2725(03)00242-5

Mutsaers, S.E., Wilkosz, S., 2007. Structure and Function of Mesothelial Cells, in: Ceelen, W.P. (Ed.), Peritoneal Carcinomatosis: A Multidisciplinary Approach. Springer US, Boston, MA, pp. 1–19. https://doi.org/10.1007/978-0-387-48993-3_1

Na, K.Y., Bacchini, P., Bertoni, F., Kim, Y.W., Park, Y.-K., 2012. Syndecan-4 and fibronectin in osteosarcoma. Pathology 44, 325–330. https://doi.org/10.1097/PAT.0b013e328353447b

Naba, A., Clauser, K.R., Hoersch, S., Liu, H., Carr, S.A., Hynes, R.O., 2012. The Matrisome: *In Silico* Definition and *In Vivo* Characterization by Proteomics of Normal and Tumor Extracellular Matrices*. Molecular & Cellular Proteomics 11, M111.014647. https://doi.org/10.1074/mcp.M111.014647

Nagai, H., Chew, S.H., Okazaki, Y., Funahashi, S., Namba, T., Kato, T., Enomoto, A., Jiang, L., Akatsuka, S., Toyokuni, S., 2013. Metamorphosis of mesothelial cells with active horizontal motility in tissue culture. Sci Rep 3, 1144. https://doi.org/10.1038/srep01144

Najy, A.J., Day, K.C., Day, M.L., 2008. ADAM15 supports prostate cancer metastasis by modulating tumor cell-endothelial cell interaction. Cancer Res 68, 1092–1099. https://doi.org/10.1158/0008-5472.CAN-07-2432

Nakada, M., Miyamori, H., Kita, D., Takahashi, T., Yamashita, J., Sato, H., Miura, R., Yamaguchi, Y., Okada, Y., 2005. Human glioblastomas overexpress ADAMTS-5 that degrades brevican. Acta Neuropathol 110, 239–246. https://doi.org/10.1007/s00401-005-1032-6

Nakamura, H., Fujii, Y., Inoki, I., Sugimoto, K., Tanzawa, K., Matsuki, H., Miura, R., Yamaguchi, Y., Okada, Y., 2000. Brevican Is Degraded by Matrix Metalloproteinases and Aggrecanase-1 (ADAMTS4) at Different Sites *. Journal of Biological Chemistry 275, 38885–38890. https://doi.org/10.1074/jbc.M003875200

Nam, K.T., Lee, H.-J., Smith, J.J., Lapierre, L.A., Kamath, V.P., Chen, X., Aronow, B.J., Yeatman, T.J., Bhartur, S.G., Calhoun, B.C., Condie, B., Manley, N.R., Beauchamp, R.D., Coffey, R.J., Goldenring, J.R., 2010. Loss of Rab25 promotes the development of intestinal neoplasia in mice and is associated with human colorectal adenocarcinomas. J Clin Invest 120, 840–849. https://doi.org/10.1172/JCI40728

Nash, M.A., Deavers, M.T., Freedman, R.S., 2002. The Expression of Decorin in Human Ovarian Tumors. Clinical Cancer Research 8, 1754–1760.

National Cancer Institute, 2024. SEER*Explorer: An interactive website for SEER cancer statistics. [WWW Document]. URL https://seer.cancer.gov/statistics-network/explorer/application.html?site=61&data_type=9&graph_type=3&compareBy=rate_type&chk_rate_type_1=1&chk_rate_type_2=2&chk_rate_type_3=3&hdn_sex=3&race=1&advopt_precision=1&advopt_show_ci=on&hdn_view=1#resultsRegion1 (accessed 3.13.25).

Nehmé, A., Baskaran, R., Aebi, S., Fink, D., Nebel, S., Cenni, B., Wang, J.Y.J., Howell, S.B., Christen, R.D., 1997. Differential Induction of c-Jun NH2-Terminal Kinase and c-Abl Kinase in DNA Mismatch Repair-proficient and -deficient Cells Exposed to Cisplatin1. Cancer Research 57, 3253–3257.

Neophytou, C.M., Panagi, M., Stylianopoulos, T., Papageorgis, P., 2021. The Role of Tumor Microenvironment in Cancer Metastasis: Molecular Mechanisms and Therapeutic Opportunities. Cancers (Basel) 13, 2053. https://doi.org/10.3390/cancers13092053

Nieman, K.M., Kenny, H.A., Penicka, C.V., Ladanyi, A., Buell-Gutbrod, R., Zillhardt, M.R., Romero, I.L., Carey, M.S., Mills, G.B., Hotamisligil, G.S., Yamada, S.D., Peter, M.E., Gwin, K., Lengyel, E., 2011. Adipocytes promote ovarian cancer metastasis and provide energy for rapid tumor growth. Nat Med 17, 1498–1503. https://doi.org/10.1038/nm.2492

Norris, J.L., Baldwin, A.S., 1999. Oncogenic Ras Enhances NF-κB Transcriptional Activity through Raf-dependent and Raf-independent Mitogen-activated Protein Kinase Signaling Pathways*. Journal of Biological Chemistry 274, 13841–13846. https://doi.org/10.1074/jbc.274.20.13841

Okuyama, E., Suzuki, A., Murata, M., Ando, Y., Kato, I., Takagi, Y., Takagi, A., Murate, T., Saito, H., Kojima, T., 2013. Molecular mechanisms of syndecan-4 upregulation by TNF-α in the endothelium-like EAhy926 cells. The Journal of Biochemistry 154, 41–50. https://doi.org/10.1093/jb/mvt024

Onyeisi, J.O.S., Lopes, C.C., Götte, M., 2021. Syndecan-4 as a Pathogenesis Factor and Therapeutic Target in Cancer. Biomolecules 11, 503. https://doi.org/10.3390/biom11040503

Paatero, I., Alve, S., Gramolelli, S., Ivaska, J., Ojala, P.M., 2018. Zebrafish Embryo Xenograft and Metastasis Assay. Bio Protoc 8, e3027. https://doi.org/10.21769/BioProtoc.3027

Paget, S., 1889. THE DISTRIBUTION OF SECONDARY GROWTHS IN CANCER OF THE BREAST. The Lancet, Originally published as Volume 1, Issue 3421 133, 571–573. https://doi.org/10.1016/S0140-6736(00)49915-0

Pang, X., He, X., Qiu, Z., Zhang, H., Xie, R., Liu, Z., Gu, Y., Zhao, N., Xiang, Q., Cui, Y., 2023. Targeting integrin pathways: mechanisms and advances in therapy. Sig Transduct Target Ther 8, 1–42. https://doi.org/10.1038/s41392-022-01259-6

Pankov, R., Yamada, K.M., 2002. Fibronectin at a glance. Journal of Cell Science 115, 3861–3863. https://doi.org/10.1242/jcs.00059

Patton, E.E., Zon, L.I., Langenau, D.M., 2021. Zebrafish disease models in drug discovery: from preclinical modelling to clinical trials. Nat Rev Drug Discov 20, 611–628. https://doi.org/10.1038/s41573-021-00210-8

Paul, N.R., Allen, J.L., Chapman, A., Morlan-Mairal, M., Zindy, E., Jacquemet, G., Fernandez del Ama, L., Ferizovic, N., Green, D.M., Howe, J.D., Ehler, E., Hurlstone, A., Caswell, P.T., 2015. α5β1 integrin recycling promotes Arp2/3-independent cancer cell invasion via the formin FHOD3. J Cell Biol 210, 1013–1031. https://doi.org/10.1083/jcb.201502040

Peduto, L., Reuter, V.E., Shaffer, D.R., Scher, H.I., Blobel, C.P., 2005. Critical function for ADAM9 in mouse prostate cancer. Cancer Res 65, 9312–9319. https://doi.org/10.1158/0008-5472.CAN-05-1063

Persikov, A.V., Ramshaw, J.A.M., Kirkpatrick, A., Brodsky, B., 2005. Electrostatic Interactions Involving Lysine Make Major Contributions to Collagen Triple-Helix Stability. Biochemistry 44, 1414–1422. https://doi.org/10.1021/bi048216r

Piek, J.M.J., van Diest, P.J., Zweemer, R.P., Jansen, J.W., Poort-Keesom, R.J.J., Menko, F.H.,

Gille, J.J.P., Jongsma, A.P.M., Pals, G., Kenemans, P., Verheijen, R.H.M., 2001. Dysplastic changes in prophylactically removed Fallopian tubes of women predisposed to developing ovarian cancer. The Journal of Pathology 195, 451–456. https://doi.org/10.1002/path.1000

Piperigkou, Z., Kyriakopoulou, K., Koutsakis, C., Mastronikolis, S., Karamanos, N.K., 2021. Key Matrix Remodeling Enzymes: Functions and Targeting in Cancer. Cancers (Basel) 13, 1441. https://doi.org/10.3390/cancers13061441

Pommler, R.F., Woltering, E.A., Milo, G., Fletcher, W.S., 1988. Synergistic cytotoxicity between dimethyl sulfoxide and antineoplastic agents against ovarian cancer in vitro. American Journal of Obstetrics and Gynecology 159, 848–852. https://doi.org/10.1016/S0002-9378(88)80151-0

Pompili, S., Latella, G., Gaudio, E., Sferra, R., Vetuschi, A., 2021. The Charming World of the Extracellular Matrix: A Dynamic and Protective Network of the Intestinal Wall. Front. Med. 8. https://doi.org/10.3389/fmed.2021.610189

Ponta, H., Sherman, L., Herrlich, P.A., 2003. CD44: from adhesion molecules to signalling regulators. Nat Rev Mol Cell Biol 4, 33–45. https://doi.org/10.1038/nrm1004

Porter, S., Scott, S.D., Sassoon, E.M., Williams, M.R., Jones, J.L., Girling, A.C., Ball, R.Y., Edwards, D.R., 2004. Dysregulated expression of adamalysin-thrombospondin genes in human breast carcinoma. Clin Cancer Res 10, 2429–2440. https://doi.org/10.1158/1078-0432.ccr-0398-3

Pradeep, S., Kim, S.W., Wu, S.Y., Nishimura, M., Chaluvally-Raghavan, P., Miyake, T., Pecot, C.V., Kim, S.-J., Choi, H.J., Bischoff, F.Z., Mayer, J.A., Huang, L., Nick, A.M., Hall, C.S., Rodriguez-Aguayo, C., Zand, B., Dalton, H.J., Arumugam, T., Lee, H.J., Han, H.D., Cho, M.S., Rupaimoole, R., Mangala, L.S., Sehgal, V., Oh, S.C., Liu, J., Lee, J.-S., Coleman, R.L., Ram, P., Lopez-Berestein, G., Fidler, I.J., Sood, A.K., 2014. Hematogenous Metastasis of Ovarian Cancer: Rethinking Mode of Spread. Cancer Cell 26, 77–91. https://doi.org/10.1016/j.ccr.2014.05.002

Provenzano, P.P., Eliceiri, K.W., Campbell, J.M., Inman, D.R., White, J.G., Keely, P.J., 2006. Collagen reorganization at the tumor-stromal interface facilitates local invasion. BMC Medicine 4, 38. https://doi.org/10.1186/1741-7015-4-38

Prydz, K., 2015. Determinants of Glycosaminoglycan (GAG) Structure. Biomolecules 5, 2003–2022. https://doi.org/10.3390/biom5032003

Quintero-Fabián, S., Arreola, R., Becerril-Villanueva, E., Torres-Romero, J.C., Arana-Argáez, V., Lara-Riegos, J., Ramírez-Camacho, M.A., Alvarez-Sánchez, M.E., 2019. Role of Matrix Metalloproteinases in Angiogenesis and Cancer. Front Oncol 9, 1370. https://doi.org/10.3389/fonc.2019.01370

Ra, H.-J., Parks, W.C., 2007. Control of Matrix Metalloproteinase Catalytic Activity. Matrix Biol 26, 587–596. https://doi.org/10.1016/j.matbio.2007.07.001

Rainero, E., Caswell, P.T., Muller, P.A.J., Grindlay, J., McCaffrey, M.W., Zhang, Q.,

Wakelam, M.J.O., Vousden, K.H., Graziani, A., Norman, J.C., 2012. Diacylglycerol kinase α controls RCP-dependent integrin trafficking to promote invasive migration. Journal of Cell Biology 196, 277–295. https://doi.org/10.1083/jcb.201109112

Rainero, E., Howe, J.D., Caswell, P.T., Jamieson, N.B., Anderson, K., Critchley, D.R., Machesky, L., Norman, J.C., 2015. Ligand-Occupied Integrin Internalization Links Nutrient Signaling to Invasive Migration. Cell Reports 10, 398–413. https://doi.org/10.1016/j.celrep.2014.12.037

Rainero, E., Norman, J.C., 2013. Late endosomal and lysosomal trafficking during integrin-mediated cell migration and invasion. https://doi.org/10.1002/bies.201200160

Ramus, S.J., Song, H., Dicks, E., Tyrer, J.P., Rosenthal, A.N., Intermaggio, M.P., Fraser, L., Gentry-Maharaj, A., Hayward, J., Philpott, S., Anderson, C., Edlund, C.K., Conti, D., Harrington, P., Barrowdale, D., Bowtell, D.D., Alsop, K., Mitchell, G., AOCS Study Group, Cicek, M.S., Cunningham, J.M., Fridley, B.L., Alsop, J., Jimenez-Linan, M., Poblete, S., Lele, S., Sucheston-Campbell, L., Moysich, K.B., Sieh, W., McGuire, V., Lester, J., Bogdanova, N., Dürst, M., Hillemanns, P., Ovarian Cancer Association Consortium, Odunsi, K., Whittemore, A.S., Karlan, B.Y., Dörk, T., Goode, E.L., Menon, U., Jacobs, I.J., Antoniou, A.C., Pharoah, P.D.P., Gayther, S.A., 2015. Germline Mutations in the BRIP1, BARD1, PALB2, and NBN Genes in Women With Ovarian Cancer. JNCI: Journal of the National Cancer Institute 107, djv214. https://doi.org/10.1093/jnci/djv214

Rashid, M., Coombs, K.M., 2019. Serum-reduced media impacts on cell viability and protein expression in human lung epithelial cells. J Cell Physiol 234, 7718–7724. https://doi.org/10.1002/jcp.27890

Reed, C.C., Iozzo, R.V., 2002. The role of decorin in collagen fibrillogenesis and skin homeostasis. Glycoconj J 19, 249–255. https://doi.org/10.1023/A:1025383913444

Remacle, A.G., Golubkov, V.S., Shiryaev, S.A., Dahl, R., Stebbins, J.L., Chernov, A.V., Cheltsov, A.V., Pellecchia, M., Strongin, A.Y., 2012. Novel MT1-MMP Small-Molecule Inhibitors Based on Insights into Hemopexin Domain Function in Tumor Growth. Cancer Research 72, 2339–2349. https://doi.org/10.1158/0008-5472.CAN-11-4149

Reunanen, N., Kähäri, V., 2013. Matrix Metalloproteinases in Cancer Cell Invasion, in: Madame Curie Bioscience Database [Internet]. Landes Bioscience.

Revell, C.K., Jensen, O.E., Shearer, T., Lu, Y., Holmes, D.F., Kadler, K.E., 2021. Collagen fibril assembly: New approaches to unanswered questions. Matrix Biology Plus 12, 100079. https://doi.org/10.1016/j.mbplus.2021.100079

Ricard-Blum, S., 2011. The Collagen Family. Cold Spring Harb Perspect Biol 3, a004978. https://doi.org/10.1101/cshperspect.a004978

Ricard-Blum, S., Ruggiero, F., van der Rest, M., 2005. The Collagen Superfamily, in: Brinckmann, J., Notbohm, H., Müller, P.K. (Eds.), Collagen: Primer in Structure, Processing and Assembly. Springer, Berlin, Heidelberg, pp. 35–84. https://doi.org/10.1007/b103819

Ricciardelli, C., Ween, M.P., Lokman, N.A., Tan, I.A., Pyragius, C.E., Oehler, M.K., 2013. Chemotherapy-induced hyaluronan production: a novel chemoresistance mechanism in ovarian cancer. BMC Cancer 13, 476. https://doi.org/10.1186/1471-2407-13-476

Richardson, T.P., Trinkaus-Randall, V., Nugent, M.A., 2001. Regulation of heparan sulfate proteoglycan nuclear localization by fibronectin. Journal of Cell Science 114, 1613–1623. https://doi.org/10.1242/jcs.114.9.1613

Rieppi, M., Vergani, V., Gatto, C., Zanetta, G., Allavena, P., Taraboletti, G., Giavazzi, R., 1999. Mesothelial cells induce the motility of human ovarian carcinoma cells. Int J Cancer 80, 303–307. https://doi.org/10.1002/(sici)1097-0215(19990118)80:2<303::aid-ijc21>3.0.co;2-w

Riggio, A.I., Varley, K.E., Welm, A.L., 2021. The lingering mysteries of metastatic recurrence in breast cancer. Br J Cancer 124, 13–26. https://doi.org/10.1038/s41416-020-01161-4

Rosel, D., Fernandes, M., Sanz-Moreno, V., Brábek, J., 2019. Migrastatics: Redirecting R&D in Solid Cancer Towards Metastasis? Trends in Cancer 5, 755–756. https://doi.org/10.1016/j.trecan.2019.10.011

Rowan, A.D., Litherland, G.J., Hui, W., Milner, J.M., 2008. Metalloproteases as potential therapeutic targets in arthritis treatment. Expert Opinion on Therapeutic Targets 12, 1–18. https://doi.org/10.1517/14728222.12.1.1

Roy, R., Yang, J., Moses, M.A., 2009. Matrix Metalloproteinases As Novel Biomarker s and Potential Therapeutic Targets in Human Cancer. JCO 27, 5287–5297. https://doi.org/10.1200/JCO.2009.23.5556

Russell, D.L., Ochsner, S.A., Hsieh, M., Mulders, S., Richards, J.S., 2003. Hormone-Regulated Expression and Localization of Versican in the Rodent Ovary. Endocrinology 144, 1020–1031. https://doi.org/10.1210/en.2002-220434

Rynne-Vidal, A., Au-Yeung, C.L., Jiménez-Heffernan, J.A., Pérez-Lozano, M.L., Cremades-Jimeno, L., Bárcena, C., Cristóbal-García, I., Fernández-Chacón, C., Yeung, T.L., Mok, S.C., Sandoval, P., López-Cabrera, M., 2017. Mesothelial-to-mesenchymal transition as a possible therapeutic target in peritoneal metastasis of ovarian cancer. J Pathol 242, 140–151. https://doi.org/10.1002/path.4889

Rynne-Vidal, A., Jiménez-Heffernan, J.A., Fernández-Chacón, C., López-Cabrera, M., Sandoval, P., 2015. The Mesothelial Origin of Carcinoma Associated-Fibroblasts in Peritoneal Metastasis. Cancers 7, 1994–2011. https://doi.org/10.3390/cancers7040872

Sacks, J.D., Barbolina, M.V., 2015. Expression and Function of CD44 in Epithelial Ovarian Carcinoma. Biomolecules 5, 3051–3066. https://doi.org/10.3390/biom5043051

Sadok, A., Marshall, C.J., 2014. Rho GTPases: Masters of cell migration. Small GTPases 5, e983878. https://doi.org/10.4161/sgtp.29710

Sahai, E., Astsaturov, I., Cukierman, E., DeNardo, D.G., Egeblad, M., Evans, R.M., Fearon, D., Greten, F.R., Hingorani, S.R., Hunter, T., Hynes, R.O., Jain, R.K., Janowitz, T., Jorgensen, C., Kimmelman, A.C., Kolonin, M.G., Maki, R.G., Powers, R.S., Puré, E., Ramirez, D.C.,

Scherz-Shouval, R., Sherman, M.H., Stewart, S., Tlsty, T.D., Tuveson, D.A., Watt, F.M., Weaver, V., Weeraratna, A.T., Werb, Z., 2020. A framework for advancing our understanding of cancer-associated fibroblasts. Nat Rev Cancer 20, 174–186. https://doi.org/10.1038/s41568-019-0238-1

Sahin, U., Weskamp, G., Kelly, K., Zhou, H.-M., Higashiyama, S., Peschon, J., Hartmann, D., Saftig, P., Blobel, C.P., 2004. Distinct roles for ADAM10 and ADAM17 in ectodomain shedding of six EGFR ligands. J Cell Biol 164, 769–779. https://doi.org/10.1083/jcb.200307137

Sakko, A.J., Ricciardelli, C., Mayne, K., Suwiwat, S., LeBaron, R.G., Marshall, V.R., Tilley, W.D., Horsfall, D.J., 2003. Modulation of prostate cancer cell attachment to matrix by versican. Cancer Res 63, 4786–4791.

Salani, R., Kurman, R.J., Giuntoli, R., Gardner, G., Bristow, R., Wang, T.-L., Shih, I.-M., 2008. Assessment of TP53 mutation using purified tissue samples of ovarian serous carcinomas reveals a higher mutation rate than previously reported and does not correlate with drug resistance. Int J Gynecol Cancer 18, 487–491. https://doi.org/10.1111/j.1525-1438.2007.01039.x

Salani, R., Neuberger, I., Kurman, R.J., Bristow, R.E., Chang, H.-W., Wang, T.-L., Shih, I.-M., 2007. Expression of Extracellular Matrix Proteins in Ovarian Serous Tumors. International Journal of Gynecological Pathology 26, 141. https://doi.org/10.1097/01.pgp.0000229994.02815.f9

Salemme, V., Centonze, G., Avalle, L., Natalini, D., Piccolantonio, A., Arina, P., Morellato, A., Ala, U., Taverna, D., Turco, E., Defilippi, P., 2023. The role of tumor microenvironment in drug resistance: emerging technologies to unravel breast cancer heterogeneity. Front Oncol 13, 1170264. https://doi.org/10.3389/fonc.2023.1170264

Sandoval, P., Jiménez-Heffernan, J.A., Rynne-Vidal, Á., Pérez-Lozano, M.L., Gilsanz, Á., Ruiz-Carpio, V., Reyes, R., García-Bordas, J., Stamatakis, K., Dotor, J., Majano, P.L., Fresno, M., Cabañas, C., López-Cabrera, M., 2013. Carcinoma-associated fibroblasts derive from mesothelial cells via mesothelial-to-mesenchymal transition in peritoneal metastasis. The Journal of Pathology 231, 517–531. https://doi.org/10.1002/path.4281

Santamaria, S., 2020. ADAMTS-5: A difficult teenager turning 20. International Journal of Experimental Pathology 101, 4–20. https://doi.org/10.1111/iep.12344

Santamaria, S., Cuffaro, D., Nuti, E., Ciccone, L., Tuccinardi, T., Liva, F., D'Andrea, F., de Groot, R., Rossello, A., Ahnström, J., 2021. Exosite inhibition of ADAMTS-5 by a glycoconjugated arylsulfonamide. Sci Rep 11, 949. https://doi.org/10.1038/s41598-020-80294-1

Santamaria, S., Yamamoto, K., Teraz-Orosz, A., Koch, C., Apte, S.S., de Groot, R., Lane, D.A., Ahnström, J., 2019. Exosites in Hypervariable Loops of ADAMTS Spacer Domains control Substrate Recognition and Proteolysis. Sci Rep 9, 10914. https://doi.org/10.1038/s41598-019-47494-w

Sato, N., Kohi, S., Hirata, K., Goggins, M., 2016. Role of hyaluronan in pancreatic cancer biology and therapy: Once again in the spotlight. Cancer Sci 107, 569–575. https://doi.org/10.1111/cas.12913

Sauk, J.J., Nikitakis, N., Siavash, H., 2005. Hsp47 a novel collagen binding serpin chaperone, autoantigen and therapeutic target. Front Biosci 10, 107–118. https://doi.org/10.2741/1513

Sawada, K., Mitra, A.K., Radjabi, A.R., Bhaskar, V., Kistner, E.O., Tretiakova, M., Jagadeeswaran, S., Montag, A., Becker, A., Kenny, H.A., Peter, M.E., Ramakrishnan, V., Yamada, S.D., Lengyel, E., 2008. Loss of E-Cadherin Promotes Ovarian Cancer Metastasis via α5-Integrin, which Is a Therapeutic Target. Cancer Res 68, 2329–2339. https://doi.org/10.1158/0008-5472.CAN-07-5167

Scheja, L., Makowski, L., Uysal, K.T., Wiesbrock, S.M., Shimshek, D.R., Meyers, D.S., Morgan, M., Parker, R.A., Hotamisligil, G.S., 1999. Altered insulin secretion associated with reduced lipolytic efficiency in aP2-/- mice. Diabetes 48, 1987–1994. https://doi.org/10.2337/diabetes.48.10.1987

Schild, T., Low, V., Blenis, J., Gomes, A.P., 2018. Unique Metabolic Adaptations Dictate Distal Organ-Specific Metastatic Colonization. Cancer Cell 33, 347–354. https://doi.org/10.1016/j.ccell.2018.02.001

Schindelin, J., Arganda-Carreras, I., Frise, E., Kaynig, V., Longair, M., Pietzsch, T., Preibisch, S., Rueden, C., Saalfeld, S., Schmid, B., Tinevez, J.-Y., White, D.J., Hartenstein, V., Eliceiri, K., Tomancak, P., Cardona, A., 2012. Fiji: an open-source platform for biological-image analysis. Nat Methods 9, 676–682. https://doi.org/10.1038/nmeth.2019

Schmalfeldt, B., Prechtel, D., Härting, K., Späthe, K., Rutke, S., Konik, E., Fridman, R., Berger, U., Schmitt, M., Kuhn, W., Lengyel, E., 2001. Increased expression of matrix metalloproteinases (MMP)-2, MMP-9, and the urokinase-type plasminogen activator is associated with progression from benign to advanced ovarian cancer. Clin Cancer Res 7, 2396–2404.

Schnitzer, T., Pueyo, M., Deckx, H., van der Aar, E., Bernard, K., Hatch, S., van der Stoep, M., Grankov, S., Phung, D., Imbert, O., Chimits, D., Muller, K., Hochberg, M.C., Bliddal, H., Wirth, W., Eckstein, F., Conaghan, P.G., 2023. Evaluation of S201086/GLPG1972, an ADAMTS-5 inhibitor, for the treatment of knee osteoarthritis in ROCCELLA: a phase 2 randomized clinical trial. Osteoarthritis Cartilage 31, 985–994. https://doi.org/10.1016/j.joca.2023.04.001

Schwartz, S.L., Cao, C., Pylypenko, O., Rak, A., Wandinger-Ness, A., 2007. Rab GTPases at a glance. J Cell Sci 120, 3905–3910. https://doi.org/10.1242/jcs.015909

Seals, D.F., Courtneidge, S.A., 2003. The ADAMs family of metalloproteases: multidomain proteins with multiple functions. Genes Dev. 17, 7–30. https://doi.org/10.1101/gad.1039703

Sekhon, B.S., 2010. Matrix metalloproteinases – an overview. RRB 1, 1–20. https://doi.org/10.2147/RRB.S12043

Seven, D., Dogan, S., Kiliç, E., Karaman, E., Koseoglu, H., Buyru, N., 2015. Downregulation of Rab25 activates Akt1 in head and neck squamous cell carcinoma. Oncology Letters 10, 1927–1931. https://doi.org/10.3892/ol.2015.3433

Shan, G., Zhou, X., Gu, J., Zhou, D., Cheng, W., Wu, H., Wang, Y., Tang, T., Wang, X., 2021. Downregulated exosomal microRNA-148b-3p in cancer associated fibroblasts enhance chemosensitivity of bladder cancer cells by downregulating the Wnt/β-catenin pathway and upregulating PTEN. Cell Oncol. 44, 45–59. https://doi.org/10.1007/s13402-020-00500-0

Sharghi-Namini, S., Fan, H., Sulochana, K.N., Potturi, P., Xiang, W., Chong, Y.-S., Wang, Z., Yang, H., Ge, R., 2008. The first but not the second thrombospondin type 1 repeat of ADAMTS5 functions as an angiogenesis inhibitor. Biochem Biophys Res Commun 371, 215–219. https://doi.org/10.1016/j.bbrc.2008.04.047

Sharma, A., Askari, J.A., Humphries, M.J., Jones, E.Y., Stuart, D.I., 1999. Crystal structure of a heparin- and integrin-binding segment of human fibronectin. EMBO J 18, 1468–1479. https://doi.org/10.1093/emboj/18.6.1468

Shen, Y., Shen, R., Ge, L., Zhu, Q., Li, F., 2012. Fibrillar Type I Collagen Matrices Enhance Metastasis/Invasion of Ovarian Epithelial Cancer Via β1 Integrin and PTEN Signals. International Journal of Gynecological Cancer 22, 1316–1324. https://doi.org/10.1097/IGC.0b013e318263ef34

Sherman-Baust, C.A., Weeraratna, A.T., Rangel, L.B.A., Pizer, E.S., Cho, K.R., Schwartz, D.R., Shock, T., Morin, P.J., 2003. Remodeling of the extracellular matrix through overexpression of collagen VI contributes to cisplatin resistance in ovarian cancer cells. Cancer Cell 3, 377–386. https://doi.org/10.1016/S1535-6108(03)00058-8

Shield, K., Riley, C., Quinn, M.A., Rice, G.E., Ackland, M.L., Ahmed, N., 2007. α2β1 integrin affects metastatic potential of ovarian carcinoma spheroids by supporting disaggregation and proteolysis. J Carcinog 6, 11. https://doi.org/10.1186/1477-3163-6-11

Shima, I., Sasaguri, Y., Kusukawa, J., Yamana, H., Fujita, H., Kakegawa, T., Morimatsu, M., 1992. Production of matrix metalloproteinase-2 and metalloproteinase-3 related to malignant behavior of esophageal carcinoma. A clinicopathologic study. Cancer 70, 2747–2753. https://doi.org/10.1002/1097-0142(19921215)70:12<2747::aid-cncr2820701204>3.0.co;2-5

Shin, J., Rhim, J., Kwon, Y., Choi, S.Y., Shin, S., Ha, C.-W., Lee, C., 2019. Comparative analysis of differentially secreted proteins in serum-free and serum-containing media by using BONCAT and pulsed SILAC. Sci Rep 9, 3096. https://doi.org/10.1038/s41598-019-39650-z

Sillanpää, S.M., Anttila, M.A., Voutilainen, K.A., Ropponen, K.M., Sironen, R.K., Saarikoski, S.V., Kosma, V.-M., 2006. Prognostic significance of matrix metalloproteinase-7 in epithelial ovarian cancer and its relation to β-catenin expression. International Journal of Cancer 119, 1792–1799. https://doi.org/10.1002/ijc.22067

Silverberg, S.G., 2000. Histopathologic Grading of Ovarian Carcinoma: A Review and Proposal. International Journal of Gynecological Pathology 19, 7–15.

Śliwa, A., Szczerba, A., Pięta, P.P., Białas, P., Lorek, J., Nowak-Markwitz, E., Jankowska, A., 2024. A Recipe for Successful Metastasis: Transition and Migratory Modes of Ovarian Cancer Cells. Cancers 16, 783. https://doi.org/10.3390/cancers16040783

Sodek, K.L., Murphy, K.J., Brown, T.J., Ringuette, M.J., 2012. Cell–cell and cell–matrix dynamics in intraperitoneal cancer metastasis. Cancer Metastasis Rev 31, 397–414. https://doi.org/10.1007/s10555-012-9351-2

Song, F., Yi, X., Zheng, X., Zhang, Z., Zhao, L., Shen, Y., Zhi, Y., Liu, T., Liu, X., Xu, T., Hu, X., Zhang, Y., Shou, H., Huang, P., 2025. Zebrafish patient-derived xenograft system for predicting carboplatin resistance and metastasis of ovarian cancer. Drug Resistance Updates 78, 101162. https://doi.org/10.1016/j.drup.2024.101162

Stadlmann, S., Amberger, A., Pollheimer, J., Gastl, G., Offner, F.A., Margreiter, R., Zeimet, A.G., 2005. Ovarian carcinoma cells and IL-1beta-activated human peritoneal mesothelial cells are possible sources of vascular endothelial growth factor in inflammatory and malignant peritoneal effusions. Gynecol Oncol 97, 784–789. https://doi.org/10.1016/j.ygyno.2005.02.017

Stadlmann, S., Pollheimer, J., Moser, P.L., Raggi, A., Amberger, A., Margreiter, R., Offner, F.A., Mikuz, G., Dirnhofer, S., Moch, H., 2003. Cytokine-regulated expression of collagenase-2 (MMP-8) is involved in the progression of ovarian cancer. European Journal of Cancer 39, 2499–2505. https://doi.org/10.1016/j.ejca.2003.08.011

Steitz, A.M., Schröder, C., Knuth, I., Keber, C.U., Sommerfeld, L., Finkernagel, F., Jansen, J.M., Wagner, U., Müller-Brüsselbach, S., Worzfeld, T., Huber, M., Beutgen, V.M., Graumann, J., Pogge von Strandmann, E., Müller, R., Reinartz, S., 2023. TRAIL-dependent apoptosis of peritoneal mesothelial cells by NK cells promotes ovarian cancer invasion. iScience 26, 108401. https://doi.org/10.1016/j.isci.2023.108401

Stewart, C., Ralyea, C., Lockwood, S., 2019. Ovarian Cancer: An Integrated Review. Seminars in Oncology Nursing, Gynecology Oncology 35, 151–156. https://doi.org/10.1016/j.soncn.2019.02.001

Stokes, A., Joutsa, J., Ala-Aho, R., Pitchers, M., Pennington, C.J., Martin, C., Premachandra, D.J., Okada, Y., Peltonen, J., Grénman, R., James, H.A., Edwards, D.R., Kähäri, V.-M., 2010. Expression profiles and clinical correlations of degradome components in the tumor microenvironment of head and neck squamous cell carcinoma. Clin Cancer Res 16, 2022–2035. https://doi.org/10.1158/1078-0432.CCR-09-2525

Streisinger, G., Walker, C., Dower, N., Knauber, D., Singer, F., 1981. Production of clones of homozygous diploid zebra fish (Brachydanio rerio). Nature 291, 293–296. https://doi.org/10.1038/291293a0

Strobel, T., Cannistra, S.A., 1999. Beta1-integrins partly mediate binding of ovarian cancer cells to peritoneal mesothelium in vitro. Gynecol Oncol 73, 362–367. https://doi.org/10.1006/gyno.1999.5388

Symowicz, J., Adley, B.P., Gleason, K.J., Johnson, J.J., Ghosh, S., Fishman, D.A., Hudson, L.G., Stack, M.S., 2007. Engagement of Collagen-Binding Integrins Promotes Matrix

Metalloproteinase-9–Dependent E-Cadherin Ectodomain Shedding in Ovarian Carcinoma Cells. Cancer Research 67, 2030–2039. https://doi.org/10.1158/0008-5472.CAN-06-2808

Szarvas, T., Reis, H., Kramer, G., Shariat, S.F., vom Dorp, F., Tschirdewahn, S., Schmid, K.W., Kovalszky, I., Rübben, H., 2014. Enhanced stromal syndecan-1 expression is an independent risk factor for poor survival in bladder cancer. Human Pathology 45, 674–682. https://doi.org/10.1016/j.humpath.2013.10.036

Takada, Y., Ye, X., Simon, S., 2007. The integrins. Genome Biology 8, 215. https://doi.org/10.1186/gb-2007-8-5-215

Takashima, S., Oka, Y., Fujiki, F., Morimoto, S., Nakajima, H., Nakae, Y., Nakata, J., Nishida, S., Hosen, N., Tatsumi, N., Mizuguchi, K., Hashimoto, N., Oji, Y., Tsuboi, A., Kumanogoh, A., Sugiyama, H., 2016. Syndecan-4 as a Biomarker to Predict Clinical Outcome for Glioblastoma Multiforme Treated with WT1 Peptide Vaccine. Future Science OA 2, FSO96. https://doi.org/10.4155/fsoa-2015-0008

Tan, D.S.P., Agarwal, R., Kaye, S.B., 2006. Mechanisms of transcoelomic metastasis in ovarian cancer. Lancet Oncol 7, 925–934. https://doi.org/10.1016/S1470-2045(06)70939-1

Tan, I. de A., Ricciardelli, C., Russell, D.L., 2013. The metalloproteinase ADAMTS1: a comprehensive review of its role in tumorigenic and metastatic pathways. Int J Cancer 133, 2263–2276. https://doi.org/10.1002/ijc.28127

Tang, L., Wang, P., Wang, Q., Zhong, L., 2019. Correlation of LAMA3 with onset and prognosis of ovarian cancer. Oncol Lett 18, 2813–2818. https://doi.org/10.3892/ol.2019.10600

Tarin, D., Price, J.E., Kettlewell, M.G.W., Souter, R.G., Vass, A.C.R., Crossley, B., 1984. Mechanisms of Human Tumor Metastasis Studied in Patients with Peritoneovenous Shunts. Cancer Res 44, 3584–3592.

Tavares, V., Marques, I.S., de Melo, I.G., Assis, J., Pereira, D., Medeiros, R., 2024. Paradigm Shift: A Comprehensive Review of Ovarian Cancer Management in an Era of Advancements. Int J Mol Sci 25, 1845. https://doi.org/10.3390/ijms25031845

Teame, T., Zhang, Z., Ran, C., Zhang, H., Yang, Y., Ding, Q., Xie, M., Gao, C., Ye, Y., Duan, M., Zhou, Z., 2019. The use of zebrafish (Danio rerio) as biomedical models. Anim Front 9, 68–77. https://doi.org/10.1093/af/vfz020

Teng, P.-N., Wang, G., Hood, B.L., Conrads, K.A., Hamilton, C.A., Maxwell, G.L., Darcy, K.M., Conrads, T.P., 2014. Identification of candidate circulating cisplatin-resistant biomarkers from epithelial ovarian carcinoma cell secretomes. Br J Cancer 110, 123–132. https://doi.org/10.1038/bjc.2013.687

Teng, Y., Xie, X., Walker, S., White, D.T., Mumm, J.S., Cowell, J.K., 2013. Evaluating human cancer cell metastasis in zebrafish. BMC Cancer 13, 453. https://doi.org/10.1186/1471-2407-13-453

Testa, U., Petrucci, E., Pasquini, L., Castelli, G., Pelosi, E., 2018. Ovarian Cancers: Genetic Abnormalities, Tumor Heterogeneity and Progression, Clonal Evolution and Cancer Stem

Cells. Medicines (Basel) 5, 16. https://doi.org/10.3390/medicines5010016

Tian, C., Markman, M., Zaino, R., Ozols, R.F., McGuire, W.P., Muggia, F.M., Rose, P.G., Spriggs, D., Armstrong, D.K., 2009. CA-125 change after chemotherapy in prediction of treatment outcome among advanced mucinous and clear cell epithelial ovarian cancers. Cancer 115, 1395–1403. https://doi.org/10.1002/cncr.24152

To, W.S., Midwood, K.S., 2011. Plasma and cellular fibronectin: distinct and independent functions during tissue repair. Fibrogenesis & Tissue Repair 4, 21. https://doi.org/10.1186/1755-1536-4-21

Tone, A.A., McConechy, M.K., Yang, W., Ding, J., Yip, S., Kong, E., Wong, K.-K., Gershenson, D.M., Mackay, H., Shah, S., Gilks, B., Tinker, A.V., Clarke, B., McAlpine, J.N., Huntsman, D., 2014. Intratumoral heterogeneity in a minority of ovarian low-grade serous carcinomas. BMC Cancer 14, 982. https://doi.org/10.1186/1471-2407-14-982

Tong, M., Chan, K.W., Bao, J.Y.J., Wong, K.Y., Chen, J.-N., Kwan, P.S., Tang, K.H., Fu, L., Qin, Y.-R., Lok, S., Guan, X.-Y., Ma, S., 2012. Rab25 Is a Tumor Suppressor Gene with Antiangiogenic and Anti-Invasive Activities in Esophageal Squamous Cell Carcinoma. Cancer Res 72, 6024–6035. https://doi.org/10.1158/0008-5472.CAN-12-1269

Tong, W.-W., Tong, G.-H., Chen, X.-X., Zheng, H.-C., Wang, Y.-Z., 2015. HIF2α is associated with poor prognosis and affects the expression levels of survivin and cyclin D1 in gastric carcinoma. International Journal of Oncology 46, 233–242. https://doi.org/10.3892/ijo.2014.2719

Trelford, C.B., Buensuceso, A., Tomas, E., Valdes, Y.R., Hovey, O., Li, S.S.-C., Shepherd, T.G., 2024. LKB1 and STRADα Promote Epithelial Ovarian Cancer Spheroid Cell Invasion. Cancers 16, 3726. https://doi.org/10.3390/cancers16223726

Tsara, M.E., Theocharis, A.D., Theocharis, D.A., 2002. Compositional and structural alterations of proteoglycans in human rectum carcinoma with special reference to versican and decorin. Anticancer Res 22, 2893–2898.

Tsoyi, K., Osorio, J.C., Chu, S.G., Fernandez, I.E., De Frias, S.P., Sholl, L., Cui, Y., Tellez, C.S., Siegfried, J.M., Belinsky, S.A., Perrella, M.A., El-Chemaly, S., Rosas, I.O., 2019. Lung Adenocarcinoma Syndecan-2 Potentiates Cell Invasiveness. Am J Respir Cell Mol Biol 60, 659–666. https://doi.org/10.1165/rcmb.2018-0118OC

Tulotta, C., He, S., Chen, L., Groenewoud, A., van der Ent, W., Meijer, A.H., Spaink, H.P., Snaar-Jagalska, B.E., 2016. Imaging of Human Cancer Cell Proliferation, Invasion, and Micrometastasis in a Zebrafish Xenogeneic Engraftment Model, in: Kawakami, K., Patton, E.E., Orger, M. (Eds.), Zebrafish: Methods and Protocols. Springer, New York, NY, pp. 155–169. https://doi.org/10.1007/978-1-4939-3771-4_11

Ueland, F.R., Desimone, C.P., Seamon, L.G., Miller, R.A., Goodrich, S., Podzielinski, I., Sokoll, L., Smith, A., van Nagell, J.R.J., Zhang, Z., 2011. Effectiveness of a Multivariate Index Assay in the Preoperative Assessment of Ovarian Tumors. Obstetrics & Gynecology 117, 1289. https://doi.org/10.1097/AOG.0b013e31821b5118

Van den Steen, P.E., Proost, P., Wuyts, A., Van Damme, J., Opdenakker, G., 2000. Neutrophil gelatinase B potentiates interleukin-8 tenfold by aminoterminal processing, whereas it degrades CTAP-III, PF-4, and GRO-alpha and leaves RANTES and MCP-2 intact. Blood 96, 2673–2681.

Vargas-Patron, L.A., Agudelo-Dueñas, N., Madrid-Wolff, J., Venegas, J.A., González, J.M., Forero-Shelton, M., Akle, V., 2019. Xenotransplantation of Human glioblastoma in Zebrafish larvae: in vivo imaging and proliferation assessment. Biology Open 8, bio043257. https://doi.org/10.1242/bio.043257

Varki, A., Cummings, R., Esko, J., Freeze, H., Hart, G., Marth, J., 1999. Proteoglycans and Glycosaminoglycans, in: Essentials of Glycobiology. Cold Spring Harbor Laboratory Press.

Viapiano, M.S., Hockfield, S., Matthews, R.T., 2008. BEHAB/brevican requires ADAMTS-mediated proteolytic cleavage to promote glioma invasion. J Neurooncol 88, 261–272. https://doi.org/10.1007/s11060-008-9575-8

Voutilainen, K., Anttila, M., Sillanpää, S., Tammi, R., Tammi, M., Saarikoski, S., Kosma, V.-M., 2003. Versican in epithelial ovarian cancer: Relation to hyaluronan, clinicopathologic factors and prognosis. International Journal of Cancer 107, 359–364. https://doi.org/10.1002/ijc.11423

Walker, C., Mojares, E., Del Río Hernández, A., 2018. Role of Extracellular Matrix in Development and Cancer Progression. International Journal of Molecular Sciences 19, 3028. https://doi.org/10.3390/ijms19103028

Wang, F., So, J., Reierstad, S., Fishman, D.A., 2005. Matrilysin (MMP-7) promotes invasion of ovarian cancer cells by activation of progelatinase. International Journal of Cancer 114, 19–31. https://doi.org/10.1002/ijc.20697

Wang, J., Markova, D., Anderson, D.G., Zheng, Z., Shapiro, I.M., Risbud, M.V., 2011. TNF-α and IL-1β Promote a Disintegrin-like and Metalloprotease with Thrombospondin Type I Motif-5-mediated Aggrecan Degradation through Syndecan-4 in Intervertebral Disc*. Journal of Biological Chemistry 286, 39738–39749. https://doi.org/10.1074/jbc.M111.264549

Wang, S., Hu, C., Wu, F., He, S., 2017. Rab25 GTPase: Functional roles in cancer. Oncotarget 8, 64591–64599. https://doi.org/10.18632/oncotarget.19571

Wang, X., Kumar, R., Navarre, J., Casanova, J.E., Goldenring, J.R., 2000. Regulation of Vesicle Trafficking in Madin-Darby Canine Kidney Cells by Rab11a and Rab25 *. Journal of Biological Chemistry 275, 29138–29146. https://doi.org/10.1074/jbc.M004410200

Wang, Y., Li, G., Wang, H., Qi, Q., Wang, X., Lu, H., 2025. Targeted therapeutic strategies for Nectin-4 in breast cancer: Recent advances and future prospects. The Breast 79, 103838. https://doi.org/10.1016/j.breast.2024.103838

Watanabe, A., Mabuchi, T., Satoh, E., Furuya, K., Zhang, L., Maeda, S., Naganuma, H., 2006. Expression of syndecans, a heparan sulfate proteoglycan, in malignant gliomas: participation of nuclear factor-κB in upregulation of syndecan-1 expression. J Neurooncol 77, 25–32.

https://doi.org/10.1007/s11060-005-9010-3

Watnick, R.S., 2012. The Role of the Tumor Microenvironment in Regulating Angiogenesis. Cold Spring Harb Perspect Med 2, a006676. https://doi.org/10.1101/cshperspect.a006676

Ween, M.P., Oehler, M.K., Ricciardelli, C., 2011. Role of versican, hyaluronan and CD44 in ovarian cancer metastasis. Int J Mol Sci 12, 1009–1029. https://doi.org/10.3390/ijms12021009

Weis, M.A., Hudson, D.M., Kim, L., Scott, M., Wu, J.-J., Eyre, D.R., 2010. Location of 3-Hydroxyproline Residues in Collagen Types I, II, III, and V/XI Implies a Role in Fibril Supramolecular Assembly*. Journal of Biological Chemistry 285, 2580–2590. https://doi.org/10.1074/jbc.M109.068726

Wennerberg, K., Rossman, K.L., Der, C.J., 2005. The Ras superfamily at a glance. J Cell Sci 118, 843–846. https://doi.org/10.1242/jcs.01660

Wewer, U.M., Mörgelin, M., Holck, P., Jacobsen, J., Lydolph, M.C., Johnsen, A.H., Kveiborg, M., Albrechtsen, R., 2006. ADAM12 Is a Four-leafed Clover: THE EXCISED PRODOMAIN REMAINS BOUND TO THE MATURE ENZYME*. Journal of Biological Chemistry 281, 9418–9422. https://doi.org/10.1074/jbc.M513580200

White, J., Bridges, L., DeSimone, D., Tomczuk, M., Wolfsberg, T., 2005. Introduction to the ADAM Family, in: Hooper, N.M., Lendeckel, U. (Eds.), The ADAM Family of Proteases. Springer US, Boston, MA, pp. 1–28. https://doi.org/10.1007/0-387-25151-0_1

White, R., Rose, K., Zon, L., 2013. Zebrafish cancer: the state of the art and the path forward. Nat Rev Cancer 13, 624–636. https://doi.org/10.1038/nrc3589

WHO, E.B., 2020. Female genital tumours, 5th ed. ed, World Health Organization classification of tumours. IARC Press, Lyon.

Wiegand, K.C., Shah, S.P., Al-Agha, O.M., Zhao, Y., Tse, K., Zeng, T., Senz, J., McConechy, M.K., Anglesio, M.S., Kalloger, S.E., Yang, W., Heravi-Moussavi, A., Giuliany, R., Chow, C., Fee, J., Zayed, A., Prentice, L., Melnyk, N., Turashvili, G., Delaney, A.D., Madore, J., Yip, S., McPherson, A.W., Ha, G., Bell, L., Fereday, S., Tam, A., Galletta, L., Tonin, P.N., Provencher, D., Miller, D., Jones, S.J.M., Moore, R.A., Morin, G.B., Oloumi, A., Boyd, N., Aparicio, S.A., Shih, I.-M., Mes-Masson, A.-M., Bowtell, D.D., Hirst, M., Gilks, B., Marra, M.A., Huntsman, D.G., 2010. ARID1A Mutations in Endometriosis-Associated Ovarian Carcinomas. New England Journal of Medicine 363, 1532–1543. https://doi.org/10.1056/NEJMoa1008433

Wight, T.N., 2017. Provisional matrix: A role for versican and hyaluronan. Matrix Biology, Special issue on Provisional Matrix 60–61, 38–56. https://doi.org/10.1016/j.matbio.2016.12.001

Wilhelm, O., Hafter, R., Coppenrath, E., Pflanz, M., Schmitt, M., Babic, R., Linke, R., Gã, W., n.d. Fibrin-Fibronectin Compounds in Human Ovarian Tumor Ascites and Their Possible Relation to the Tumor Stroma. 1988.

Witz, C.A., Montoya-Rodriguez, I.A., Cho, S., Centonze, V.E., Bonewald, L.F., Schenken, R.S., 2001. Composition of the extracellular matrix of the peritoneum. J Soc Gynecol Investig

8, 299–304. https://doi.org/10.1016/s1071-5576(01)00122-8

Wong, K.-K., Izaguirre, D.I., Kwan, S.-Y., King, E.R., Deavers, M.T., Sood, A.K., Mok, S.C., Gershenson, D.M., 2013. Poor survival with wild-type *TP53* ovarian cancer? Gynecologic Oncology 130, 565–569. https://doi.org/10.1016/j.ygyno.2013.06.016

Woolas, R., Jacobs, I., Davies, A.P.R.Y.S., Leake, J., Brown, C., Grudzinskas, J.G., Oram, D., 1994. What is the true incidence of primary fallopian tube carcinoma? International Journal of Gynecological Cancer 4, 384–388. https://doi.org/10.1046/j.1525-1438.1994.04060384.x

Wu, J., Jiang, J., Chen, B., Wang, K., Tang, Y., Liang, X., 2021. Plasticity of cancer cell invasion: Patterns and mechanisms. Translational Oncology 14, 100899. https://doi.org/10.1016/j.tranon.2020.100899

Wu, J., Sheng, S., Liang, X., Tang, Y., 2017. The role of tumor microenvironment in collective tumor cell invasion. Future Oncology 13, 991–1002. https://doi.org/10.2217/fon-2016-0501

Wu, M., Cronin, K., Crane, J.S., 2025. Biochemistry, Collagen Synthesis, in: StatPearls. StatPearls Publishing, Treasure Island (FL).

Wu, Y.-H., Chang, T.-H., Huang, Y.-F., Huang, H.-D., Chou, C.-Y., 2014. COL11A1 promotes tumor progression and predicts poor clinical outcome in ovarian cancer. Oncogene 33, 3432–3440. https://doi.org/10.1038/onc.2013.307

Wu, Y.J., Pierre, D.P.L., Wu, J., Yee, A.J., Yang, B.B., 2005. The interaction of versican with its binding partners. Cell Res 15, 483–494. https://doi.org/10.1038/sj.cr.7290318

Xiao, J., McGill, J.R., Nasir, A., Lekan, A., Johnson, B., Wilkins, D.J., Pearson, G.W., Tanner, K., Goodarzi, H., Glasgow, E., Schlegel, R., Agarwal, S., 2022. Identifying drivers of breast cancer metastasis in progressively invasive subpopulations of zebrafish-xenografted MDA-MB-231. Mol Biomed 3, 16. https://doi.org/10.1186/s43556-022-00080-5

Xiong, J.P., Stehle, T., Diefenbach, B., Zhang, R., Dunker, R., Scott, D.L., Joachimiak, A., Goodman, S.L., Arnaout, M.A., 2001. Crystal structure of the extracellular segment of integrin alpha Vbeta3. Science 294, 339–345. https://doi.org/10.1126/science.1064535

Xu, L., Nagai, Y., Kajihara, Y., Ito, G., Tomita, T., 2021. The Regulation of Rab GTPases by Phosphorylation. Biomolecules 11, 1340. https://doi.org/10.3390/biom11091340

Xu, S., Xu, H., Wang, W., Li, S., Li, H., Li, T., Zhang, W., Yu, X., Liu, L., 2019. The role of collagen in cancer: from bench to bedside. Journal of Translational Medicine 17, 309. https://doi.org/10.1186/s12967-019-2058-1

Xu, Shouying, Cao, B., Xuan, G., Xu, Shu, An, Z., Zhu, C., Li, L., Tang, C., 2024. Function and regulation of Rab GTPases in cancers. Cell Biol Toxicol 40, 28. https://doi.org/10.1007/s10565-024-09866-5

Xu, W., Foster, B.A., Richards, M., Bondioli, K.R., Shah, G., Green, C.C., 2018. Characterization of prostate cancer cell progression in zebrafish xenograft model. International Journal of Oncology 52, 252–260. https://doi.org/10.3892/ijo.2017.4189

Yamamoto, K., Owen, K., Parker, A.E., Scilabra, S.D., Dudhia, J., Strickland, D.K., Troeberg, L., Nagase, H., 2014. Low density lipoprotein receptor-related protein 1 (LRP1)-mediated endocytic clearance of a disintegrin and metalloproteinase with thrombospondin motifs-4 (ADAMTS-4): functional differences of non-catalytic domains of ADAMTS-4 and ADAMTS-5 in LRP1 binding. J Biol Chem 289, 6462–6474. https://doi.org/10.1074/jbc.M113.545376

Yang, F., Xiao-Yan, X., Bi-Liang, C., Xiangdong, M., 2006. Knockdown of Rab25 expression by RNAi inhibits growth of human epithelial ovarian cancer cells *in vitro* and *in vivo*. Pathology 38, 561–567. https://doi.org/10.1080/00313020601024037

Yang, H., Liu, Y., Zhao, M.-M., Guo, Q., Zheng, X.-K., Liu, D., Zeng, K.-W., Tu, P.-F., 2021. Therapeutic potential of targeting membrane-spanning proteoglycan SDC4 in hepatocellular carcinoma. Cell Death Dis 12, 1–16. https://doi.org/10.1038/s41419-021-03780-y

Yang, X., Cui, W., Gu, A., Xu, C., Yu, S., Li, T., Cui, Y., Zhang, X., Bian, X., 2013. A Novel Zebrafish Xenotransplantation Model for Study of Glioma Stem Cell Invasion. PLOS ONE 8, e61801. https://doi.org/10.1371/journal.pone.0061801

Yao, J., Li, W.-Y., Li, S.-G., Feng, X.-S., Gao, S.-G., 2014. Midkine promotes perineural invasion in human pancreatic cancer. World J Gastroenterol 20, 3018–3024. https://doi.org/10.3748/wjg.v20.i11.3018

Yao, J., Zhang, L.-L., Huang, X.-M., Li, W.-Y., Gao, S.-G., 2017. Pleiotrophin and N-syndecan promote perineural invasion and tumor progression in an orthotopic mouse model of pancreatic cancer. World J Gastroenterol 23, 3907–3914. https://doi.org/10.3748/wjg.v23.i21.3907

Yao, S., Liu, X., Feng, Y., Li, Y., Xiao, X., Han, Y., Xia, S., 2024. Unveiling the Role of HGF/c-Met Signaling in Non-Small Cell Lung Cancer Tumor Microenvironment. Int J Mol Sci 25, 9101. https://doi.org/10.3390/ijms25169101

Yeung, T.-L., Leung, C.S., Wong, K.-K., Samimi, G., Thompson, M.S., Liu, J., Zaid, T.M., Ghosh, S., Birrer, M.J., Mok, S.C., 2013. TGF-β Modulates Ovarian Cancer Invasion by Upregulating CAF-Derived Versican in the Tumor Microenvironment. Cancer Research 73, 5016–5028. https://doi.org/10.1158/0008-5472.CAN-13-0023

Yeung, T.-L., Leung, C.S., Yip, K.-P., Au Yeung, C.L., Wong, S.T.C., Mok, S.C., 2015. Cellular and molecular processes in ovarian cancer metastasis. A Review in the Theme: Cell and Molecular Processes in Cancer Metastasis. Am J Physiol Cell Physiol 309, C444–C456. https://doi.org/10.1152/ajpcell.00188.2015

Yokoi, A., Yoshioka, Y., Yamamoto, Y., Ishikawa, M., Ikeda, S., Kato, T., Kiyono, T., Takeshita, F., Kajiyama, H., Kikkawa, F., Ochiya, T., 2017. Malignant extracellular vesicles carrying MMP1 mRNA facilitate peritoneal dissemination in ovarian cancer. Nat Commun 8, 14470. https://doi.org/10.1038/ncomms14470

Yoshida, Y., Hosokawa, K., Dantes, A., Kotsuji, F., Kleinman, H.K., Amsterdam, A., 2001. Role of laminin in ovarian cancer tumor growth and metastasis via regulation of Mdm2 and Bcl-2 expression. Int J Oncol 18, 913–921. https://doi.org/10.3892/ijo.18.5.913

Yoshihara, M., Yamakita, Y., Kajiyama, H., Senga, T., Koya, Y., Yamashita, M., Nawa, A., Kikkawa, F., 2020. Filopodia play an important role in the trans-mesothelial migration of ovarian cancer cells. Experimental Cell Research 392, 112011. https://doi.org/10.1016/j.yexcr.2020.112011

Yousif, N.G., 2014. Fibronectin promotes migration and invasion of ovarian cancer cells through up-regulation of FAK–PI3K/Akt pathway. Cell Biology International 38, 85–91. https://doi.org/10.1002/cbin.10184

Yuan, S., Bacchetti, R., Adams, J., Cuffaro, D., Rossello, A., Nuti, E., Santamaria, S., Rainero, E., 2025. The protease ADAMTS5 controls ovarian cancer cell invasion, downstream of Rab25. The FEBS Journal. https://doi.org/10.1111/febs.70080

Yuan, S., Bacchetti, R., Adams, J., Rainero, E., 2024. The protease ADAMTS5 controls ovarian cancer cell invasion, downstream of Rab25. https://doi.org/10.1101/2024.07.08.602517

Zand, L., Feng, Q., Roskelley, C.D., Leung, P.C.K., Auersperg, N., 2003. Differential effects of cellular fibronectin and plasma fibronectin on ovarian cancer cell adhesion, migration, and invasion. In Vitro Cell.Dev.Biol.-Animal 39, 178–182. https://doi.org/10.1007/s11626-003-0013-0

Zeller, C., Dai, W., Steele, N.L., Siddiq, A., Walley, A.J., Wilhelm-Benartzi, C.S.M., Rizzo, S., van der Zee, A., Plumb, J.A., Brown, R., 2012. Candidate DNA methylation drivers of acquired cisplatin resistance in ovarian cancer identified by methylome and expression profiling. Oncogene 31, 4567–4576. https://doi.org/10.1038/onc.2011.611

Zerial, M., McBride, H., 2001. Rab proteins as membrane organizers. Nat Rev Mol Cell Biol 2, 107–117. https://doi.org/10.1038/35052055

Zhang, J., Wei, J., Lu, J., Tong, Z., Liao, B., Yu, B., Zheng, F., Huang, X., Chen, Z., Fang, Y., Li, B., Chen, W., Xie, D., Luo, J., 2013. Overexpression of Rab25 contributes to metastasis of bladder cancer through induction of epithelial–mesenchymal transition and activation of Akt/GSK-3β/Snail signaling. Carcinogenesis 34, 2401–2408. https://doi.org/10.1093/carcin/bgt187

Zhang, J., Yang, N., Kreeger, P.K., Notbohm, J., 2021. Topological defects in the mesothelium suppress ovarian cancer cell clearance. APL Bioengineering 5, 036103. https://doi.org/10.1063/5.0047523

Zhao, H., Yang, Z., Wang, X., Zhang, X., Wang, M., Wang, Y., Mei, Q., Wang, Z., 2012. Triptolide inhibits ovarian cancer cell invasion by repression of matrix metalloproteinase 7 and 19 and upregulation of E-cadherin. Exp Mol Med 44, 633–641. https://doi.org/10.3858/emm.2012.44.11.072

Zheng, A., Wei, Y., Zhao, Y., Zhang, T., Ma, X., 2022. The role of cancer-associated mesothelial cells in the progression and therapy of ovarian cancer. Front Immunol 13, 1013506. https://doi.org/10.3389/fimmu.2022.1013506

Zheng, W., Ge, D., Meng, G., 2020. Reversing microtubule-directed chemotherapeutic drug resistance by co-delivering α2β1 inhibitor and paclitaxel with nanoparticles in ovarian cancer. Cell Biology International 44, 610–620. https://doi.org/10.1002/cbin.11261

Zhou, J., Du, Y., Lu, Y., Luan, B., Xu, C., Yu, Y., Zhao, H., 2019. CD44 Expression Predicts Prognosis of Ovarian Cancer Patients Through Promoting Epithelial-Mesenchymal Transition (EMT) by Regulating Snail, ZEB1, and Caveolin-1. Front. Oncol. 9. https://doi.org/10.3389/fonc.2019.00802

Zhu, H., Wang, J., Nie, W., Armando, I., Han, F., 2021. ADAMs family in kidney physiology and pathology. eBioMedicine 72, 103628. https://doi.org/10.1016/j.ebiom.2021.103628

Zhu, Z., Xu, J., Wu, X., Lin, S., Li, L., Ye, W., Huang, Z., 2021. In Silico Identification of Contradictory Role of ADAMTS5 in Hepatocellular Carcinoma. Technol Cancer Res Treat 20, 1533033820986826. https://doi.org/10.1177/1533033820986826

Zitka, O., Kukacka, J., Krizkova, S., Huska, D., Adam, V., Masarik, M., Prusa, R., Kizek, R., 2010. Matrix metalloproteinases. Curr Med Chem 17, 3751–3768. https://doi.org/10.2174/092986710793213724

Zollinger, A.J., Smith, M.L., 2017. Fibronectin, the extracellular glue. Matrix Biology, Special issue on Provisional Matrix 60–61, 27–37. https://doi.org/10.1016/j.matbio.2016.07.011